Expression, Structure and Mechanism of Manganese Peroxidase from *Phanerochaete chrysosporium*

Katsuyuki Kishi

B.S., Tokyo University, 1988

M.S., Tokyo University, 1990

A dissertation submitted to the faculty of the

Oregon Graduate Institute of Science and Technology

in partial fulfillment of the

requirements for the degree

Doctor of Philosophy

in

Biochemistry

April 1997

The dissertation "Expression, Structure and Mechanism of Manganese Peroxidase from *Phanerochaete chrysosporium*" by Katsuyuki Kishi has been examined and approved by the following examination committee:

_____

Michael H. Gold, Advisor
Professor

_____

James K. Hurst
Professor, Washington State University

Thomas M. Loehr
Professor

_____

V. Renganathan
Associate Professor

ACKNOWLEDGMENTS

TABLE OF CONTENTS

LIST OF TABLES

LIST OF FIGURES

ABSTRACT

Expression, Structure and Mechanism of Manganese Peroxidase from *Phanerochaete chrysosporium*

Katsuyuki Kishi, Ph.D.

Supervising Professor: Michael H. Gold

Manganese peroxidase (MnP) is one of two extracellular peroxidases secreted by the lignin-degrading fungus *Phanerochaete chrysosporium*. MnP oxidizes Mn(II) to Mn(III) and the latter, complexed with a chelator, in turn oxidizes the plant polymer, lignin, and aromatic pollutants.

The role of organic acid chelators in the MnP reaction was examined using transient state kinetic techniques. Maximal stimulation of the rate of MnP compound II reduction occurs at physiological concentrations of oxalate, suggesting that a 1:1 complex of Mn(II)-chelator may be the substrate for MnP compound II reduction.

An homologous expression system in *P. chrysosporium* was developed in order to study structure/function relationships in MnP via site-directed mutagenesis. In this system, the promoter region of the glyceraldehyde-3-phosphate dehydrogenase gene (*gpd*) is used to drive expression of the gene encoding MnP isozyme 1 (MnP1) during primary metabolic growth of *P. chrysosporium*. The expressed MnP protein is secreted and fully active and has kinetic and spectral properties which are essentially identical to the wild-type MnP.

Site-directed MnP mutants were created using the polymerase chain reaction and variant proteins were produced using our homologous expression system. MnP mutants of the potential Mn(II) ligands, D179N, E35Q, E39Q, and D179N-E35Q, were

generated, expressed and characterized. All of these variants exhibit dramatically reduced Mn(II) binding and rates of oxidation, strongly suggesting that MnP has only one productive site for Mn(II) oxidation. This site consists of Asp179, Glu35, Glu39, the heme 6-propionate and two water molecules.

The role of the Phe190 residue in the heme pocket also was examined by site-directed mutagenesis. The F190Y, F190L, F190I, and F190A variants exhibit steady-state kinetic properties similar to the wild-type enzyme. In contrast, the stability of both the native and oxidized states of MnP are significantly altered in several of the Phe190 variants. Moreover, a pH-dependent Fe(III) high- to low-spin transition occurs at considerably lower pHs for the F190A and F190I variants. These results suggest that Phe190 plays a critical role in stabilizing the heme environment of MnP.

CHAPTER 1

INTRODUCTION

1.1 BIODEGRADATION OF LIGNIN

Lignin is the second most abundant carbon source after cellulose and the most abundant renewable aromatic resource on earth (Sarkanen & Ludwig, 1971; Crawford, 1981). It comprises 15-36 % of the total lignocellulosic material in wood (Lin & Dence, 1992). It provides increased rigidity to the plant cell wall and also protects plants from pathogenic organisms (Sarkanen & Ludwig, 1971; Higuchi, 1985). In addition, lignin minimizes water permeation across the cell walls of xylem tissues (Sarkanen & Ludwig, 1971; Higuchi, 1985). Since the biodegradation of cellulose is retarded by the presence of this polymer (Crawford, 1981; Buswell & Odier, 1987; Kirk & Farrell, 1987; Gold *et al.*, 1989), the breakdown and potential utilization of lignin are of enormous significance.

Although wood was known to be degraded by living organisms, particularly fungi (Kirk & Shimada, 1985; Kirk & Farrell, 1987; Blanchette, 1991), substantial progress in lignin biodegradation research did not commence until a better understanding of the lignin structure was gained in the 1960s. Furthermore, an effective and simple assay to evaluate lignin biodegradation either qualitatively or quantitatively was not developed until the 1970s. During the 1970s, assays for lignin biodegradation using lignin model compounds and ^{14}C-labeled lignins were finally developed (Crawford, 1981). From the 1970s to the present day, model compounds have been used as substitutes for the natural polymer to obtain a better understanding of the individual steps involved in lignin biodegradation. Radioisotopic assay techniques have been applied successfully to a wide range of lignin related research problems, such as the determination of the range of microbial taxa involved and the screening of lignin-degrading microorganisms.

This section comprises a brief overview of lignin structure, the microorganisms involved in lignin biodegradation, and a review of studies on lignin degradation by white

rot basidiomycetes.

1.1.1 Lignin: Structure and Classification

Lignin is a complex, heterogeneous and random phenylpropanoid polymer (Freudenberg, 1968; Sarkanen & Ludwig, 1971) and is found in all vascular plants and in certain primitive plant groups such as ferns and club mosses, but not in *Bryophyta* (true mosses) and algae (Crawford, 1981). Lignin is synthesized from three substituted cinnamyl alcohols: p-coumaryl [1-(4-hydroxyphenyl)-], coniferyl [1-(4-hydroxy-3-methoxyphenyl)-], and sinapyl alcohols [1-(3,5-dimethoxy-4-hydroxyphenyl)-3-hydroxy-1-propane] (Figure 1.1). These substructures have been commonly called p-coumaryl, guaiacyl, and syringyl nuclei, respectively. The proportions of these nuclei are dependent on the plant examined. Guaiacyl lignin is predominantly found in softwoods. Hardwoods contain guaiacyl-syringyl lignin, which is derived from approximately equal amounts of coniferyl and sinapyl alcohols and grasses produce a mixed polymer of p-coumaryl, guaiacyl, and syringyl alcohols (Musha & Goring, 1975; Effland, 1977). Free radical condensation of these alcohols, initiated by plant cell wall peroxidases (Harkin & Obst, 1973), results in the formation of a heterogeneous, amorphous, optically inactive, random, and highly branched polymer (Figure 1.2). More than two thirds of the phenylpropane units in lignin are linked by ether bonds and the remainder are linked by carbon-to-carbon bonds. Figure 1.3 shows the principal bonds in lignin. The major functional groups in lignin consist of phenolic hydroxyl, benzylic hydroxyl, and carbonyl groups. The frequency of individual functional group varies with the origin of the lignins.

1.1.2 Lignin-Degrading Microorganisms

Most wood-decaying microorganisms degrade wood polysaccharides by means of hydrolases, such as cellulases and xylanases. Many organisms are able to chemically modify lignin but few can actually degrade lignin to CO_2 and H_2O owing to its complex and heterogenous structure. Thus, the biodegradation of lignin is believed to be accomplished by special groups of some bacteria and fungi (Kirk & Shimada, 1985; Kirk & Farrell, 1987; Blanchette, 1991).

1.1.2.1 Lignin-degrading bacteria

Bacteria are known to be involved in the degradation of lignin, particularly low-molecular weight lignin-related aromatic compounds (Buswell & Odier, 1987; McCarthy, 1987; Vicuna, 1988; Zimmermann, 1990). Lignin-degrading bacteria belong to
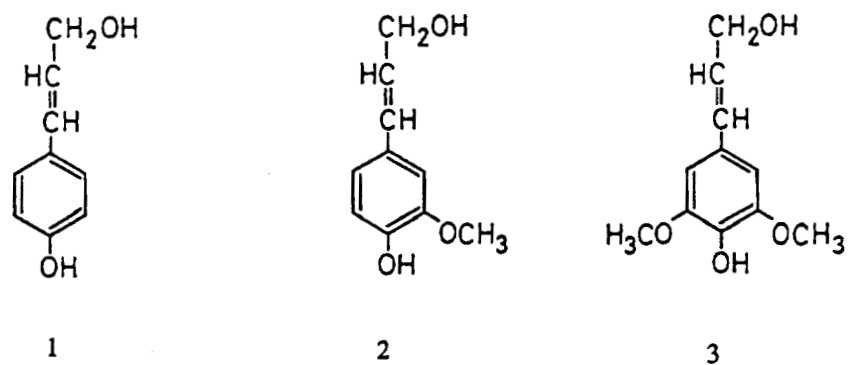
Figure 1.1. Lignin precursors. (1) *p*-coumaryl, (2) coniferyl, and (3) sinapyl alcohol (Eriksson, 1990).
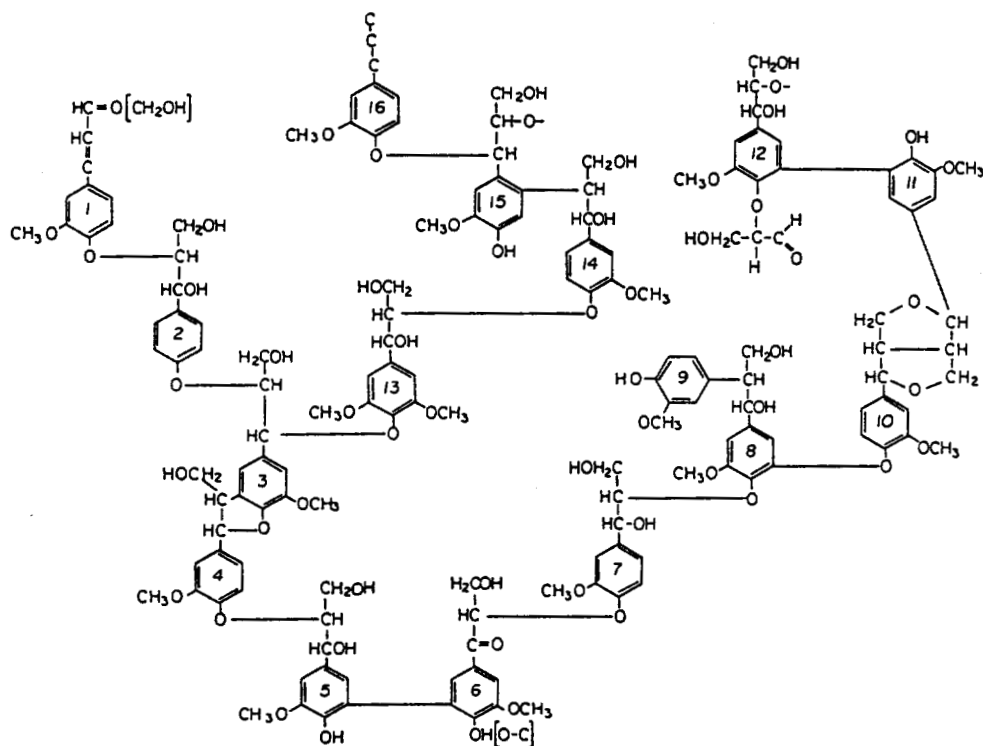
Figure 1.2. Schematic structure of spruce lignin (Adler, 1977).
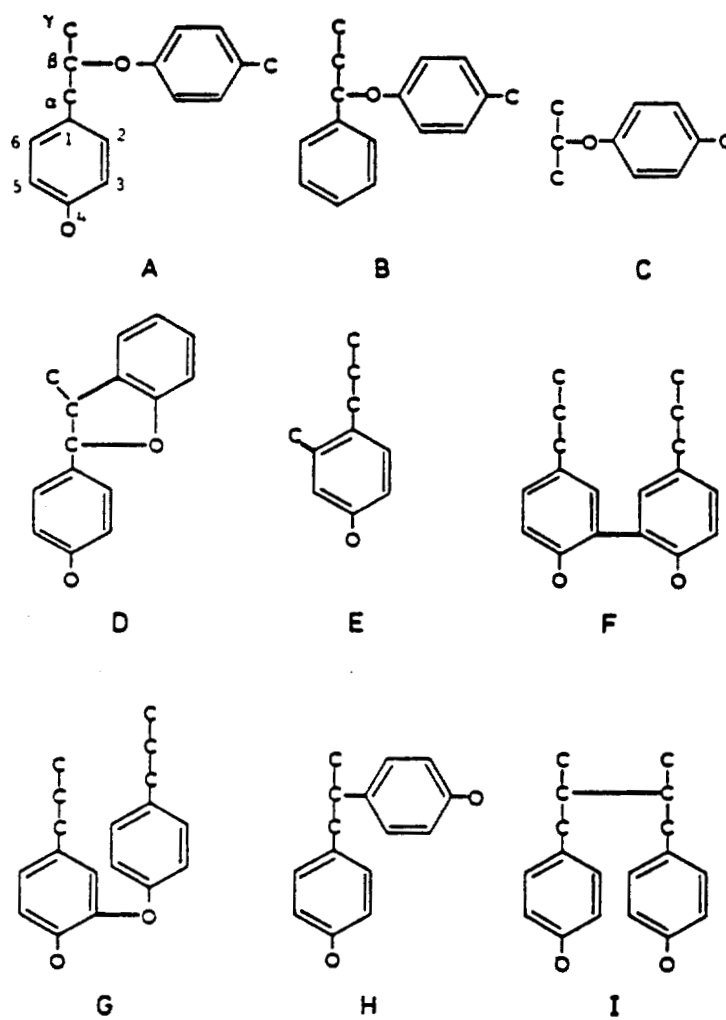
Figure 1.3. The common linkages between phenylpropane units: A, arylglycerol-β-aryl ether; B, nonphenolic benzyl aryl ether; C, glycerolaldehyde-2-aryl ether; D, phenylcoumarane; E, 2-, or 6-condensed; F, biphenyl; G, diphenyl ether; H, diarylpropane; I, β,β-linked units.

actinomycetes (*Streptomyces* spp.) and some Gram-negative eubacteria (*Pseudomonas* and *Xanthomonas* spp.). Lignin degradation by bacteria is, however, generally much slower than by wood-decaying fungi. Most of the enzymes involved in the bacterial degradation of lignin are intracellular, explaining the restricted effect on polymeric lignin. Interestingly, peroxidases possibly involved in lignin degradation have recently been discovered in several streptomycetes (Ramachandra *et al.*, 1988; Adhi *et al.*, 1989; Mliki & Zimmermann, 1992) and a lignin peroxidase-like enzyme (Chapter 1.2.2) secreted by *Streptomyces viridosporus* has been characterized (Ramachandra *et al.*, 1988; Wang *et al.*, 1990b). This suggests that actinomycetous bacteria may utilize a ligninolytic system related to that of white-rot fungi (Chapters 1.1.3 and 1.2.2).

1.1.2.2 Lignin-degrading fungi

Wood-rotting fungi have been classified into three categories: white-rot, brown-rot, and soft-rot fungi, according to the morphology of wood decay (Kirk & Cowling, 1984; Blanchette, 1991). White-rot fungi extensively decompose all major components of wood (Kirk & Farrell, 1987). The name "white-rot" comes from the observation that these organisms degrade cell wall lignin leaving the colorless cellulose. More than a thousand species of white-rot fungi have been identified. The majority belong to *Basidiomycotina* (Gilbertson, 1980). Among the ligninolytic microorganisms, white-rot basidiomycetes are the most efficient of all known lignin degraders.

Brown-rot fungi typically decompose wood carbohydrates (cellulose and hemicellulose) but leave the lignin intact. This lignin appears dark brown in color and is almost equal in weight to the lignin in sound wood (Eriksson, 1990; Blanchette, 1991). Brown-rot fungi predominantly attack softwood, whereas white-rot fungi primarily decompose hardwood. Brown-rot fungi are taxonomically very similar to white-rot fungi and also belong to the *Basidiomycotina*. Analysis of brown-rotted lignin has shown that brown-rot fungi cause some modification of lignin including a decreased methoxy content (Kirk & Adler, 1970; Kirk, 1975). As a result, a significant amount of phenolic hydroxyl groups are introduced into brown-rotted lignin (Kirk, 1975; Crawford, 1981; Jin *et al.*, 1990). The dark brown color is caused by the generation of additional quinones and conjugated carbonyl groups in the decayed lignin.

Soft-rot fungi preferably attack hardwood, especially when the moisture content is high (Blanchette, 1991). Most of these fungi belong to the *Ascomycotina* and *Deuteromycotina*. Soft-rot fungi decompose softwood, though generally more slowly than white- or brown-rot fungi (Kirk, 1971) and leave a modified lignin residue

(Eslyn *et al.*, 1975). It has been shown that soft-rot fungi are poor at degrading synthetic lignin, dehydrogenated polymerizates (DHPs), whereas they rapidly mineralize lignin-related phenolic compounds (Ander *et al.*, 1984, 1988). Although it seems likely that soft-rot fungi have an important role as lignin degraders in nature, cultivation of these organisms in the laboratory is difficult, and little is known about the enzymes they use to decompose lignin.

1.1.3 Lignin Biodegradation by White-Rot Basidiomycetes

Most of our knowledge about the biochemistry of lignin biodegradation comes from studies of lignin degraded by white-rot basidiomycetes. One white-rot fungus, *Phanerochaete chrysosporium*, has become the model for current studies of lignin biodegradation. The advantages of studying this fungus are: (a) it efficiently degrades both lignin and cellulose, (b) it is thermotolerant (an optimal growth temperature of 38 °C), (c) it produces asexual (conidia) spores prolifically - an advantage for genetic manipulation, and (d) it forms sexual fruiting structures in culture (Burdsall & Eslyn, 1974; Gold & Cheng, 1978). The ligninolytic activity in *P. chrysosporium* is triggered by the switch to idiophase, the physiological state of secondary metabolism when the nutrient carbon, sulfur, or nitrogen is depleted and the primary growth of the organism stops (Keyser *et al.*, 1978; Wessels, 1987; Kirk *et al.*, 1976; Jeffries *et al.*, 1981; Faison & Kirk, 1985). The addition of ammonium or glutamate to nitrogen-limiting cultures raises the concentration of intracellular glutamate (Fenn & Kirk, 1981), sharply decreases the concentration of cAMP (MacDonald *et al.*, 1984), restores primary growth (Fenn & Kirk, 1981), and halts lignin degradation (Fenn & Kirk, 1981).

Elemental and functional group analyses of lignin decayed by white-rot fungi, mainly *P. chrysosporium*, suggest that the degradation of lignin is an oxidative process, since the oxygen content of white-rotted lignin is generally higher than the control lignin from sound wood (Kirk & Chang, 1974). There also is a decrease in methoxyl groups and an increase in carbonyl and carboxyl groups. Product analysis of released fragments indicates that lignin degradation occurs mainly through C_α-C_β cleavage of the propyl side chains and through aryl-ether cleavage followed by modification of side chains, and aromatic ring fission (Kirk & Chang, 1974, 1975; Chen *et al.*, 1982; Chen & Chang, 1985; Higuchi, 1990; Tai *et al.*, 1990). However, detailed studies of the degradation of lignin by white-rot fungi are difficult owing to the complex and heterogeneous structure of lignin. Therefore, various lignin-related model compounds have been utilized to elucidate the mechanisms of lignin degradation. Dimeric and trimeric aromatic compounds

containing the most frequent lignin substructures, such as β-O-4 and β-1 dimers (Figure 1.3), are only degraded under conditions in which lignin is also degraded (Enoki *et al.*, 1980, 1981; Enoki & Gold, 1982; Goldsby *et al.*, 1980; Nakatsubo *et al.*, 1981, 1982; Kirk *et al.*, 1983; Higuchi, 1985, 1990; Weinstein *et al.*, 1980). In addition, analyses of degradation products indicate that the β-ether and C_α-C_β bonds of those model compounds are cleaved by fungi, in agreement with the results for polymeric lignin degradation (Kirk *et al.*, 1978; Bar-Lev & Kirk, 1981; Enoki & Gold, 1982).

1.2 ENZYMES INVOLVED IN LIGNIN BIODEGRADATION

Extracellular phenol oxidization was observed in cultures of white-rot fungi in the 1930s (Eriksson *et al.*, 1990). Bavendamm showed that most white-rot fungi produce a colored zone around mycelium on agar plates containing tannin and that the color is caused by phenol oxidases secreted by the fungi (Bavendamm, 1928). Later it was confirmed that the ligninolytic activity of wood-rotting fungi and the positive Bavendamm's test are almost parallel with only a few exceptions (Kirk & Kelman, 1965). Three distinct types of enzymes have been considered as phenol oxidases: tyrosinases, laccases, and peroxidases (Ander & Eriksson, 1976). Tyrosinases are copper enzymes that use oxygen to oxidize monophenols, yielding *o*-diphenols or *o*-quinones. They can also oxidize catechols to *o*-quinones. These enzymes, however, have a relatively narrow substrate specificity and are found intracellularly. Therefore, tyrosinases have not been considered as key enzymes in the nonspecific oxidation of lignin. Laccases are also multicopper enzymes that catalyze the oxidation of a variety of phenolic compounds by abstraction of one electron and one proton from phenolic hydroxyl groups to form phenoxy radicals. Free radicals produced by the enzyme undergo disproportionation or polymerization via radical coupling. Laccases use oxygen as an electron acceptor which is ultimately reduced to water. Peroxidases are heme enzymes that perform a similar reaction, but use hydrogen peroxide rather than oxygen as the cosubstrate. In addition, several other enzymes such as H_2O_2-producing enzymes and various reductases appear to play important roles in lignin breakdown.

1.2.1 Laccase

Laccase (EC 1.10.3.2, benzenediol:oxygen oxidoreductase) is a copper-containing oxidase (blue copper oxidase) (Reinhammar, 1984) and is produced by nearly all white-rot

fungi and by higher plants. Laccase catalyzes the one-electron oxidation of a variety of phenolic substrates, reducing O_2 to H_2O by four electrons. Laccases are glycoproteins with a carbohydrate content of 11-25 %.

Among fungal laccases, the laccases from the ascomycete *Neurospora crassa* (Froehner & Eriksson, 1974; Lerch *et al.*, 1978) and the basidiomycete *Trametes* (*Coriolus, Polyporus*) *versicolor* (Fahraeus & Reinhammar, 1967; Reinhammar, 1984) have been investigated in detail. Gene sequences of laccase have been reported from the ascomycetes, *N. crassa* (Germann & Lerch, 1986) and *Aspergillus nidulans* (Aramayo & Timberlake, 1990) and the basidiomycetes *Trametes* (*Coriolus*) *hirsuta* (Kojima *et al.*, 1990), *Phlebia radiata* (Saloheimo *et al.*, 1991), and *Agaricus bisporus* (Perry *et al.*, 1993). These gene sequences reveal a close similarity with ascorbate oxidase from higher plants (Messerschmidt & Huber, 1990).

T. versicolor laccase contains four copper atoms with three structural types: 1 type I, 1 type II, and 2 type III copper ions. The catalytic cycle of laccase has been proposed based upon the catalytic model for ascorbate oxidase (Reinhammar, 1984; Messerschmidt *et al.*, 1989). The type I copper is reduced by one electron by a phenol, and the electron is transferred to the trinuclear copper complex (type II and III) through amino acid ligands. All of the four copper ions are eventually reduced to Cu(I) ions which, in turn, reduce the O_2 bound to the type II copper generating two molecules of H_2O. Since a three-dimensional crystal structure of laccase is not available, the topology and coordination of the active site of laccase are not precisely known. In addition, laccases purified from various fungi are highly diverse in terms of molecular mass, copper content, presence of subunits, and substrate specificity. The molecular weight of laccases range from 60 to 100 kDa (Reinhammar, 1984), and non-blue laccases with only two copper atoms in the active site have been reported in *Agaricus bisporus* (Wood, 1980) and *Phlebia radiata* (Karhunen *et al.*, 1990). More investigation is required to determine if these results are accurate.

Research using phenolic lignin model dimers, particularly with guaiacyl type models, has revealed that polymerization rather than depolymerization occurs with laccase, although certain degradative reactions also are observed with syringyl models (Kirk *et al.*, 1968; Kawai *et al.*, 1988a,b; Morohoshi & Haraguchi, 1987; Wariishi *et al.*, 1987; Higuchi, 1989; Leonowicz *et al.*, 1984). The primary effect on lignin by laccase seems to be further polymerization, although some modification of lignin may occur (Ishihara & Miyazaki, 1972; Morohoshi *et al.*, 1987). Furthermore, most laccases cannot oxidize nonphenolic lignin related compounds (Kirk *et al.*, 1968; Wariishi *et al.*, 1987;

Kawai *et al.*, 1988). Normally, lignin contains only 15-20% free phenolic hydroxyl groups in its phenylpropanoid units (Adler, 1977; Sarkanen & Ludnig, 1971; Fengel & Wegener, 1989). Therefore, lignin might be a poor substrate for laccase. However, it should be noted that *T. versicolor* laccase has been shown to oxidize non-phenolic lignin model compounds in the presence of 2,2´-azido-bis(3-ethylbenzthiazoline-6-phosphate) (ABTS) (Bourbonnais & Paice, 1990; Muheim *et al.*, 1992) or syringaldehyde (Kawai *et al.*, 1989). The laccase-ABTS system is also able to delignify hardwood Kraft pulp (Bourbonnais & Paice, 1992).

Other roles for laccase have been suggested. One possible function of laccase may be detoxification of low-molecular-mass phenols released during lignin degradation (Bollag *et al.*, 1988). Additionally, laccase may produce specific chemical transformations required for degradation by other enzymes (Trojanowski & Leonowicz, 1969). Finally, laccase indirectly oxidizes Mn(II) in the presence of phenolic substrates (Archibald & Roy, 1992). These results suggest a more complicated role for laccase in lignin degradation.

1.2.2 Lignin and Manganese Peroxidases

Although most basidiomycetous white-rot fungi secrete laccase, *P. chrysosporium* produces no detectable laccase activity under commonly used ligninolytic culture conditions. Studies on activated oxygen species generated by *P. chrysosporium* led to the discovery of extracellular hydrogen peroxide in the culture medium (Forney *et al.*, 1982; Kustuki & Gold, 1982; Faison & Kirk, 1983). H_2O_2 was detected in the medium when *P. chrysosporium* degraded lignin, suggesting the presence of H_2O_2 requiring enzyme(s) in ligninolytic culture medium of *P. chrysosporium*.

In 1983, Gold's and Kirk's groups simultaneously announced the discovery in *P. chrysosporium* of an extracellular H_2O_2-requiring enzyme involved in lignin degradation (Gold *et al.*, 1983; Kirk & Tien, 1983; Glenn *et al.*, 1983; Tien & Kirk, 1983). The enzyme was named lignin peroxidase (LiP, EC 1.11.1.14). Subsequently, a second enzyme involved in lignin degradation, manganese peroxidase (MnP, EC 1.11.1.13), was isolated in Gold's laboratory (Kuwahara *et al.*, 1984). Both enzymes exist as a series of isozymes, which are encoded by multiple related genes (Leisola *et al.*, 1987; Farrell *et al.*, 1989; Glumoff *et al.*, 1990; Gold & Alic, 1993; Stewart *et al.*, 1992). MnP is found in all white-rot fungi known to degrade lignin (Hatakka, 1994; Périé & Gold, 1991; Orth *et al.*, 1993). The major isozymes of LiP and MnP have been isolated and purified to homogeneity from the extracellular culture medium of *P. chrysosporium* and have been characterized as heme containing enzymes (Kuwahara *et al.*, 1984; Gold *et al.*, 1984;

Tien & Kirk, 1984; Renganathan *et al.*, 1985; Kirk *et al.*, 1986; Leisola *et al.*, 1987; Glenn & Gold, 1985; Paszczynski *et al.*, 1986).

Both LiP and MnP are able to oxidize lignin, lignin derivatives, and a variety of lignin model compounds (Hammel *et al.*, 1985; Kirk & Farrell, 1987; Gold *et al.*, 1989; Wariishi *et al.*, 1989b; Higuchi, 1990; Schoemaker, 1990; Hammel & Moen, 1991; Wariishi *et al.*, 1991b). The main difference between LiP and MnP is in the nature of the substrates. LiP oxidizes non-phenolic aromatics generating aryl π-cation radicals (Buswell & Odier, 1987; Kirk & Farrell, 1987; Gold *et al.*, 1989; Enoki *et al.*, 1981; Enoki & Gold, 1982; Schoemaker, 1990; Tien, 1987). In contrast, the primary reducing substrate for MnP is a Mn(II) ion rather than a phenol, producing highly reactive Mn(III) which, chelated with organic acids, oxidizes various phenolic compounds (Glenn & Gold, 1985; Glenn *et al.*, 1986; Wariishi *et al.*, 1992; Kuan *et al.*, 1993; Kuan & Tien, 1993; Tuor *et al.*, 1992; Wariishi *et al.*, 1991b), as well as possible mediator molecules (Bao *et al.*, 1994; Wariishi *et al.*, 1989b). The general properties of heme peroxidases and the catalytic cycle and structure of MnP are discussed in detail in Sections 1.3 and 1.4.

1.2.3 H₂O₂-Generating Enzymes

White-rot fungi produce a variety of intracellular and extracellular H_2O_2-generating enzymes which can provide H_2O_2 for peroxidase activity. The enzymes most studied are the intracellular glucose-1-oxidase (β-D-glucose:oxygen 1-oxidoreductase, EC 1.1.3.4) (Kelly & Reddy, 1986), pyranose-2-oxidase (pyranose:oxygen 2-oxidoreductase, EC 1.1.3.10) (Eriksson *et al.*, 1986), and methanol oxidase (alcohol oxidase, EC 1.1.3.13) (Nishida & Eriksson, 1987), and the extracellular glyoxal oxidase (EC 1.2.3.5) (Kersten & Kirk, 1987) and aryl-alcohol oxidase (EC 1.1.3.7) (Waldner *et al.*, 1988; Muheim *et al.*, 1990; Bourbonnais & Paice, 1988). The intracellular enzymes, glucose-1-oxidase, pyranose-2-oxidase, and methanol oxidase possess FAD as a prosthetic group. The preferred substrate for glucose-1-oxidase is glucose, whereas pyranose-2-oxidase oxidizes glucose and xylose (Eriksson *et al.*, 1990; Daniel *et al.*, 1990, 1992; Evans *et al.*, 1991). Methanol oxidase reacts with primary alcohols and unsaturated alcohols (Nishida & Eriksson, 1987).

The extracellular enzyme, aryl-alcohol oxidase, also contains FAD (Muheim *et al.*, 1990; Guillen *et al.*, 1992). This glycoprotein was first found in cultures of *Trametes* (*Coriolus, Polyporus, Polystictus*) *versicolor* (Farmer *et al.*, 1960) and was purified from *Bjerkandera adusta* (Waldner *et al.*, 1988; Muheim *et al.*, 1990). The enzyme oxidizes

various non-phenolic aromatic alcohols to the corresponding aldehydes via a two-electron oxidation with concomitant reduction of O_2 to H_2O_2 (Guillen *et al.*, 1992; Bourbonnais & Paice, 1988). Another extracellular enzyme, glyoxal oxidase, has been purified from ligninolytic cultures of *P. chrysosporium* (Kersten & Kirk, 1987). Spectroscopic and biochemical studies have demonstrated that this enzyme has a free radical-coupled copper complex in the catalytic site which is similar to that found in galactose oxidase (Whittaker *et al.*, 1996; Whittaker & Whittaker, 1988). The enzyme oxidizes glyoxal, methyl glyoxal, and several other α-hydroxy carbonyl and dicarbonyl compounds coupled to the reduction of O_2 to H_2O_2. Both glyoxal and methyl glyoxal have been identified in the extracellular culture medium under ligninolytic conditions (Kersten & Kirk, 1987).

1.2.4   Reductases

Various quinone intermediates are generated during lignin biodegradation. White-rot fungi are able to reduce the various quinones to the corresponding phenols by intracellular and extracellular enzymes. An intracellular quinone-reducing enzyme, NAD(P)H: quinone oxidoreductase (EC 1.6.99.2) has been characterized (Buswell *et al.*, 1979; Buswell & Eriksson, 1988; Constam *et al.*, 1991; Brock *et al.*, 1995; Brock & Gold, 1996; Schoemaker *et al.*, 1989). This enzyme contains FMN as a cofactor and has broad substrate specificity (Brock & Gold, 1996). Quinone reductase is expressed under both primary and secondary metabolic conditions, suggesting that the enzyme is regulated independently of LiP and MnP (Brock *et al.*, 1995). In addition to quinone reductases, an intracellular aryl aldehyde reductase has been characterized (Muheim *et al.*, 1991). This enzyme reduces veratraldehyde to veratryl alcohol which is a substrate for LiP. Veratryl alcohol is produced by several white-rot fungi including *P. chrysosporium* (Lundquist & Kirk, 1978) and *T. versicolor* (Kawai *et al.*, 1986).

Among the extracellular quinone reducing enzymes, cellobiose:quinone oxidoreductase (CBQ, EC1.1.5.1) and cellobiose dehydrogenase (CDH, EC 1.1.99.18) have been purified and extensively characterized from several white-rot fungi. CBQ was first discovered in cultures of *T. versicolor* and *P. chrysosporium* (Westermark & Eriksson, 1974a,b). CBQ is produced by many other white-rot fungi (Ander & Eriksson, 1977; Eriksson *et al.*, 1990) and also by a brown-rot fungus (Schmidhalter & Canevascini, 1992). This is FAD-containing glycoprotein and catalyzes the oxidation of cellobiose to cellobiono-δ-lactone with simultaneous reduction of *ortho-*

and *para*-quinones. CDH, formerly named cellobiose oxidase, has been purified from *P. chrysosporium* (Ayers *et al.*, 1978). CDH has two distinct domains: a heme *b*-containing domain and an FAD-containing domain (Ayers *et al.*, 1978; Bao *et al.*, 1993). CDH catalyzes the oxidation of cellobiose using a variety of electron acceptors such as cytochrome *c* and dichlorophenol-indophenol and benzoquinones (Samejima *et al.*, 1992; Samejima & Eriksson, 1992; Bao *et al.*, 1993) . However, unlike CBQ, CDH is able to reduce cytochrome *c*, which is dependent on the heme domain of CDH (Samejima *et al.*, 1992; Samejima & Eriksson, 1992; Ander, 1994). Recently, it has been proposed that CBQ is a proteolytically cleaved product of CDH (Kremer & Wood, 1992a,b,c; Henriksson *et al.*, 1991; Eriksson *et al.*, 1993). One important function of CBQ and CDH is the reduction of phenoxy or cation radicals generated by peroxidases, thus preventing repolymerization of lignin (Ander *et al.*, 1990; Samejima & Eriksson, 1992; Ander *et al.*, 1993; Eriksson *et al.*, 1993; Ander, 1994). Another proposed role of CDH is the generation of hydroxyl radicals through a Fenton's reaction in the presence of H_2O_2 (Ander, 1994; Kremer & Wood, 1992a,b,c). However, since these enzymes are not produced in cultures of *P. chrysosporium* under nitrogen-limited ligninolytic conditions, further studies are required to elucidate the role of CBQ and CDH in lignin biodegradation by white-rot fungi.

1.3 HEME PEROXIDASES

1.3.1 Occurrence and Function of Peroxidases

Peroxidases are found in most organisms from bacteria to animals. One of the most extensively studied peroxidases has been purified from horseradish roots (horseradish peroxidase; HRP, EC 1.11.1.7). Other well known plant peroxidases are turnip peroxidase (Mazza, 1968), Japanese radish peroxidase (Dunford & Stillman, 1976), peanut peroxidase (Buffard *et al.*, 1990; Rodríguez-Maranón *et al.*, 1994; Schuller *et al.*, 1996), and ascorbate peroxidase (Patterson & Poulos, 1995). All of these peroxidases contain a ferric protoporphyrin IX (Figure 1.4). Plant peroxidases are thought to participate in a variety of pathways, including synthesis of the cell wall components, lignin and suberin, metabolism of hormones such as indole-3-acetic acid (IAA), stress response, and fatty acid metabolism (Grisebach, 1981; Higuchi, 1989; Yang, 1967).

In addition to the plant peroxidases, bacteria and other microorganisms also produce peroxidases. One of the best characterized peroxidases, cytochrome *c* peroxidase (CCP), is obtained from the intermembrane space of the mitochondria of baker's and
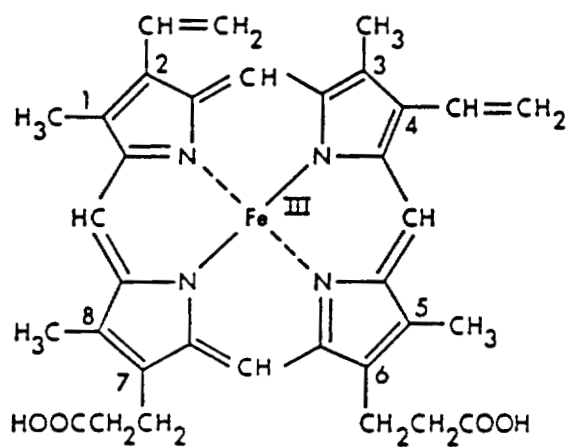
Figure 1.4. Ferric protoporphyrin IX (ferric heme).

brewer's yeasts (Maccecchini *et al.*, 1979; Williams & Stewart, 1976). CCP catalyzes the oxidation of ferrocytochrome *c*. CCP has also been isolated from *Pseudomonas aeruginosa* (Ellfolk & Soininen, 1970, 1971). Although there is evidence suggesting that CCP may support oxidative phosphorylation in the absence of cytochrome *c* oxidase (Erecínska *et al.*, 1973), the role of CCP *in vivo* is still unclear. The fungal chloroperoxidase isolated from the mold *Caldarimyces fumago* (Morris & Hager, 1966) and the marine algal bromoperoxidase from *Penicillus capitatus* (Ahern *et al.*, 1980; Manthey & Hager, 1981) have also been characterized. The chloroperoxidase is able to catalyze the oxidation of chloride ion, although a wide variety of compounds are substrates for chloroperoxidase (Thomas *et al.*, 1970; Kedderis *et al.*, 1980; Shahangian & Hager, 1981). Bromoperoxidase use bromide ion (but not chloride ion) to generate brominated organic compounds which may be involved in an antimicrobial defense system (Manthey & Hager, 1981). Another fungal peroxidase, *Coprinus cinereus* peroxidase (CIP), has been isolated from the ink-cap basidiomycete (Morita *et al.*, 1988). CIP has been demonstrated to be identical to the commercial *Coprinus macrorhizus* peroxidase (CMP) and *Arthromyces ramosus* peroxidase (ARP) in covalent structure and enzymatic properties. Differences among these related peroxidases include the extent of glycosylation and the presence of an additional glycine residue adjacent to residue 4 of ARP (Kjalke *et al.*, 1992; Baunsgaard *et al.*, 1993; Petersen *et al.*, 1994; Kunishima *et al.*, 1994; Limongi *et al.*, 1995). Although CIP shows 40-45% sequence identity to LiPs and MnPs from *P. chrysosporium*, CIP is unable to degrade lignin. CIP resembles HRP in terms of enzymatic specificity (Petersen *et al.*, 1994; Kunishima *et al.*, 1994).

LiP and MnP each contain an iron-protoporphyrin IX prosthetic group (Kuwahara *et al.*, 1984; Gold *et al.*, 1984; Tien & Kirk, 1984; Renganathan *et al.*, 1985; Kirk *et al.*, 1986; Leisola *et al.*, 1987; Glenn & Gold, 1985; Paszczynski *et al.*, 1986), sharing this structural feature with other plant and fungal peroxidases. Among these peroxidases, HRP and CCP have been the most extensively characterized. Therefore, HRP and CCP have served as excellent models for the characterization of LiP and MnP.

Peroxidases have also been isolated and characterized from mammalian sources but these enzymes are beyond the scope of this review.

1.3.2 Catalytic Mechanism of Peroxidase

Peroxidases form distinct and relatively long-lived reaction intermediates facilitating kinetic and biophysical studies. Plant and fungal peroxidases contain a ferriprotoporphyrin IX prosthetic group (Figure 1.4). The oxidation state of the heme iron in the resting state

of the enzyme has been demonstrated to be Fe(III) by Mössbauer, electron paramagnetic resonance (EPR) and resonance Raman spectroscopic studies (Dunford & Stillman, 1976).

Plant and fungal peroxidases have common features in their reaction mechanisms. The peroxidase reaction can be generalized as follows:

Native enzyme + $H_2O_2 \rightarrow$ Compound I + H_2O

Compound I + substrate $\rightarrow$ Compound II + oxidized substrate

Compound II + substrate $\rightarrow$ Native enzyme + H_2O + oxidized substrate
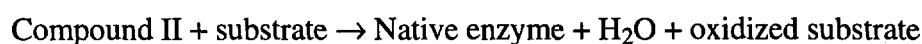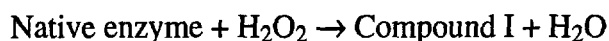
This peroxidase reaction is described as a modified bi-bi ping-pong mechanism (Dunford, 1982):

$$\begin{array}{cccccc} H_2O_2 & H_2O & AH_2 & \cdot AH & AH_2 & \cdot AH + H_2O \\ \downarrow & \uparrow & \downarrow & \uparrow & \downarrow & \uparrow \end{array}$$

Native   Compound I   Compound II   Native
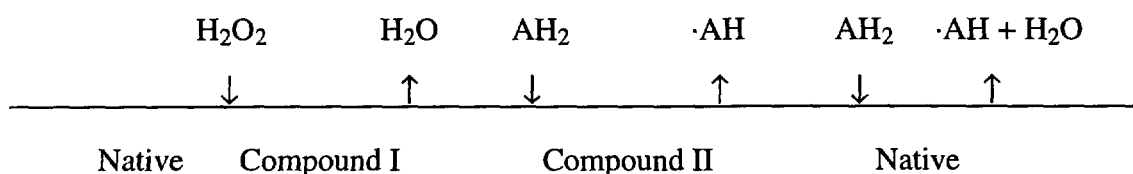
The first step in the catalytic cycle is the 2-electron oxidation of the enzyme by peroxide to generate compound I. In the second step, one molecule of substrate reduces compound I by one electron to a second intermediate, compound II. Finally, one-electron reduction of compound II regenerates the native enzyme.

A variety of chemical studies have demonstrated that peroxidase compound I contains two oxidizing equivalents over the native state of the enzyme. Thus, compound I is an Fe(V) form of the enzyme. Compound I is reduced to compound II by one electron derived from a substrate. Therefore, compound II is a formal Fe(IV) form of the enzyme. All known heme peroxidases have a common compound II structure in which the single oxidizing equivalent is stored as a ferryl (Fe(IV)=O) species, established by Mössbauer (Maeda, 1967; Moss et al., 1969; Schultz et al., 1984), NMR (LaMar et al., 1983), X-ray absorption (Penner-Hahn et al., 1983, 1986; Chance et al., 1984), electron nuclear double resonance (ENDOR) (Roberts et al., 1981), and resonance Raman (Terner et al., 1985; Sitter et al., 1985; Hashimoto et al., 1986a,b,c) spectroscopic techniques.

The same ferryl species is known to be present in compound I (Schultz et al., 1984; Penner-Hahn et al., 1986; Chance et al., 1984; Edwards et al., 1987). Therefore, compound I species must store an additional oxidizing equivalent somewhere other than at the iron center. There are two possible sites for the location of the second oxidizing equivalent. The second oxidizing equivalent in compound I of HRP and most other plant and fungal peroxidases occurs as a porphyrin π-cation radical (Dolphin et al., 1971; DiNello & Dolphin, 1981). Therefore, the HRP compound I structure can be described as

$(Fe(IV)=O, P^{\cdot+})$. The direct evidence for the π-cation radical in HRP compound I obtained by proton and ^{14}N ENDOR studies (Roberts *et al.*, 1981), and NMR (La Mar *et al.*, 1981), and resonance Raman (Felton *et al.*, 1976) studies strongly supports this interpretation.

In contrast, compound I of CCP was recognized quite early on as being different from that of other peroxidases, since its absorption spectrum resembles that of HRP compound II, although both intermediates contain three unpaired electrons. Therefore, CCP compound I has often been called "compound ES" to emphasize this difference (Yonetani & Schleyer, 1966). CCP compound I shows a narrow free-radical-like EPR signal at 77K (Yonetani, 1976; Yonetani & Schleyer, 1966), suggesting that the second oxidizing equivalent is removed from the heme center and exists as a free radical on an amino acid residue. Recent studies, including ENDOR (Sivaraja *et al.*, 1989, Huyett *et al.*, 1995), EPR (Hori & Yonetani, 1985), and site-directed mutagenesis (Fishel *et al.*, 1987; Goodin *et al.*, 1987; Mauro *et al.*, 1988), strongly suggest that the unpaired electron is stored at a Trp191 located on the proximal side of the heme (Chapter 1.3.4). Radical formation on Trp191 also is known to be essential for electron transfer between CCP and its substrate, cytochrome *c* (Mauro *et al.*, 1988). Some of the structural features which promote the formation of a protein radical in CCP have been proposed (Poulos & Fenna, 1994; Bonagura *et al.*, 1996; Houseman *et al.*, 1993; Goodin & McRee, 1993; Fitzgerald *et al.*, 1994), but the factors that stablize a porphyrin π-cation radical in other peroxidases with respect to oxidation of amino acid residues remain unclear.

Figure 1.5 shows the electronic absorption spectra of native HRP, and HRP compounds I and II (Dunford & Stillman, 1976). The Soret peak at ~400 nm is characteristic for heme proteins. The electronic spectrum of native HRP is typical of the high-spin Fe(III), exhibiting a Soret band at 406 nm and Q-bands near 500 and 640 nm. The reduced intensity of the Soret band of HRP compound I is due to its π-cation radical nature (Dolphin *et al.*, 1971), and the peak at 650 nm is due to an A_{2u} type ground state (Dolphin *et al.*, 1971; DiNello & Dolphin, 1981). HRP compound II exhibits a Soret band at 420 nm, and β and α bands at 525 and 555 nm, respectively, suggesting a low-spin iron (Dunford & Stillman, 1976). The distinct electronic absorption spectra of these oxidized intermediates of peroxidases are particularly useful for studying the kinetics of the formation or reactions of these intermediates since the absorption changes in the Soret band region are sufficiently large at low (≤ 1 μM) enzyme concentrations.

The second-order rate constant for the reaction between H_2O_2 and peroxidase is ~10^7 M^{-1} s^{-1} (Hewson & Dunford, 1975; Yonetani & Ray, 1966;
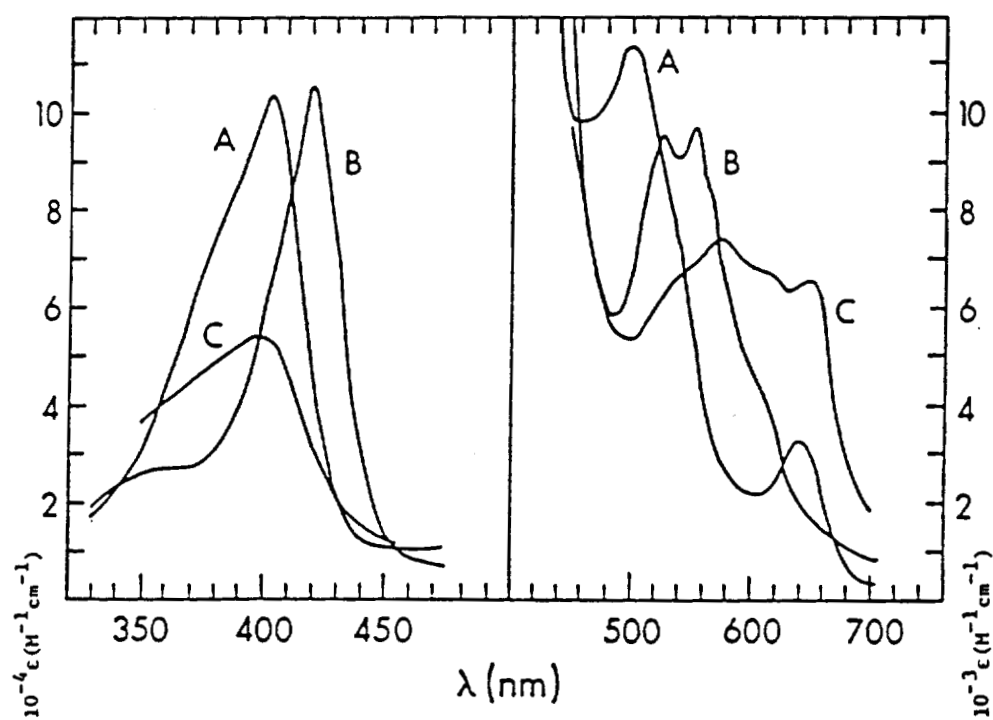
Figure 1.5. Electronic absorption spectra of native HRP, HRP compound I, and HRP compound II. A, native HRP; B, HRP compound II; C, HRP compound I (Dunford & Stillman, 1976).

Dunford & Stillman, 1976) which is significantly higher than that for the reaction between heme and peroxide at physiological pH (10^3 M^{-1} s^{-1}) (Kelly *et al.*, 1977). In order to account for this remarkable rate enhancement, the enzyme should have a high affinity for H_2O_2, a stabilized activated transition-state complex, and the ability to stabilize the energetically unfavorable charge separation generated by the heterolytic cleavage of the O-O bond of H_2O_2. The critical amino acid residues for these functions in peroxidases are the distal His and Arg, and the proximal His. The proposed mechanism of compound I formation involves the following stages: (1) binding of H_2O_2 to the active site facilitated by the distal His and Arg; (2) proton transfer from H_2O_2 to the distal His, ligation of an oxygen atom into the iron coordination sphere, and hydrogen bonding of the His to another oxygen atom of peroxyanion; (3) heterolytic cleavage of the O-O bond to develop a negative charge on the leaving oxygen which is stablized by the positive charge on the distal Arg residue, resulting in the release of H_2O (Dawson, 1988; Poulos & Kraut, 1980b; Poulos & Fenna, 1994). Thus, the distal His acts as an acid-base catalyst. The proximal His is believed to stablize the oxidized intermediates by coordinating to the Fe(IV)=O center (Poulos & Fenna, 1994). The function of catalytic amino acid residues has been elucidated by a variety of studies, particularly site-directed mutagenesis (Chapter 1.3.4).

The reduction of peroxidase compound I to the ferric native enzyme by a reducing substrate normally occurs via compound II formation. In most cases, the reaction of peroxidase compound II with various reducing substrates is the rate-limiting step in the peroxidase catalytic cycle and is 10-100 times slower than that of compound I reduction (Cormier & Prichard, 1968; Hewson & Dunford, 1976; Critchlow & Dunford, 1972a,b; Dunford & Cotton, 1975). One possible explanation for this may be that compound I has a higher redox potential than compound II. However, the redox potentials determined for compounds I and II of a few peroxidases, E_0 (compound I/compound II) and E_0' (compound II/native enzyme), are essentially the same (Hayashi & Yamazaki, 1979; Farhangrazi *et al.*, 1994). Therefore, the redox potential does not explain the higher reactivity of compound I compared with compound II. Since the reactions of compounds I and II are electron transfer reactions, it is useful to refer to an electron transfer theory (Marcus & Sutin, 1985; McLendon *et al.*, 1985; DeVault, 1980). The activation energy of an electron transfer reaction, ΔG^*, is determined by the driving force of the reaction, $\Delta G°$, and the reorganization energy, λ, according to the following equation:

$$\Delta G^* = (\Delta G° - \lambda)^2/4\lambda$$

The rate of the reaction is proportional to $\exp(-\Delta G^*/\lambda)$. The reorganization energy represents the energy required to reorganize protein (ligand)-metal bond distances and geometry prior to electron transfer. In addition, this electron transfer process is affected by the medium through which the electron passes and by the distance between redox centers. The ferryl oxygen atom and most of the heme of HRP compound I are believed to be inaccessible to reducing substrates based primarily on suicide inhibition studies with substituted hydrazines (Ator & Ortiz de Montellano, 1987; Ator et al., 1987; Ortiz de Montellano et al., 1987, 1988; Ortiz de Montellano, 1987). The higher reactivity of compound I may result from exposure of the porphyrin π-cation radical at a peripheral site, thus minimizing the distance to the reducing substrate (Ortiz de Montellano, 1987). Reorganization energy may also contribute to the different reactivities of compounds I and II. The reduction of compound II may require higher reorganization energy, since the reduction of compound II includes the release of an H_2O molecule and the low- to high-spin transition of the iron center, whereas essentially no change of heme geometry is involved in the reduction of compound I. Further investigations on the reactions of compounds I and II are continuing.

The reduction of CCP compound I appears to be more complex and the detailed mechanism remains unclear. In CCP, the oxidizing equivalents of peroxide are stored at two sites: one site is the iron, which is converted from the ferric to ferryl (Fe(IV)=O) state, and the other is Trp191, which produces a stable indolyl cation radical (Sivaraja et al., 1989; Huyett et al., 1995; Hori & Yonetani, 1985; Fishel et al., 1987; Goodin, 1987; Mauro et al., 1988; Poulos & Fenna, 1994; Bonagura et al., 1996). The main questions about CCP compound I reduction are: (1) Which of the two sites is reduced first? (2) Can the two sites be reduced independently or only in ordered fashion? It has been proposed that the mechanism is ordered: the Trp191 radical is reduced initially, followed by reduction of the oxy-ferryl heme as shown in Scheme 1.1 (Geren et al., 1991; Hahm et al., 1992, 1993, 1994):

Scheme 1.1

$$\text{Fe(IV)=O, Trp}^{\cdot+} + \text{Cytochrome } c \text{ (II)} \rightarrow \text{Fe(IV)=O, Trp} + \text{Cytochrome } c \text{ (III)} \quad (1)$$

$$\text{Fe(IV)=O, Trp} + 2\text{H}^+ \rightleftharpoons \text{Fe(III), Trp}^{\cdot+} + \text{H}_2\text{O} \quad (2)$$

$$\text{Fe(III), Trp}^{\cdot+} + \text{Cytochrome } c \text{ (II)} \rightleftharpoons [\text{Fe(III), Trp}^{\cdot+} - \text{Cytochrome } c \text{ (II)}] \quad (3)$$

$$[\text{Fe(III), Trp}^{\cdot+} - \text{Cytochrome } c \text{ (II)}] \rightarrow [\text{Fe(III), Trp} - \text{Cytochrome } c(\text{III})] \quad (4)$$
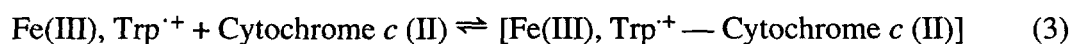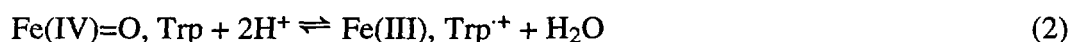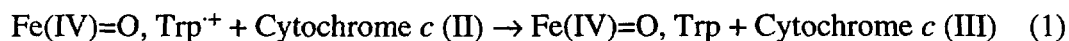
In equation 1, cytochrome c (II) reduces the Trp191 radical. Equilibrium between the

oxy-ferryl species and the Trp191 then generates an intermediate with a ferric iron center and a Trp radical (equation 2). The Trp191 radical produced is then reduced by cytochrome c (II), generating the resting ferric enzyme (equations 3 and 4). In contrast, others have argued that the two sites can be reduced independently (Hazzard & Tollin, 1991; Kang et al., 1977). This independent reduction mechanism may be consistent with the evidence that CCP has two binding sites for cytochrome c (Wang & Margoliash, 1995; Zhou et al., 1995; Mauk et al., 1994) and with the result obtained using CCP and cytochrome c substituted with a Zn-heme (Stemp & Hoffman, 1993; Zhou & Hoffman, 1994). Site-directed mutagenesis studies have also been carried out to elucidate the role of the Trp191 in the electron transfer between CCP and cytochrome c (Chapter 1.3.4).

1.3.3 Recombinant Peroxidase Expression Systems

Although a variety of studies have been carried out to elucidate the catalytic mechanism of the peroxidases, the roles of particular amino acid residues in peroxidase reactions has remained obscure. This is particularly true for HRP, for which no high resolution crystal structure is available. Along with crystallographic and spectroscopic studies, site-directed mutagenesis is a powerful tool for understanding the roles and functions of potentially important amino acid residues. To conduct site-directed mutagenesis, an efficient expression system is required to produce quantities of variant proteins sufficient for further characterization. To date, several heterologous expression systems have been established for plant and fungal peroxidases, including CCP, HRP, LiP, MnP, CIP, and ascorbate peroxidase.

1.3.3.1 Prokaryotic expression systems

To date, CCP has served as the best enzyme for site-directed mutagenesis studies. One of the reasons for this is the relative ease of producing active recombinant CCP in E. coli. CCP is produced in E. coli essentially as the apoprotein (Fishel et al., 1987). However, the CCP holoprotein is readily reconstituted (Yonetani, 1967; Fishel et al., 1987). Crystallization can be used to purify the recombinant CCP and the final yield of the recombinant CCP protein is normally 20-80 mg per liter of cell culture (Fishel et al., 1987; Choudhury et al., 1994; Studier et al., 1990; Goodin et al., 1991; Ferrer et al., 1994). The crystal structures and spectral properties of the recombinant and wild-type yeast CCPs are indistinguishable (Wang et al., 1990; Sundaramoorthy et al., 1991), suggesting that the expression of the recombinant CCP in E. coli and reconstitution of the holoenzyme is an excellent system for conducting site-directed mutagenesis studies.

In contrast, the expression and production of other peroxidases in *E. coli* have presented serious problems. Many plant and fungal peroxidases have disulfide bonds and are normally glycosylated (Welinder, 1985, 1992; Gold & Alic, 1993; Limongi *et al.*, 1995). The expression of these peroxidases in bacteria may be complicated since disulfide bonds are difficult to form in the reducing bacterial environment. Furthermore, bacteria do not glycosylate proteins. Moreover, the expressed proteins frequently appear as insoluble inclusion bodies in *E. coli* from which it is difficult to recover active enzymes in significant yields (Marston, 1986). Thus, multiple steps including solubilization, folding of the protein, and heme insertion into the apoprotein are required to obtain active enzyme. Smith et al. (1990) have successfully produced active recombinant HRP isozyme C in *E. coli*, by denaturing the recombinant protein with urea and then refolding the protein in the presence of Ca(II), heme, and oxidized glutathione. Results have demonstrated that the presence of Ca(II) is essential for folding recombinant HRP C (Smith *et al.*, 1990). Ca(II) ions are known to have important structural roles in many proteins (Bajorath *et al.*, 1989), including HRP (Haschke & Friedhoff, 1978; Ogawa *et al.*, 1979; Shiro *et al.*, 1986; Morishima *et al.*, 1986). Currently, this system is being used to conduct site-directed mutagenesis studies of HRP. The yield of active recombinant HRP C isolated from *E. coli* is, however, only 3-4% in terms of conversion of inactive protein to active enzyme (Smith *et al.*, 1990).

Similar attempts have been made to express ascorbate peroxidase (Patterson & Poulos, 1994; Ishikawa *et al.*, 1995; Dalton *et al.*, 1996), LiP (Doyle & Smith, 1996), and MnP (Whitwarm *et al.*, 1995) in *E. coli*. Patterson and Poulos (1994) have developed an *E. coli* system for expression of recombinant ascorbate peroxidase in which the protein expressed is fully active although the yield of the recombinant enzyme is relatively low (~3 mg of enzyme per liter of cell culture). Recently, the yield of the recombinant ascorbate peroxidase has been increased (16 mg of pure holoenzyme per liter of cell culture) by reconstitution of apoprotein with heme (Dalton *et al.*, 1996). The reconstitution of the recombinant ascorbate peroxidase appears to be as straightforward as that of CCP. Addition of glutamate or δ-aminolevulinic acid (a precursor of heme synthesis) to the culture medium also increases the yield of holoenzyme (Dalton *et al.*, 1996).

The production of active recombinant LiP or MnP using *E. coli* has not been successful. The reconstitution of LiP and MnP expressed in *E. coli* using similar methods to those described for HRP (Smith *et al.*, 1990) yields only a small amount of active enzyme (< 1% of total protein). At present, this system is insufficient for structural and

functional studies of recombinant LiP and MnP (Doyle & Smith, 1996; Whitwarm *et al.*, 1995).

1.3.3.2   Eukaryotic expression systems

Eukaryotic expression systems, unlike prokaryotic systems, can produce fully active enzymes which do not require reconstitution with heme. Many eukaryotic proteins have been successfully produced in insect tissue culture using a baculovirus transfer vector (Smith *et al.*, 1983; Miller, 1988). Active mammalian cytochrome P450 (Asseffa *et al.*, 1989), as well as glycosylated proteins from a variety of mammalian viruses, have been expressed in this system (Miller, 1988; Van Wyke Coelingh *et al.*, 1987). HRP has been successfully expressed in the baculovirus systems (Hartmann & Ortiz de Montellano, 1992). The recombinant HRP is fully active and contains heme, although the addition of heme to the cell culture significantly increases activity. Moreover, spectroscopic and kinetic properties of the recombinant HRP are essentially identical to those of the wild-type enzyme (Hartmann & Ortiz de Montellano, 1992).

A cDNA clone encoding LiP isozyme H8 has been used to express protein which is glycosylated, contains heme, and is capable of oxidizing iodide and veratryl alcohol (Johnson & Li, 1991). However, the recombinant LiP is only about 50% active toward veratryl alcohol compared with wild-type LiP. Likewise, a cDNA encoding MnP isozyme H4 has been expressed and extracellularly produces a MnP antibody-reactive and heme-containing protein which has a molecular weight similar to that of wild-type MnP (Pease *et al.*, 1991). The enzyme is active and dependent on both Mn(II) and H_2O_2 for activity. However, the yields of LiP and MnP in this system are very low (< 1 mg of protein per 1 liter of cell culture after purification) (Johnson & Li, 1991; Pease *et al.*, 1991). In addition, the baculovirus system is relatively expensive and thus may not be suitable for large-scale enzyme production. Finally, these recombinant enzymes often are produced in multiple forms which complicates the purification process (Hartmann & Ortiz de Montellano, 1992; Johnson & Li, 1991). Therefore, it may be difficult to produce site-directed mutants of these peroxidases with the baculovirus expression system in quantities sufficient for detailed analysis. In fact, no site-directed mutagenesis study of LiP or MnP using the baculovirus system has been reported.

Another fungal peroxidase, CIP has been successfully expressed in the filamentous fungus *Aspergillus oryzae* (Dalbøge *et al.*, 1992; Tams *et al.*, 1993; Petersen *et al.*, 1993, 1994). Recombinant CIP expressed in the *Aspergillus* system is identical to fungal CIP in all respects, including sites of glycosylation and N-terminal proccessing (Baunsgaard *et al.*,

1993; Kjalke *et al.*, 1992; Tam *et al.*, 1993; Petersen *et al.*, 1994). The recombinant CIP can be obtained with high purity and thus, has been extensively characterized using a variety of techniques including X-ray crystallography (Petersen *et al.*, 1993, 1994) and resonance Raman (Smulevich *et al.*, 1994a) and NMR (Veitch *et al.*, 1994) spectroscopies. In addition, site-directed mutagenesis of CIP has been performed using the *Aspergillus* expression system (Veitch *et al.*, 1994; Smulevich *et al.*, 1996) (Chapter 1.3.4). Recombinant MnP has also been expressed in the *Aspergillus* system (Stewart *et al.*, 1996). However, the addition of heme to the culture medium is required to obtain active recombinant MnP and the yields of protein are low. Moreover, the rates of recombinant MnP compound I and II reduction with Mn(II) are only 35 and 65%, respectively, of those of wild-type MnP (Stewart *et al.*, 1996).

1.3.4 Site-Directed Mutagenesis of Peroxidases

A high resolution crystal structure is not yet available for HRP but such structures are available for CCP (Poulos *et al.*, 1980; Finzel *et al.*, 1984), LiP (Edwards *et al.*, 1993; Poulos *et al.*, 1993; Piontek *et al.*, 1993), MnP (Sundaramoorthy *et al.*, 1994b), CIP (Kunishima *et al.*, 1994; Petersen *et al.*, 1994), ascorbate peroxidase (Patterson & Poulos, 1995), peanut peroxidase (Schuller *et al.*, 1996), and chloroperoxidase (Sundaramoorthy *et al.*, 1995). Alignment of the highly conserved sequences suggests that these peroxidases share similar structural elements (Welinder, 1992; Welinder *et al.*, 1995). Additionally, spectroscopic studies suggest that the heme environment is very similar in these peroxidases (Dunford, 1991). However, crystal structures alone cannot answer questions about detailed mechanisms such as the role of amino acid residues, the electron transfer pathways, and the locations of possible free radical sites on the protein. A combination of structural and kinetic studies is required to understand the mechanisms of peroxidases. In addition, site-directed mutagenesis of the key amino acids has revealed various important functions for these residues. Most of the site-directed mutagenesis studies of peroxidases have involved HRP, CCP, and CIP (Table 1.1).

1.3.4.1 Free radical site in compound I

The first step in the peroxidase catalytic cycle is the 2-electron oxidation of the enzyme by peroxide to generate compound I. It has been established for all known heme peroxidases that the single oxidizing equivalent is stored as a ferryl (Fe(IV)=O) species. An unique protein-centered radical is proposed to exist in CCP compound I

Table 1.1. Site-Directed Mutagenesis of Cytochrome c Peroxidase (CCP), Horseradish Peroxidase (HRP), and *Coprinus cinereus* Peroxidase (CIP).

Enzyme	Mutation	Description
CCP	*Distal Site*	
	His52 - Leu	The rate of compound I formation decreased by 5 orders of magnitude (Smulevich *et al.*, 1991; Erman *et al.*, 1993).
	Arg48 - Leu - Lys	The H-bond between Asp235 and His175 was lost. Saturation kinetics was observed for compound I formation. The rate of compound I decreased by 2 and 10 orders of magnitude for R48K and R48L, respectively. The rate of CO dissociation for R48K and R48L increased 5- and 20-fold, respectively (Miller *et al.*, 1990a,b; Vitello *et al.*, 1993).
	Asn82 - Ala - Asp	H-bond between His52 and CN^- was disrupted (Alam *et al.*, 1995). The binding affinity of CN^- and F^- for Fe(III) decreased by one or two orders of magnitude (DeLauder *et al.*, 1994; Satterlee *et al.*, 1994).

	Trp51 - Ala
	     - Phe
	     - Met
	     - Thr
	     - Cys
	     - Gly
		Monooxygenation reaction was observed (W51A). The oxidation of substituted anilines was enhanced. H-bond between Asp245 and His175 was lost (W51F). Cytochrome c oxidation was enhanced for W51F, W51M, and W51T. The rate of cytochrome c oxidation decreased for W51C, W51A, and W51G (Goodin *et al.*, 1991; Miller *et al.*, 1992; Roe & Goodin, 1993; Turano *et al.*, 1995).

	Proximal Site	

	His175 - Glu
	      - Gln
	      - Cys
	      - Gly
		H175E and H175Q retained activity (Choudhury *et al.*, 1992, 1994; Smulevich *et al.*, 1995) H175G formed bis-aquo heme. The addition of imidazole restored some activity (~5%) (McRee *et al.*, 1994).

	Asp235 - Asn
	      - Glu
	      - Ala
		The reactivity for H_2O_2 was ~20% of wild-type enzyme. The strength of His175-Fe(III) bond was weakened. In D235A and D235N, low-spin Fe(III) was observed. H-bond between His175 and Glu235 was weaker. Trp radical was destablized (Smulevich *et al.*, 1988a,b, 1991; Satterlee *et al.*, 1990; Wang *et al.*, 1990a; Fishel *et al.*, 1991; Miller *et al.*, 1992; Vitello *et al.*, 1992; Goodin & McRee, 1993; Ferrer *et al.*, 1994).

	Trp191 - Gly - Phe	The binding of imidazoles restored activity. K^+ ion binding near Asp235 was observed (W191G) (Fitzgerald *et al.*, 1994, 1995; Miller *et al.*, 1994a). The reaction for H_2O_2 was increased (~40%) (F191F). Porphyrin π cation radical formation was observed instead of protein radical. The rate of electron transfer from cytochrome c was 10,000 times lower (Hazzard *et al.*, 1987; Mauro *et al.*, 1988; Erman *et al.*, 1989; Smulevich *et al.*, 1990; Vitello *et al.*, 1990; Fishel *et al.*, 1991; Liu *et al.*, 1994; Miller *et al.*, 1995a). H175Q-W191F double mutant retained 20% of activity (Choudhury *et al.*, 1994).

Table 1.1.   (continued)

Enzyme	Mutation	Description
	Cation Binding Site	
	Gly192 - Thr Ala194 - Asn Thr199 - Asp Glu201 - Ser	Introducing the ascorbate peroxidase cation binding site into CCP destablized the Trp191 radical and significantly lowered the activity (< 1% of wild-type enzyme) (Bonagura *et al.*, 1996).
	Solvent Access Channel	
	Ala147 - Met - Tyr	The oxidation of small molecules was significantly inhibited (Wilcox *et al.*, 1996).
	Electron Transfer or Cytochrome *c* *Binding Site*	
	Glu32 - Gln Glu35 - Gln Glu290 - Asn - Cys Glu291 - Gln Asp34 - Asn Asp37 - Lys Asp217 - Lys Lys149 - Cys Tyr39 - Phe Tyr42 - Phe Tyr229 - Phe His181 - Gly Trp223 - Phe	Except D34N, E290N, and E290C, these mutants exhibited essentially the same activity for cytochrome *c* oxidation. The rate of cytochrome *c* oxidation for D34N, E290N, and E290C was ~25-50% of the value for the wild-type enzyme (Pappa & Poulos, 1995; Pappa *et al.*, 1996; Miller *et al.*, 1994; Hahm *et al.*, 1994; Corin *et al.*, 1991, 1993; Miller *et al.*, 1988; Edwards *et al.*, 1988).
HRP	*Distal Site* His42 - Ala - Val - Leu - Arg	The rate of compound I formation decreased (H42A and H42V). Compound II was not detectable. Thioanisole sulfoxidation was 10 times faster for H42A than for the wild-type enzyme. Styrene epoxidation was also observed with H42A. By the reaction of phenyldiazene, H42A and H42V each formed a phenyl-iron complex (Newmyer & Ortiz de Montellano, 1995). CO binding to ferrous iron increased for H42R and H42L. CN^- did not bind to either H42R or H42L (Meunier *et al.*, 1995).
	Arg38 - Leu - Lys	The affinity for H_2O_2 decreased ~1000 fold (R38L). The binding of guaiacol, *p*-cresol, and ABTS decreased 2-3 fold (Rodriguez-Lopez *et al.*, 1996). R38K was 2-fold more sensitive to H_2O_2 and exhibited a compound I formation rate of half that of the wild-type protein Fe(III)-His170 bond strength was weakened (Smulevich *et al.*, 1994b; Hiner *et al.*, 1995).

Table 1.1.   (continued)

Enzyme	Mutation	Description
	Asn70 - Val	The rate of compound I formation decreased ~30 fold. The rate of compound II reduction also decreased 60-70 fold. However, compound II was more stable than that of the wild-type enzyme (Nagano *et al.*, 1995).
	Phe41 - Ala - Val - Trp - Leu	Thioanisole sulfoxidation by F41A was 100 times faster than with the wild-type enzyme (Newmyer & Ortiz de Montellano, 1995). The rate of compound I formation decreased 8 fold (F41V). The activity increased ~2- fold with *p*-aminobenzoic acid but decreased 5-10 fold with ABTS. F41W did not bind benzhydroxamic acid (BHA). F41V showed a 2-fold increase in affinity for BHA (Smith *et al.*, 1992a,b; Smulevich *et al.*, 1994b). The rate of thioether sulfoxidation increased 2-4 fold (Ozaki & Ortiz de Montellano, 1994).
	Substrate Binding Site Phe142 - Ala Phe143 - Ala - Glu	F142A exhibited 3-4 times weaker binding for aromatics, but F143A showed essentially the same binding affinity for aromatics (Veitch *et al.*, 1995). F143E inhibited the binding of negatively charged molecules (Gazaryan *et al.*, 1994).
	Protein Radical Phe172 - Tyr	Phenoxy radical formation was detected in compound I (Miller *et al.*, 1995b).
CIP	*Proximal Site* Asp245 - Asn	D245N significantly weakened Fe(III)-His bond strength and the Fe-His bond was broken at alkaline pH (Smulevich *et al.*, 1996).
	Substrate Binding Site Gly156 - Phe Asn157 - Phe	ABTS oxidation increased 2 fold for G157F-N157F double mutant (Veitch *et al.*, 1994).

(Yonetani, 1976), unlike HRP compound I wherein a porphyrin π-cation radical is formed (Dolphin *et al.*, 1971; DiNello & Dolphin, 1981). Early site-directed mutagenesis studies of CCP focused on the identification of the amino acid-centered radical in CCP compound I. In the crystal structure of CCP, Trp51 is found parallel to and near the heme (Poulos *et al.*, 1980). Thus, Trp51 was proposed as the site of the free radical (Finzel *et al.*, 1984; Poulos & Finzel, 1984). However, various spectroscopic studies argued against a tryptophan radical. Using ENDOR spectroscopy, Hoffman et al. (1981) suggested that the free radical should be a sulfur-based radical and could be derived from a methionine instead of a tryptophan. The CCP crystal structure shows that, in fact, a methionine residue, Met172, is located in a proximal site near the heme (Poulos *et al.*, 1980; Finzel *et al.*, 1984). In addition, magnetic circular dichroism (MCD) spectra of CCP compound I does not support the proposed tryptophan radical (Myers & Palmer, 1985). However, Hori and Yonetani (1985) reexamined this issue using single-crystal EPR and showed evidence, once again, for a tryptophan radical.

Site-directed mutations of possible free radical sites in CCP have helped to resolve this question. Neither the Met172Ser nor the Trp51Phe mutant exhibits perturbed EPR signals upon H_2O_2 oxidation (Goodin *et al.*, 1986, 1987; Fishel *et al.*, 1991). In contrast, the Trp191Phe mutant does show a significantly altered EPR signal (Mauro *et al.*, 1988). These results strongly suggest that Trp191 is the site for the free radical and prove that neither Trp51 nor Met172 is the radical site. However, an alteration in a property of a mutated enzyme can be an indirect consequence of replacing an amino acid residue. Hence, although site-directed mutagenesis may be able to eliminate an amino acid residue as an active site, it cannot identify a site absolutely. Moreover, the location of the radical site could not be identified by X-ray crystallography of CCP compound I (Edwards *et al.*, 1987; Fulop *et al.*, 1994). However, the expression system for CCP has facilitated the preparation of CCP which is isotopically enriched in specific atoms within particular amino acid residues. ENDOR spectroscopy of the labeled CCP compound I suggests that the radical species is a Trp residue and, almost certainly, Trp191 (Hoffman, 1991; Hoffman *et al.*, 1993; Sivaraja *et al.*, 1989). Finally, an ENDOR study using enzyme labeled with ^2H at specific positions on Trp, with ^{15}N at N_1 of the indole ring, and with ^{13}C at C_2 of the ring and at C_β of the side chain (Huyett *et al.*, 1995), provides further evidence for the formation of a radical at Trp191.

In contrast to CCP, most other plant and fungal peroxidases possess a Phe, rather than a Trp, in the proximal site of the heme pocket. It has been postulated that porphyrin

π-cation radical formation in compound I of these peroxidases occurs mainly because the Phe residue cannot be oxidized as easily as a Trp residue (Poulos & Fenna, 1994). Recently, the characterization of cytosolic peroxidase, ascorbate peroxidase, has provided additional criteria for the location of the free radical (Patterson & Poulos, 1995; Patterson *et al.*, 1995; Pappa *et al.*, 1996). The crystal structure of ascorbate peroxidase shows that this enzyme has a Trp179 residue in the proximal pocket at the same location as the Trp191 in CCP (Patterson & Poulos, 1995). A recent EPR study has demonstrated that ascorbate peroxidase compound I forms a porphyrin π-cation radical rather than a Trp radical (Patterson *et al.*, 1995). In addition, the replacement of the Trp179 with Phe does not significantly affect ascorbate peroxidase activity, suggesting that the Trp179 is not essential (Pappa *et al.*, 1996). The refined crystal structure of ascorbate peroxidase shows that the enzyme has a cation located about 8 Å from the proximal Trp179 residue (Patterson & Poulos, 1995). This cation binding site in ascorbate peroxidase is homologous to the proximal Ca(II) binding site in other plant and fungal peroxidases (Edwards *et al.*, 1993; Poulos *et al.*, 1993; Piontek *et al.*, 1993; Schuller *et al.*, 1996; Kunishima *et al.*, 1994; Peterson *et al.*, 1994; Sundaramoorthy *et al.*, 1994b). Although CCP has the same polypeptide conformation in this region, the side chain ligands in CCP are not suitable to bind a cation (Bonagura *et al.*, 1996). Therefore, Patterson and Poulos (1995) have suggested that the presence of this cation may increase the electrostatic potential in the proximal pocket, inhibiting the formation of a stable radical on the Trp179. Recently, Bonagura et al. (1996) has successfully introduced the ascorbate peroxidase cation binding site into CCP by changing Gly192, Ala194, Thr199, and Glu201 to the corresponding residues in ascorbate peroxidase. The mutant CCP is no longer able to form a stable Trp191 radical, supporting this hypothesis. Moreover, Miller et al. (1995b) has replaced Phe172 in HRP, which is close to the γ-meso edge of the heme, with a Tyr residue. The mutant enzyme forms a Tyr radical upon the addition of H_2O_2. However, only ~10% of the mutant HRP compound I carries a Tyr radical (Miller *et al.*, 1995b), suggesting that other factors besides the distance between the heme and an oxidizable amino acid residue are involved in locating the second oxidizing equivalent in peroxidase compound I. Most plant and fungal peroxidases, including HRP, have a Ca(II) binding site on the proximal side of the heme at the same location as the cation binding site in ascorbate peroxidase (Patterson & Poulos, 1995). Therefore, most peroxidases may generate a porphyrin π-cation radical for efficient substrate oxidation, by preventing an oxidizing equivalent from "leaking" through the protein. In contrast, the substrate for CCP is a protein, cytochrome *c*, which cannot be oxidized at a site close to the heme. It has been

demonstrated that the electron transfer between CCP and cytochrome c occurs through the protein and that Trp191 is essential for the electron transfer reaction (Mauro *et al.*, 1988). Thus, the location of the free radical in peroxidases is physiologically relevant. Nevertherless, further studies are required to elucidate factors which localize the free radical.

1.3.4.2 Distal side: H-bonding and reaction with H_2O_2

Peroxidase compound I formation involves the heterolytic cleavage of the RO-OH bond (Dawson, 1988; Poulos & Kraut, 1980b; Poulos & Fenna, 1994). Two essential steps in the formation of compound I are the acid-base catalysis by a distal His and the charge stabilization of a precursor enzyme-substrate complex by a distal Arg. Site-directed mutagenesis has been used to examine the proposed roles of the distal His and Arg in compound I formation. When distal His52 in CCP is mutated to a Leu, the rate of compound I formation decreases by 5 orders of magnitude (Erman *et al.*, 1993). Similar results are obtained for the His42Ala and His42Val mutants of HRP (Newmyer & Ortiz de Montellano, 1995), supporting the premise that the distal His plays an essential role as an acid-base catalyst in the formation of compound I. Changing the distal Arg to Leu reduces the rate of compound I formation by 2-3 orders of magnitude for CCP and HRP (Vitello *et al.*, 1993; Meunier *et al.*, 1995; Rodriguez-Lopez, 1996). Saturation kinetics are observed for compound I formation in the Arg to Leu mutation and the rate of O-O bond cleavage appears to be 10-100 times lower than that of the wild-type enzyme (Vitello *et al.*, 1993). These results suggest that the distal Arg plays an important role in binding peroxide on the distal side of heme and may also stablize a transient enzyme-substrate complex prior to the cleavage of the RO-OH bond. Moreover, the crystal structure of CCP indicates that the distal Arg is able to rotate allowing the optimal hydrogen bonding interactions with the ferryl oxygen atom of compounds I and II (Edwards *et al.*, 1987; Edwards & Poulos, 1990). This suggests that the distal Arg plays a role in stablizing compounds I and II. Interestingly, changing the Arg to Lys does not significantly affect the rate of CCP compound I formation whereas the same mutation in HRP shows a 500-fold decrease in the rate of compound I formation (Sanders *et al.*, 1994; Vitello *et al.*, 1993), indicating that the orientation of the distal Arg of HRP may be different from that in CCP.

Amino acid residues which form important hydrogen bonding networks at both distal and proximal sites are conserved in all known plant and fungal peroxidases except chloroperoxidase (Welinder *et al.*, 1995; Sundaramoorthy *et al.*, 1995). On the distal side,

two side chains and one carbonyl backbone are conserved: His, Asn, and Glu (Welinder et al., 1995). An H-bond between the His and Asn has been proposed to ensure that $N\epsilon2$ of the distal His is available for accepting a proton from the peroxide (Welinder et al., 1995; Poulos & Fenna, 1994; Poulos & Finzel, 1984). Changing the distal Asn82 in CCP to Ala or Asp disrupts the H-bond between the distal His and cyanide ligated to the iron center (Satterlee et al., 1994; Alam et al., 1995; DeLauder et al., 1994), lowering the affinity of CN^- and F^- for the iron center by one or two orders of magnitude. In addition, an Asn70 to Val mutation in HRP decreases the rates of compound I formation and reduction ~30 and ~70 fold, respectively, compared with wild-type HRP, and compound II becomes extremely unstable (Nagano et al., 1995). These results suggest that the H-bond between the distal His and Asn residues stablizes compounds I and II.

To date, no study has been carried out to elucidate the role of the H-bond between the distal Asn and the carbonyl backbone of the nearby Glu residue. Conservation of the Glu residue in plant and fungal peroxidases is puzzling as the H-bond is formed with the backbone, not the side chain, of the Glu residue (Welinder et al., 1995). It is possible that the distal Glu may play other roles besides forming the H-bonding network with the distal His and Asn.

1.3.4.3 Proximal side: the role of His and Asp residues

Two other key amino acid residues in CCP have been examined by site-directed mutagenesis: Asp235 and the proximal ligand, His175. Asp235 forms an H-bond with the proximal His175. This H-bond has been postulated to impart a greater anionic character to the proximal ligand (Poulos & Finzel, 1984) which, in turn, lowers the redox potential of the iron center of the heme and stablizes the oxyferryl iron in compounds I and II (Wang et al., 1990a; Smulevich et al., 1991). In addition, the proximal Asp residue is particularly important in CCP since it forms an H-bond with the indole nitrogen of Trp191 (Smulevich et al., 1988a,b, 1991). Thus, Asp235 may participate in stabilizing a cationic radical at Trp191 in CCP compound I. Crystallographic and resonance Raman studies of CCP variants in which Asp235 has been replaced by Asn, Glu, and Ala have demonstrated that these substitutions produce significant changes involving the hydrogen-bonding interactions on both sides of the heme pocket (Wang et al., 1990a; Goodin & McRee, 1993; Smulevich et al., 1988a,b, 1991). The heme irons of CCP Asp235Asn and Asp235Ala variants are hexacoordinated and are in the low-spin state at pH 6.0 (Vitello et al., 1992; Satterlee et al., 1990; Ferrer et al., 1994). The Trp191 indole ring

also rotates out of its native position, resulting in the formation of an H-bond between an indole nitrogen and the peptide carbonyl oxygen of Leu177 (Wang *et al.*, 1990a). The Fe(III)/Fe(II) redox potentials of the CCP Asp235 to Asn, Glu, and Ala increase and the steady-state activities of those variants are 3-5 orders of magnitude lower than that of wild-type CCP (Goodin & McRee, 1993). Likewise, a recent resonance Raman spectroscopic study of the CIP proximal Asp245Asn variant shows a significantly weakened Fe-His bond. Furthermore, the Fe-His bond is broken at alkaline pH, a phenomenon not observed in wild-type CIP (Smulevich *et al.*, 1996).

In contrast, the Asp235-His175 H-bond does not appear to be essential for either the formation or stability of the oxyferryl center in CCP compound I (Miller *et al.*, 1994a; Wang *et al.*, 1990a; Fishel *et al.*, 1991). More importantly, Asp235 appears to stablize the π-cation radical at Trp191 (Miller *et al.*, 1994a; Fitzgerald *et al.*, 1995). Replacing Trp191 with Gly or Gln generates a K^+ binding site in the cavity formerly occupied by the side chain of Trp191. The calculated free enegy for cation binding in this site is sufficient to account for the stability of the Trp191 radical (Miller *et al.*, 1994a). These data confirm that the Asp-His-Fe interaction in the proximal site is important in defining the redox properties and imidazolate character of the distal His as has been proposed. Furthermore, its role in peroxidase function may be to maintain a high-spin pentacoordinate heme iron center by increasing the strength of the His-Fe bond and, in CCP, to correctly orient the Trp191 for efficient coupling of the free radical to the heme (Wang *et al.*, 1990a; Goodin & McRee, 1993).

The proximal ligand, His175, in CCP has been converted to both Glu and Gln (Choudhury *et al.*, 1992, 1994; Smulevich *et al.*, 1995). The crystal structures of the mutants show that the Glu and Gln residues are ligated to the iron center and interact with Asp235 (Choudhury *et al.*, 1992, 1994). The His175 to Gln mutant retains enzyme activity and the His175 to Glu mutant is approximately 7 times more active than the wild-type CCP. This suggests that the negative charge on the Glu residue provides additional electrostatic stabilization to the iron center and thus, increases the thermodynamic driving force for electron transfer (Goodin *et al.*, 1991; Choudhury *et al.*, 1994). His175 has also been replaced by a Cys residue which is oxidized to a cysteic acid (Choudhury *et al.*, 1994). Although the Cys also ligates to the iron center of the heme, the mutant enzyme exhibites only ~7% of the wild-type activity (Choudhury *et al.*, 1994). In addition, the compounds I of all of these mutants are less stable than that of the wild-type enzyme (Choudhury *et al.*, 1992, 1994). In the wild-type CCP, the indole ring of Trp191 and the imidazole ring of His175 form a parallel π stacking interaction which appears to

stablize the free radical of CCP compound I (Goodin & McRee, 1993). Changing the His to Glu, Gln, or Cys disrupts this π interaction (Choudhury *et al.*, 1994). Therefore, the nature of the proximal ligand may not be important for activity but the ligand appears to be critical for the stability of CCP compound I. However, most other plant and fungal peroxidases possess a Phe residue in the proximal site instead of a Trp residue, raising a question as to the role of the proximal His in these peroxidases. Thus far, no site-directed mutagenesis study of the proximal His for these peroxidases has been reported. In addition, other heme enzymes such as P-450, chloroperoxidase, and catalase possess different proximal ligands: Cys in P-450 and chloroperoxidase and Tyr in catalase (Morrison & Schonbaum, 1976; Peisach, 1975; Dawson *et al.*, 1976; Dawson & Sono, 1987; Dawson, 1988). The role of the proximal ligands in heme enzymes, in general, remains obscure and requires further study.

1.3.4.4 Small substrate binding and oxidation

Although the biological functions of peroxidases are diverse (Chapter 1.3.1), most plant and fungal peroxidases are able to oxidize small molecules such as aromatics, organic acids, halides, and metal complexes. There has been considerable interest in understanding the interaction of peroxidases with these compounds, particularly aromatic molecules. In contrast, CCP primarily oxidizes a macromolecule, ferrocytochrome *c*. This unique reaction will be discussed in the next section. This section presents a summary of the site-directed mutagenesis studies attempting to identify the aromatic donor molecule binding sites in peroxidases, particularly HRP.

One of the major difficulties in identifying the aromatic donor molecule binding site of HRP is the lack of high-resolution crystallographic data. Although crystal structures are available for other plant and fungal peroxidases such as CCP (Poulos *et al.*, 1980; Finzel *et al.*, 1984), ascorbate peroxidase (Patterson & Poulos, 1995), peanut peroxidase (Schuller *et al.*, 1996), LiP (Edwards *et al.*, 1993; Poulos *et al.*, 1993; Piontek *et al.*, 1993), MnP (Sundaramoorthy *et al.*, 1994b), and CIP (Kunishima *et al.*, 1994; Petersen *et al.*, 1994), the co-crystallization of these peroxidases with aromatic molecules has not been successful, due, in part, to weak binding of most aromatics to peroxidases (dissociation constants = ~2-8 mM) (Veitch, 1995). Thus, other methods, particularly proton NMR spectroscopy, have been extensively applied to studies of peroxidases (La Mar & de Ropp, 1993; Satterlee *et al.*, 1993; Veitch, 1995; Veitch & Williams, 1991). Results indicate that donor molecules bind relatively close to the heme methyl 8-CH$_3$ (near the δ-meso edge of the heme) (Veitch, 1995; Sakurada *et al.*, 1986; Banci *et al.*, 1993;

Veitch & Williams, 1990, 1991, 1995) (Figure 1.4). The side chains of the distal His42, an Ile residue and two Phe residues called PheA and PheB are also implicated in the binding site (Veitch & Williams, 1990, 1991, 1995; La Mar et al., 1992; Veitch, 1995). In addition to the NMR spectroscopic studies, enzyme inactivation studies using suicide inhibitors also have suggested that the aromatic donor molecules are oxidized at a site close to the δ-meso edge of the heme (DePillis et al., 1991; Ortiz de Montellano, 1992; Ortiz de Montellano et al., 1988; Harris et al., 1993). This idea has been further supported by a recent site-directed mutagenesis study of CCP in which Ala147, a residue located near the δ-meso edge of the heme and along the solvent access channel, was replaced with Met and Tyr residues (Wilcox et al., 1996). The oxidation of small molecule substrates by CCP is significantly inhibited by these mutations (Wilcox et al., 1996). While these studies reveal some properties of the aromatic binding site in peroxidases, they have not been able to identify the specific amino acid residues participating in binding of aromatic molecules. Until now, only a few HRP and CIP mutants have been characterized by proton NMR and limited studies have been carried out using benzhydroxamic acid (Veitch et al., 1992a,b, 1994, 1995; Gazaryan et al., 1994; Tams et al., 1993).

There are several Phe residues surrounding the heme in HRP (Figure 1.6) (Smith et al., 1995; Veitch et al., 1995). These hydrophobic Phe residues may form suitable binding sites for aromatic molecules. A combination of amino acid sequence comparisons, examination of model HRP structures, and analysis of NMR spectra of several different plant peroxidases initially suggested Phe142 and Phe143 as reasonable candidates for the proposed PheA and PheB residues (Veitch & Williams, 1991; Welinder, 1992; Welinder & Nørskov-Lauritsen, 1986). Phe142 and Phe143 to Ala mutants of HRP have been constructed (Veitch et al., 1995). Comparison with the NMR spectrum of wild-type HRP indicates that PheA or PheB cannot be assigned to either the Phe142 or 143. However, the ablity of the Phe142 to Ala mutant to bind benzhydroxamic acid is decreased ~4-fold with respect to the wild-type HRP (Veitch et al., 1995). Thus, substitution of Phe142 clearly affects aromatic donor binding, although this Phe residue may not be directly involved in the binding site. In addition, replacement of the Phe143 with Glu (Gazaryan et al., 1994) appears to disrupt the binding of negatively charged molecules. It has been proposed that the Phe142 and Phe143 residues are located at the entrance of the heme access channel (Smith et al., 1995; Veitch et al., 1995) (Figure 1.6), supporting the indirect effect of these Phe residues on small molecule binding. In contrast, a molecular-modeling study predicted Phe68 as the aromatic residue in contact with
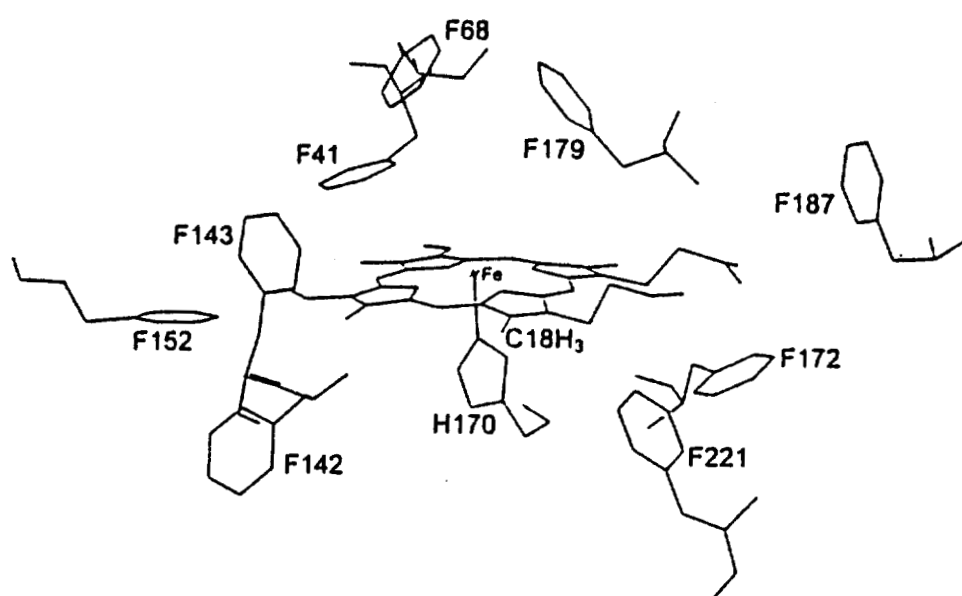
Figure 1.6. Phenylalanine side chains in the heme pocket and heme access channel of horseradish peroxidase isozyme C (Smith *et al.*, 1995; Veitch *et al.*, 1995).

substrate (Banci *et al.*, 1994). An NMR study of HRP isozyme A2, in which three Phe residues in HRP C are substituted by amino acids with aliphatic side chains, suggests that Phe179 or 221 and Ile244 in HRP C are important for aromatic molecule binding (de Ropp *et al.*, 1995). Further studies of mutants at positions 68, 179, 221 or others are required to provide definitive identification of PheA and PheB. In fact, an X-ray crystallographic study of HRP is underway showing that benzhydroxamic acid binds Phe68 and 179 (Gajhede, M., Copenhagen Univ., personal communication). Site-directed mutants of CIP have also been examined (Tams *et al.*, 1993; Veitch *et al.*, 1994). The mutants, G156F, N157F, and G156F-N157F, have Phe residues replacing Gly156 and Asn157. These residues are aligned with Phe142 and Phe143 of HRP C, respectively and, in addition, Gly156 is aligned with Phe148 of LiP, a residue in a proposed veratryl alcohol binding site (Poulos *et al.*, 1993). However, NMR studies of these mutants indicate that these residues only have an indirect effect on substrate binding (Veitch *et al.*, 1994, Tams *et al.*, 1993).

The conserved aromatic residue adjacent to the distal His in plant and fungal peroxidases has also been altered. The residue at this position is a Phe in all of the peroxidases except CCP and ascorbate peroxidase, in which it is a Trp (Finzel *et al.*, 1984; Patterson & Poulos, 1995; Welinder, 1992). Although its precise role is not known, this aromatic residue may affect heme reactivity and substrate specificity. Several HRP mutants at this position have been characterized, including F41A, F41V, F41L, and F41W (Newmyer & Ortiz de Montellano, 1995; Smulevich *et al.*, 1994b; Smith *et al.*, 1992a,b, 1993; Veitch *et al.*, 1992a,b). The HRP F41W mutant does not bind benzhydroxamic acid, whereas the F41V mutant shows a 2-fold increase in affinity (Smith *et al.*, 1992a,b; Smulevich *et al.*, 1994b). However, both F41W and F41V show decreased activities towards ABTS with respect to wild-type HRP (~12% and ~40%, respectively) (Smith *et al.*, 1992a,b). The rate constant for compound I formation with H_2O_2 decreases 8-fold for the HRP F41V mutant in comparison with the wild-type HRP (Smith *et al.*, 1992a,b), whereas the rate of oxidation of *p*-aminobenzoic acid increases 1.3-2.5-fold (Smith *et al.*, 1992a,b). Moreover, the HRP F41A variant catalyzes thioanisole sulfoxidation 100 times faster than the wild-type HRP (Newmyer & Ortiz de Montellano, 1995) and the Phe41 to Leu mutation increases the enantioselectivity of thioether sulfoxidation (Ozaki & Ortiz de Montellano, 1994). Similarly, mutations at Trp51 of CCP significantly affect the coordination and functional properties of the enzyme (Goodin *et al.*, 1987, 1991; Wang *et al.*, 1990a; Smulevich *et al.*, 1990; Roe & Goodin, 1993; Turano *et al.*, 1995). CCP W51F and W51A mutants exhibit hyperactivity towards

a number of substituted anilines (Roe & Goodin, 1993). The rate constants for aniline derivative oxidation are 10-400-fold larger for the CCP W51F and W51A than those for the wild-type CCP. Furthermore, the HRP F41A and CCP W51A mutants also show monooxygenase activity. They are able to epoxidate styrene whereas wild-type HRP and CCP cannot (Newmyer & Ortiz de Montellano, 1995; Miller *et al.*, 1992). These results suggest that the aromatic residue at the distal site affects substrate specificity. Replacement of Trp51 with an Ala residue significantly alters the spin states, coordination chemistry, and anion binding near the heme (Turano *et al.*, 1995). Thus, the Trp residue at the distal site in CCP appears also to be important in maintaining the heme environment.

1.3.4.5 Interprotein electron transfer between CCP and cytochrome *c*

As mentioned in earlier sections, CCP catalyzes the oxidation of ferrocytochrome *c*. The reaction between two redox proteins generally involves at least three distinct steps: (1) formation of a transient binary complex between the two proteins, (2) electron transfer within the binary complex, and (3) dissociation of the products. The reaction between cytochrome *c* and CCP has served as a paradigm for the protein interactions and the electron transfer pathway of other proteins (Finzel *et al.*, 1984; Edwards *et al.*, 1987; Wang *et al.*, 1990a; Everest *et al.*, 1991; Wallin *et al.*, 1991; Northrup *et al.*, 1988a). High-resolution crystallographic structures have been determined for both redox states of cytochrome *c* from a number of different organisms (Takano & Dickerson, 1981a,b; Louie & Brayer, 1990). X-ray crystal structures have also been determined for native CCP and CCP compound I (Finzel *et al.*, 1984; Edwards *et al.*, 1987). Cytochrome *c* forms a stable complex with CCP at low ionic strength, and both the stability of the complex and the rate of the electron transfer decreases significantly as the ionic strength increases, indicating the importance of electrostatic interactions between these two proteins (Yonetani & Ray, 1966; Kang *et al.*, 1977). Poulos and Kraut (1980a) proposed a hypothetical model for the 1:1 complex between tuna cytochrome *c* and CCP, stabilized by charge-pair interactions between Lys13, 27, 72, 86, and 87 of cytochrome *c* and Asp34, 37, 79, and 217 of CCP (Figure 1.7). Subsequently, Pelletier and Kraut (1992) determined the three-dimensional structure of a 1:1 complex between CCP and yeast iso-1-cytochrome *c* crystallized at high ionic strength (150 mM NaCl, pH 7.0). The binding domain is different from that proposed in the Poulos-Kraut model, and hydrophobic and van der Waals interactions are particularly important in stablizing the complex (Figure 1.8). Although no direct hydrogen bond between the two proteins is present, the positive charges on Lys 73 and 87 of cytochrome *c* are each about 4.0 Å from
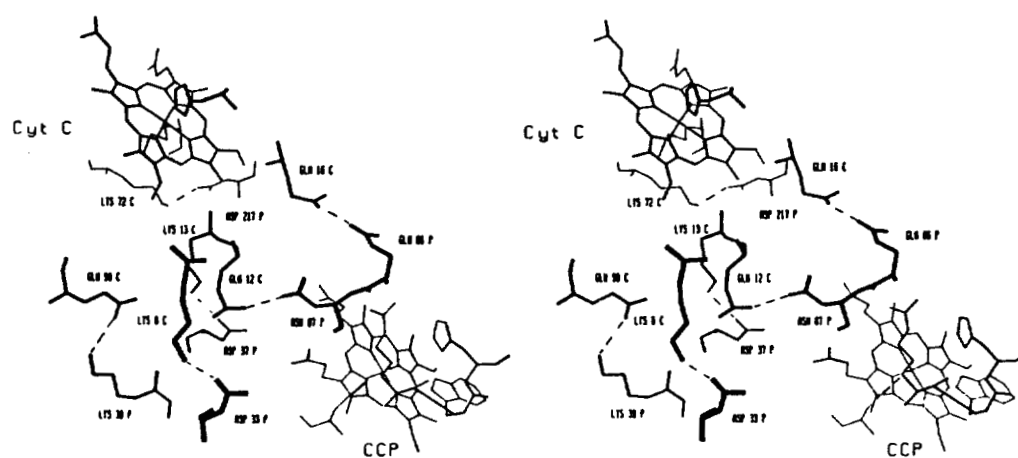
Figure 1.7. Stereoscopic model of the hypothetical CCP-cytochrome c complex showing the ionic and/or hydrogen bonding interactions (Poulos & Kraut, 1980a). CCP residues are labeled with a P and cytochrome c with a C.
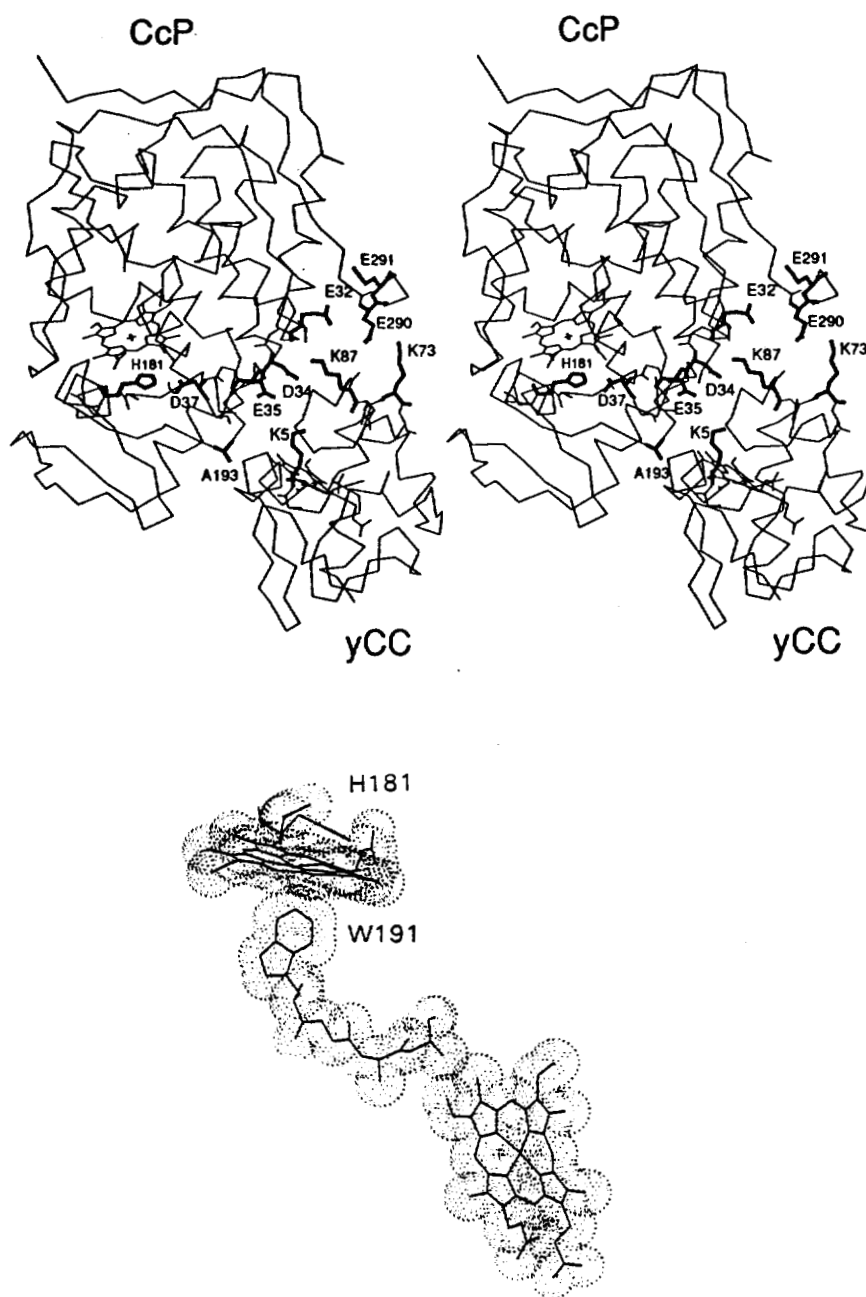
Figure 1.8. X-ray crystal structure of the yeast CCP-yeast iso-1-cytochrome c complex (Pelletier & Kraut, 1992). The side chains of CCP residues E32, D34, E35, D37, H181, A193, E290, and E291, and of cytochrome c residues K5, K73, and K87, are shown and labeled (*top*). The heme groups and the CCP residues Trp191, Gly192, Ala193, and Ala194 proposed to be involved in the electron transfer pathway are enclosed in Connolly surfaces (*bottom*).

the negative charges on Glu290 and Asp34 of CCP, respectively (Pelletier & Kraut, 1992). Therefore, electrostatic interactions involving these residues, as well as others, could help to stablize the complex. CCP mutants Asp34 to Asn and Glu290 to Asn exhibit 25-50% of the wild-type CCP activity for cytochrome c oxidation (Miller *et al.*, 1994b), confirming that the electrostatic interaction by Asp34 and Glu290 of CCP is important for the electron transfer between CCP and cytochrome c. Importantly, the crystal structure reveals a potential electron transfer pathway extending from the exposed heme methyl group of cytochrome c through CCP residues, Ala194, Ala193, and Gly192 to the indole group of Trp191, which is in van der Waals contact with the heme (Figure 1.8) (Pelletier & Kraut, 1992). Changing the Ala193 to Phe, which presumably disrupts this proposed interprotein electron transfer pathway, results in a 2-4-fold decrease in the catalytic rate of CCP (Miller *et al.*, 1994b), indicating the importance of the proposed pathway for the electron transfer reaction.

There is, however, a question as to whether CCP interacts with cytochrome c at only one site or at multiple sites. Fluorescence-quenching experiments (Leonard & Yonetani, 1974), spectrophotometric titrations (Erman & Vitello, 1980), and NMR studies (Moench *et al.*, 1992, 1993) are consistent with a 1:1 ratio of CCP:cytochrome c. In contrast, there is growing evidence that cytochrome c interacts with CCP at multiple sites. Biphasic steady-state kinetics observed with the CCP-catalyzed oxidation of cytochrome c may be attributed to a two-binding site mechanism for catalysis in which CCP has both a high-affinity and a low-affinity binding site for cytochrome c (Kang *et al.*, 1977). Stempf and Hoffman (1993) measured triplet state quenching of the zinc- or magnesium-substituted CCP binding to cytochrome c and the fraction of the quenching which is due to electron transfer. The results led to the proposal of a mechanism involving two cytochrome c-binding sites on CCP. Subsequently, Zhou and Hoffman (1994) observed similar properties using modified horse cytochrome c in which the heme iron was replaced with zinc. Moreover, similar experiments, in the presence of copper-substituted cytochrome c as an inhibitor of the electron transfer, support the sequential binding model which postulates that the first cytochrome c binds strongly at a nonreactive domain and the second binds weakly at a reactive site (Zhou *et al.*, 1995). Potentiometric data at low ionic strength also are in agreement with two binding sites possessing different ionic properties (Mauk *et al.*, 1994). The site identified in the crystal structure of the CCP-cytochrome c complex (Pelletier & Kraut, 1992) has been proposed as a high-affinity site with low electron transfer efficiency (Zhou & Hoffman, 1994; Mauk *et al.*, 1994). Brownian dynamics simulations of the CCP-cytochrome c complex (Northrup *et al.*, 1988a,b)

provides some insights regarding sites of interaction. The predicted primary site is near that observed in the crystal structure, whereas the second site is predicted to be near Asp148 of CCP.

To identify the cytochrome c binding sites, site-directed mutagenesis has been used to introduce Cys residues into CCP and cytochrome c to form site-specific cross-linked intermolecular complexes (Pappa & Poulos, 1995; Pappa *et al.*, 1996). In this way, the proposed cytochrome c binding site of CCP can be blocked. Approximately 40-50% of activity is retained by cross-linking between the Cys290 of CCP and Cys73 of ccytochrome c (Pappa & Poulos, 1995), suggesting that the site revealed in the crystal structure is indeed involved in the electron transfer reaction but that CCP also has a second site for electron transfer. In contrast, the CCP mutant in which the second proposed site near Asp148 is blocked shows essentially wild-type activity towards cytochrome c (Pappa *et al.*, 1996), suggesting that this region is not important for electron transfer. Extensive studies are continuing to determine the number and location of cytochrome c binding sites in CCP.

It is well established that a free radical is formed on the Trp191 in CCP compound I (Hoffman, 1991; Hoffman *et al.*, 1993; Sivaraja *et al.*, 1989; Huyett *et al.*, 1995). Site-directed mutagenesis studies have also suggested that the Trp191 radical formation is important for the electron transfer reaction between CCP and cytochrome c (Mauro *et al.*, 1988). The rate of electron transfer from cytochrome c to CCP in a Trp191 to Phe mutant is decreased by at least 10^4-fold relative to the wild-type CCP (Mauro et al. 1988; Hazzard *et al.*, 1987; Liu *et al.*, 1995b). Kinetic analyses of the CCP W191F compounds I and II reduction by cytochrome c have demonstrated that the electron transfer reaction occurs through Trp191 in both (Miller *et al.*, 1995a), in agreement with the ordered mechanism (Chapter 1.3.2.2) (Geren *et al.*, 1991; Hahm *et al.*, 1992, 1993, 1994; Liu *et al.*, 1994, 1995a,b). In addition, another CCP mutant, in which a cation binding site has been introduced near Trp191, is unable to generate a stable Trp radical (Bonagura *et al.*, 1996). The activity of this CCP mutant towards cytochrome c is <1% of that of wild-type CCP, once again supporting the involvement of Trp191 in the electron transfer between CCP and cytochrome c. However, electron transfer between Trp191 and the oxyferryl center in CCP compound II, which is required for the ordered mechanism, appears to be too slow to account for the turnover rates observed in the steady-state reaction (Ho *et al.*, 1983; Summers & Erman, 1988; Hazzard & Tollin, 1991; Liu *et al.*, 1994). Furthermore, the double mutant, His175 to Gln/Trp191 to Phe, retains 20% of the wild-type activity (Choudhury *et al.*, 1994) whereas the single Trp191 to Phe mutant is

essentially inactive (Mauro *et al.*, 1988). These results suggest either the existence of more than one electron pathway in CCP or that the presence of Trp191 is not sufficient to ensure rapid electron transfer from cytochrome *c* to the oxy-ferryl center of the heme. The Trp191 to Phe mutant, in fact, forms a cross-linked dimer in the reaction of the mutant enzyme with peroxide (Miller *et al.*, 1995a), suggesting that a protein-centered radical can be generated even without the Trp191 residue. Therefore, Trp191 and the Trp191 radical may play only secondary roles in controlling the rate and specificity of electron transfer.

In summary, site-directed mutagenesis has been an invaluable tool for understanding the mechanisms of peroxidases, particularly CCP and HRP. Although a variety of questions still remain, the future is promising. Recently, crystal structures of several other plant and fungal peroxidases have been determined. Moreover, various recombinant peroxidase proteins have been expressed and produced in significant quantity, facilitating further study by site-directed mutagenesis of peroxidases. Biochemical analyses of mutant peroxidases will give us additional insights as to the relationships between structure and function in peroxidases, including the substrate binding sites, electron transfer pathways, factors controlling stability of enzymes, and the reactivity of intermediates.

1.4 MANGANESE PEROXIDASE: STRUCTURE AND FUNCTION

Although a variety of studies have demonstrated that the structure and catalytic cycle of MnP are similar to those of other plant and fungal peroxidases, MnP is unique in its ablity to oxidize a metal ion, Mn(II) to Mn(III). The generated Mn(III) is released from the protein and then acts as a redox mediator. None of the other plant and fungal peroxidases utilize Mn(II) in this fashion. Thus, it is extremely important to determine the specific Mn(II) binding site(s) in MnP, the location of the Mn(II) oxidation site(s), and the amino acid residues involved in the Mn(II) binding site(s). This information is required to elucidate the unique mechanism of Mn(II) oxidation by MnP. This chapter describes previous studies on MnP, particularly the crystal structure of MnP and the prediction of the Mn(II) binding site.

1.4.1 General Properties

When cultured under ligninolytic conditions, the white-rot fungus *P. chrysosporium*, produces two extracellular heme peroxidases, LiP and MnP. These enzymes have been demonstrated to be major components of the lignin degradation system of this organism (Kirk & Farrell, 1987; Buswell & Odier, 1987; Gold & Alic, 1993;

Wariishi *et al.*, 1991b; Kuwahara *et al.*, 1984; Hammell *et al.*, 1993). MnP has been purified and extensively characterized. It contains one iron protoporphyrin IX prosthetic group, is a glycoprotein of molecular mass 45 to 47 kDa, and exists as a series of isozymes with pIs ranging from 4.2 to 4.9 (Glenn & Gold, 1985; Gold & Alic, 1993; Paszczynski *et al.*, 1986; Leisola *et al.*, 1987; Mino *et al.*, 1988; Wariishi *et al.*, 1988). Enzyme characterization has been conducted with the major isozyme, referred to as MnP isozyme 1 in our laboratory.

Electronic absorption maxima for MnP, oxidized intermediates of MnP, and various ligated forms of the enzyme are listed in Table 1.2. All of these spectra of MnP are similar to those of HRP, indicating that the heme environment of MnP is similar to that of other plant and fungal peroxidases (Glenn & Gold, 1985; Glenn *et al.*, 1986; Renganathan & Gold, 1986; Mino *et al.*, 1988; Gold *et al.*, 1989; Dunford & Stillman, 1976; Wariishi *et al.*, 1988, 1989a). Detailed EPR, NMR, and resonance Raman spectral studies of LiP and MnP have also demonstrated that the native forms of these enzymes exist as ferric, high-spin, pentacoordinate heme proteins with the protein ligated to the heme iron through a proximal His residue, similar to HRP (Andersson *et al.*, 1985; Banci *et al.*, 1992; de Ropp *et al.*, 1991; Gold *et al.*, 1989; Kirk & Farrell, 1987; Mino *et al.*, 1988). In addition, the sequences of *mnp* cDNA (Gold & Alic, 1993; Pribnow *et al.*, 1989; Pease *et al.*, 1989) and genomic clones (*mnp1* and *mnp2*) (Gold & Alic, 1993; Godfrey *et al.*, 1990; Mayfield *et al.*, 1994a) encoding two *P. chrysosporium* MnP isozymes have been determined. Comparison of cDNA sequences confirms that a proximal and distal His and a distal Arg are conserved in the active site of MnP (Pribnow *et al.*, 1989; Gold & Alic, 1993; Ritch *et al.*, 1991; Welinder, 1976; Kaput *et al.*, 1982). The crystal structures of both LiP and MnP have been reported (Edwards *et al.*, 1993; Poulos *et al.*, 1993; Piontek *et al.*, 1993; Sundaramoorthy *et al.*, 1994b) and also confirm that the heme environments of MnP and LiP are similar to those of other plant and fungal peroxidases (Poulos *et al.*, 1993; Sundaramoorthy *et al.*, 1994b).

MnP oxidizes Mn(II) to Mn(III) as shown in Scheme 1.2 (Glenn & Gold, 1985; Glenn *et al.*, 1986; Wariishi *et al.*, 1992) and the Mn(III) generated, in turn, oxidizes organic substrates such as lignin substructure model compounds (Tuor *et al.*, 1992), synthetic lignin (Wariishi *et al.*, 1991b; Bao *et al.*, 1994), and aromatic pollutants (Valli & Gold, 1991; Valli *et al.*, 1992a,b; Joshi & Gold, 1993).

Scheme 1.2

$$MnP + H_2O_2 \rightarrow MnP \text{ compound I} + H_2O$$

Table 1.2. Electronic Absorption Spectral Maxima of MnP, LiP, and HRP.

System	Absorption Maxima (nm)				References
Ferric, resting state					
MnP, pH 4.5	406	502	632		Glenn & Gold, 1985
LiP, pH 4.5	408	500	632		Gold et al., 1984; Renganathan & Gold, 1986
HRP, pH 6.0	403	500	641		Dunford & Stillman, 1976
Compound I					
MnP	407	558	617	650	Wariishi et al., 1988
LiP	408	550	608	650	Gold et al., 1984; Renganathan & Gold, 1986
HRP	400	557	622	650	Dunford, 1982
Compound II					
MnP	420	528	555		Wariishi et al., 1988
LiP	420	525	556		Gold et al., 1984; Renganathan & Gold, 1986
HRP	420	527	554		Dunford, 1982
Ferric, low-spin					
CN^--MnP	421	546			Glenn & Gold, 1985
CN^--LiP	423	540			Gold et al., 1984
CN^--HRP	422	539			Dunford & Stillman, 1976
N_3^--MnP	417	542	580		Glenn & Gold, 1985
N_3^--LiP	418	540	575		Gold et al., 1984
N_3^--HRP	416	534	565		Dunford & Stillman, 1976
Ferrous					
MnP	433	554			Glenn & Gold, 1985
LiP	435	556			Gold et al., 1984
HRP	437	556			Dunford & Stillman, 1976
CO-MnP	423	541	570		Glenn & Gold, 1985
CO-LiP	420	535	568		Gold et al., 1984
CO-HRP	423	541	575		Dunford & Stillman, 1976

$$\text{MnP compound I} + \text{Mn(II)} \rightarrow \text{MnP compound II} + \text{Mn(III)}$$

$$\text{MnP compound II} + \text{Mn(II)} \rightarrow \text{MnP} + \text{Mn(III)} + H_2O$$
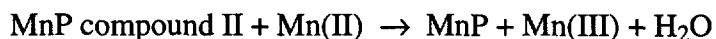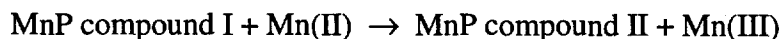
The manganese ion acts as a redox mediator rather than an enzyme-binding activator. This is supported by results which show that when the MnP/Mn(II)/H_2O_2 system is separated from the organic substrate by a semipermeable membrane, the substrate is oxidized by the diffusible Mn(III) generated by the enzyme (Glenn *et al.*, 1986). Since free Mn(III) is extremely unstable in aqueous solution, Mn(III) needs to be stabilized by an organic acid chelator such as oxalate, which is also secreted by the fungus (Wariishi *et al.*, 1992; Kuan & Tien, 1993). The Mn(III)-chelator complexes can be spectroscopically detected and the generation of Mn(III) by MnP is confirmed by measuring the Mn(III)-chelator complex formation (Glenn & Gold, 1985; Paszczynski *et al.*, 1986; Wariishi *et al.*, 1989a, 1992; Kuan *et al.*, 1993; Kuan & Tien, 1993). This unique ability of MnP to oxidize Mn(II) to Mn(III) strongly indicates that MnP has at least one Mn(II) binding and oxidation site. The next section describes the proposed Mn(II) binding sites in MnP.

1.4.2 Mn(II) Binding Site: Proposed Mechanism of Mn(II) Oxidation

The nature of the Mn(II) binding site in MnP has been under investigation for several years. Harris et al. (1991) demonstrated that suicide inhibitors such as azide and organic hydrazines completely inactivate MnP but that the modified MnP is able to react with H_2O_2, indicating that modification of the δ-meso edge of the heme suppresses Mn(II) oxidation by MnP. They also showed that binding of Mn(II) does not inhibit the inactivation of MnP by azide or organic hydrazines (Harris *et al.*, 1991). Therefore, it was suggested that a Mn(II) ion binds close to the δ-meso position (above or below the plane of the heme) without blocking the approach of small molecules to the δ-meso edge (Figure 1.9) (Harris *et al.*, 1991). Similarly, based upon the perturbation of NMR spectrum of MnP upon the binding of Mn(II), Banci et al. (1993) suggested a Mn(II) binding site at the δ-meso side of the heme. Disappearance of the 8-CH_3 resonance and the distal side proton signals are observed upon addition of 1 equivalent of Mn(II) to MnP, suggesting that Mn(II) approaches the heme in a position near the 8-CH_3 and the distal side protons (Banci *et al.*, 1993). This is consistent with the work done by Harris et al. (1991). In contrast, Johnson et al. (1993) used homology modeling and energetic considerations to predict the Mn(II) binding sites in MnP (Figure 1.10). They predicted five Mn(II) binding sites and proposed
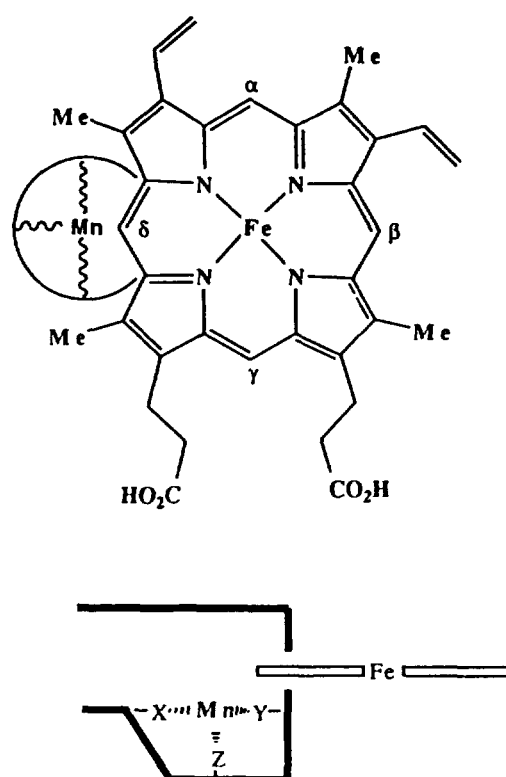
Figure 1.9. A model of the active site of MnP proposed by Harris *et al.* (1991). The upper drawing shows the approximate placement of the Mn(II) binding site relative to the heme edge. The bottom drawing shows that the proposed Mn(II) site is on one side of the heme plane.
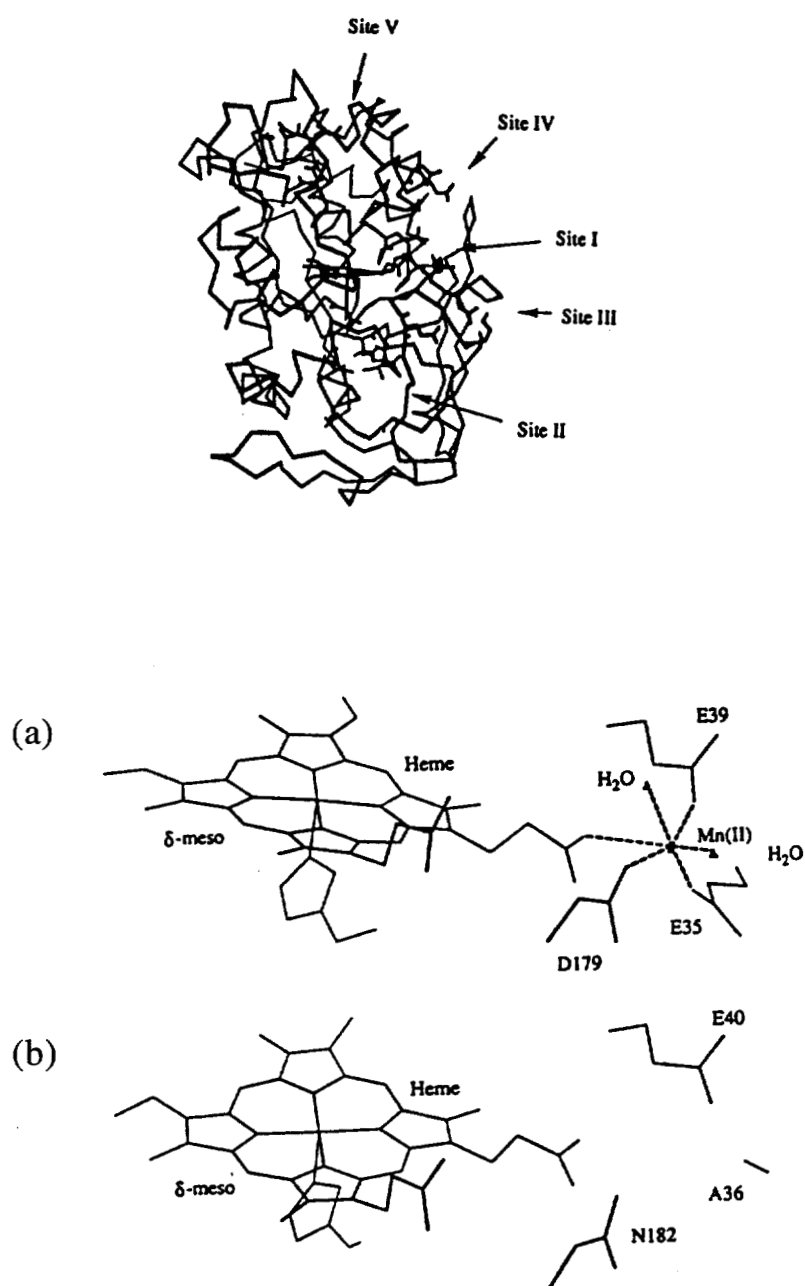
Figure 1.10. *Top,* C_α trace of the predicted model structure of MnP (Johnson *et al.,* 1993). The five candidate Mn(II) binding sites in MnP are highlighted. *Bottom,* the first candidate Mn(II) binding site in MnP (a) and the corresponding region in LiP (b).

that the most likely stable binding site consists of the ligands Asp179, Glu35, Glu39, and one of the heme propionates. This places the Mn(II) binding site close to the γ-meso rather than δ-meso position of the heme. According to this model structure, the region near the δ-meso edge of the heme is unlikely to bind a Mn(II) ion since it lacks anionic or polar amino acid side chains to act as the Mn(II) ligands (Johnson *et al.*, 1993). The recently solved crystal structure of MnP (Sundaramoorthy *et al.*, 1994b) supports this latter prediction for the binding site (Chapter 1.4.3).

1.4.3 Crystal Structure of Manganese Peroxidase

Recently, the crystal structure of MnP has been solved and refined to R = 0.20 at 2.06 Å (Sundaramoorthy *et al.*, 1994b).

1.4.3.1 Heme environment

As in other plant and fungal peroxidases, MnP consists of two domains with the heme sandwiched between them (Figure 1.11). There are ten major helices and one minor helix, all of which also are found in LiP (Edwards *et al.*, 1993; Poulos *et al.*, 1993; Piontek *et al.*, 1993). The two minor helices present in LiP and CIP are in a 3_{10} helical conformation in MnP. In addition to these two helices, MnP and LiP have six other 3_{10} helical segments (Edwards *et al.*, 1993; Poulos *et al.*, 1993; Piontek *et al.*, 1993). In the heme pocket (Figure 1.12), the distal His46 and Arg42 peroxide binding site, the H-bond between the distal His46 and Asn80, and the H-bond between the proximal ligand, His173 and Asp242, are all conserved among plant and fungal peroxidases (Gold & Alic, 1993).

In addition to the Fe-His173 interaction, the heme in MnP is stabilized by the interaction of propionates with Mn(II) as well as H-bonds with protein and solvent molecules. There are some major differences in these interactions as compared with LiP. The outer propionate in LiP interacts with Asp183 through an unusual carboxylate-carboxylate H-bond (Poulos *et al.*, 1993), analogous to the propionate-Asn183 interaction in CCP. In MnP, the corresponding residue, Lys180 (Gly191 in CIP), points away from the heme and does not interact directly with the heme propionate. In contrast, the propionate in MnP rotates approximately 60° relative to that in LiP to make H-bonds with the main chain peptide nitrogens of Asp179 and Lys180 and two water molecules. CIP has a similar structure. Because of the different orientations of the outer propionate in MnP, the distal Arg42 cannot form a H-bond with the propionate, whereas in LiP, the distal Arg directly interacts with the propionate. In CIP and CCP, a water molecule bridges the distal
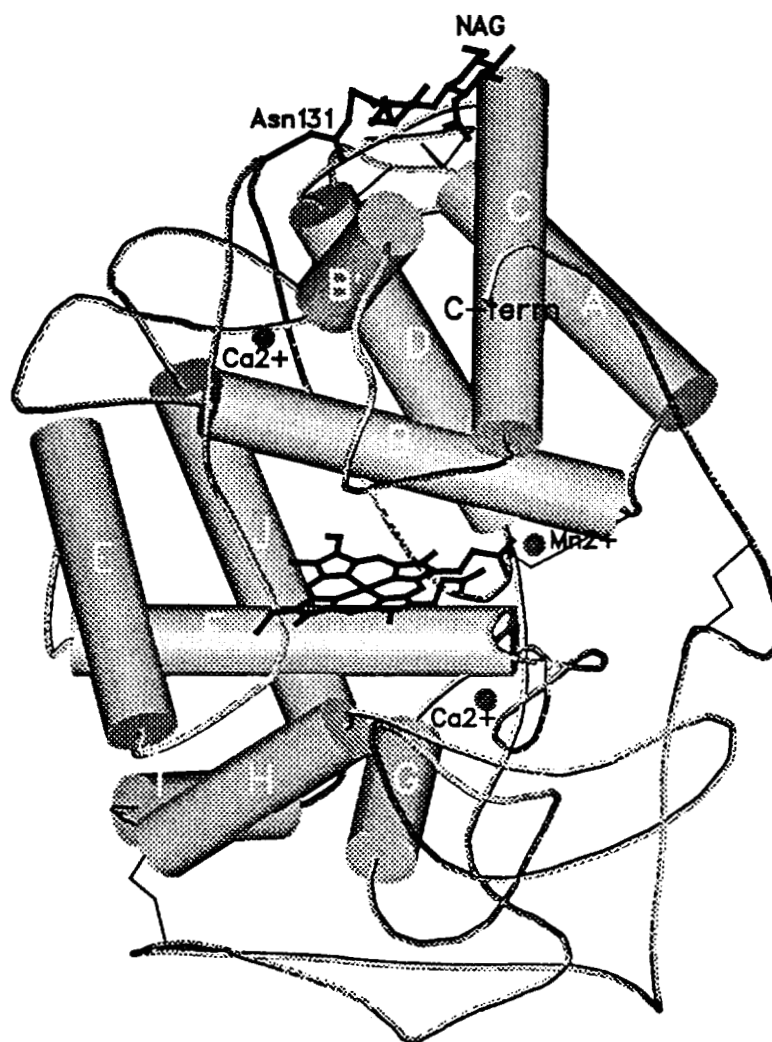
Figure 1.11. Schematic representation of the complete MnP polypeptide chain (Sundaramoorthy *et al.*, 1994b). The helices are represented as cylinders. The heme, carbohydrate, calcium ions, and manganous ions are highlighted.
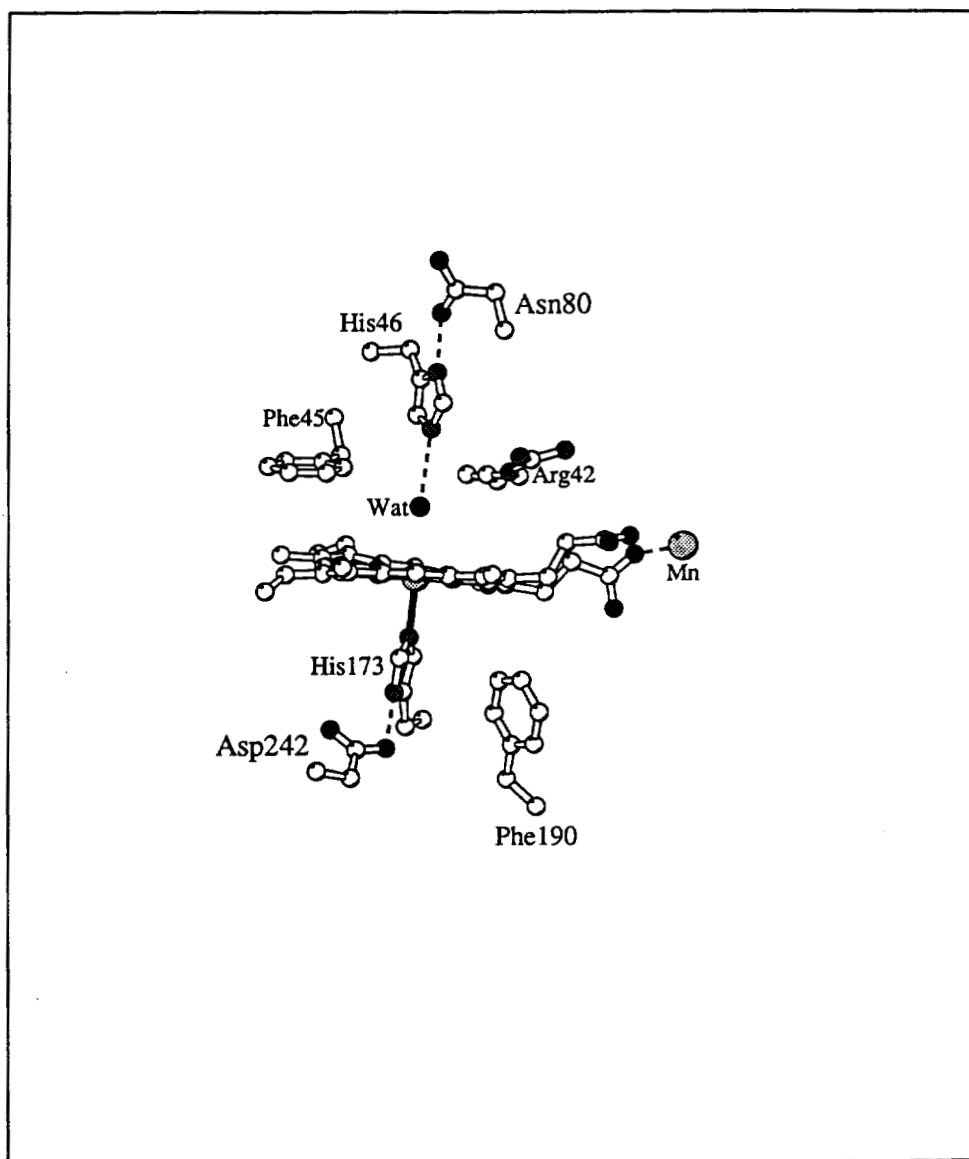
Figure 1.12. The active site environment of MnP (Sundaramoorthy *et al.*, 1994b). The hydrogen bonds are represented as dashed lines.

Arg and the heme propionate. The second propionate in MnP interacts directly with Mn(II) ion, water molecules, and the peptide NH group of Arg177. The interaction of a propionate with a main chain peptide nitrogen also is found in LiP and CIP. However, the effects of these H-bonds on the function of peroxidases are not clear.

MnP has two Phe residues in the heme pocket (Figure 1.12). One of these Phe residues, Phe190 on the proximal side, may play an important role in MnP. CCP and ascorbate peroxidase have Trp residues at this site (Finzel *et al.*, 1984; Patterson & Poulos, 1995) and CIP has a Leu at this position (Kunishima *et al.*, 1994; Petersen *et al.*, 1994). Other peroxidases such as LiP and HRP have Phe residues at this position. Comparison of the LiP and MnP crystal structures indicates that the orientation of the plane of these proximal Phe residues differs between LiP and MnP. In LiP, the Phe ring is approximately parallel to the proximal His imidazole ring (Edwards *et al.*, 1993; Poulos *et al.*, 1993; Piontek *et al.*, 1993) whereas in MnP, the Phe190 ring is orientated almost perpendicular to the plane of the proximal His.

1.4.3.2 Mn(II) binding site

There are three large 10σ F_0-F_c difference electron density peaks in the MnP crystal, suggesting three metals are bound to MnP. Two of these sites correspond to the calcium-binding sites in other plant and fungal peroxidases (Figures 1.11 and 1.13). The third site is unique to MnP and is identical to the predicted most probable Mn(II) binding site based upon homology modeling and energetic considerations as mentioned above (Figure 1.10) (Johnson *et al.*, 1993). The Mn(II) ion is hexacoordinated to the carboxylate oxygens of Glu35, Glu39 and Asp179, a heme propionate oxygen, and two water oxygens (Figure 1.14). One of the water ligands is H-bonded to the second heme propionate. The bond distances between the Mn(II) ion and its ligands are shown in Table 1.3. The coordination around the Mn(II) ion is octahedral which is typical of Mn(II) coordination complexes (Demmer *et al.*, 1980). Another potentially important interaction is an H-bond between Arg177 and one of the Mn(II) ligands, Glu35. This interaction may be important for the correct orientation of the Glu35 or may affect the electronic property of the Glu35. An Arg cannot be accommodated in LiP, wherein Arg177 is replaced by Ala. In MnP, there is sufficient room for an Arg at this position since the C-terminal tail is further away from the main part of the protein because of an extra Cys341:Cys348 disulfide bond. Because LiP lacks this unique disulfide bond, only a small amino acid side chain can be accommodated (Figure 1.15). Table 1.3 also lists the residues in LiP, CCP, and CIP corresponding to the Mn(II) ligands in MnP. Two of the three anionic residues found in
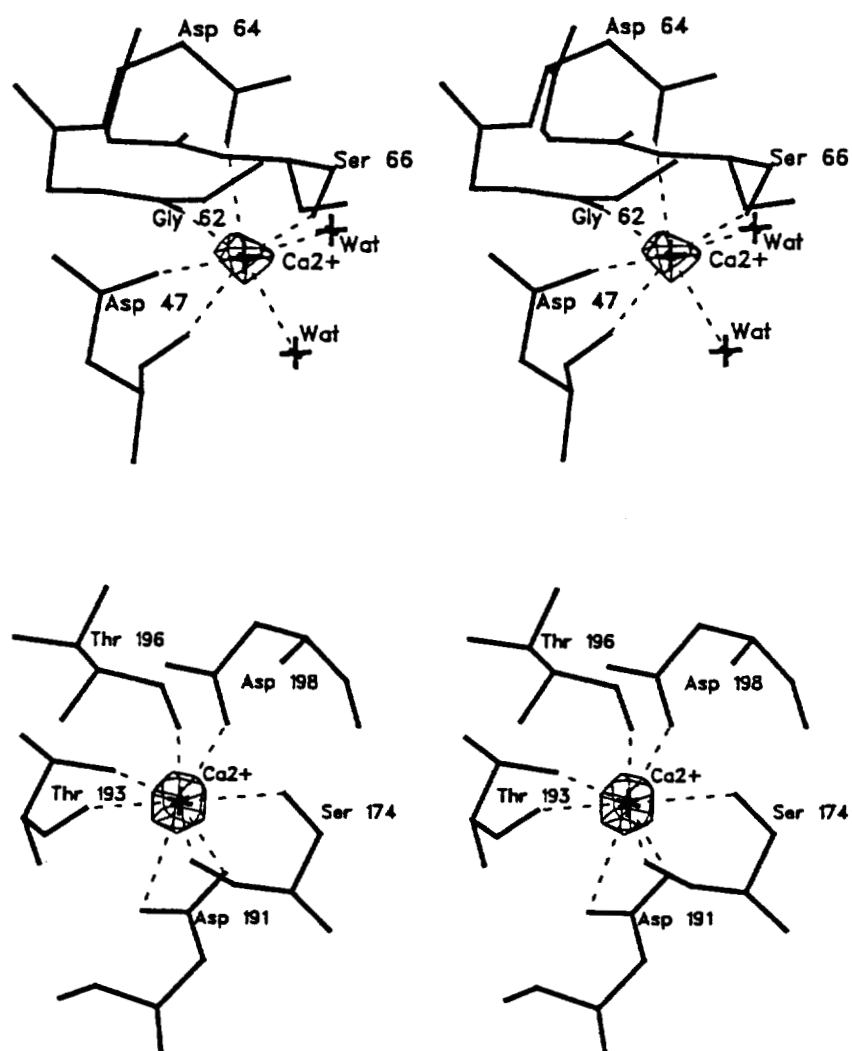
Figure 1.13. Stereo view of two calcium sites in MnP (Sundaramoorthy *et al.*, 1994b). *Top*, the distal site and *bottom*, the proximal site.
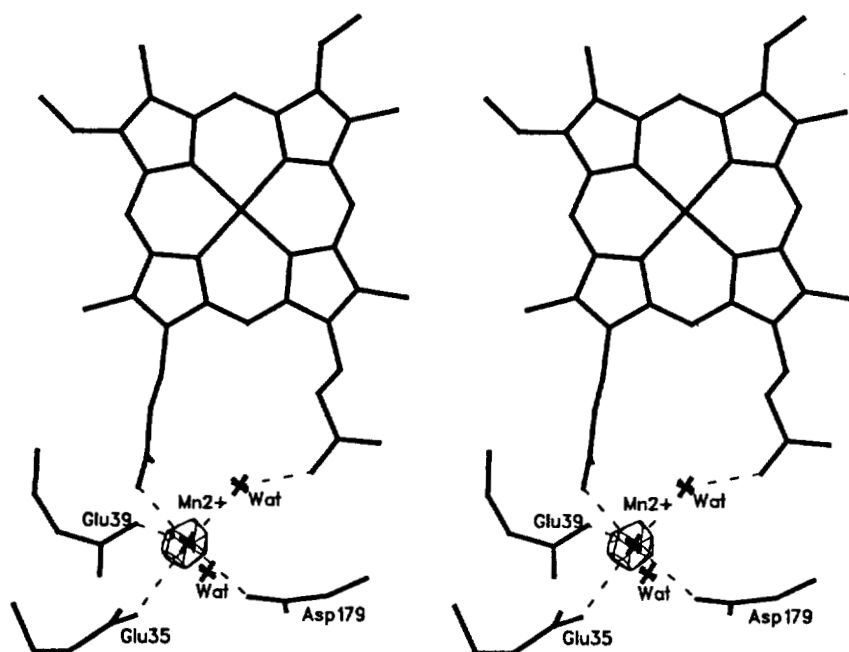
Figure 1.14. Stereo view of the Mn(II) binding site in MnP (Sundaramoorthy *et al.*, 1994b).
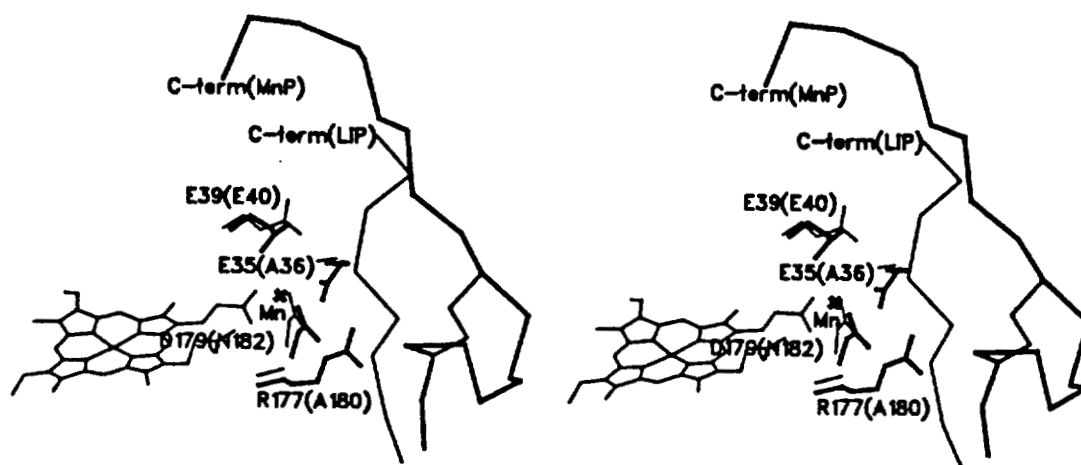
Figure 1.15. A close-up view of the Mn(II) binding site of MnP (thick lines) superimposed on LiP (thin lines) (Sundaramoorthy *et al.*, 1994b). The LiP residues are shown in parentheses.

Table 1.3. Manganese Ligands and Bond Distances in MnP, and Comparison with Other Peroxidases (Sundaramoorthy *et al.*, 1994b).

Ligand	Distance Å	Corresponding residue in		
		LiP	CIP	CCP
Heme propionate	2.34	same	same	same
Side chain carboxyl E35	2.69	A36	S45	G41
Side chain carboxyl E39	2.82	E40	K49	V45
Side chain carboxyl D179	2.57	N182	E190	H181
Water 520	2.35			
Water 441	2.57			

MnP are replaced by non-charged residues in LiP: Ala36 for Glu35 and Asn182 for Asp179. Only Glu39 in MnP is conserved as Glu40 in LiP. In addition, the heme propionate in LiP is not positioned for favorable Mn(II) binding (Johnson *et al.*, 1993) (Figure 1.10 and 1.15). The unique anionic environment in MnP is also absent in CCP and CIP (Table 1.3). This appears to be the reason why MnP is the only known peroxidase capable of oxidizing Mn(II) efficiently. Current views of electron transfer proteins envision an electron transfer pathway through covalent bonds (Onuchic & Beratan, 1990). In MnP, the electron could be transferred from the Mn(II) to the porphyrin periphery or to the iron center via the heme propionate, using a nearly continuous σ-bond.

Using a homologous expression system (Mayfield *et al.*, 1994b) (Chapter 3), we have carried out site-directed mutagenesis of MnP to understand structure/function relations in this unique protein (Chapters 4-6).

1.5. SUMMARY OF RESEARCH

Biochemical and physiological studies of *P. chrysosporium* have demonstrated that two peroxidases, LiP and MnP, along with an H_2O_2-generating system, appear to be the major components of its extracellular lignin degradative system. Considerable evidence suggests that MnP is essential for lignin depolymerization *in vivo*. The white-rot fungus, *Dichomitus squalens*, which lacks LiP isozymes, still degrades lignin and, importantly, the degradation of lignin by this fungus is stimulated by Mn(II) ion, which induces MnP protein expression (Périé & Gold, 1991). Moreover, MnP activity is found in all white-rot fungi known to degrade lignin (Périé & Gold, 1991; Hatakka, 1994; Orth *et al.*, 1993). Therefore, the characterization of the MnP mechanism should increase our understanding of the biodegradation of lignin and the environmental pollutants by white-rot fungi.

Although a variety of studies have demonstrated that the heme environment and catalytic cycle of MnP are very similar to those of other plant and fungal peroxidases, MnP is uniquely able to catalyze the one electron oxidation of Mn(II) to Mn(III). Whereas phenolic compounds are oxidized directly by MnP compound I, direct oxidation of phenols by MnP compound II is extremely slow compared with Mn(II) oxidation. Thus, Mn(II) is required to complete the MnP catalytic cycle (Wariishi *et al.*, 1988, 1989a). In addition, the Mn(III) generated by MnP is released from the protein and then acts as a redox mediator, oxidizing a second substrate such as phenolic compounds. The Mn(III) species in aqueous solution needs to be stablized by an organic acid, such as lactate, malonate, or oxalate (Glenn & Gold, 1985; Paszczynski *et al.*, 1986; Wariishi *et al.*, 1989a, 1992;

Demmer *et al.*, 1980). In particular, oxalate appears to be a physiological chelator for Mn(II) and Mn(III) in the cultures of the white-rot fungi. The production of millimolar concentrations of oxalate by *P. chrysosporium* under defined conditions has been demonstrated (Wariishi *et al.*, 1992; Barr *et al.*, 1992; Kuan & Tien, 1993; Dutton *et al.*, 1993). In addition, it has been shown that optimal enzyme activity is obtained in the presence of 0.5-2.0 mM oxalate, a concentration found in *P. chrysosporium* cultures (Kuan & Tien, 1993; Kishi *et al.*, 1994). Therefore, white-rot fungi utilize the enzymatically generated Mn(III), complexed with oxalate, as a freely diffusible oxidant, enabling the fungi to degrade polymeric lignin within the wood matrix.

The role of chelators in the MnP reaction has been under investigation for several years. Besides stablizing the Mn(III) species in aqueous solution, chelators such as C_2 and C_3 dicarboxylic and α-hydroxy acids dramatically stimulate the catalytic activity of MnP (Glenn & Gold, 1985; Wariishi *et al.*, 1988, 1992; Glenn *et al.*, 1986; Kuan & Tien, 1993; Kuan *et al.*, 1993). Wariishi et al. (1992) have demonstrated that some chelators exhibit competitive inhibition with Mn(III)-malonate formation and that the Mn(II) ion binds the enzyme more tightly in the absence of chelators than in the presence of chelators. Based upon these results, they proposed that the enzyme reacts with free non-chelated Mn(II) and that chelators stimulate enzyme activity by facilitating the release of Mn(III) from the enzyme. However, the chelators also form complexes with the Mn(II) ion. In addition, the stronger binding of free Mn(II) by MnP does not necessarily indicate that the free Mn(II) ion is a substrate for MnP even in the presence of chelators; the chelated Mn(II) ion may be oxidized by MnP more readily than the free non-chelated Mn(II). Recently, by using kinetic analysis, it was suggested that a monooxalate complex of Mn(II), rather than the free Mn(II), reacts with MnP (Kuan *et al.*, 1993; Kishi *et al.*, 1994). Further investigation of this issue using transient-state kinetics is presented in Chapter 2. These kinetic results do not agree with the crystallographic results suggesting that free Mn(II) is bound to the enzyme (Sundaramoorthy *et al.*, 1994b).

Another important aspect of the MnP reaction mechanism is the location of the Mn(II) binding site. At the start of the present work, it had been proposed that the Mn(II) binding site is located near the δ-meso edge of the heme (Harris *et al.*, 1991). However, amino acid residues involved in Mn(II) binding had not been determined, nor was the crystal structure of MnP available. Therefore, site-directed mutagenesis was deemed to be the best technique for identifying the Mn(II) binding site in MnP. To conduct site-directed mutagenesis of MnP, an efficient expression system for recombinant MnP protein was

required. Attempts to produce MnP in heterologous expression systems had been of limited success. The variety of post-translational events required to produce active MnP protein extracellularly, including heme insertion, glycosylation, disulfide bond formation, and secretion of the protein, proved to be problematic for heterologous expression systems. Homologous expression, using *P. chrysosporium*, would bypass these difficulties. However, a method to distinguish recombinant protein from endogenous protein was required. In *P. chrysosporium*, MnP is expressed only during the secondary metabolic (idiophasic) stage of growth, which is triggered by depletion of nutient nitrogen (Gold & Alic, 1993; Kirk & Farrell, 1987). It has been demonstrated that *mnp* gene transcription is regulated by both nutrient nitrogen and Mn(II) ion levels (Brown *et al.*, 1990, 1991; Pribnow *et al.*, 1989). This limitation can be used to express recombinant MnP separately from endogenous MnP by placing the coding region of the *mnp* gene under the control of a primary metabolic promoter. The recombinant MnP protein is then produced under primary metabolic conditions when the endogenous *mnp* genes are not expressed. Chapter 3 describes the first homologous expression system for MnP isozyme 1. In this system, the *P. chrysosporium* glyceraldehyde-3-phosphate dehydrogenase (*gpd*) promoter is used to drive expression of the *mnp1* gene during the primary metabolic growth phase. This expression system produces recombinant MnP1 in amounts which are comparable to the endogenous MnP1 produced by the wild-type strain. Moreover, biochemical characterization suggests that the recombinant MnP is essentially identical to the wild-type enzyme. This expression system makes the generation of site-directed MnP mutants possible. Chapters 4 through 6 describe several site-directed mutants of MnP.

The characterization of Mn(II) binding site mutants of MnP is described in Chapters 4 and 5. The site-directed mutation of the Mn(II) binding site was initially conducted based on the prediction made by Johnson et al. (1993) (Figure 1.10). Subsequently, the crystal structure of MnP was solved (Sundaramoorthy *et al.*, 1994b). Although the crystal structure strongly suggested the Mn(II) binding site in MnP (Figures 1.14 and 1.15), it was not clear whether the enzyme-bound metal in the MnP crystal was a Mn(II) or whether that Mn(II) binding site was the productive site (Chapter 1.4.3). The studies on the Mn(II) binding site mutants, the D179N, E35Q, and E39Q single mutants, and the D179N-E35Q double mutant, demonstrate that the proposed Mn(II) binding site is indeed the productive site and that MnP has only one site for Mn(II) oxidation.

Although the heme environment of MnP is similar to that of other plant and fungal peroxidases, the nature of the proximal residue (Phe190 in MnP) (Figure 1.12) varies

among these peroxidases. CCP and ascorbate peroxidase have Trp residues and CIP has a Leu residue at this site. Other peroxidases such as LiP, and HRP have Phe residues. In CCP, a protein-centered radical is generated at the proximal Trp residue in CCP compound I and the Trp residue is required for electron transfer between CCP and cytochrome c, whereas ascorbate peroxidase does not generate a radical at the Trp residue and does not require the Trp residue for its catalytic activity (Chapters 1.3.2.2 and 1.3.4.1). In contrast, the role of the proximal Phe residue in MnP, LiP, and HRP is unknown. The fact that CIP has a Leu residue at this position suggests that peroxidase activity does not require an aromatic amino acid residue such as a Trp or Phe at this position. Site-directed mutagenesis of the Phe190 of MnP should enable us to understand the role of this amino acid residue for peroxidase catalysis and structure. Chapter 6 presents data pertaining to the role of the Phe190 residue with regard to the heme environment, the reactivity, and the stability of MnP protein.

In summary, this research involves the further characterization of MnP, particularly focusing on analyses of the MnP active site: the Mn(II) binding site, the nature of the substrate, and the role of an amino acid residue in the heme binding pocket. It increases our understanding of the unique function of this enzyme. This work also involves the first homologous expression and site-directed mutagenesis of MnP. These systems provide us with powerful tools for probing the structure/function relationships of MnP in detail.

CHAPTER 2

MECHANISM OF MANGANESE PEROXIDASE COMPOUND II REDUCTION. THE EFFECT OF ORGANIC ACID CHELATORS AND pH

2.1 INTRODUCTION

White rot basidiomycete fungi are primarily responsible for the initiation of the decomposition of lignin in wood (Gold *et al.*, 1989; Kirk & Farrell, 1987; Buswell & Odier, 1987). When cultured under ligninolytic conditions, the white rot fungus *Phanerochaete chrysosporium* produces two extracellular heme peroxidases, LiP and MnP, which along with an H_2O_2-generating system are major components of its lignin degradative system (Kirk & Farrell, 1987; Buswell & Odier, 1987; Tien 1987; Hammel & Moen, 1991; Wariishi et al, 1991b; Kuwahara *et al.*, 1984). MnP has been purified and characterized. The enzyme contains one iron protoporphyrin IX prosthetic group, is a glycoprotein of Mr ~46,000 and exists as a series of isoenzymes (Glenn & Gold, 1985; Paszczynski *et al.*, 1986; Leisola *et al.*, 1987; Mino *et al.*, 1988; Wariishi *et al.*, 1988; Harris *et al.*, 1991). Spectroscopic studies and cDNA sequences reveal that the heme environment of manganese peroxidase is similar to that of other plant and fungal peroxidases (Glenn & Gold, 1985; Mino *et al.*, 1988; Harris *et al.*, 1991; Dunford & Stillman, 1976; Banci *et al.*, 1992; Pribnow *et al.*, 1989; Pease *et al.*, 1989). In addition, kinetic and spectral characterization of the oxidized intermediates, compounds I and II, indicate that the catalytic cycle of MnP is similar to that of horseradish peroxidase and LiP (Gold *et al.*, 1989; Wariishi *et al.*, 1988; Renganathan & Gold, 1986; Wariishi *et al.*, 1989a; Glenn *et al.*, 1986; Wariishi *et al.*, 1992). Importantly, the enzyme oxidizes Mn(II) to Mn(III) and the latter, in turn, oxidizes phenolic substrates, including lignin model compounds (Tuor *et al.*, 1992), lignin (Wariishi *et al.*, 1991b) and chlorinated phenols (Joshi & Gold, 1993). Transient state kinetic analysis has confirmed that Mn(II)/Mn(III) acts as a redox couple rather than as an enzyme binding activator (Wariishi *et al.*, 1989a). Thus, enzymatically generated Mn(III) is utilized as a freely diffusible oxidant, enabling the enzyme to oxidize polymeric lignin within the woody

58

matrix (Wariishi *et al.*, 1988; Glenn *et al.*, 1986; Wariishi *et al.*, 1992; Tuor *et al.*, 1992; Joshi & Gold, 1993).

We previously have emphasized the importance of organic acid chelators in the manganese peroxidase system. Organic acids, including lactate, malonate and oxalate, chelate enzymatically generated Mn(III), stabilizing this species in aqueous solution (Paszczynski *et al.*, 1986; Renganathan & Gold, 1986; Wariishi *et al.*, 1989a; Demmer *et al.*, 1980), and as we shall show, ensuring the efficiency of Mn(II) oxidation. Recently, the production and secretion of oxalate and malonate by *P. chrysosporium* were demonstrated (Wariishi *et al.*, 1992; Barr *et al.*, 1992; Kuan & Tien, 1993; Dutton *et al.*, 1992). In particular, the production of millimolar concentrations of oxalate by this fungus under defined conditions was reported (Wariishi *et al.*, 1992; Barr *et al.*, 1992; Kuan & Tien, 1993; Dutton *et al.*, 1992). We previously reported that relatively high concentrations of malonate or lactate are required to stimulate optimal MnP activity (Glenn & Gold, 1985; Paszczynski *et al.*, 1986; Wariishi *et al.*, 1992); however, these high concentrations are not physiological (Wariishi *et al.*, 1992; Kuan & Tien, 1993). Recently it was shown that optimal enzyme activity is obtained in the presence of 500 μM oxalate, a concentration found in *P. chrysosporium* cultures (Kuan & Tien, 1993); a kinetic analysis was published in a subsequent paper (Kuan *et al.*, 1993). In the present study, we reinvestigated the effect of several organic acid chelators under a variety of conditions which shed light upon the behavior of both Mn(II) and Mn(III) in the MnP system. Our results confirm that physiological concentrations of oxalate stimulate the reduction of the oxidized enzyme intermediates and probably stabilize the enzyme-generated Mn(III) by chelation. In addition, we report detailed analysis of the pH dependence of the overall MnP reaction. We show that succinate exhibits a complex behavior in contrast to a report that it has little effect on the reactions of MnP (Kuan *et al.*, 1993).

2.2 MATERIALS AND METHODS

2.2.1 Chemicals

H_2O_2 (30% solution) was obtained from BDH Chemicals. *m*CPBA, 2,6-DMP, and veratryl alcohol were obtained from Aldrich. The concentration of H_2O_2 and *m*CPBA stock solutions were determined as described (Cotton & Dunford, 1973). All other chemicals were reagent grade. Solutions were prepared using deionized water obtained from a Milli Q system (Millipore).

2.2.2 Enzyme Preparation

MnP isozyme 1 was purified from the extracellular medium of acetate-buffered agitated cultures of *P. chrysosporium* strain OGC101 (Alic *et al.*, 1987) as described (Glenn & Gold, 1985; Wariishi *et al.*, 1989a). The purified enzyme was electrophoretically homogeneous and had an RZ (A_{406}/A_{280}) value of 6. The enzyme concentration was determined at 406 nm using an extinction coefficient of 129 mM^{-1} cm^{-1} (Glenn & Gold, 1985). Oxalate oxidase and horseradish peroxidase were purchased from Sigma. LiP was assayed utilizing veratryl alcohol as described (Gold *et al.*, 1989; Kirk & Farrell, 1987). MnP was routinely assayed by following the formation of Mn(III)-malonate as described (Glenn & Gold, 1985; Glenn *et al.*, 1986).

2.2.3 Oxalate Produced by *P. chrysosporium*

P. chrysosporium was grown from a conidial inoculum at 38°C in shaking cultures, with 2% glucose and 1.2 mM ammonium tartrate as the carbon and nitrogen sources, as described (Wariishi *et al.*, 1992; Kirk *et al.*, 1978). The extracellular concentration of oxalate produced in the cultures was determined via two independent methods: (i) using HPLC (Wariishi *et al.*, 1992) and (ii) using oxalate oxidase as previously described (Barr *et al.*, 1992; Kuan & Tien, 1993; Laker *et al.*, 1980) except that 2,6-DMP was used as the peroxidase substrate.

2.2.4 Kinetic and Rapid Scan Spectral Measurements

Kinetic measurements were conducted at 25.0 ± 0.5 °C using a Photal RA601 Rapid Reaction Analyzer. One reservoir contained the enzyme in water at a concentration of 2 μM for MnP compound I formation and 5 μM for compound II reduction experiments. The other reservoir contained the substrate (H_2O_2 or Mn(II)), in buffer, in at least 10 fold excess. Experiments were performed with the following buffers as indicated: K-malonate, -oxalate, -lactate, and -succinate (ionic strength 0.1 adjusted with K_2SO_4). The pH was varied from 3.34 to 6.95. The final pH of reactions was measured using an Accumet 50 pH meter (Fisher Scientific). Compound II was formed by the successive addition of 1.0 equiv of *m*CPBA and 0.9 equiv of K-ferrocyanide to the native enzyme. Compound II samples were freshly prepared for each experiment. All of the kinetic traces exhibited single exponential character from which pseudo-first order rate constants were calculated. In each kinetic experiment several substrate concentrations were used and plots of pseudo-first order rate constants versus substrate concentrations were obtained.

Rapid scan spectra were recorded on a multichannel photodiode array

(Photal RA601) equipped with a 1-cm observation cell at 25.0 ± 0.5 °C. The spectral region from 345 to 445 nm was scanned. Electronic absorption spectra obtained on a conventional time scale were recorded on a Shimadzu UV-260 or Beckman DU 650 spectrophotometer.

2.2.5 Oxidation of 2,6-Dimethoxyphenol by MnP

Oxidation of 2,6-DMP by MnP was followed spectrophotometrically at 469 nm for quinone dimer formation (Wariishi *et al.*, 1992). Reaction mixtures (1 ml) contained manganese peroxidase (0.5 µg), $MnSO_4$ (0.5 mM), 2,6-DMP (0.2 mM) and H_2O_2 (0.1 mM) in each of the buffers described above (ionic strength 0.1).

2.3 RESULTS

2.3.1 Enzyme Preparation

The effect of freeze-thaw cycles on manganese peroxidase activity was examined. One freeze-thaw cycle of the enzyme (1 mg/ml in water) resulted in an activity loss of ~12% and 5 cycles resulted in an activity loss of 50%. The freeze-thaw treated enzyme showed a similar Soret and visible absorption spectrum to the untreated enzyme. In our previous transient state kinetic study (Wariishi *et al.*, 1989a), MnP was stored frozen and the stock solution was thawed whenever enzyme was needed. Probably owing to this treatment, smaller rate constants were reported for compound I formation and compound II reduction (Wariishi *et al.*, 1989a) as compared to those found in the present study. However the previously reported kinetic features such as a saturation phenomenon and reversibility were similar to those described below. In our present work we utilized freshly prepared enzyme and eliminated freeze-thaw cycles.

2.3.2 Fungal Secretion of Oxalate and Peroxidases

A time course for oxalate and peroxidase accumulation in the extracellular medium of shaking cultures of *P. chrysosporium* is shown in Figure 2.1. Under these conditions oxalate accumulation reached a maximum of 2.4 mM on day 5 and decreased on day 6, leveling off at ~1 mM. Extracellular MnP activity also was maximal on day 5 and decreased thereafter. In contrast LiP activity first appeared on day 6, when the oxalate concentration was decreasing, and was maximal on day 8 (Figure 2.1).
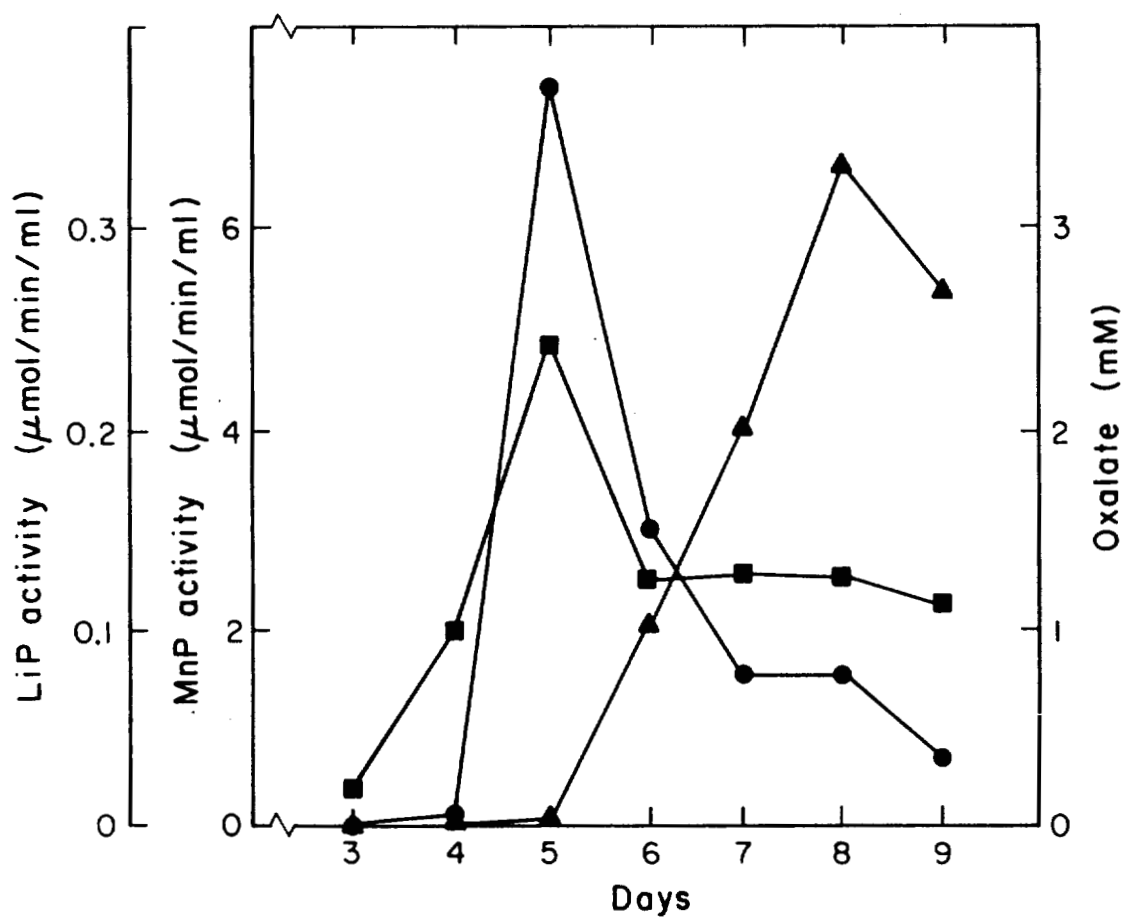
Figure 2.1. Production of manganese and lignin peroxidases and oxalate in agitated cultures of *P. chrysosporium*. Oxalate concentrations (■), and lignin (▲) and manganese peroxidase activities (●) in the extracellular medium were assayed as described in the text.

2.3.3 Effect of Chelators on the Oxidation of 2,6-DMP by MnP

The rate dependence of 2,6-DMP oxidation by Mn(III), generated by the MnP system, on the concentrations of malonate and oxalate is shown in Figure 2.2. Enzyme activity increased with increasing malonate concentration reaching a maximum at ~50 mM. Similar results were observed with lactate although the maximal activity in 50 mM lactate was ~80% of that in 50 mM malonate (data not shown). In contrast, maximum enzyme activity was observed with 2 mM oxalate. At concentrations above 2 mM, enzyme activity slowly decreased with increasing oxalate concentrations. The maximum MnP activity in 2 mM oxalate was ~90% of that in 50 mM malonate. No 2,6-DMP oxidation by manganese peroxidase was observed in reactions conducted in succinate buffer (Wariishi et al., 1992). These results are consistent with our previous studies conducted with chelator concentrations of 50 mM (Wariishi et al., 1992).

2.3.4 Reduction of Compound II in the Presence of Oxalate

When the reduction of compound II was examined at low concentrations of K-oxalate (1-5 mM), the plot of the observed rate constants versus [Mn(II)] leveled off at high [Mn(II)]. This reaction can be described by a simple binding interaction between the reactants according to Equations 1-3:
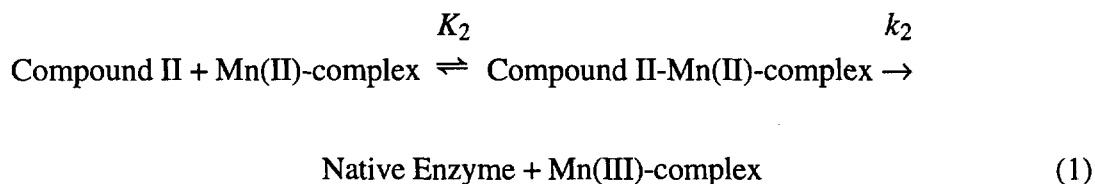
$$\text{Compound II} + \text{Mn(II)-complex} \x;\overset{K_2}{\rightleftharpoons}\; \text{Compound II-Mn(II)-complex} \overset{k_2}{\rightarrow}$$

$$\text{Native Enzyme} + \text{Mn(III)-complex} \tag{1}$$

$$k_{2obs} = \cfrac{k_2}{1 + \cfrac{K_2}{[\text{Mn(II)-complex}]}} \tag{2}$$

$$K_2 = \frac{[\text{Compound II}][\text{Mn(II)-complex}]}{[\text{Compound II- Mn(II)-complex}]} \tag{3}$$

where k_2 is a first order rate constant (s^{-1}) and K_2 is a dissociation constant (M).
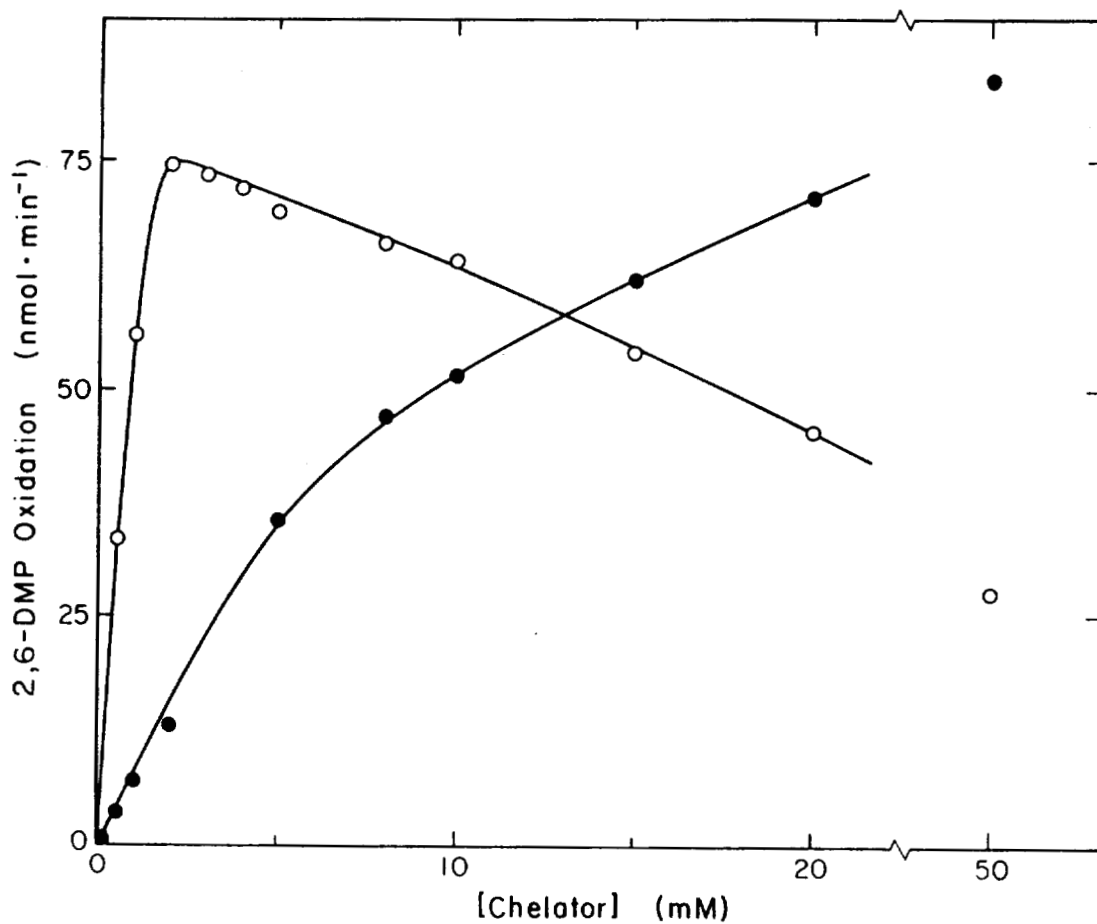
Figure 2.2. The effect of the chelator concentration on 2,6-dimethoxyphenol oxidation by MnP. Reaction mixtures contained MnP (0.5 μg/ml), MnSO$_4$ (0.5 mM), 2,6-DMP (0.2 mM), and H$_2$O$_2$ (0.1 mM) in oxalate (O) and malonate (●) at pH 4.5. The reaction was followed by measuring the increase in absorbance at 469 nm, indicating quinone dimer formation (Wariishi *et al.*, 1992).

The calculated values for k_2 and K_2 are listed in Table 2.1.

When the reaction was conducted in higher concentrations of oxalate (10 and 20 mM), the plot of observed rate constants versus Mn(II) concentration was linear and passed through the origin within experimental error (Figure 2.3), indicating that, under these conditions, the reduction of compound II obeyed second order kinetics and was irreversible. The second order rate constants were calculated from the slopes of the plots in Figure 2.3 and are listed in Table 2.1. Saturation behavior might be expected at higher concentrations of Mn(II).

2.3.5 Reduction of Compound II in Malonate and Lactate Buffers

The reduction of MnP compound II to native enzyme was followed at 406 nm in K-malonate, pH 4.60 and in K-lactate, pH 4.56, under pseudo-first order conditions with the reducing substrate, Mn(II), in excess. When the reaction was conducted in either 10 or 20 mM K-malonate, the plot of the observed rate constants (k_{2obs}) versus Mn(II) concentration leveled off at high Mn(II) concentration (Figure 2.4A) suggesting a binding interaction between reactants. In contrast, when the reaction was conducted in lower concentrations of malonate (1-5 mM), the dependence of k_{2obs} on substrate concentration (0-100 μM) was linear and the plot had a positive y-axis intercept (Figure 2.4B), suggesting that, at these concentrations, the reaction was reversible as expressed by Equations 4 and 5:

$$\text{Compound II} + \text{Mn(II)-complex} \overset{k_{2app}}{\underset{k_{-2}}{\rightleftharpoons}} \text{Native Enzyme} + \text{Mn(III)-complex} \qquad (4)$$
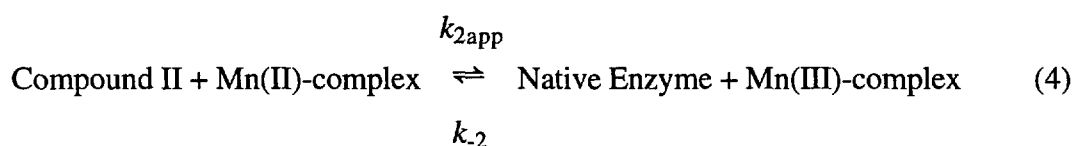
$$k_{2obs} = k_{2app}[\text{Mn(II)-complex}] + k_{-2} \qquad (5)$$

where k_{2app} is a second order rate constant for the forward reaction and k_{-2} is a first order rate constant for the reverse reaction. The kinetic parameters are summarized in Table 2.1. Similar behavior was observed in K-lactate, where saturation kinetics were observed at a 20 mM chelator concentration and a reversible reaction was observed at 2 mM (data not shown). All data are summarized in Table 2.1. Saturation kinetics for this reaction in 20 mM lactate have been reported previously (Wariishi et al., 1989a).

Table 2.1. Kinetic parameters for the reduction of MnP compound II by Mn(II) in several different organic acid chelators. Data obtained by fits to the plots of the pseudo-first order rate constant, k_{obs}, vs. [Mn(II)].

Organic acid (pH)	Conc.	Hyperbolic[a]		Linear[b]	
		First order rate const.	Equilibrium dissociation const.	Forward second order rate const.	Reverse First order rate const.
	mM	s^{-1}	M	$M^{-1}s^{-1}$	s^{-1}
Oxalate (4.62)	1	$(2.3 \pm 0.2) \times 10^2$	$(5.6 \pm 1.0) \times 10^{-5}$	--	--
	2	$(2.9 \pm 0.1) \times 10^2$	$(8.7 \pm 0.7) \times 10^{-5}$	--	--
	5	$(5.6 \pm 0.6) \times 10^2$	$(4.4 \pm 0.6) \times 10^{-4}$	--	--
	10	--	--	$(6.2 \pm 0.2) \times 10^5$	--
	20	--	--	$(3.3 \pm 0.1) \times 10^5$	--
Malonate (4.60)	1	--	--	$(1.8 \pm 0.1) \times 10^5$	$(1.8 \pm 0.1) \times 10$
	2	--	--	$(6.0 \pm 0.1) \times 10^5$	$(2.1 \pm 0.1) \times 10$
	5	--	--	$(9.1 \pm 0.4) \times 10^5$	$(2.1 \pm 0.2) \times 10$
	10	$(3.6 \pm 0.3) \times 10^2$	$(1.9 \pm 0.2) \times 10^{-4}$	--	--
	20	$(8.9 \pm 0.5) \times 10^2$	$(1.9 \pm 0.1) \times 10^{-4}$	--	--
Lactate (4.56)	2	--	--	$(3.9 \pm 0.2) \times 10^5$	$(2.3 \pm 0.1) \times 10$
	20	$(1.2 \pm 0.3) \times 10^3$	$(9.0 \pm 0.3) \times 10^{-4}$	--	--
Succinate I[c] (4.58)	20	$(5.5 \pm 0.6) \times 10$	$(2.4 \pm 0.9) \times 10^{-5}$	--	--
II		--	--	$(6.7 \pm 0.7) \times 10^4$	6.9 ± 0.4
III		$(2.3 \pm 0.3) \times 10^{-1}$ [d]	--	--	--

[a] A nonlinear least square fit was applied to the data showing saturation kinetics.

[b] A linear least square fit was applied to the data showing a linear relationship.

[c] The reduction of compound II by Mn(II) in succinate occurred via triphasic kinetics (Figure 2.5).

[d] The first order rate for the phase III reaction was [Mn(II)] independent (Figure 2.6C).
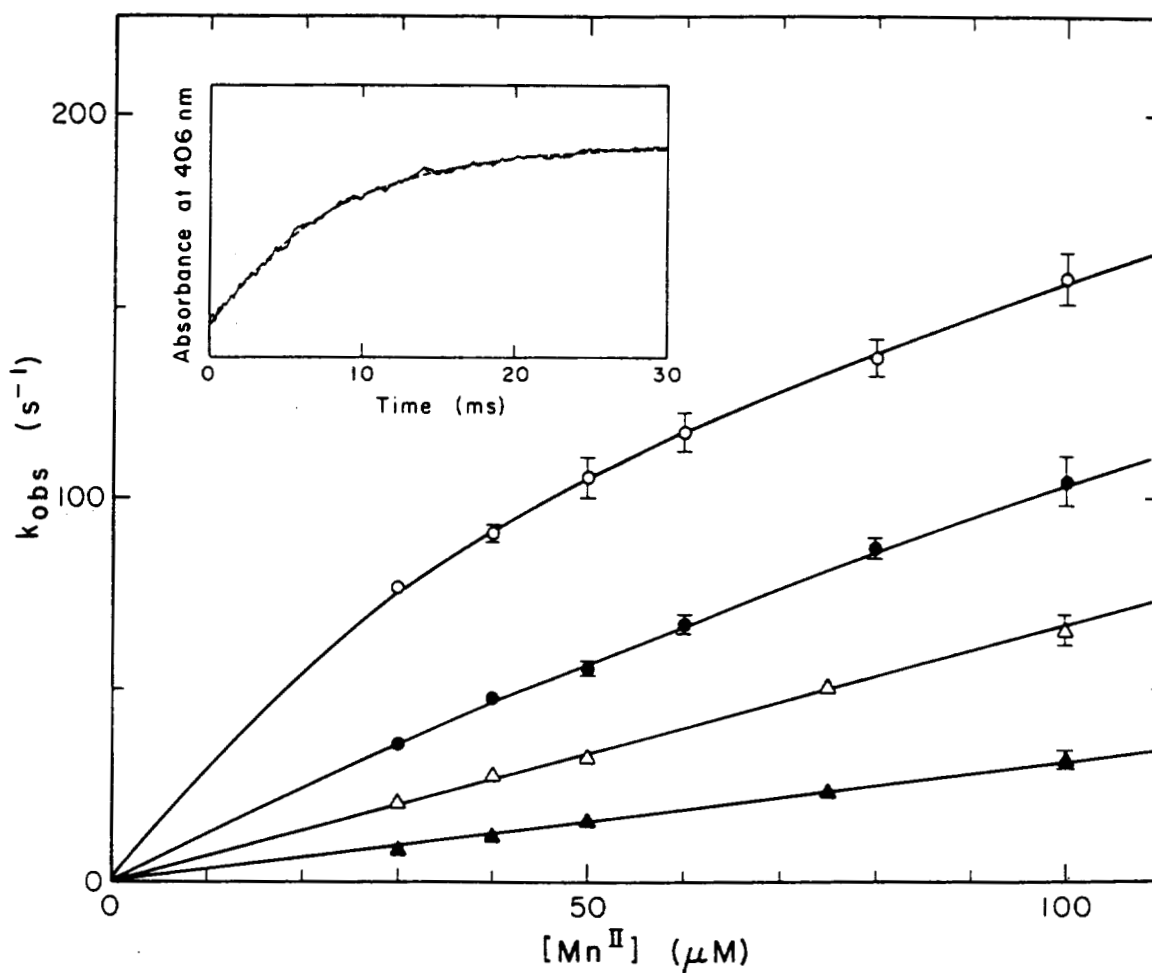
Figure 2.3. Reduction of manganese peroxidase compound II by Mn(II) in oxalate at pH 4.62. Observed pseudo-first order rate constants were plotted against [Mn(II)] at 2 mM (O), 5 mM (●), 10 mM (Δ) and 20 mM (▲) oxalate. *Inset* shows a typical kinetic trace for the reduction of compound II by Mn(II) (50 µM) in 2 mM oxalate, showing single exponential character from which a pseudo-first order rate constant was calculated. 5 µM MnP converted to compound II as described in text, ionic strength 0.1 M.
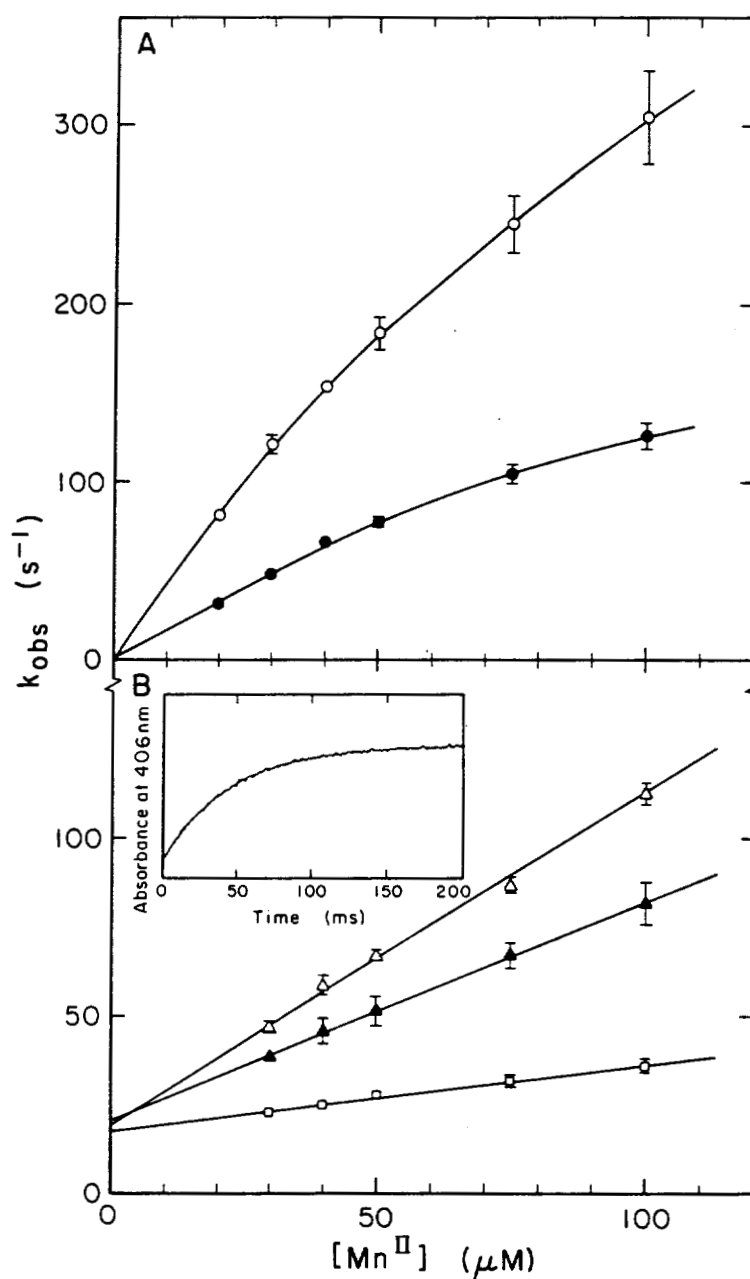
Figure 2.4. Reduction of MnP compound II by Mn(II) in malonate at pH 4.60. Observed pseudo-first order rate constants were plotted against [Mn(II)] at 10 mM (●) and 20 mM (O) malonate (A); and at 1 mM (□), 2 mM (▲) and 5 mM (Δ) malonate (B). Reaction conditions were as described in the text. *Inset*; a typical trace at 406 nm of compound II reduction by 75 μM Mn(II) in 5 mM malonate. The curve exhibited single exponential character. Concentration of enzyme 5 μM, ionic strength 0.1.

2.3.6 Reduction of Compound II in Succinate Buffer

The reduction of compound II by Mn(II) also was carried out in 20 mM K-succinate (pH 4.58), which does not chelate Mn(III) readily (Wariishi *et al.*, 1989a; Wariishi *et al.*, 1992; Demmer *et al.*, 1980). The resultant kinetic traces exhibited a triphasic character (Figure 2.5). The plots of k_{obs} versus Mn(II) concentration for each reaction phase are shown in Figure 2.6. The first phase of the reaction (phase I) displayed saturation kinetics (Figures 2.5 and 2.6). In the second phase (phase II), k_{obs} was linearly dependent on Mn(II) concentration and the plot had a positive y-intercept (Figure 2.6), suggesting that the reduction of compound II in phase II was reversible. Approximately 60% of compound II was converted to native enzyme in phases I and II. In the third phase of the reaction (phase III), k_{obs} values were independent of the Mn(II) concentration in the range 20 to 100 μM (Figure 2.6). The kinetic parameters listed in Table 2.1 show that the rates for the reactions carried out in succinate buffer are slower than the rates in other buffers. The rate for the phase III reaction in succinate is particularly slow.

The rapid scan spectrum for the conversion of compound II to native enzyme in K-succinate displayed an apparent isosbestic point at 417 nm (data not shown). This isosbestic point also was observed in the conversion of compound II to native MnP by Mn(II) in malonate, lactate, and oxalate (data not shown). Thus, the triphasic plot for reactions carried out in succinate apparently was not caused by the contamination of compound II with compound I or with unreacted *m*CPBA. Our results with succinate are in contrast to an earlier report that succinate has little effect on the reaction (Kuan *et al.*, 1993).

2.3.7 pH Dependence of Compound II Reduction

The pH dependence of the reduction of compound II by Mn(II) also was examined. At low Mn(II) concentrations, k_{2obs} was linearly proportional to Mn(II) concentration in reactions carried out in 2 mM oxalate and in 20 mM malonate (Figure 2.3 and 2.4). Therefore, the k_{app} at low Mn(II) concentrations (20-30 μM) was measured over the pH range of 3.34-6.95. For these experiments k_{2obs} was measured using 6 different Mn(II) concentrations in 20 mM malonate at pH 3.53, 4.60, 4.99, and 5.99. All reactions displayed saturation kinetics with no apparent reverse reaction (data not shown). The pH dependence of k_{app} (k_{2obs}/[Mn(II)]) for compound II reduction is shown in Figure 2.7. Maximum rates were obtained at pHs 5.0 and 5.4 in 2 mM oxalate and 20 mM malonate, respectively. The pH profiles for compound II reduction by Mn(II) (Figure 2.7) were
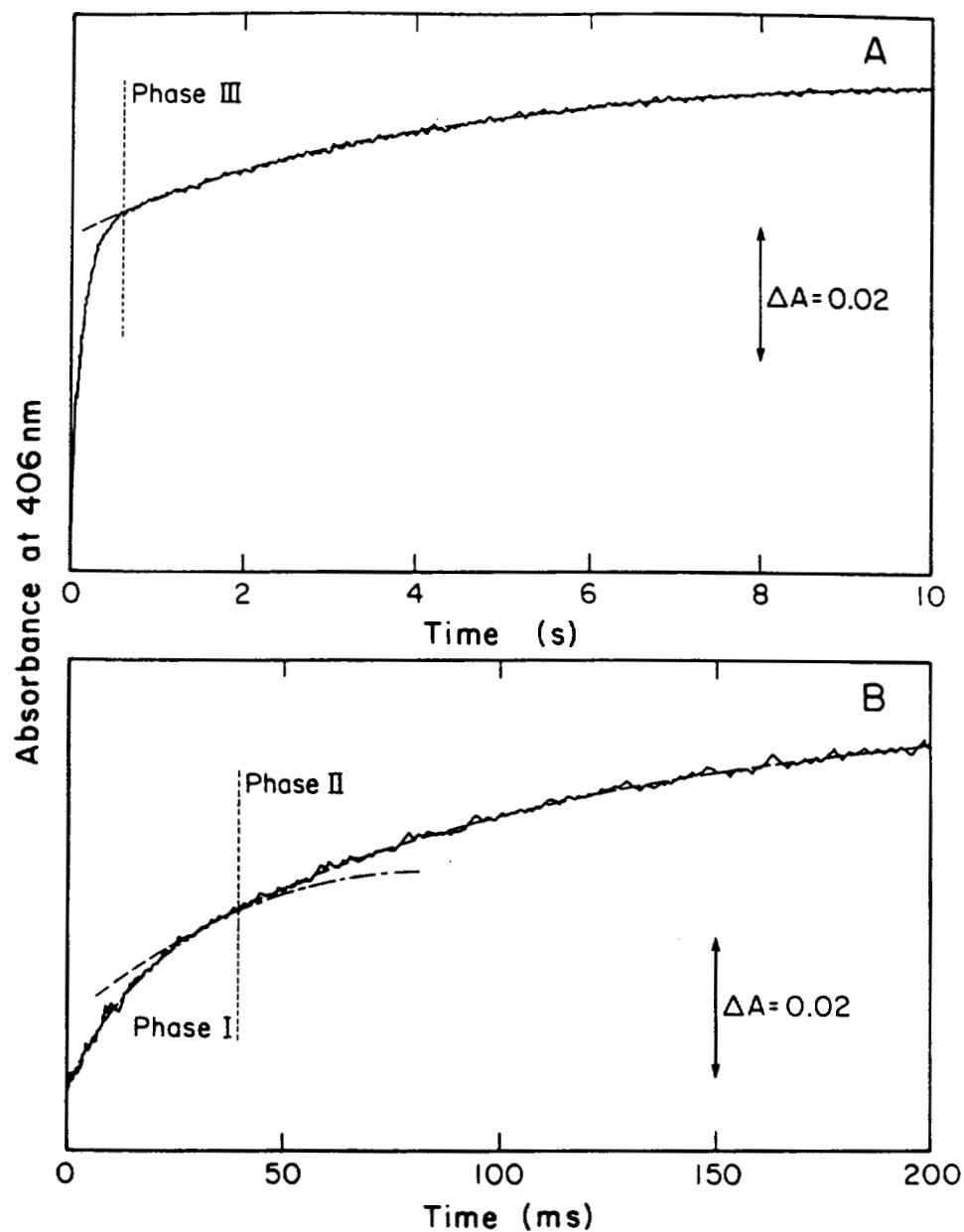
Figure 2.5. Time course of the reduction of MnP compound II by Mn(II) in succinate. (A) Kinetic trace for the reduction of compound II by Mn(II) (50 μM) in 20 mM succinate, pH 4.58. The sampling period was 10 s. (B) The same as (A) except a sampling period of 200 ms was used. Dashed lines are computer-fitted single exponential curves from which observed pseudo-first order rate constants were calculated for each phase of the triphasic reaction.
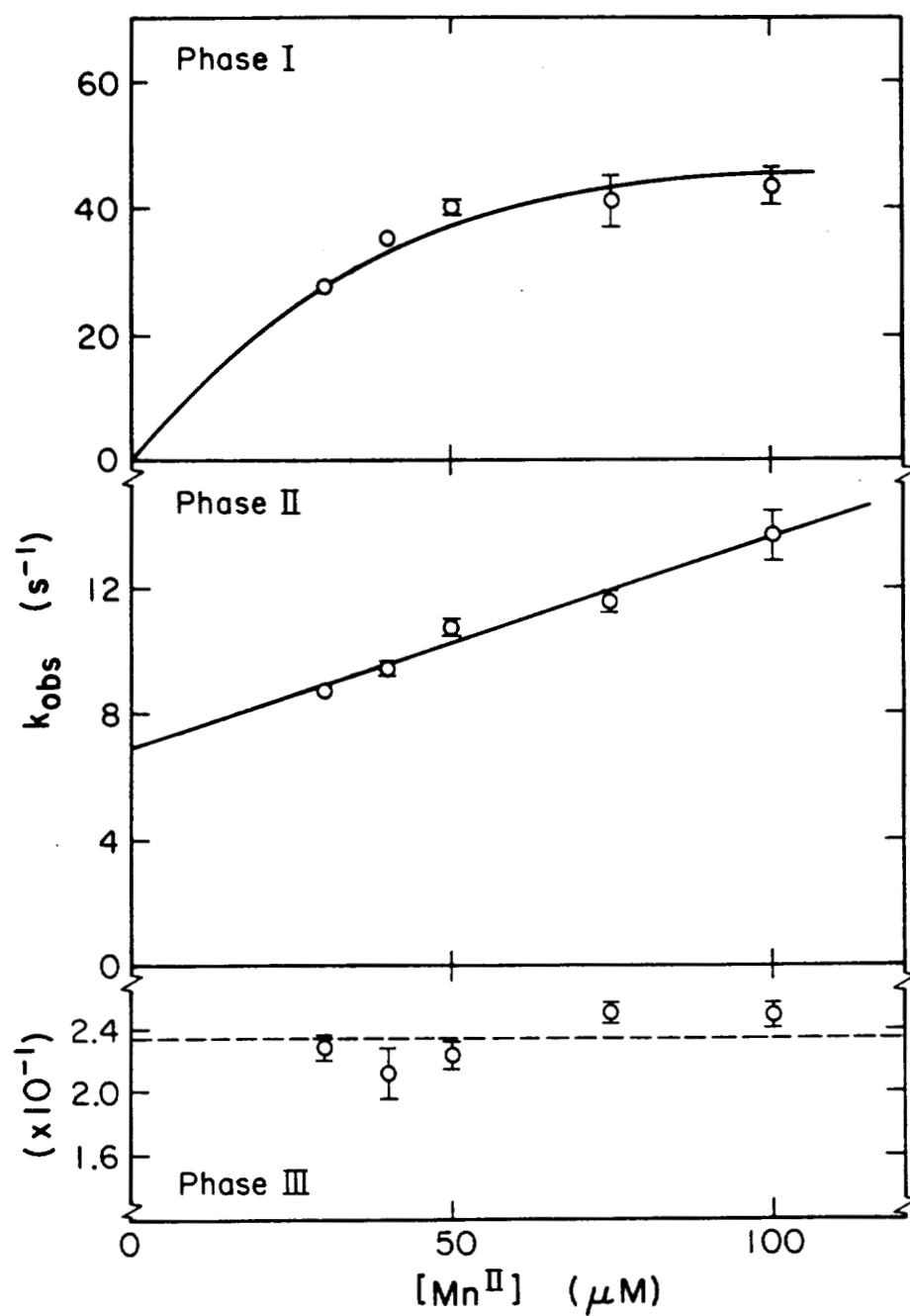
Figure 2.6. Reduction of MnP compound II by Mn(II) in succinate at pH 4.58. Analysis of each phase of the tri-phasic reaction. Observed pseudo-first order rate constants k_{obs} are plotted against [Mn(II)] for each of phases I, II, and III.
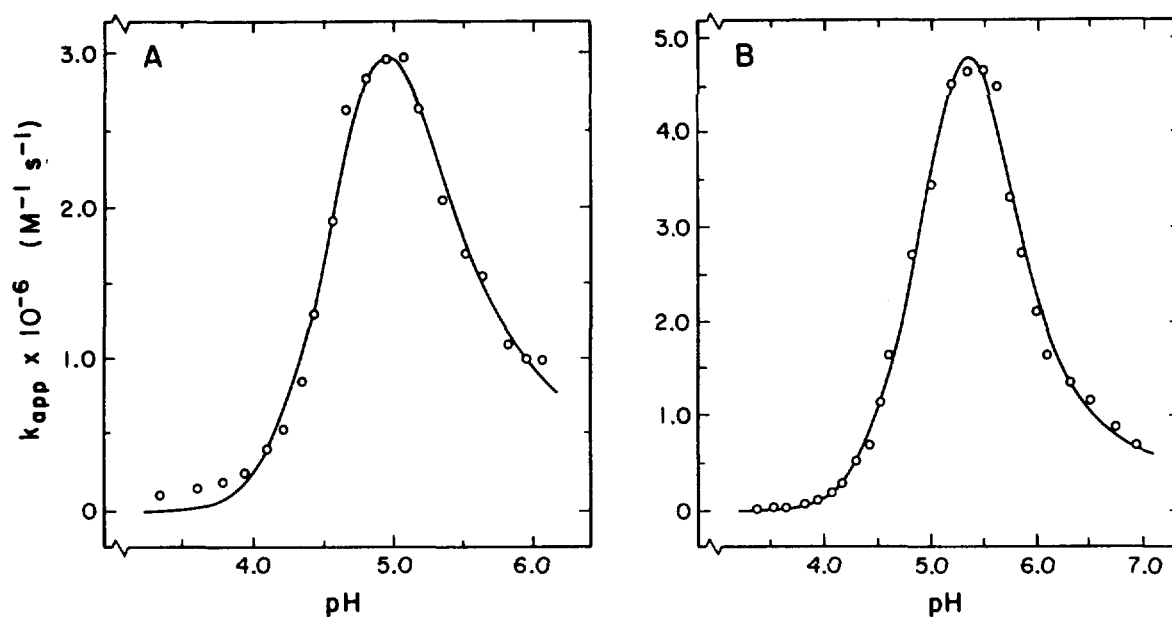
Figure 2.7. pH dependence of the reduction of MnP compound II by Mn(II) in oxalate and malonate. Observed pseudo-first order rate constants divided by [Mn(II)] generated second order rate constants which are plotted as a function of pH. The solid curves are calculated on the basis of two rate constants, two ionization constants on the enzyme and one ionization constant of the chelator. All parameters have the same value for both curves within experimental error, except the constants calculated for the chelators: pK values of 4.5 and 5.6 for oxalate and malonate, which agree within experimental error with their pK_{a2} values. (A) Reduction of MnP compound II in 2 mM oxalate, pH 4.62; (B) Reduction of MnP compound II in 20 mM malonate, pH 4.60.

similar to those for oxidation of 2,6-DMP (data not shown).

2.3.8 pH Dependence of 2,6-DMP Oxidation

The pH profiles for 2,6-DMP oxidation by Mn(II), produced by the action of MnP, exhibited maxima at pH 4.56 in 2 mM oxalate and at pH 4.60 in 20 mM malonate (data not shown). Above the optimal pH the decrease in MnP activity was steeper in oxalate than in malonate. In contrast, below the optimal pH the decrease in MnP activity was steeper in malonate than in oxalate. These differences suggest that organic acid chelators may be controlling the pH dependence of the reactions.

2.3.9 Rate of Compound I Formation

The rate of MnP compound I formation from native enzyme and H_2O_2 was determined at pH 4.6 in oxalate, malonate, lactate and succinate buffers. Compound I formation was measured at 397 nm, the isosbestic point between compounds I and II, excluding interference from the possible conversion of compound I to II. Each trace displayed single exponential character. The observed rate constants (k_{1obs}) were linearly proportional to the H_2O_2 concentrations at 10 to 50 fold excess. The second order rate constants (k_{1app}) for compound I formation (Table 2.2) were not affected by the type or concentration of the organic acid.

2.4 DISCUSSION

We have confirmed (Wariishi *et al.*, 1989a) that the reduction rate for MnP compound I by Mn(II) is >20 times faster than that for compound II (data not shown). Therefore, provided sufficient hydroperoxide is present, the rate determining step in the catalytic cycle is the reduction of compound II to native enzyme. Using only 1.0 equiv of *m*CPBA and 0.9 equiv of ferrocyanide to generate compound II assures a single turnover. Thus the rate of compound II reduction can be measured directly at 406 nm, the Soret maximum for native MnP.

2.4.1 Effect of Chelators on MnP Compound II Reduction

2.4.1.1 Oxalate

In oxalate, the pseudo-first order rate constant k_{obs} for compound II reduction decreases as the concentration of the chelator increases beyond 2 mM (Figure 2.3), which

Table 2.2 Rate of formation of Manganese Peroxidase Compound I in the presence of several different chelators

Organic acid (pH)	Concentration mM	k_{app}[a] $M^{-1}s^{-1}$
Oxalate (4.62)	2	$(3.9 \pm 0.1) \times 10^6$
	20	$(3.8 \pm 0.1) \times 10^6$
Malonate (4.60)	2	$(3.6 \pm 0.2) \times 10^6$
	20	$(3.6 \pm 0.1) \times 10^6$
Lactate (4.56)	2	$(3.6 \pm 0.5) \times 10^6$
	20	$(3.6 \pm 0.3) \times 10^6$
Succinate (4.58)	2	$(3.4 \pm 0.4) \times 10^6$
	20	$(3.8 \pm 0.1) \times 10^6$

[a]MnP Compound I formation was followed at 397 nm, the isosbestic point between compounds I and II. Traces showed single exponential character from which pseudo-first order rate constants were calculated. These rate constants were linearly proportional to [H_2O_2] with zero intercept.

is consistent with the effect of oxalate concentration on the MnP oxidation of 2,6-DMP (Figure 2.2). A plausible explanation is that the dioxalate complex of Mn(II) binds less well to the enzyme than the monooxalate complex. At low concentrations (1, 2, and 5 mM) of oxalate, plots of k_{obs} versus Mn(II) concentration are hyperbolic, requiring the introduction of a binding constant to fit the data quantitatively (Equations 1-3). In contrast, at higher concentrations of oxalate, the reaction does not show saturation phenomenon (Figure 2.3). If the dioxalate complex of Mn(II) is oxidized, then Mn(III) may be released faster since further chelation is apparently not required. However, at sufficiently high concentrations of Mn(II), one would expect the linear plots of k_{obs} versus Mn(II) concentration at 20 mM oxalate to exhibit curvature, showing the same behavior observed at lower oxalate concentrations. Thus the data displayed in Figure 2.3 are consistent with a smooth transition from lowest to highest chelator concentration. In contrast to the results obtained with malonate and lactate, the reduction of compound II by Mn(II)-oxalate shows saturation kinetics at low concentrations of oxalate (Figure 2.3). Furthermore, at either low or high concentrations of oxalate the reduction of compound II is irreversible.

2.4.1.2 Malonate and Lactate

The value of k_{obs} for compound II reduction increases with increasing concentration of malonate (Figure 2.4), consistent with the effect of malonate on the oxidation of 2,6-DMP (Figure 2.2). At high concentrations of malonate (10 and 20 mM) the plots of k_{obs} versus Mn(II) concentration are hyperbolic (Figure 2.4A). Nonlinear saturation responses have been observed previously for the reactions of MnP compounds I and II with Mn(II) in lactate (Wariishi et al., 1989a), for the reductions of horseradish peroxidase compounds I and II with p-cresol (Hewson & Dunford, 1976; Critchlow & Dunford, 1972a) and p-aminobenzoic acid (Dunford & Cotton, 1975), and for the reduction of LiP compound II with veratryl alcohol (Wariishi et al., 1991a). This can be attributed to the binding interaction between the enzyme and substrate followed by enzyme reduction (Equations 1-3). In contrast, when the reaction is conducted in low concentrations of malonate (Figure 2.4B), plots of k_{obs} versus [Mn(II)] are linear. These differences imply different lifetimes for the compound II- Mn(II) complex dependent upon the concentration of malonate. Furthermore, at low concentrations of malonate the reaction is reversible and the rate of the reverse reaction is essentially independent of malonate concentration (1, 2, and 5 mM). These differences in the kinetic features of the reaction at high and low chelator concentrations also are observed for compound II reduction in lactate (Table 2.1). The reversibility of the reaction in low malonate and lactate concentrations

may be explained as follows. At low concentrations of malonate and lactate, the Mn(III) produced by compound II may not be chelated effectively and thus is not stabilized. Owing to the high redox potential of the Mn(II)/Mn(III) couple in water (1.54 eV), reoxidation of native enzyme to compound II by Mn(III) may occur. The single-step, one-electron oxidation of native horseradish peroxidase to compound II by the $[IrCl_6]^{3-}/[IrCl_6]^{2-}$ couple, which has a reduction potential of 0.93 V, has been reported (Hayashi & Yamazaki, 1979).

2.4.1.3 Succinate

The rate of reduction of compound II in succinate is triphasic. Three successive exponential curves are observed when absorbance change is plotted versus time, with the rate becoming progressively slower (Figure 2.5). As shown in Figure 2.6, the phase I reaction exhibits saturation kinetics with excess Mn(II). In phase II, the plot of k_{obs} versus Mn(II) is linear with a finite intercept. In phase III of the reaction in succinate, the values of k_{obs} are extremely low ($\sim 2.4 \times 10^{-1}$ s^{-1}) and independent of Mn(II) concentrations in the range from 20 to 100 μM (Figure 2.6). The reverse reaction, the oxidation of native enzyme to compound II by Mn(III), seems to occur with weak chelators such as succinate (Wariishi et al., 1989a; Demmer et al., 1980) which apparently are unable to form a stable complex with Mn(III). The lack of 2,6-DMP oxidation by MnP in succinate (Wariishi et al., 1992) can be explained by this ineffective chelation and hence stabilization of Mn(III) (Wariishi et al., 1988).

2.4.2 pH Dependence of Compound II Reduction and 2,6-DMP Oxidation

The pH optimum for oxidation of phenolic substrates by MnP is ~4.5 (Glenn & Gold, 1985; Paszczynski et al., 1986; Glenn et al., 1986; Aitken & Irvine, 1990), despite a higher reactivity of Mn(III) complexes at lower pHs (Glenn et al., 1986; Demmer et al., 1980), suggesting that the pH dependency is at least partially controlled by enzyme bound ionizable groups. Compound II reduction is usually rate-controlling. Therefore in order to elucidate the factors involved we have examined the pH dependence of compound II reduction in the presence of malonate and oxalate.

For the reduction of compound II by Mn(II), the plots of k_{app} vs pH in 2 mM oxalate and 20 mM malonate both exhibit a sharp peak at the pH optimum (Figure 2.7). The optimum is pH 5.0 in oxalate and pH 5.4 in malonate, both of which are slightly higher than the optimal pH for oxidation of 2,6-DMP in the same buffers (pH 4.56 and pH 4.6 for oxalate and malonate respectively). The lower pH optimum for the oxidation of

2,6-DMP may be a result of the low pH optimum for the reaction of Mn(III)-complexes with aromatic substrates. For example, a pH optimum of 2.5 has been reported for the oxidation of aromatic substrates by Mn(II)-lactate (Glenn *et al.*, 1986).

Plots of the pH dependence of compound II reduction in both oxalate and malonate display at least two inflection points. When the logarithm of k_{app} is plotted against pH, a linear region with a slope of ~1.6 is obtained in the pH range 4-5 for both oxalate and malonate. If a single kinetically important ionization occurs, a slope of 1.0 would be expected (Hayashi & Yamazaki, 1979); however the value of $\log(k_{app})$ increases more rapidly with increasing pH. This observation strongly suggests an additional important ionization in the region where rate increases with increasing pH. The inflection point at higher pH where the rate is decreasing implies a role for another acid group. Thus three kinetically important ionizations may be involved in the pH range shown in Figure 2.7. A non-linear least squares program was applied to the data in Figure 2.7, in which three acid dissociation constants (two for the enzyme, K_{E1} and K_{E2}, and one for the chelator) and three rate constants were introduced as adjustable parameters. It turned out that only two rate constants were required, the value for the third was negligible. All parameters except that for the chelator were essentially the same within experimental error for both oxalate and malonate (Figure 2.7A and B) and are as follows: $pK_{E1} = 6.1 \pm 0.5$, $pK_{E2} = 3.4 \pm 0.5$, $k_1 = (4.6 \pm 1.0) \times 10^5$ $M^{-1}s^{-1}$ and $k_2 = (1.8 \pm 0.6) \times 10^8$ $M^{-1}s^{-1}$, with the most acid form of the enzyme being most reactive and the most basic form unreactive. The values for the chelators are $pK = 4.5 \pm 0.2$ for oxalate and 5.6 ± 0.5 for malonate; these are the same within experimental error as the pK_{a2} values for these chelators (4.28 for oxalate and 5.69 for malonate). Undoubtedly ionizations of oxalate and malonate affect their chelating ability. Specific assignment of dissociation constants to acid groups in the enzyme active site would be premature.

2.4.3 Compound I Formation Rate and Effect of Chelators

The primary reaction product of peroxidases with H_2O_2 is the oxidized intermediate compound I. MnP compound I is similar to other peroxidase compounds I in its spectral features and in the activation energy for its formation (Wariishi *et al.*, 1988; Dunford & Stillman, 1976; Renganathan & Gold, 1986; Wariishi *et al.*, 1989a; Marquez *et al.*, 1988; Hewson & Dunford, 1975; Andrawis *et al.*, 1988; Job *et al.*, 1978). We have shown that the second order rate constant for MnP compound I formation with H_2O_2 as the substrate is independent of pH over the range 3.1-8.3 (Wariishi *et al.*, 1989a).

In this study, utilizing a better enzyme preparation, we confirm that the compound I formation rate (k_{1app}) is independent of pH (data not shown) and that k_{1app} is twice as large as that which we reported previously (Table 2.2) (Wariishi et al., 1989a). In addition, the value of k_{1app} is independent of both the type and the concentration of the organic acid chelator (Table 2.2), suggesting that both the pH and chelator dependencies of MnP reactions (Figures 2.2 and 2.7) (Glenn & Gold, 1985; Wariishi et al., 1988; Glenn et al., 1986) are dictated by effects on the reductions of MnP compounds I and II.

2.4.4 General Discussion

Kinetic and inhibition studies suggest that MnP has a single binding site for Mn(II) in the vicinity of the heme (Harris et al., 1991; Wariishi et al., 1992) and that Mn(II) is the substrate for the enzyme (Harris et al., 1991; Wariishi et al., 1989a; Wariishi et al., 1992). The catalytic activity of MnP is stimulated dramatically by C_2 and C_3 dicarboxylic or α-hydroxy acids such as oxalate, malonate and lactate (Glenn & Gold, 1985; Wariishi et al., 1988; Glenn et al., 1986; Wariishi et al., 1992; Kuan & Tien, 1993; Kuan et al., 1993). These organic acid chelators (i) stabilize Mn(III) in aqueous solution (Wariishi et al., 1988; Wariishi et al., 1989a; Glenn et al., 1986), and (ii) chelate Mn(II).

Under ligninolytic conditions, P. chrysosporium secretes several organic acid metabolites including oxalate, malonate, citrate and glyoxylate (Wariishi et al., 1992; Barr et al., 1992; Kuan & Tien, 1993; Dutton et al., 1992). Oxalate, a common secondary metabolite of wood-rotting basidiomycetes (Takao, 1965), is the major organic acid secreted by this fungus (Figure 2.1) (Wariishi et al., 1992; Barr et al., 1992; Kuan & Tien, 1993; Dutton et al., 1992). Furthermore, oxalate is the only organic acid secreted at the concentrations required to stimulate MnP (Kuan & Tien, 1993). Maximal production of oxalate and MnP occur simultaneously in agitated cultures of P. chrysosporium (Figure 2.1). Furthermore, maximal enzyme activity is observed with 2 mM oxalate, approximately the maximal oxalate concentration secreted by the fungus in agitated culture (Figures 2.1 and 2.2). In contrast, maximal MnP activity requires 50 mM malonate (Figure 2.2) (Wariishi et al., 1992) although the concentration of malonate secreted by this organism in agitated cultures is approximately 20-30 μM (Wariishi et al., 1992). High concentrations (> 20 mM) of the C_2 acids glyoxylate (2-oxoacetate) and glycolate (2-hydroxy-acetate) also are required to stimulate the enzyme maximally (data not shown). Recently, others have observed maximal MnP activity with 500 μM oxalate (Kuan & Tien, 1993) although we observe optimal activity at ~2 mM

oxalate (Figure 2.2). This suggests that oxalate is the physiologically relevant chelator (Barr et al., 1992; Kuan & Tien, 1993; Dutton et al., 1992). This led us in the present study to examine the effect of several organic acid chelators and pH on various steps in the manganese peroxidase catalytic cycle in order to better understand the unique effects of oxalate.

While optimal activity is observed at higher concentrations (>10 mM) of malonate and lactate, oxalate stimulates MnP optimally at low physiological concentrations (1-2 mM) (Table 2.1). In addition, at low concentrations of malonate and lactate, the reverse reaction (native enzyme oxidation to compound II) occurs. In contrast, this reverse reaction is not observed at any concentration of oxalate. Since the C_2 acids glyoxalate and glycolate exhibit behavior similar to malonate, our results suggest that oxalate may act in a unique manner. It is possible that the binding of C_3 chelators is sterically hindered. Furthermore, the C_2 chelators glyoxalate and glycolate are less effective chelators than oxalate. Thus only oxalate is able to facilitate effectively the chelation and stabilization of Mn(III), resulting in optimal activity at relatively low oxalate concentrations. At high oxalate concentrations, a higher degree of Mn(II) complexation occurs (Demmer et al., 1980; Taube, 1948), suggesting that dichelated Mn(II) is not a good substrate. At the physiological concentration of oxalate, Mn(III) forms a dioxalate complex, whereas Mn(II) is mono-chelated (Demmer et al., 1980; Taube, 1948).

A mono-oxalate complex of Mn(II) (Kuan et al., 1993), rather than aquo- Mn(II) as previously suggested (Wariishi et al., 1992), reacts with oxidized forms of MnP. However, our data suggest that Mn(III) is released from the enzyme in its dichelated form. Thus further chelation apparently occurs after oxidation of Mn(II) to Mn(III). Our results on compound I formation rates indicate that chelators do not bind directly to the iron(III) of the native enzyme. This does not preclude a binding site close to the heme. Inhibition of Mn(III) reactions with other oxidizable molecules by higher concentrations of oxalate is probably caused by a higher degree of chelation of Mn(II) making it less reactive.

With our present state of knowledge a satisfactory mechanism for compound II reduction by Mn(II) in the presence of oxalate is shown in Equations 6 and 7:

$$\text{Compound II} + \text{Mn(II) (mono-chelated)} \xrightarrow{\text{slow}} \text{Native MnP} + \text{Mn(III) (mono-chelated)} \quad (6)$$

$$\text{Mn(III) (mono-chelated)} + \text{Chelator} \xrightarrow{\text{fast}} \text{Mn(III) (di-chelated)} \quad (7)$$
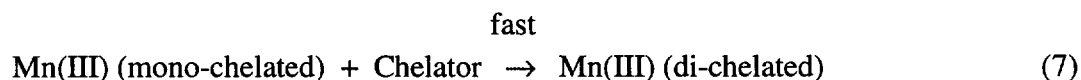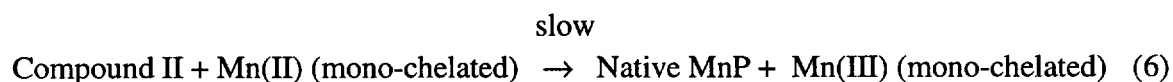
CHAPTER 3

HOMOLOGOUS EXPRESSION OF RECOMBINANT MANGANESE PEROXIDASE IN *PHANEROCHAETE CHRYSOSPORIUM*

3.1 INTRODUCTION

The white-rot basidiomycete *Phanerochaete chrysosporium* has been the focus of numerous studies on the degradation of lignin (Buswell & Odier, 1987; Gold *et al.*, 1989; Kirk & Farrell, 1987) and aromatic pollutants (Bumpus & Aust, 1987; Hammel, 1989; Joshi & Gold, 1993). Two families of extracellular peroxidases, manganese peroxidase (MnP) and lignin peroxidase (LiP), along with an extracellular H_2O_2-generating system, are thought to be the major components of this organism's extracellular lignin-degrading system (Gold & Alic, 1993; Gold *et al.*, 1989; Kirk & Farrell, 1987). Significantly, both LiP and MnP depolymerize synthetic lignins *in vitro* (Hammel *et al.*, 1993; Wariishi *et al.*, 1991b). Furthermore, MnP has been detected in cultures of essentially all white-rot fungi which efficiently degrade lignin (Hatakka, 1987; Orth *et al.*, 1993; Périé & Gold, 1991). MnP has been purified and extensively characterized (Glenn & Gold, 1985; Gold & Alic, 1993; Gold *et al.*, 1989; Kishi *et al.*, 1994; Kuan & Tien, 1993; Paszczynski *et al.*, 1986; Wariishi *et al.*, 1988). The enzyme oxidizes Mn(II) to Mn(III). The latter, complexed with an organic acid chelator such as oxalate, secreted by *P. chrysosporium*, oxidizes the substrates either directly, as in the case of lignin and phenolic lignin model compounds (Tour *et al.*, 1992; Wariishi *et al.*, 1991b), or possibly through the mediation of organic radicals (Moen & Hammel, 1994; Wariishi *et al.*, 1989b). MnP occurs as a series of isozymes encoded by a family of genes and the sequences of cDNA and genomic clones encoding two MnP isozymes have been determined (Godfrey *et al.*, 1990; Gold & Alic, 1993; Mayfield *et al.*, 1994a). These studies, as well as spectroscopic and kinetic studies (Banci *et al.*, 1993; Kishi *et al.*, 1994; Mino *et al.*, 1988), indicate that the heme environment of MnP is similar to that of other plant and fungal peroxidases (Dunford & Stillman, 1976). The crystal structure of LiP has been reported (Piontek *et al.*, 1993; Poulos *et al.*, 1993) and studies on the crystal structure of MnP are in progress

80

(Sundaramoorthy *et al.*, 1994a).

Efficient expression systems for recombinant MnP (rMnP) and LiP are required for structure/function studies with these enzymes. To our knowledge, the successful expression of MnP or LiP in heterologous prokaryotic or eukaryotic microbial systems has not been achieved. Although the heterologous expression of these proteins has been achieved in the baculovirus system (Johnson & Li, 1991; Pease *et al.*, 1991), the latter has several disadvantages including a relatively high cost as compared to microbial systems, a relatively low yield of recombinant protein, and an apparent requirement for exogenous heme for optimal expression. In *P. chrysosporium*, the various isozymes of MnP and LiP are expressed only during the secondary metabolic (idiophasic) stage of growth, which is triggered by depletion of nutrient nitrogen (Gold & Alic, 1993; Kirk & Farrell, 1987). Previously we demonstrated that *mnp* gene transcription is regulated by both nutrient nitrogen and Mn ion levels (Brown *et al.*, 1991; Gold & Alic, 1993; Pribnow *et al.*, 1989). In this report we describe the first homologous expression system for MnP, wherein the coding region of the *mnp1* gene was placed under the control of the *P. chrysosporium* glyceraldehyde-3-phosphate dehydrogenase (*gpd*) primary metabolic promoter.

3.2 MATERIAL AND METHODS

3.2.1 Organisms

P. chrysosporium wild-type strain OGC101, auxotrophic strain OGC107-1 (Ade1) and prototrophic transformants were maintained as described previously (Alic *et al.*, 1990). *Escherichia coli* XL1-Blue and DH5αF′ were used for subcloning plasmids.

3.2.2 Cloning and Sequencing the *P. chrysosporium gpd* Gene

Plaque lifts from a *P. chrysosporium* λEMBL3 genomic library (Godfrey *et al.*, 1990) were probed with a 1.8 kb *Sca*I fragment from the *Aspergillus nidulans gpdA* gene in the plasmid pAN5-22 (Punt *et al.*, 1988). Heterologous hybridizations were carried out at 28°C with washing at 34°C as previously described (Alic *et al.*, 1991). Fourteen positive clones were analyzed by Southern blotting of restriction digests to select a clone which appeared to include the entire *P. chrysosporium gpd* gene. A 5.8-kb *Pst*I fragment identified by further Southern analysis was subcloned into BluescriptII SK+ (Stratagene). Using exonuclease III to generate overlapping deletion subclones (Henikoff, 1987), 3.2 kb of the clone was sequenced by the dideoxy method (Sanger *et al.*, 1977) using a Sequenase

2.0 kit (U.S. Biochemicals) and [α-^{35}S]-dATP (NEN-Dupont). A 1.8-kb *Stu*I fragment containing 1.06 kb of the *gpd* promotor region was subcloned into the *Sma*I site of BluescriptII SK+.

3.2.3 Construction of pAGM1

A 1.06-kb *Xba*I–*Nsp*I fragment containing the *gpd* promoter, including the ATG translation initiation codon at the 3′ end, was used in a three-way ligation with a *Nsp*I–*Not*I 35-bp synthetic linker (Oligos Etc. Inc.) with 5′ and 3′ overhangs on the noncoding strand, and BluescriptII SK+ digested with *Xba*I and *Not*I. The 35-bp linker was identical to nucleotides 4 through 38 of the *mnp1* coding region (Figure 3.1A). The *Xba*I–*Not*I insert fragment, containing the *gpd* promoter and linker, and a 3.6-kb *Not*I–*Eco*RI fragment of the *mnp1* genomic clone (Godfrey *et al.*, 1990), including the entire *mnp1* coding region from nt 39, were used in a second three-way ligation with the pOGI18 shuttle vector containing the *Schizophyllum commune* *ade5* gene as a selectable marker (Godfrey *et al.*, 1994) to give pAGM1 (Figure 3.1B).

3.2.4 *P. chrysosporium* Transformations

Protoplasts of the *P. chrysosporium* Ade1 strain were transformed with 2 µg of *Eco*RI-linearized pOGI18 or pAGM1 as described previously (Alic *et al.*, 1990, 1991). Prototrophic transformants were picked to minimal medium and purified by isolating single basidiospores as previously described (Alic *et al.*, 1987, 1990, 1991).

3.2.5 Screening for Expression of rMnP1

pAGM1 transformants were inoculated to petri dishes containing 10 ml of high carbon, high nitrogen (HCHN) medium (standard basal media) (Kirk *et al.*, 1978), supplemented with 0.2% tryptone, 2% glucose, 24 mM ammonium tartrate, 20 mM sodium 2,2-dimethysuccinate (DMS) buffer (pH 4.8), 1.7% agar, and the peroxidase substrate *o*-anisidine (2 mM). Plates were incubated at 37°C for 48 hours, after which they were flooded at RT with a 1-ml solution of 2 mM MnSO$_4$ and 0.5 units of glucose oxidase in 100 mM Na-malonate buffer, pH 4.5.

3.2.6 Production of rMnP1

pAGM1 transformants were grown from a conidial inoculum at 38°C in 20-ml stationary cultures in 250-ml Erlenmeyer flasks for 2 days. The medium used was as

(A)

gpd 5' UTR	oligo	mnp

CTACTTGAACATG	GCCTTCAAGTCCCTCATCGCCTTCGTCGCCCTCGC	GGCCGCTGTTCGTG
GATGAACTT	GTACCGGAAGTTCAGGGAGTAGCGGAAGCAGCGGGAGCGCCGG	CGACAAGCAC
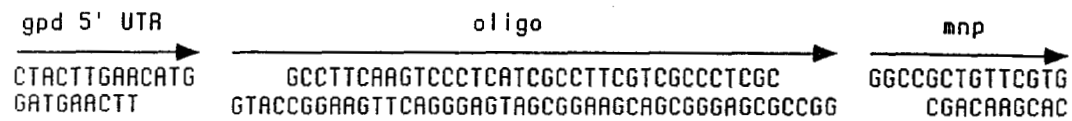
(B)
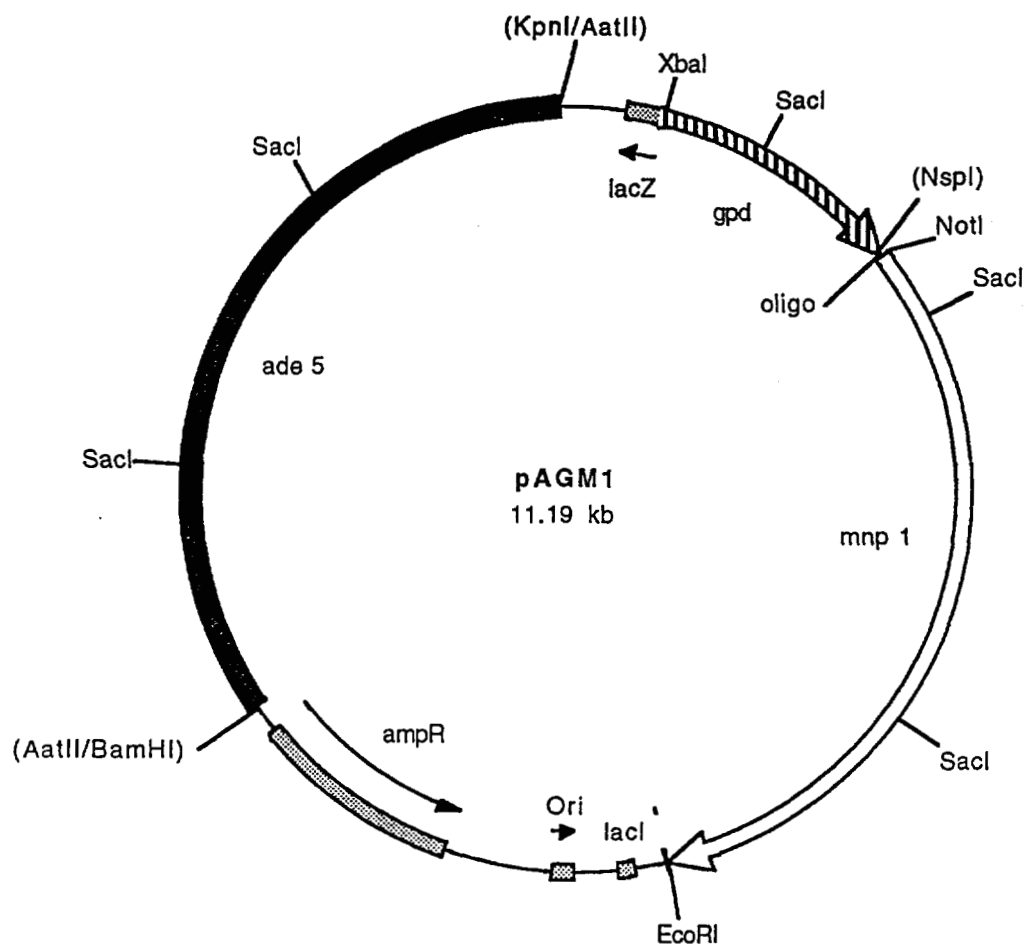
Figure 3.1. Construction of MnP1 expression vector. (A) Junction of the *gpd* promoter-*mnp1* coding region *gpd 5′*. UTR, 5′ untranslated region of the *gpd* gene. Oligo is the synthetic oligonucleotide linker, spanning nt positions 4-38 of the *mnp1* coding region. (B) Restriction map of pAGM1 containing the *ade5* gene and the *gpd* promoter fused to the *mnp1* coding region as indicated. Restriction sites in parentheses are absent from pAGM1.

described elsewhere (Kirk *et al.*, 1978), but supplemented with 2% glucose, 12 mM ammonium tartrate and 20 mM DMS, pH 4.5. The mycelial mat from one flask was homogenized for 20 sec in a blender and used to inoculate a 2-liter Erlenmeyer flask containing 1 liter of the above medium, except in the large cultures the pH was adjusted to pH 6.5 and Na-succinate was used instead of DMS. Cultures were grown at 38°C on a rotary shaker (200 rpm) for 60 hours.

3.2.7 Purification of rMnP1

The filtrate from 6 1-liter cultures was concentrated to ~200 ml and dialyzed against 20 mM Na-acetate (pH 6.0) at 4°C using a hollow fiber filter system (Amicon, 10,000 MW cutoff).

3.2.7.1 DEAE Sepharose chromatography

The concentrate was applied to a DEAE Sepharose CL-6B column (2.5 × 20 cm) equilibrated with 30 mM Na-acetate buffer (pH 6.0). The protein was eluted at 4°C with a linear gradient (400 ml total volume) of decreasing pH from 6.0 to 4.0 in 30 mM Na-succinate. The fractions containing MnP activity were concentrated by membrane ultrafiltration.

3.2.7.2 Blue Agarose chromatography

The DEAE Sepharose fraction was applied to a Cibacron Blue 3GA Agarose column (1.0 × 25 cm) equilibrated with 10 mM Na-succinate buffer (pH 4.5) at 4°C. MnP was eluted at 4°C with a linear NaCl-gradient (0 to 0.5 M). Fractions containing MnP activity were concentrated and desalted by membrane ultrafiltration.

3.2.7.3 Mono Q chromatography

The Blue Agarose fraction was applied to a Mono Q HR 5/5 column (Pharmacia) equilibrated with 10 mM Na-acetate (pH 6.0) in an FPLC system. The protein was eluted at RT with a linear two-phase gradient of increasing concentrations of Na-acetate (pH 6.0), 0.01-0.1 M followed by 0.1-0.3 M. Active MnP fractions were pooled and desalted with a Centricon microconcentrator.

3.2.8 SDS-Polyacrylamide Gel Electrophoresis

SDS-polyacrylamide gel electrophoresis was carried out in a 12% Tris/glycine gel system (Laemmli, 1970) in a MiniProtean II apparatus (Bio-Rad), followed by staining with Coomassie blue (Hames & Rickwood, 1981).

3.2.9 Spectroscopic Procedures and Enzyme Assays

Enzyme absorption spectra were recorded on a Shimadzu UV-260 spectrophotometer at room temperature using a 1-cm light path cuvette. MnP activity was determined by following the formation of Mn(III)-malonate at 270 nm as described (Glenn & Gold, 1985; Wariishi et al., 1992). Reaction mixtures (1 ml) contained MnP (0.5 μg/ml), $MnSO_4$ (0.025-0.5 mM), and H_2O_2 (0.02-0.1 mM) in 50 mM Na-malonate, pH 4.5. Oxidation of 2,6-dimethoxyphenol (2,6-DMP) by MnP was followed by measuring quinone dimer formation at 469 nm as described (Wariishi et al., 1992).

3.2.10 Chemicals

Glucose oxidase, DEAE Sepharose CL-6B, and Cibacron Blue 3GA Agarose were obtained from Sigma. Molecular biology reagents were from New England Biolabs and U.S. Biochemical. o-Anisidine (2-methoxyaniline), H_2O_2 and 2,6-DMP were obtained from Aldrich. The concentration of the H_2O_2 stock solution was determined as described (Cotton & Dunford, 1973). 2,6-DMP was purified by recrystallization before use. All other chemicals were reagent grade.

3.3 RESULTS

3.3.1 Expression of rMnP1

The 82 Ade+ transformants obtained with pAGM1 were screened on plates by the o-anisidine assay. Although the level of expression among individual transformants varied considerably, all but one of the pAGM1 transformants were positive for MnP activity under primary metabolic conditions, whereas the Ade1 auxotroph and three different Ade+ transformants obtained with pOGI18 were negative under these conditions. Three of the pAGM1 transformants expressing the highest levels of rMnP in this initial screening were purified by isolation of single basidiospores (Alic et al., 1987) and analyzed further in liquid culture.

Time courses for the appearance of MnP activity in nitrogen-sufficient stationary cultures of purified pAGM1 transformants, the wild-type strain OGC101, the Ade1

auxotroph, and Ade+ pOGI18 transformants are shown in Figure 3.2. Extracellular MnP activity was detected only in the strains transformed with pAGM1. MnP activity reached a maximum after 60 hours and decreased thereafter. No new activity peak appeared on days 5 or 6 in any of the cultures. This is the period during which endogenous MnP is expressed in low-nitrogen cultures (Brown *et al.*, 1991; Godfrey *et al.*,1994). These observations indicated that the activity observed in the transformants was due to rMnP. Furthermore, when transformant 15 (T15) was grown in HCHN medium in the absence of exogenous Mn, extracellular MnP activity levels were similar to those found in cultures containing Mn (data not shown). The maximum MnP activity for Mn(II) oxidation obtained from T15 cultures was ~2 μmole·ml^{-1}·min^{-1}. Although this is approximately 30% of the MnP activity expressed under nitrogen-limited conditions by the wild-type strain OGC101, it is approximately 2-fold higher than the MnP activity expressed in nitrogen-limited cultures of either the Ade1 auxotroph or pOGI18 transformants (data not shown). Total intracellular MnP activity in T15 was ~0.04% of the extracellular activity.

The influences of several culture parameters on the expression of rMnP were examined. The effect of pH on rMnP expression was examined in high-nitrogen, stationary cultures using DMS as the buffer. As shown in Figure 3.3, an initial culture medium pH of 6.5 resulted in a two-fold increase in maximum MnP activity as compared with an initial pH of 4.5. Increasing the pH beyond 6.5 likewise resulted in a decrease in the amount of rMnP expressed. Maximum rMnP activity observed with either phosphate or acetate buffers was approximately two-thirds of that observed in DMS buffer. Furthermore, rMnP protein was efficiently expressed without the addition of exogenous hemin to the culture medium. Addition of Tween 80 (0.1% v/v) in shaking cultures also increased extracellular MnP activity approximately 1.5-fold, whereas varying the concentration of nutrients such as glucose (0.1-2%) or nitrogen had no apparent effect on rMnP production (data not shown).

3.3.2 Purification of rMnP1

rMnP1 was purified by successive column chromatography on DEAE Sepharose, Cibachron Blue Agarose and Mono Q. One major peak of rMnP activity eluted from both the DEAE Sepharose (Figure 3.4A) and the Blue Agarose columns. The RZ value (A406/A280) of the pooled Blue Agarose fractions was ~4.0. For further purification, the Blue Agarose fraction was applied to a Mono Q column. A typical elution profile for
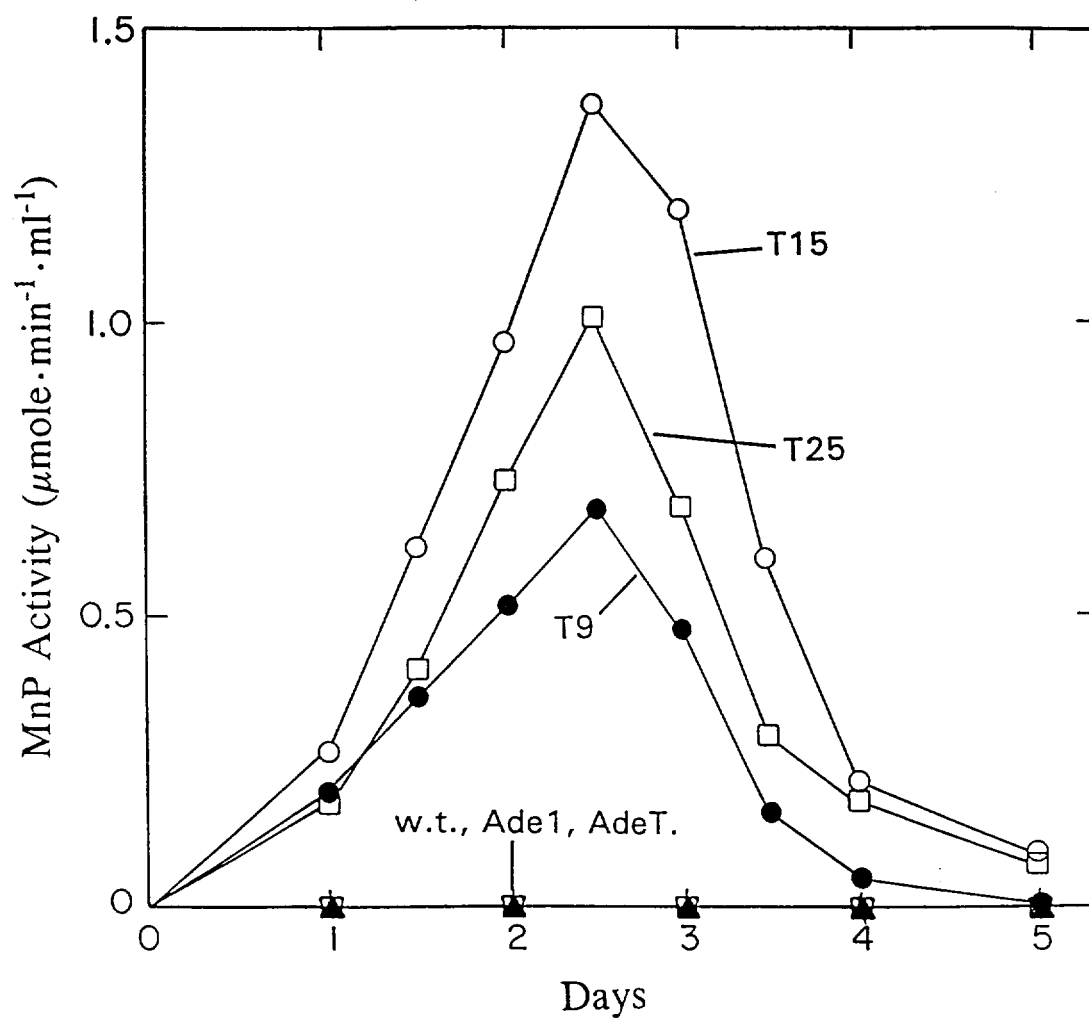
Figure 3.2. MnP activity in the extracellular medium of primary metabolic cultures of *P. chrysosporium*. T9, T15 and T25 are pAGM1 transformants. Ade1 is the host strain; AdeT is a pOGI18 transformant; wt is wild-type strain OGC101. Stationary cultures were grown under high-carbon, high-nitrogen conditions and MnP activity was measured as described in the text.
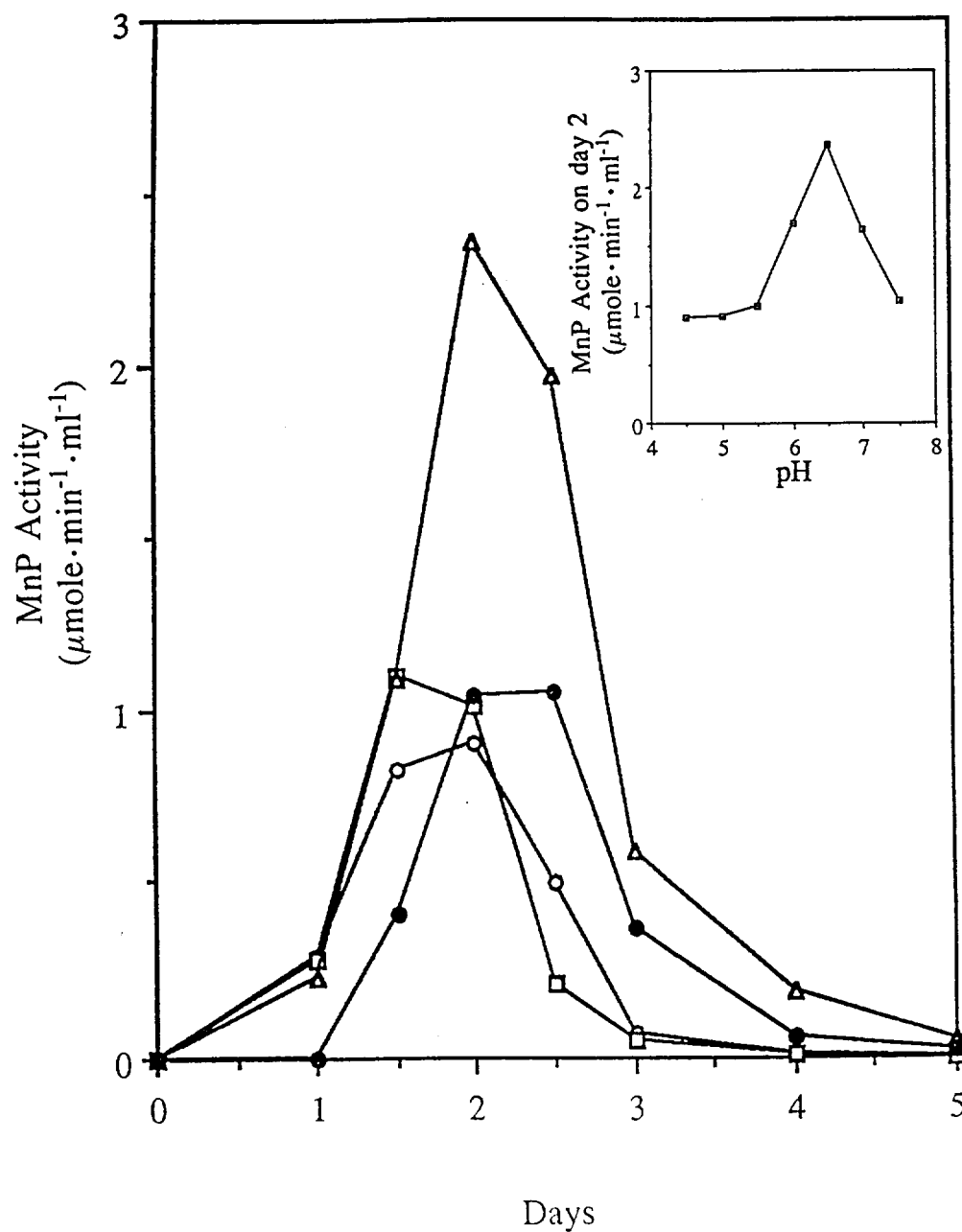
Figure 3.3. The effect of culture pH on extracellular MnP activity from pAGM1 transformant 15. Cultures were grown as described in the text with 20 mM DMS, pH 4.5 (O), 5.5 (□), 6.5 (Δ) or 7.5 (●). MnP activity was measured as described in the text. Inset: extracellular MnP activity on day 2 from cultures buffered with DMS at the indicated pHs.
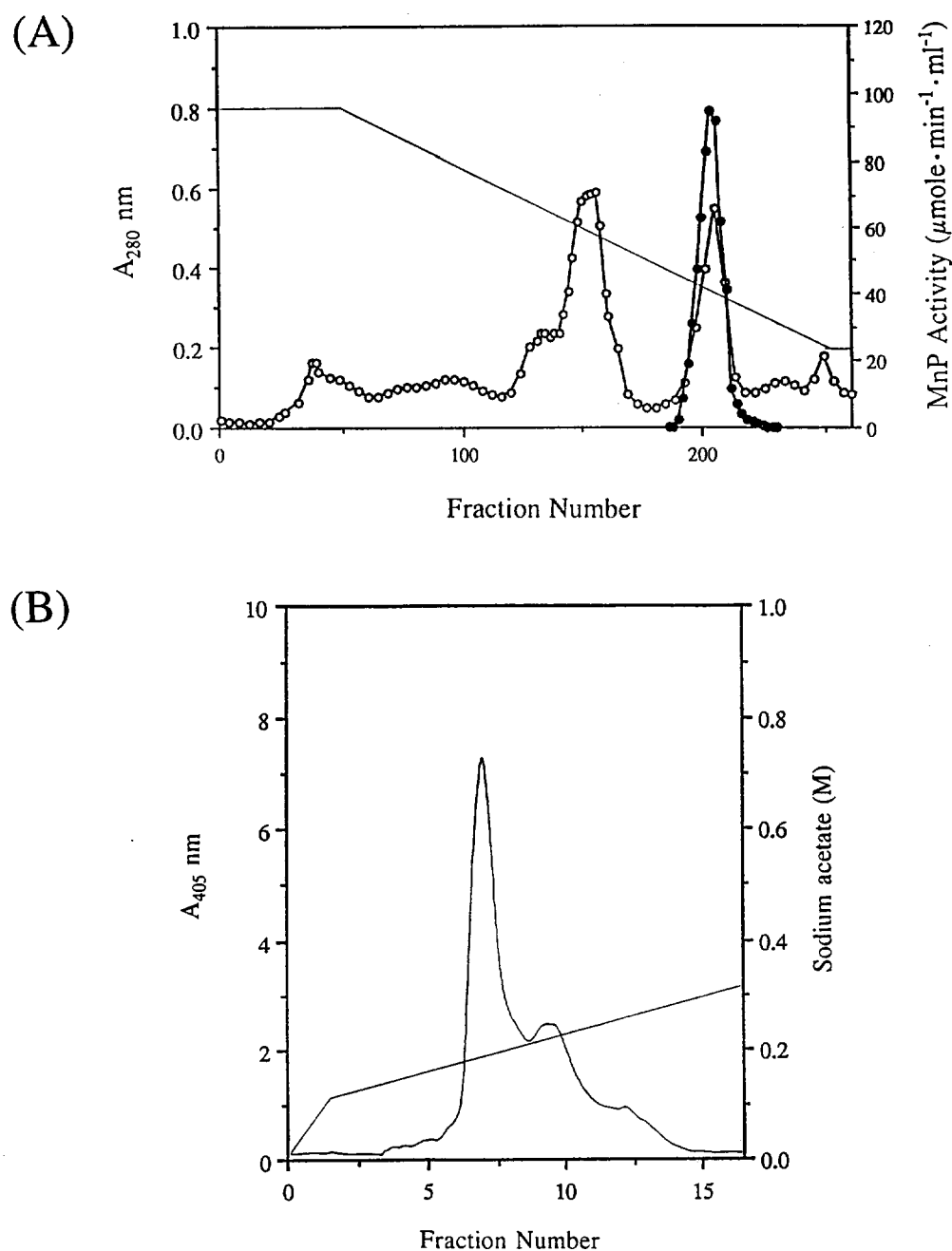
Figure 3.4. Ion exchange chromatography of rMnP1. (A) Chromatography on a DEAE Sepharose column (2.5 × 20 cm). The column was eluted with 30 mm Na-succinate using a decreasing pH gradient from pH 6.0 to 4.0 as shown. Absorbance at 280 nm (O) and MnP activity (●) were measured as described in the text. (B) Chromatography on a Mono Q column. The column was eluted with a gradient of increasing Na-acetate concentration as described in the text.

rMnP on the Mono Q column is shown in Figure 3.4B. Several peaks were detected at 405 nm, including a major peak with the same retention time as that of wtMnP. The MnP activity profile correlated with the A405 profile (data not shown). The RZ value, as well as the SDS-PAGE, suggested that the purity of the recombinant protein was ~95%. This compares to a value of 6.0 for the homogenous wild-type enzyme (Glenn & Gold, 1985; Wariishi et al., 1988). The major Mono Q peak was pooled, concentrated and subjected to SDS-PAGE (Figure 3.5). One intense band, similar to the wild-type enzyme, with an M_r of ~46,000 was observed. The specific activity of the purified rMnP1 for the oxidation of Mn(II) was 341.3 μmole/min/mg (Table 3.1). The specific activity of the enzyme in crude extracellular filtratres was 16.1 μmole/min/mg. Total purification was 21.2-fold.

The absorption spectrum of purified rMnP1, shown in Figure 3.6, had a Soret maximum at 406 nm and visible bands at 502 and 632 nm. The shapes and intensities of these spectral bands were identical to that of wtMnP1 (Figure 3.6) (Glenn & Gold, 1985; Wariishi et al., 1988), suggesting that rMnP1 and the wild-type enzyme have similar heme environments. Like the wild-type enzyme, rMnP oxidized Mn(II) to Mn(III) and the oxidation of 2,6-DMP by rMnP was strictly dependent on both Mn(II) and H_2O_2 (Table 3.1). Furthermore, the specific activity of purified rMnP was similar to that of wtMnP1 with either Mn(II) or 2,6-DMP as substrate (Table 3.1).

Under steady-state conditions, linear Lineweaver-Burk plots were obtained for $1/v$ versus $1/Mn(II)$ and for $1/v$ versus $1/H_2O_2$ over a range of substrate concentrations (data not shown). Most importantly, calculated K_m, V_m and k_{cat} ($V_m/[E]$) values for the substrates Mn(II) and H_2O_2 were similar for wtMnP1 and rMnP1 (Table 3.2).

3.4 DISCUSSION

MnP is a component of the lignin degradation system of most, if not all, white-rot fungi (Hatakka, 1994; Orth et al., 1993; Périé & Gold, 1991), including P. chrysosporium, in which it is expressed during idiophasic growth (Glenn & Gold, 1985; Godfrey et al., 1994; Gold et al., 1989; Pribnow et al., 1989). MnP is an unique peroxidase in that its primary substrate is Mn(II) which is oxidized to Mn(III) and MnP activity is stimulated by various organic acid chelators, especially oxalate, which is secreted by P. chrysosporium. A variety of spectroscopic and kinetic studies have been carried out on MnP (Banci et al., 1993; Glenn & Gold, 1985; Kishi et al., 1994; Kuan & Tien, 1993; Mino et al., 1988; Wariishi et al., 1988, 1992). However, there are many questions about this unique enzyme which could be addressed by the use of site-directed mutagenesis

Figure 3.5. SDS-PAGE of wtMnP1 (lane 1) and rMnP (lane 2). 5 μg of each protein were loaded on a 12% Tris/glycine polyacrylamide gel system (Laemmli, 1970). The gel was stained with Coomassie brilliant blue. Migration of the molecular weight standards: bovine serum albumin, 66.3 kDa; glutamate dehydrogenase, 55.4 kDa; lactate dehydrogenase, 36.5 kDa; carbonic anhydrase, 31 kDa; trypsin inhibitor, 21.5 kDa; lysozyme, 14.4 kDa is indicated.

Table 3.1. Reactions of rMnP1 and wtMnP1[a]

	Specific activity (μmole·min^{-1}·mg^{-1})			
		Substrate		
	Mn(II)	2,6-DMP		
		+ Mn(II), H$_2$O$_2$	– Mn(II)	– H$_2$O$_2$
rMnP1	341.3	158.3	N[b]	N
wtMnP1	332.2	161.1	N	N

[a]MnP activity was determined in 50 mM sodium malonate, pH 4.5, as described in the text. Mn(III)-malonate formation was followed at 270 nm as described in the text and previously (Glenn & Gold, 1985; Wariishi et al., 1992). 2,6-DMP oxidation was followed at 469 nm for the formation of quinone dimer (Wariishi et al., 1992).

[b]Negligible.
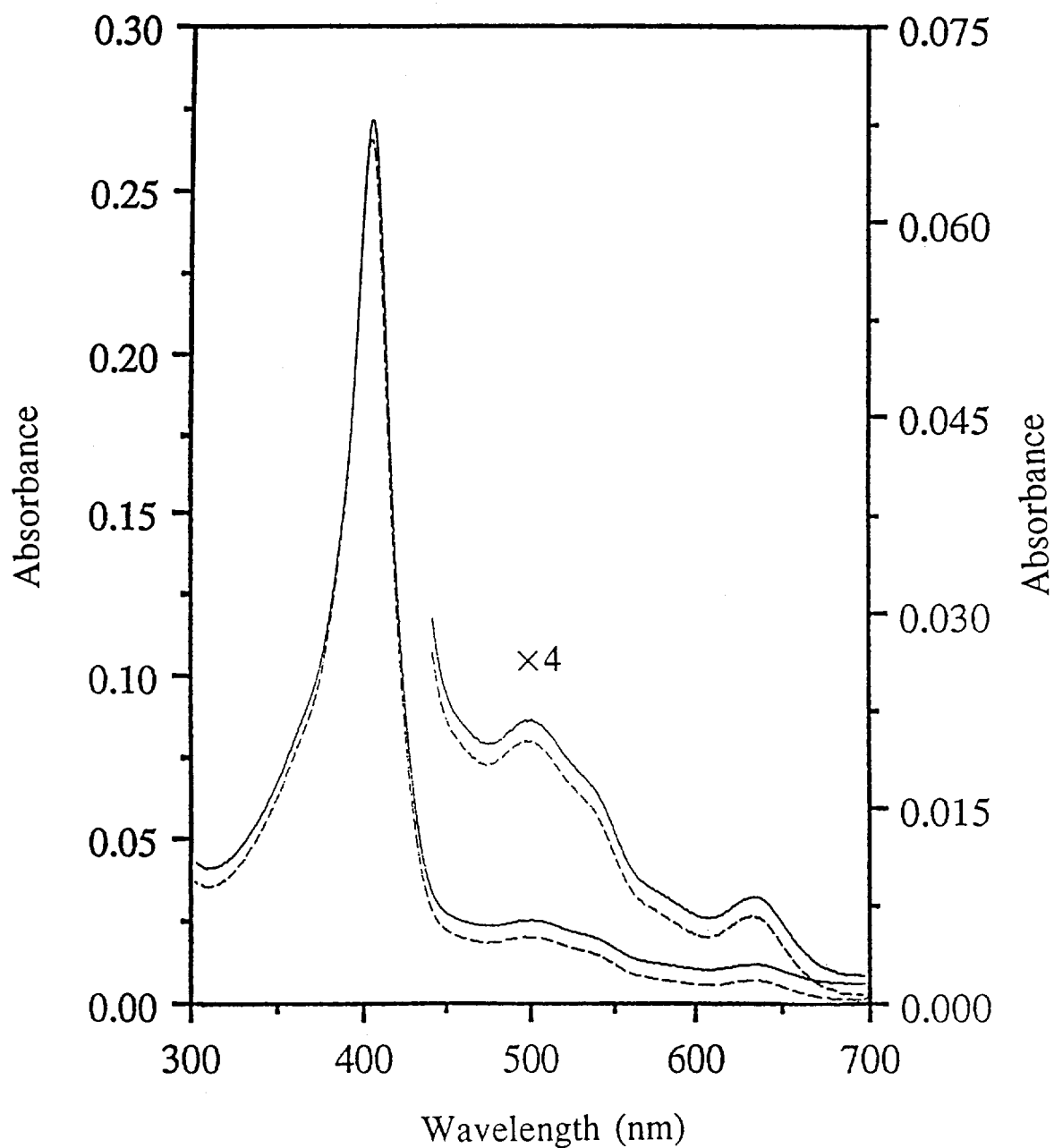
Figure 3.6. Comparison of the electronic absorbance spectra of rMnP1 (solid line) and wtMnP1 (dashed line). Spectra of protein (2 µM) were recorded in 20 mM Na-succinate, pH 4.5, as described in the text.

Table 3.2. Steady-state kinetic parameters for rMnP1 and wtMnP1[a]

	Substrate	K_m (μM)	V_m ($\mu mole \cdot mg^{-1} \cdot min^{-1}$)	k_{cat} (s^{-1})
rMnP1	Mn(II)	69.4	390.6	300.7
	H_2O_2	39.2	465.1	358.1
wtMnP1	Mn(II)	73.2	377.4	289.3
	H_2O_2	41.7	454.4	348.4

[a]Reactions were carried out in 50 mM Na-malonate, pH 4.5. Apparent K_m, V_m, and k_{cat} for Mn(II) were determined using 0.1 mM H_2O_2. Apparent K_m, V_m and k_{cat} for H_2O_2 were determined using 0.5 mM Mn(II).

coupled with kinetic and structural studies. These questions include the nature of the Mn binding site (Johnson *et al.*, 1993; Wariishi *et al.*, 1992) and the heme access channel for Mn and H_2O_2. While the crystal structure of LiP has been published (Piontek *et al.*, 1993; Poulos *et al.*, 1993) and that of MnP1 is currently under investigation (Sundaramoorthy *et al.*, 1994a), the heterologous expression of LiP and MnP has not been achieved in a microbial host. Although these enzymes have been expressed in the baculovirus system (Johnson & Li, 1991; Pease *et al.*, 1991), this system is not well suited for the cost-effective production of the large quantities of enzyme needed for structural analysis. Previously, we developed a DNA transformation system for *P. chrysosporium*, based upon the complementation of auxotrophic mutants by heterologous or homologous biosynthetic genes (Alic *et al.*, 1990, 1991). We recently utilized this system to study the expression of a reporter gene under the control of the *mnp* gene promoter (Godfrey *et al.*, 1994). Herein, we report the homologous expression of *mnp1* under the control of the *gpd* promoter. This system allows production of rMnP under primary metabolic conditions when the endogenous *mnp* genes are not expressed, facilitating purification of the recombinant protein.

The *P. chrysosporium gpd* gene was cloned from a λEMBL3 library of wild-type strain OGC101. The nucleotide sequence of this gene, which will be published elsewhere, is similar to the recently published *gpd* sequence from wild-type strain ME-446 (Harmsen *et al.*, 1992). The *gpdA* promoter from *A. nidulans* has been used for the high level constitutive expression of intracellular and extracellular homologous and heterologous proteins in that organism (Punt *et al.*, 1991). Here we demonstrate that the *P. chrysosporium gpd* promoter region can direct transcription of the *mnp1* coding region under conditions of sufficient carbon and nitrogen when the endogenous *mnp* genes are not expressed.

Almost all of the Ade+ transformants obtained with pAGM1 produced MnP under carbon- and nitrogen-sufficient conditions, as measured by *o*-anisidine screening and enzyme assays. None of the pOGI18 transformants, nor the wild-type or Ade1 auxotrophic strains produced MnP under these conditions (Figure 3.2). This indicates that the pAGM1 transformants are expressing MnP1 under control of the constitutive *gpd* promoter. Maximum MnP activity is obtained from pH 6.5 cultures (Figure 3.3) whereas endogenous MnP activity is maximal from pH 4.5 cultures. Furthermore, we have shown that expression of endogenous MnP protein in *P. chrysosporium* requires the presence of Mn ion (Brown *et al.*, 1991; Godfrey *et al.*, 1994; Gold & Alic, 1993) and *mnp1* promoter

reporter studies have shown that the Mn requirement resides in the *mnp1* promoter region (Godfrey *et al.*, 1994). However, the pAGM1 transformants produce MnP in the absence of Mn (data not shown). Finally, using pAGM1, we have recently constructed mutant *mnp* genes by site-directed mutagenesis. When *P. chrysosporium* is transformed with plasmids containing the mutant genes, only mutant proteins are expressed. No wild-type proteins are observed (Kusters-van Someren *et al.*, 1995). All of these results indicate that rMnP1 in the pAGM1 transformants is being produced under the control of the constitutive *gpd* promoter. The results indicate that any additional requirements for production of active MnP, including insertion of the heme and protein secretion, must be available during primary as well as secondary metabolism and that *cis*-acting factors restricting transcription of endogenous *mnp* genes to secondary metabolism reside in the *mnp* promoter regions.

Although most Ade+ transformants obtained with pAGM1 gave some degree of positive reaction in the *o*-anisidine screening, indicating expression of rMnP, individual transformants varied considerably. Our previous results have indicated that integration of transforming DNA in *P. chrysosporium* is predominately ectopic with single or multiple plasmid copies integrating at various chromosomal locations (Alic *et al.*, 1990,1991; Gold & Alic, 1993). The results presented here suggest that although the position of pAGM1 integration may affect the level of rMnP expression, there may not be specific chromosomal sites that determine expression during primary or secondary metabolism.

rMnP was readily purified to near-homogeneity using a combination of anion-exchange and Blue Agarose column chromatographies (Figure 3.4A). FPLC with a Mono Q column separated several protein peaks (Figure 3.4B). These multiple peaks may have arisen from alternate post-transcriptional modification, such as glycosylation. The major Mono Q column protein peak was examined further. SDS-PAGE analysis suggests that rMnP1 has an M_r of 46,000 which is nearly identical to wtMnP1 (Figure 3.5). The wild type and rMnP also exhibit identical UV-vis spectral features (Figure 3.6), suggesting that the environment and orientation of the heme in both enzymes are similar. Significantly, heme insertion appears to be normal and exogenous heme is not required for expression of this recombinant heme protein. This contrasts with the baculovirus system where exogenous heme is apparently required for MnP expression (Pease *et al.*, 1991). The addition of exogenous heme can lead to the adventitious binding of extra heme to protein (unpublished observations). As with wtMnP1, the rMnP1 is able to oxidize Mn(II) to Mn(III) and the 2,6-DMP oxidation activity of rMnP is dependent on both Mn(II) and H_2O_2 (Table 3.1). Furthermore, rMnP exhibits K_m, V_m and k_{cat} values for Mn(II) and

H_2O_2 that are very similar to those for wtMnP1 (Table 3.2), suggesting that the substrate binding and catalytic efficiency of rMnP has not been altered.

The level of rMnP1 produced in either stationary or agitated cultures is about 30% of the total MnP produced by multiple *mnp* genes in the heterokaryotic wild-type strain OGC101 (a derivative of BKM-F-1767) under ligninolytic conditions and about twice that produced by the Ade1 parental homokaryon. This suggests that the *P. chrysosporium gpd* promoter is more efficient than the combined activity of the multiple *mnp* promoters present in the Ade1 strain. Alternatively, the higher yield of rMnP may reflect increased metabolic activity during primary as compared with idiophasic metabolism. Most importantly, this expression system enables the efficient purification of a single rMnP isozyme.

To our knowledge, this constitutes the first report of efficient protein expression in *P. chrysosporium*. Whereas we previously demonstrated the ability of a secondary metabolic promoter (*mnp1*) to direct expression of a primary metabolic gene (*ura1*) (Godfrey *et al.*, 1994), here we demonstrate the expression of a secondary metabolic gene under the control of a primary metabolic promoter. The expression system described here will enable us to generate site-directed MnP mutants for structure/function studies. Similar studies on the homologous expression of recombinant LiP are planned.

CHAPTER 4

THE MANGANESE BINDING SITE OF MANGANESE PEROXIDASE: CHARACTERIZATION OF AN ASP179ASN SITE-DIRECTED MUTANT PROTEIN

4.1 INTRODUCTION

Phanerochaete chrysosporium and other white-rot fungi are capable of degrading the plant cell wall polymer, lignin (Gold *et al.*, 1989; Kirk & Farrell, 1987; Buswell & Odier, 1987), and a variety of environmentally persistent aromatic pollutants (Bumpus & Aust, 1987; Hammel, 1989; Valli & Gold, 1991; Valli *et al.*, 1992b; Joshi & Gold, 1993). When cultured under ligninolytic conditions, *P. chrysosporium* secretes two families of extracellular peroxidases, lignin peroxidase (LiP) and manganese peroxidase (MnP), which, along with an H_2O_2-generating system, comprise the major components of its extracellular lignin-degrading system (Kirk & Farrell, 1987; Buswell & Odier, 1987; Gold & Alic, 1993; Wariishi *et al.*, 1991b; Kuwahara *et al.*, 1984; Hammel *et al.*, 1993). Both LiP and MnP depolymerize lignin *in vitro* (Wariishi *et al.*, 1991b; Hammel *et al.*, 1993). Moreover, MnP activity is produced by all white-rot fungi known to degrade lignin (Hatakka, 1994; Perie & Gold, 1991; Orth *et al.*, 1993).

MnP has been purified and characterized both biochemically and kinetically (Gold *et al.*, 1989; Gold & Alic, 1993; Glenn & Gold, 1985; Glenn *et al.*, 1986; Wariishi *et al.*, 1989a; 1992). In addition, the sequences of *mnp* cDNA (Gold & Alic, 1993; Pribnow *et al.*, 1989; Pease *et al.*, 1989) and genomic clones (*mnp1* and *mnp2*) (Gold & Alic, 1993; Godfrey *et al.*, 1990; Mayfield *et al.*, 1994a) encoding two *P. chrysosporium* MnP isozymes have been determined. Spectroscopic studies and DNA sequences suggest that the heme environment of MnP is similar to that of other plant and fungal peroxidases (Glenn *et al.*, 1986; Pribnow *et al.*, 1989; Harris *et al.*, 1991; Banci *et al.*, 1992; Dunford & Stillman, 1976; Mino *et al.*, 1988; Wariishi *et al.*, 1988). Kinetic and spectral characterization of the oxidized intermediates—MnP compounds I, II, and III—indicate that the catalytic cycle of MnP is similar to that of horseradish peroxidase

98

and LiP (Gold *et al.*, 1989; Glenn *et al.*, 1986; Wariishi *et al.*, 1988, 1992; Renganathan & Gold, 1986). The crystal structure of LiP has been reported (Edwards *et al.*, 1993; Poulos *et al.*, 1993; Piontek *et al.*, 1993), and the structure of MnP recently has been solved (Sundaramoorthy *et al.*, 1994a,b). These structures confirm that the heme environment of MnP and LiP are similar to that of cytochrome *c* peroxidase and other plant and fungal peroxidases (Poulos *et al.*, 1993; Sundaramoorthy *et al.*, 1994b). MnP is unique in its ability to catalyze the one-electron oxidation of Mn(II) to Mn(III) (Glenn & Gold, 1985; Glenn *et al.*, 1986; Wariishi *et al.*, 1992) as shown in Scheme 4.1.

Scheme 4.1

$$MnP + H_2O_2 \rightarrow MnPI + H_2O \tag{1}$$

$$MnPI + Mn(II) \rightarrow MnPII + Mn(III) \tag{2}$$

$$MnPII + Mn(II) \rightarrow MnP + Mn(III) + H_2O \tag{3}$$
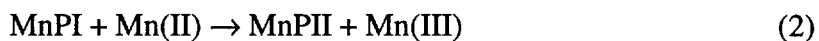
The enzyme-generated Mn(III) is stabilized by organic acid chelators such as oxalate which also is secreted by the fungus (Wariishi *et al.*, 1992; Kuan *et al.*, 1993). The Mn(III)–organic acid complex, in turn, oxidizes phenolic substrates such as lignin substructure model compounds (Tuor *et al.*, 1992), synthetic lignin (Wariishi *et al.*, 1991b), and aromatic pollutants (Valli & Gold, 1991; Valli *et al.*, 1992b; Joshi & Gold, 1993).

To study structure/function relationships in MnP via site-directed mutagenesis, an expression system is required for the efficient production and purification of large quantities of enzyme. We recently developed a homologous expression system for MnP isozyme 1 (MnP1) (Mayfield *et al.*, 1994b). In this system, the *P. chrysosporium* glyceraldehyde-3-phosphate-dehydrogenase (*gpd*) promoter is used to drive expression of the *mnp* gene during the primary metabolic growth phase when endogenous MnP is not expressed. This expression system produces recombinant MnP1 (rMnP1) in amounts which are comparable to the endogenous MnP1 produced by the wild-type strain (Mayfield *et al.*, 1994b). Furthermore, biochemical characterization suggests that the rMnP1 is very similar to the wild-type enzyme (Mayfield *et al.*, 1994b). In this study, Asp179, one of the potential ligands for manganese binding in MnP (Sundaramoorthy *et al.*, 1994b; Johnson *et al.*, 1993), was converted to Asn179 using overlap extension PCR. Kinetic and spectroscopic properties of the purified D179N mutant protein were investigated.

4.2 MATERIALS AND METHODS

4.2.1 Organisms

P. chrysosporium wild-type strain OGC101, auxotrophic strain OGC107-1 (Ade 1), and prototrophic transformants were maintained as described previously (Alic *et al.*, 1990). *Escherichia coli* XL1-Blue and DH5αF′ were used for subcloning plasmids.

4.2.2 Oligodeoxyribonucleotides

Four oligonucleotides were used for site-directed mutagenesis of Asp179 of *mnp1* (Pribnow *et al.*, 1989; Godfrey *et al.*, 1990). Oligonucleotide $B1_{norm}$ is a 17-mer corresponding to *mnp1* positions 554–570 (Godfrey *et al.*, 1990). Oligonucleotide $D1_{rev}$ is complementary to the *mnp1* sequence over nucleotide positions 1156–1140. Oligonucleotides $N179_{norm}$ and $N179_{rev}$ are 28-mers and are partly overlapping: $N179_{norm}$ spans nucleotides 841–868 and $N179_{rev}$ is complementary to nucleotides 858–830. Oligonucleotides were synthesized at the Center for Gene Research and Biotechnology, Oregon State University, Corvallis, OR. $N179_{norm}$ and $N179_{rev}$ contain the preferred (Ritch & Gold, 1992) codon and anticodon, respectively, for Asn, AAC replacing GAC, which encodes Asp179.

4.2.3 Site-Directed Mutagenesis by PCR

A 554 bp *Bpu*1102I-*Dra*III fragment containing the D179N mutation was generated by overlap extension (Ho *et al.*, 1989) using the polymerase chain reaction (PCR). Amplification of the first two fragments (Figure 4.1) was achieved using 30 ng pGM1 (the *gpd–mnp* construct subcloned in pUC18 (Mayfield *et al.*, 1994b)) as target DNA, 400 μM of each dNTP, 1 U Deep Vent polymerase (New England Biolabs), and 1 μM of either oligonucleotides $B1_{norm}$ and $N179_{rev}$ or $N179_{norm}$ and $D1_{rev}$ in a total volume of 50 μl. Samples were overlaid with mineral oil, heated for 2 min at 94 °C, and subjected to 25 cycles of denaturation (1 min at 94 °C), annealing (0.5 min at 55 °C), and extension (1 min at 72 °C), followed by a final incubation for 5 min at 72 °C in a thermocycler (Ericomp). The reaction products of both reactions were analyzed by electrophoresis on a 1% agarose gel; fragments were visualized by ethidium bromide under UV-light and those of the correct size were excised. The DNA was purified by GeneClean (BIO101). These two fragments which partially overlap were combined and used as template DNA in a third reaction with
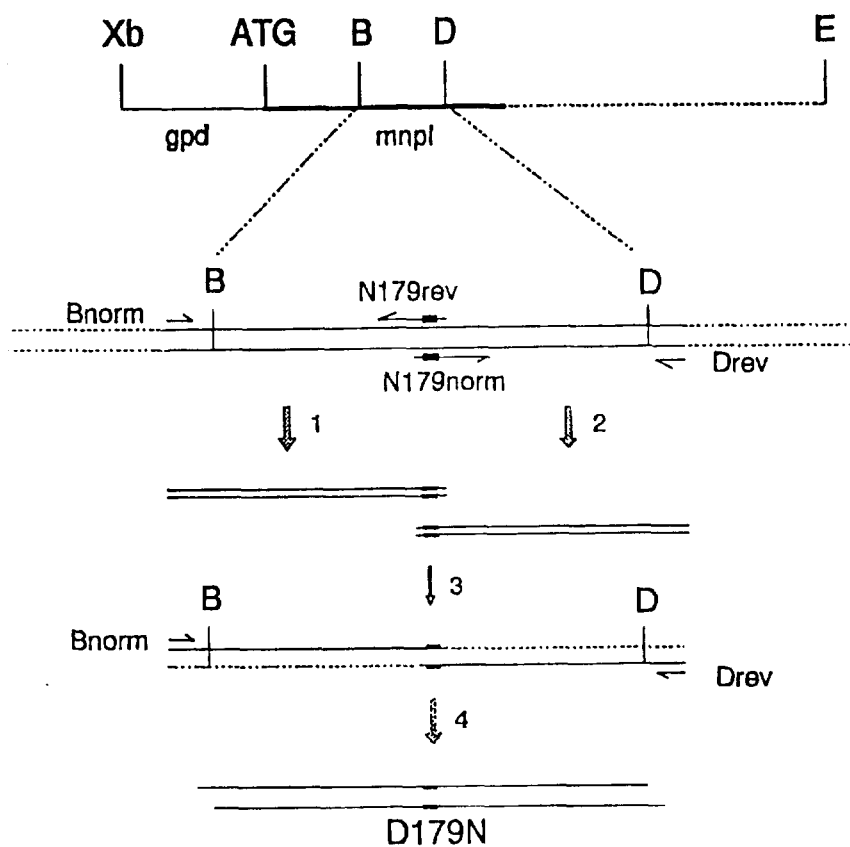
Figure 4.1. Site-directed mutagenesis strategy. In the map of the construct, the thin solid line indicates the *gpd* promoter fragment, the thick solid line indicates the *mnp1* coding region, and the dashed line represents the non-coding 3′ region of the *mnp1* gene. XB, *Xba*I; ATG, translation start codon; B, *Bpu*1102I; D, *Dra*III; E, *Eco*RI. *1*: PCR using oligonucleotides B_{norm} and $N179_{rev}$; *2*: PCR using oligonucleotides $N179_{norm}$ and D_{rev}; *3*: PCR by overlap extension with oligonucleotides B_{norm} and D_{rev}; *4*: Digestion with *Bpu*1102I and *Dra*III.

oligonucleotides B1$_{norm}$ and D1$_{rev}$ under the conditions described above, but without pGM1 DNA (Figure 4.1). The final PCR product was analyzed by agarose gel electrophoresis, excised, purified by GeneClean, and digested with *Bpu*1102I and *Dra*III (New England Biolabs).

4.2.4 Construction of pAGM4

The *Bpu*1102I-*Dra*III fragment containing the D179N mutation was first subcloned into pGM1, containing unique *Bpu*1102I and *Dra*III sites, replacing the wild-type *mnp1* fragment with the mutant fragment, to generate pGM4. The entire *Bpu*1102I-*Dra*III fragment was analyzed by double-stranded DNA sequencing using the four oligonucleotides described above, and a Sequenase Version 2.0 DNA sequencing kit (USB) with a 7-deaza-dGTP labeling mix and termination mixes (USB). Subsequently, the 4.0-kb *Xba*I-*Eco*RI fragment of pGM4 containing the *gpd* promoter and the mutated *mnp1* gene was subcloned into pOGI18 (Godfrey *et al.*, 1994), generating pAGM4. The presence of the D179N mutation in pAGM4 was confirmed by double-stranded DNA sequencing of the appropriate sequence, using oligonucleotide B1$_{norm}$ as a primer.

4.2.5 Transformation of *Phanerochaete chrysosporium*

P. chrysosporium strain Ade1 (Gold *et al.*, 1982; Alic *et al.*, 1987) was transformed as described previously (Alic *et al.*, 1990), using 1 μg of pAGM4 as the transforming DNA. Thirty-five transformants were transferred to minimal slants (Gold *et al.*, 1982) to confirm adenine prototrophy and, subsequently, were assayed for MnP activity using the *o*-anisidine plate assay as described (Mayfield *et al.*, 1994b). The six transformants showing the strongest activity by the plate assay were purified by fruiting as described (Alic *et al.*, 1987), and the progeny again were assayed for MnP activity by the plate assay.

4.2.6 Production of the D179N Mutant Protein

Transformant strain D179N-6 was maintained on 2% malt agar slants and grown from a conidial inoculum at 37 °C in 20-ml stationary cultures in 250-ml Erlenmeyer flasks for 2 days. The medium was as described elsewhere (Kirk *et al.*, 1978) except that it was supplemented with 2% glucose, 12 mM ammonium tartrate, and 20 mM dimethyl succinate (pH 4.5). The mycelial mat from one flask was homogenized for 20 s in a blender and used to inoculate a 2-l Erlenmeyer flask containing 1 l of the medium described above, except that in the large cultures the pH was adjusted to 6.5 and sodium succinate was used

instead of dimethyl succinate. Cultures were grown at 37 °C on a rotary shaker at 200 rpm for 60 h. The MnP mutant protein is produced under primary metabolic conditions when endogenous *mnp* genes are not expressed (Mayfield *et al.*, 1994b), enabling purification of the mutant protein.

4.2.7 Purification of the MnP D179N Mutant Protein

The MnP D179N mutant protein was purified by the protocol described for the wild-type recombinant MnP1 (Mayfield *et al.*, 1994b). The extracellular fluid from 6 l of 60-h-old cultures was concentrated to 200 ml and dialyzed against 20 mM sodium acetate (pH 6.0) at 4 °C, using a Hollow fiber filter system (10,000 MW cut-off; Amicon). Chromatography was as described (Mayfield *et al.*, 1994b) and included DEAE Sepharose column chromatography, Cibacron Blue 3GA agarose column chromatography, and fast-protein liquid chromatography using a Mono Q column (Pharmacia).

4.2.8 SDS-PAGE and Western Analysis

Sodium dodecyl sulfate-polyacrylamide gel electrophoresis (SDS-PAGE) was performed using a 12% Tris-glycine gel system (Laemmli, 1970) and a Mini-Protean II apparatus (Bio-Rad). The gels were stained with Coomassie Blue. For Western (immunoblot) analysis, proteins were electroblotted (Sambrook *et al.*, 1989) onto nitrocellulose (Micron Separations, Inc.) and MnP protein was detected as described (Pribnow *et al.*, 1989; Mayfield, *et al.*, 1994b).

4.2.9 Enzyme Assay and Spectroscopic Procedures

MnP activity was measured by following the formation of Mn(III)-malonate at 270 nm as previously described (Wariishi *et al.*, 1992), except that the final concentration of $MnSO_4$ in the reaction mixture was increased to 5.0 mM. UV-absorption spectra of the various oxidation states of MnP D179N, as well as rMnP1, were recorded at room temperature using a Shimadzu UV-260 spectrophotometer. The enzyme was maintained in 20 mM potassium succinate or malonate buffer, pH 4.5. The ionic strength of the buffers was adjusted to 0.1 M using K_2SO_4. Enzyme concentrations were determined at 406 nm using an extinction coefficient of 129 mM^{-1} cm^{-1} (Glenn & Gold, 1985). MnP D179N compound I was prepared by mixing 1.0 equiv of H_2O_2 with the native enzyme. Compound II was prepared by the successive addition of 1.0 equiv of H_2O_2 and 1.0 equiv of Mn(II) or ferrocyanide.

4.2.10 Kinetic Analyses

To determine apparent K_m and k_{cat} values of the mutant enzyme for Mn(II) and H_2O_2, 1/initial velocity versus 1/[substrate] was plotted at fixed concentrations of H_2O_2 or Mn(II). Reaction mixtures contained MnP D179N (10 μg/ml), MnSO$_4$ (0.5–5.0 mM), and H_2O_2 (0.02–0.1 mM) in 50 mM sodium malonate, pH 4.5. Kinetic measurements with rMnP1 were carried out as described (Mayfield et al., 1994b). The reduction of MnP compound II (2 μM) in 20 mM potassium malonate, pH 4.5, or 0.5–5 mM potassium oxalate, pH 4.6 (ionic strength 0.1 M, adjusted with K$_2$SO$_4$), was followed at 406 nm, which is the Soret absorbance maximum of the native enzyme (see "Results"). Compound II of MnP D179N and wild-type MnP1 were freshly prepared for each experiment and the reaction was initiated by adding reducing substrate, Mn(II) or p-cresol, in at least 10-fold excess. All of the kinetic traces displayed single exponential character from which pseudo-first-order rate constants were calculated. Several substrate concentrations were used and plots of pseudo-first-order rate constants versus substrate concentration were obtained.

4.2.11 Chemicals

DEAE-Sepharose CL-6B, Cibacron Blue 3GA agarose, and H_2O_2 (30% solution) were obtained from Sigma. p-Cresol was obtained from Aldrich. The concentration of the H_2O_2 stock solution was determined as described (Cotton & Dunford, 1973). p-Cresol was purified by thin-layer chromatography before use. All other chemicals were reagent grade. Solutions were prepared using deionized water obtained from a Milli Q purification system (Millipore).

4.3 RESULTS

4.3.1 Expression and Purification of Mutant Protein

The presence of the D179N mutation was confirmed by double-stranded DNA sequencing of the altered Bpu1102I-DraIII restriction fragment in pGM4 and in the complete transformation vector pAGM4. Six out of 35 selected transformants displayed readily detectable MnP activity on the plate assay. These six transformants expressed extracellular mutant MnP protein within three days of growth in liquid high-carbon, high-nitrogen shake cultures, as verified by Western (immunoblot) detection (data not shown), under conditions in which the wild-type enzyme was not expressed. The amount of mutant

protein secreted by the pAGM4 transformants was similar to the level of recombinant wild-type MnP1 (rMnP1) reported previously (Mayfield *et al.*, 1994b). However, the six transformant strains displayed only slow Mn(II)-oxidizing activity as assayed by monitoring the formation of Mn(III)-malonate complex (Wariishi *et al.*, 1992). MnP D179N from transformant 6 was purified using anion-exchange, blue agarose, and Mono Q chromatography as described (Mayfield *et al.*, 1994b). As shown in Figure 4.2, one major peak and a later eluting minor peak were separated on Mono Q column chromatography. The major peak eluted essentially at the same time as rMnP1 when the latter was chromatographed under identical conditions (Mayfield *et al.*, 1994b). Furthermore, as shown in Figure 4.2 *inset*, the molecular weight (46 kDa) of the predominant form of MnP D179N was identical to that of rMnP1 and wild-type MnP.

4.3.2 Spectral Properties of MnP D179N

Figure 4.3 shows the absorption spectra of the native, compound I, and compound II states of MnP D179N. Upon the addition of 1.0 equiv of H_2O_2 to the native enzyme, the Soret band at 406 nm rapidly decreased and red shifted to yield a band at 398 nm. The visible region of compound I displayed a peak at 650 nm with a broad absorption at 530–600 nm. Approximately 40% of compound I was spontaneously converted to compound II in 30 min (data not shown). Upon the addition of 1.0 equiv of Mn(II) to compound I, a spectrum for compound II slowly developed with maxima at 420, 527, and 555 nm. An isosbestic point between compounds I and II was observed at 398 nm (Figures 4.3 and 4.4*A*). Compound II was stable for more than 20 min and only ~10% of the compound II was converted spontaneously to the native enzyme in 1 h (data not shown). However, with the addition of 10 equiv of Mn(II) to compound II, the enzyme returned slowly to the native state, with an absorbance maximum at 406 nm and an isosbestic point at 414 nm (Figure 4.4*B*). The spectral maxima of the various oxidized states of the D179N protein were essentially identical to those of the wild-type enzyme (Table 4.1), suggesting that replacement of Asp179 with an Asn did not change the heme environment of the protein significantly.

4.3.3 Kinetic Properties of MnP D179N

The specific activity of MnP D179N for Mn(II) oxidation was 0.946 μmol mg^{-1} min^{-1} as determined by following the formation of the Mn(III)-malonate complex at 270 nm (Wariishi *et al.*, 1992). This specific activity was approximately 1/350 of the values obtained for wild-type MnP1 or rMnP1 (341 and 332 μmol mg^{-1} min^{-1}, respectively)
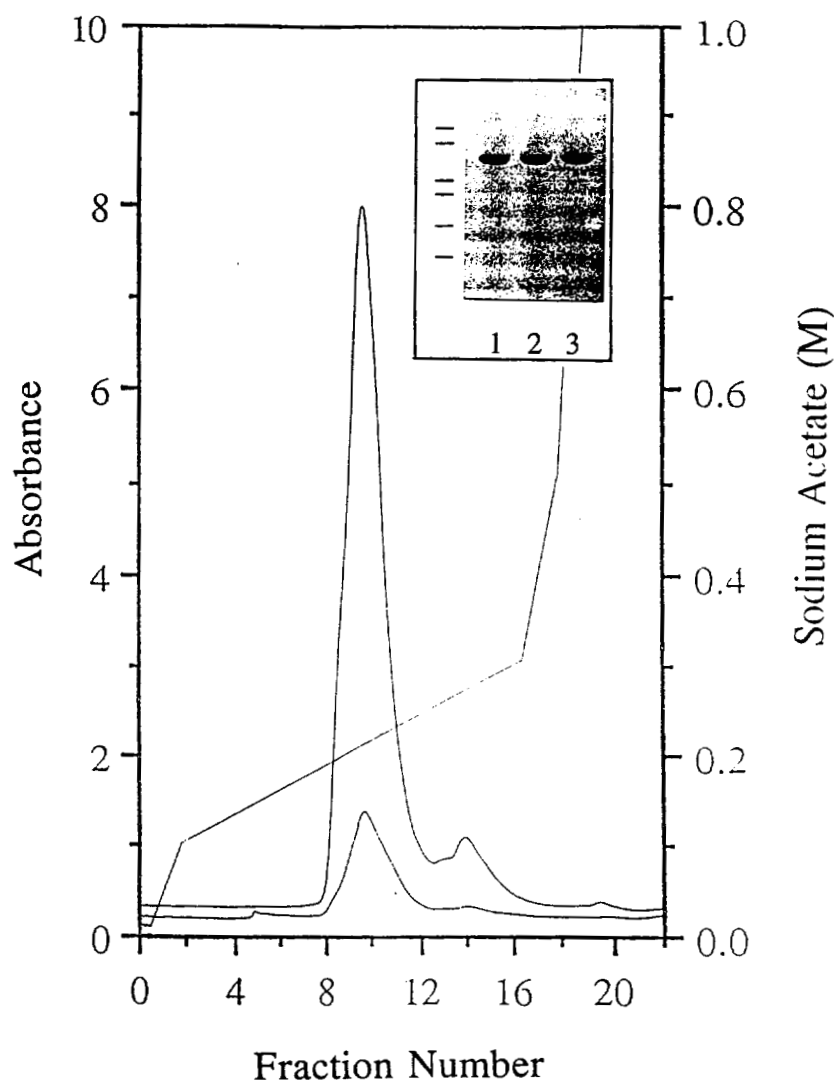
Figure 4.2. Mono Q anion exchange chromatography of the MnP D179N protein. The column was equilibrated with 10 mM sodium acetate, pH 6.0, and eluted by an increasing sodium acetate (pH 6.0) gradient as shown. Absorbance at 405 nm (*top trace*) and 280 nm (*bottom trace*) were measured. MnP activity was measured as described in the text and correlated with the absorbance at 405 nm. *Inset:* SDS PAGE of various forms of Mn peroxidase: SDS-PAGE of wild-type MnP1 (*lane 1*), rMnP1 (*lane 2*), and MnP D179N (*lane 3*). 5 μg of each protein were loaded on a 12% Tris/glycine polyacrylamide gel system (Laemmli, 1970). Proteins were visualized by Coomasie Blue staining. Migration of the molecular weight standards (from the top): bovine serum albumin, 66.3 kDa; glutamate dehydrogenase, 55.4 kDa; lactate dehydrogenase, 36.5 kDa; carbonic anhydrase, 31 kDa; trypsin inhibitor, 21.5 kDa; lysozyme, 14.4 kDa, as indicated.
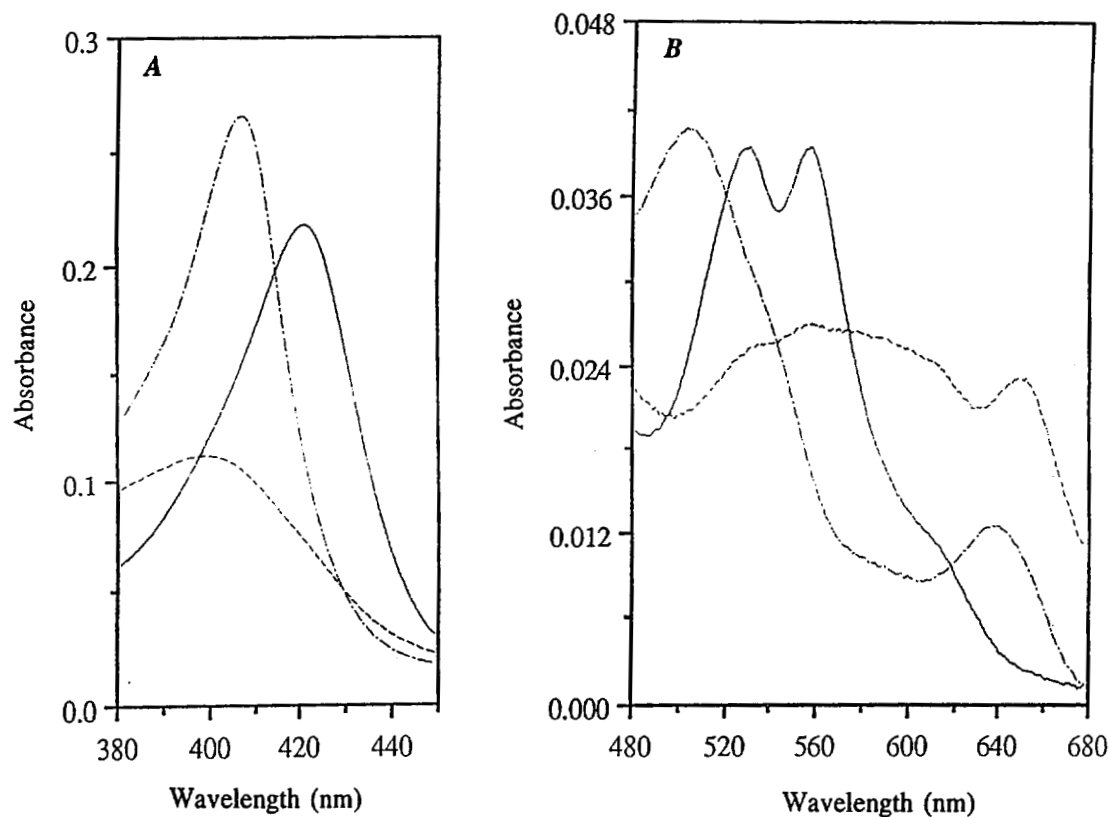
Figure 4.3. Electronic absorption spectra of oxidized states of MnP D179N. Comparison of UV/vis absorption spectra of native MnP D179N (-·-), MnP D179N compound I (---), and compound II (—). Spectra were recorded in 20 mM potassium malonate, pH 4.5, at 25 °C. The enzyme concentrations were 2 μM (A, Soret spectra) and 4 μM (B, visible spectra). MnP D179N compound I (---) was prepared by adding 1 equiv of H_2O_2 to native MnP D179N in 20 mM potassium malonate, pH 4.5 (μ = 0.1). MnP D179N compound II (—) was prepared by the successive additions of 1.0 equiv of H_2O_2 and 1.0 equiv of Mn(II) to the native enzyme in the same buffer.
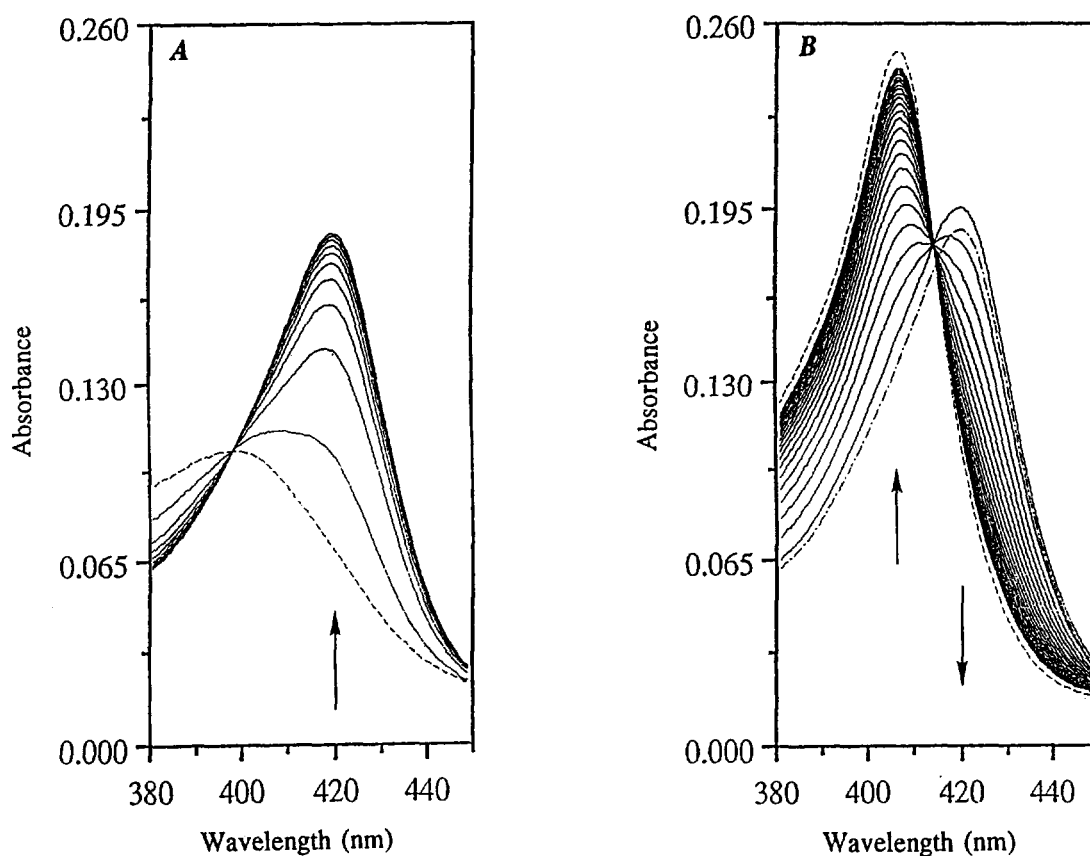
Figure 4.4. Reduction of MnP D179N compounds I and II. Reduction of MnP D179N compounds I (*A*) and II (*B*) with Mn(II). *A*, MnP D179N compound I (---) was prepared as described in the legend to Figure 4.3. Soret spectra were taken at 0.5 min intervals from 0.5–5.0 min. Final reactant concentrations: MnP D179N compound I, 2 μM; Mn(II), 2 μM (1 equiv). Arrow indicates progress of reaction. *B*, MnP D179N compound II (---) was prepared as described in the legend to Figure 4.3. Spectra were taken at 1 min intervals from 1–25 min. Final reactant concentrations: MnP D179N compound II, 2 μM; Mn(II), 20 μM (10 equiv). Dashed line represents native MnP D179N (2 μM). Arrows indicate progress of reaction.

Table 4.1. Absorbance maxima (nm) of native and oxidized intermediates of wild-type MnP1 and the MnP D179N mutant.

	Native	Compound I	Compound II
wild-type MnP1[a]	406, 502, 632	407, 558, 617 (sh)[b], 650	420, 528, 555
MnP D179N[c]	406, 502, 635	398, 557, 615 (sh)[b], 650	420, 528, 556

[a] Wariishi *et al.*, 1988.

[b] Shoulder.

[c] This work.

(Mayfield *et al.*, 1994b). Under steady-state conditions, linear Lineweaver-Burk plots were obtained over a range of Mn(II) and H_2O_2 concentrations using 50 mM malonate as the chelator (Wariishi *et al.*, 1992; Mayfield *et al.*, 1994b) (data not shown). The apparent K_m and k_{cat} values for Mn(II) and H_2O_2 are listed in Table 4.2. The apparent K_m for H_2O_2 was the same for both the wild-type MnP1 and MnP D179N. In contrast, the apparent K_m of MnP D179N for Mn(II) was ~50-fold higher than that for the wild-type MnP1 (Table 4.2). In addition, the apparent k_{cat} of MnP D179N for Mn(II) was more than 260 times lower than that for the wild-type MnP1.

The comparative rates of MnP compound II reduction for the mutant and wild-type enzyme also were examined since this is the rate-limiting step in the MnP catalytic cycle (Wariishi *et al.*, 1989a; Kuan *et al.*, 1993; Kishi *et al.*, 1994). The reduction was followed at 406 nm under pseudo-first-order conditions using an excess of reducing substrate. The plot of observed pseudo-first-order rate constants versus Mn(II) concentration leveled off at high Mn(II) concentrations (Figure 4.5) (Kishi *et al.*, 1994). This reaction can be explained by a simple binding interaction between the reactants, according to eqs. 4-6:

$$\text{compound II} + \text{Mn(II)-complex} \overset{K_D}{\rightleftharpoons}$$

$$\text{compound II} - \text{Mn(II)-complex} \overset{k}{\rightarrow}$$

$$\text{native enzyme} + \text{Mn(III)-complex} \tag{4}$$
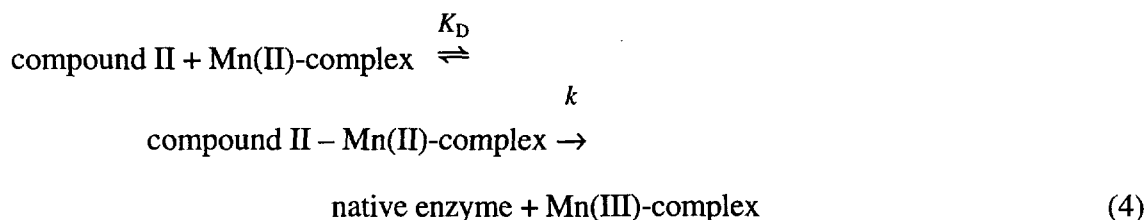
$$k_{obs} = \frac{k}{1 + K_D/[\text{Mn(II)-complex}]} \tag{5}$$

$$K_D = \frac{[\text{compound II}][\text{Mn(II)-complex}]}{[\text{compound II} - \text{Mn(II)-complex}]} \tag{6}$$

where k is a first-order rate constant (s^{-1}) and K_D is a dissociation constant (M). The calculated values are listed in Table 4.3. With *p*-cresol as the reductant in the conversion of compound II to native enzyme, the plots of pseudo-first-order rate constants versus *p*-cresol concentrations were linear for both wild-type MnP1 and MnP D179N (Figure 4.6). The second-order rate constants were calculated as 1.94×10^2 and 1.59×10^2 $M^{-1}s^{-1}$ for wild-type MnP1 and MnP D179N, respectively (Table 4.3).

Table 4.2. Steady-state kinetic parameters for wild-type rMnP1 and MnP D179N mutant.[a]

| | K_m (μM) | | k_{cat} (s^{-1}) | k_{cat}/K_m (M^{-1}s^{-1}) |
	Mn(II)	H_2O_2	Mn(II)	Mn(II)
wild-type MnP1[b]	73.2	41.7[c]	3.01×10^2	4.11×10^6
wild-type rMnP1[b]	69.4	39.2[c]	2.89×10^2	4.17×10^6
MnP D179N[d]	3.7×10^3	34.1[e]	1.09	2.95×10^2

[a] Reactions were conducted in 50 mM Na-malonate, pH 4.51.

[b] Mayfield *et al.*, 1994b.

[c] Apparent K_m for H_2O_2 was determined at 0.5 mM Mn(II).

[d] This work.

[e] Apparent K_m for H_2O_2 was determined at 5.0 mM Mn(II).
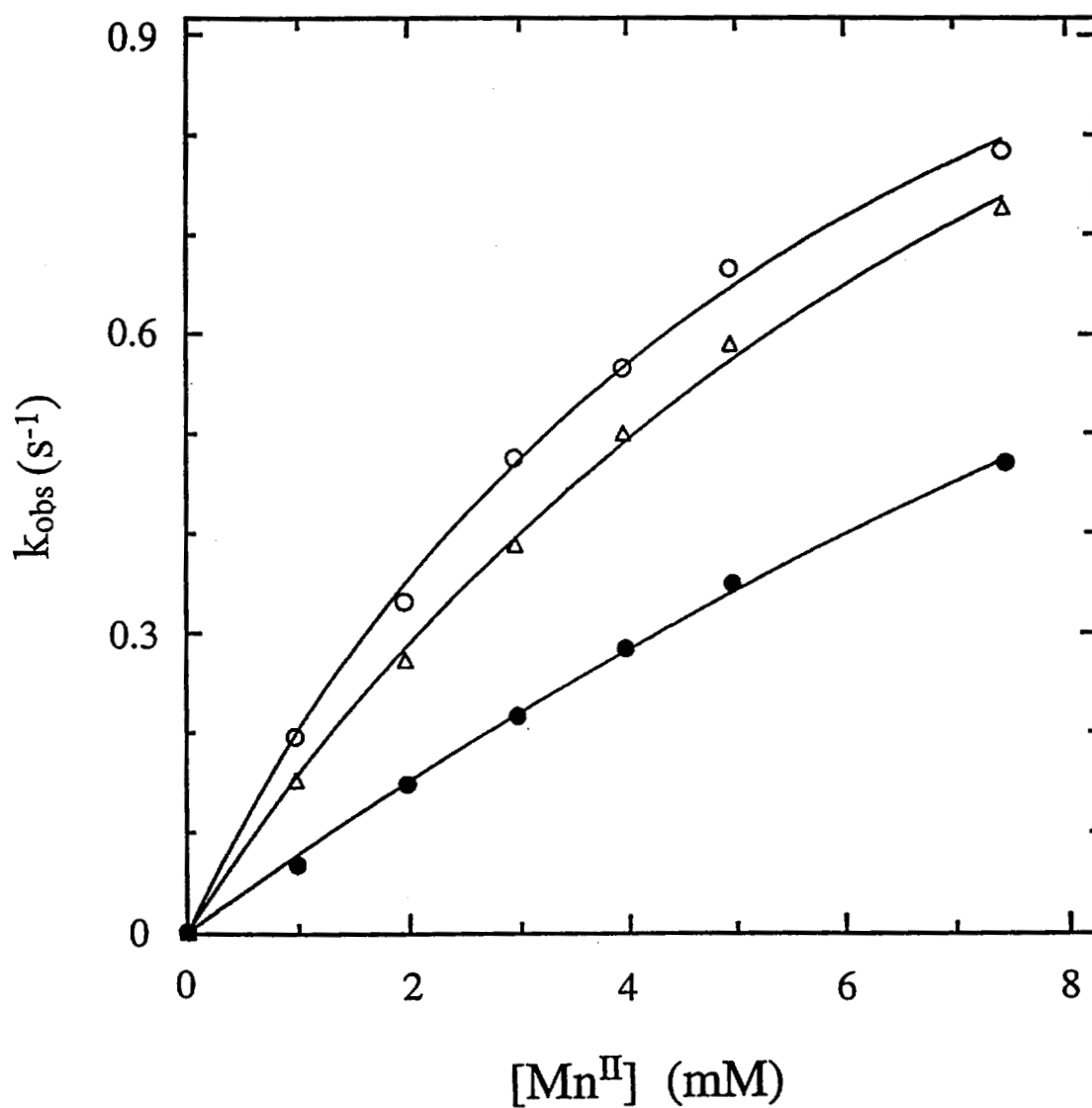
Figure 4.5. Kinetics of reduction of MnP D179N compound II. Reduction of MnP D179N compound II by Mn(II) in 0.5 (O), 2 (Δ), and 5 (●) mM potassium oxalate, pH 4.6, $\mu = 0.1$. Each k_{obs} was obtained from the exponential change in absorbance at 406 nm.
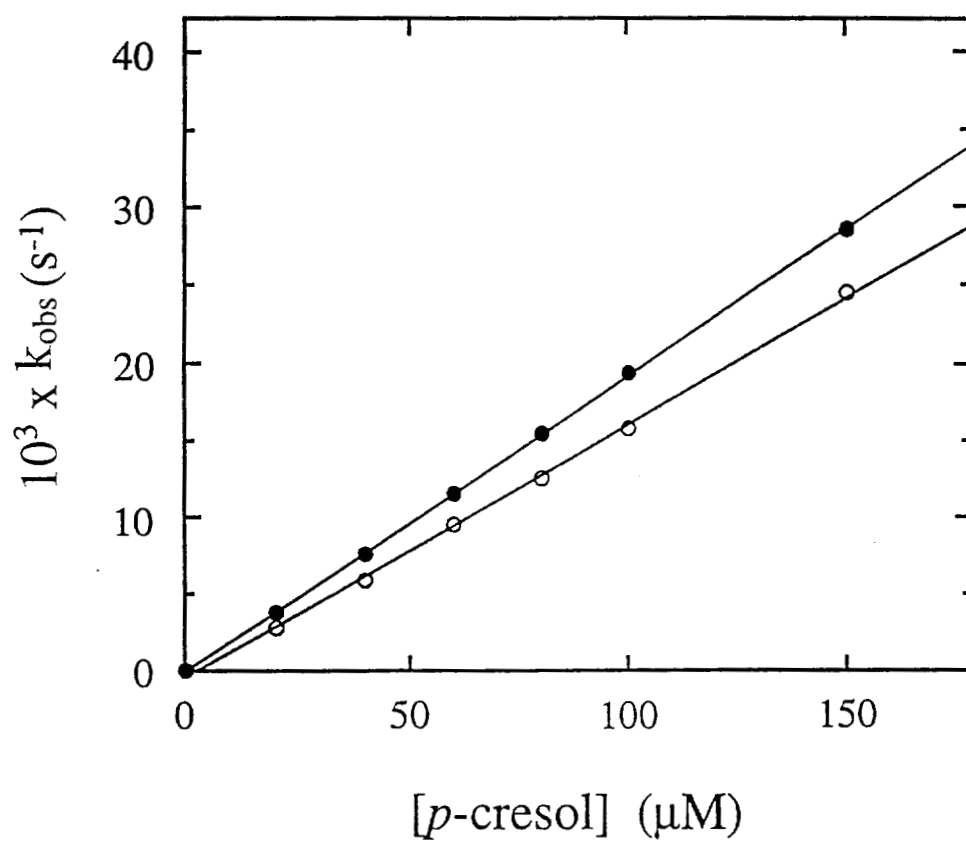
Figure 4.6. Kinetics of reduction of mutant and wild-type MnP compound II by p-cresol. Reduction of MnP D179N (O) and wild-type (●) compound II by p-cresol in 20 mM potassium malonate, pH 4.5. Each k_{obs} was obtained from the exponential change in absorbance at 406 nm.

Table 4.3. Kinetic parameters for reduction of MnP compound II.[a]

| enzyme | chelators (pH) (mM) | substrates | hyperbolic | | linear |
			first-order rate constant (s^{-1})	equilibrium dissociation constants (M)	second-order rate constants $(M^{-1}s^{-1})$[b]
	Oxalate (4.6)[c]				
wild-type MnP1	1	Mn(II)	$(2.3 \pm 0.2) \times 10^2$	$(5.6 \pm 1.0) \times 10^{-5}$	
	2		$(2.9 \pm 0.1) \times 10^2$	$(8.7 \pm 0.7) \times 10^{-5}$	
	5		$(5.6 \pm 0.6) \times 10^2$	$(4.4 \pm 0.6) \times 10^{-4}$	
	Malonate (4.5)				
	20	p-cresol			1.94×10^2
MnP D179N	Oxalate (4.6)				
	0.5	Mn(II)	1.46 ± 0.08	$(6.42 \pm 0.62) \times 10^{-3}$	
	1		1.30 ± 0.07	$(5.64 \pm 0.56) \times 10^{-3}$	
	2		1.70 ± 0.13	$(1.00 \pm 0.12) \times 10^{-2}$	
	5		2.11 ± 0.32	$(2.64 \pm 0.48) \times 10^{-2}$	
	Malonate (4.5)				
	20				1.59×10^2

[a]Reaction mixtures contained 2 μM MnP. The ionic strength was adjusted to 0.1 M.

[b]Forward second-order rate constant.

[c]Kishi et al., 1994.

4.4 DISCUSSION

Although the catalytic cycle of MnP is similar to that of other plant and fungal peroxidases (Gold *et al.*, 1989; Wariishi *et al.*, 1989a; Dunford & Stillman, 1976; Wariishi *et al.*, 1988; Renganathan & Gold, 1986), this enzyme is uniquely capable of oxidizing Mn(II) to Mn(III) (Glenn *et al.*, 1986; Wariishi *et al.*, 1989a, 1992). The latter, complexed with an organic acid, diffuses from the enzyme to oxidize the terminal phenolic substrate (Glenn *et al.*, 1986; Tuor *et al.*, 1992). This suggests that the primary substrate, Mn(II), binds directly to the enzyme. We have shown that free Mn(II) binds in the vicinity of the heme of the native enzyme with an apparent dissociation constant of 9.6 μM (Wariishi *et al.*, 1992). It is noteworthy that a variety of dicarboxylic chelators, including oxalate and malonate, increased the apparent dissociation constant 5-fold, although a chelator is required for enzymatic activity (Wariishi *et al.*, 1992).

The nature of the Mn(II) binding site in MnP has been under investigation for several years. Results of reactivity studies with azide and organic hydrazines as suicide inhibitors led Harris et al. (1991) to suggest that the binding of Mn(II) does not interfere with reactions at the δ meso position of the heme. However, they suggested that Mn(II) binds close to the δ meso position (above or below the plane of the heme). Similarly, based upon the perturbation of the NMR spectrum of MnP upon the binding of Mn(II), Banci et al. (1993) suggested a Mn(II) binding site close to the δ meso position of the heme. In contrast, Johnson et al. (1993) used homology modeling and energetic considerations to predict the Mn(II) binding site in MnP. They reported that the most likely binding site consists of the ligands Asp179, Glu35 and Glu39, and one of the heme propionates (Johnson *et al.*, 1993). This would place the Mn(II) binding site closer to the γ-meso position of the heme. As shown in Figure 4.7, the recent crystal structure of MnP (Sundaramoorthy *et al.*, 1994b) supports this latter prediction for the binding site.

This binding site is defined by three acidic amino acid ligands, including Asp179, Glu35 and Glu39, and one of the heme propionates. The final two ligands of the hexacoordinate Mn(II) ion are water molecules. Comparison of the Mn(II) binding ligands in MnP to corresponding amino acid residues in the LiP crystal structure (Sundaramoorthy *et al.*, 1994b; Johnson *et al.*, 1993) reveals that two of the three anionic residues found in MnP are replaced by noncharged residues in LiP: Ala36 for Glu35 and
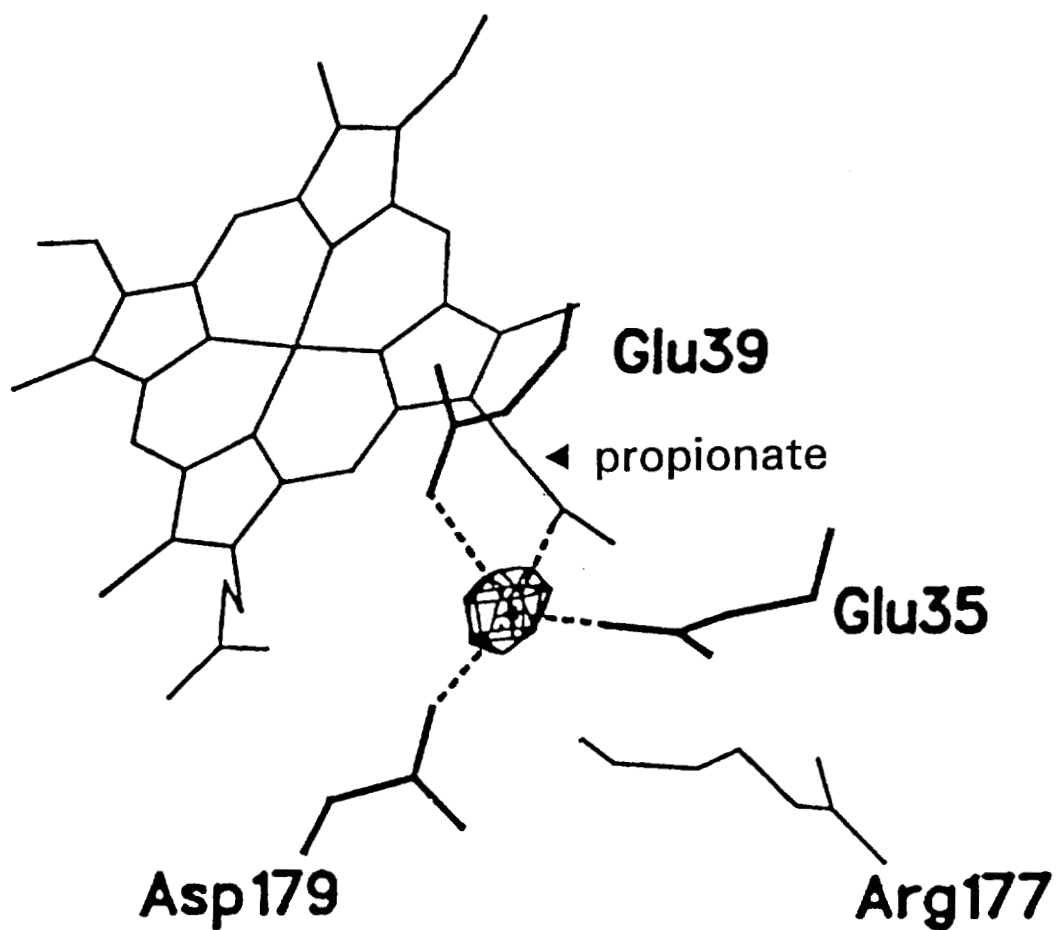
Figure 4.7. Mn(II) ligands in the binding site of Mn peroxidase (Sundaramoorthy *et al.*, 1994b).

Asn182 for Asp179. Only Glu39 in MnP is conserved as Glu40 in LiP. In addition, the heme propionate in LiP is not positioned for favorable Mn(II) binding (Sundaramoorthy *et al.*, 1994b; Johnson *et al.*, 1993). The presence of a single anionic ligand in LiP would not constitute a stable Mn(II) binding site. Mutation of the proposed Mn(II) ligands in MnP would aid our understanding of the unique specificity of this peroxidase. Furthermore, a mutation would test whether the proposed Mn(II) binding site (Sundaramoorthy *et al.*, 1994b) is productive. Herein, we report on the characterization of the site-directed mutant D179N, which transforms one of the proposed acidic amino acid ligands in the Mn(II) binding site.

We recently demonstrated the homologous expression of recombinant MnP isozyme 1 (rMnP1) of *P. chrysosporium* (Mayfield *et al.*, 1994b). In this system the expression of the *mnp*1 gene is under the control of the *P. chrysosporium gpd* gene promoter. This allows expression of rMnP1 during the primary metabolic phase of growth when the endogenous MnPs are not expressed. Both the spectral and kinetic properties of the recombinant enzyme were very similar to wild-type MnP1, indicating that this expression system is suitable for conducting structure/function studies of MnP by site-directed mutagenesis. Overlap extension PCR was used to create the D179N mutation. The mutant gene in pOGI18 was transformed into the Ade1 strain of *P. chrysosporium* as described (Mayfield *et al.*, 1994b; Alic *et al.*, 1990). The MnP D179N protein was purified as described (Mayfield *et al.*, 1994b). The Mono Q chromatographic profile suggests that one major heme protein is produced (Figure 4.2).

The D179N protein is essentially identical to the wild-type enzyme with respect to chromatographic properties and molecular weight (Figure 4.2), suggesting that this mutation does not lead to gross conformational changes in the protein. Furthermore, the native D179N mutant protein exhibits essentially identical spectral features to those of wild-type MnP (Figure 4.3, Table 4.1) (Wariishi *et al.*, 1988). The spectra of the catalytic intermediates, compounds I and II, of the mutant protein also are essentially identical to those of the wild-type MnP intermediates, except that the Soret band of MnP D179N compound I was red shifted 9 nm with a peak at 398 nm (Figure 4.3, Table 4.1). This difference may be explained by the possible contamination of wild-type MnP compound I preparations with compound II (Wariishi *et al.*, 1988). The latter has a Soret peak at 420 nm (Table 4.1). The spectral similarities of the mutant MnP D179N and the wild-type MnP strongly suggest that the heme environment of MnP is not affected significantly by this mutation.

In contrast to the minimal effect on the UV/vis spectral properties, the mutation D179N had a dramatic affect on the steady-state kinetic properties of the enzyme. Both the specific activity and the turnover number (k_{cat}) for Mn(II) oxidation by the MnP D179N protein decrease considerably in comparison to the wild-type enzyme (1/350 and 1/260, respectively). Moreover, the apparent K_m for Mn(II) of MnP D179N is 50 times higher than that for the wild-type MnP (Table 4.2). This suggests that Asp179 is one of the ligands in the Mn(II) binding site and that the Mn(II) binding site predicted by modeling and crystallographic results is the productive site (Sundaramoorthy *et al.*, 1994b; Johnson *et al.*, 1993).

In comparison, the mutation does not affect the apparent K_m for H_2O_2. This suggests that the affinity of D179N for H_2O_2 and probably the rate of compound I formation in the mutant are not altered. These results suggest that the environment of the amino acid residues thought to be involved in the formation of compound I, including the distal His, distal Arg and proximal His, has not been altered in this mutant.

Since the reduction of compound II to the native enzyme is the rate-limiting step in the MnP catalytic cycle (Wariishi *et al.*, 1988, 1989a; Kuan *et al.*, 1993; Kishi *et al.*, 1994), the rate of the MnP D179N compound II reduction by Mn(II) was examined. In potassium oxalate (0.5–5 mM, pH 4.6), the plot of k_{obs} versus Mn(II) concentration is hyperbolic (Figure 4.5), indicating a binding interaction between Mn(II) and MnP. The reduction of wild-type MnP compound II also exhibits saturation kinetics in the presence of low concentrations of oxalate (1–5 mM) but at much lower concentrations of Mn(II) (Table 4.3) (Kishi *et al.*, 1994). At 1 mM oxalate, the equilibrium dissociation constant for the wild-type enzyme is ~5.6×10^{-5} M while that for the D179N mutant is 5.6×10^{-3} M.

Thus, the binding constant for the mutant is $100 \times$ lower. This strongly suggests that D179 is a Mn(II) ligand. In contrast to the kinetics observed for the reduction of MnP compound II by Mn(II), the reduction of compound II by *p*-cresol obeys second-order kinetics and is irreversible for both wild-type MnP1 and MnP D179N (Figure 4.6). The rate of reduction of wild-type MnP1 compound II by *p*-cresol is similar to that of MnP D179N compound II. In comparison, the first-order rate constant for Mn(II) reduction of wild-type compound II in 1 mM oxalate is approximately 200 times that for the reduction of MnP D179N compound II (Table 4.3), whereas the dissociation constant for Mn(II) is approximately 1/100 of the value obtained for MnP D179N. These results strongly suggest that the low reactivity of MnP D179N for Mn(II) oxidation is a consequence of the

decreased binding affinity of Mn(II) for the mutant protein. However, the results do not rule out an additional effect on the electron transfer rate. The results also suggest that *p*-cresol binds to the enzyme at a site other than the Mn(II) binding site. A recent molecular modeling study indicates that *p*-cresol binds to horseradish peroxidase at a site on the distal side of the heme adjacent to Phe68 (Banci *et al.*, 1994). This site is distinct from the Mn(II) binding site shown in Figure 4.7.

In conclusion, the results of this study demonstrate that changing Asp179 to Asn significantly affects the oxidation of Mn(II), most probably by decreasing the affinity of the enzyme for Mn(II). In contrast, neither the apparent K_m for H_2O_2 or the rate of compound II reduction by *p*-cresol are significantly affected by this mutation. These results strongly support the assignment of the Mn(II) binding site shown in Figure 4.7 (Sundaramoorthy *et al.*, 1994b; Johnson *et al.*, 1993). This site consists of Asp179, Glu39, Glu35, a heme propionate and two water molecules. The coordination of the Mn(II) at this site is octahedral which is typical of Mn(II) coordination complexes (Demmer *et al.*, 1980). Current views envision electron transfer pathways in proteins through covalent bonds (Onuchic & Beratan, 1990). The structure of this site suggests that the electron may be transferred from Mn(II) to the porphyrin via the heme propionate ligand, using a nearly continuous σ-bonded path. Additional mechanistic, structural, and mutagenesis studies will be required in order to elucidate further the electron transfer pathway in this system.

CHAPTER 5

CHARACTERIZATION OF MN(II) BINDING SITE MUTANTS OF MANGANESE PEROXIDASE

5.1 INTRODUCTION

White-rot basidiomycete fungi are capable of degrading the plant cell wall polymer lignin (Gold *et al.*, 1989; Kirk & Farrell, 1987; Buswell & Odier, 1987) and a variety of aromatic pollutants (Bumpus & Aust, 1987; Hammel, 1989; Valli & Gold, 1991; Valli *et al.*, 1992b). When cultured under ligninolytic conditions, the white-rot fungus *Phanerochaete chrysosporium* secretes two families of extracellular peroxidases, lignin peroxidase (LiP) and manganese peroxidase (MnP), which, along with an H_2O_2-generating system, comprise the major extracellular components of its lignin-degrading system (Kirk & Farrell, 1987; Buswell & Odier, 1987; Gold & Alic, 1993; Wariishi *et al.*, 1991b; Bao *et al.*, 1994; Hammel *et al.*, 1993). Both LiP and MnP are able to depolymerize lignin *in vitro* (Wariishi *et al.*, 1991b; Bao *et al.*, 1994; Hammel *et al.*, 1993). Moreover, MnP activity is found in all white-rot fungi known to degrade lignin (Hatakka, 1994; Périé & Gold, 1991; Orth *et al.*, 1993).

P. chrysosporium MnP has been purified and characterized extensively by a variety of biochemical and biophysical methods (Gold *et al.*, 1989; Gold & Alic, 1993; Glenn & Gold, 1985; Glenn *et al.*, 1986; Wariishi *et al.*, 1992). In addition, the sequences of cDNA and genomic clones encoding several *P. chrysosporium* MnP isozymes (*mnp*1 and *mnp*2) have been determined (Gold & Alic, 1993; Pribnow *et al.*, 1989; Peace *et al.*, 1989; Godfrey *et al.*, 1990; Mayfield *et al.*, 1994a). Spectroscopic studies and DNA sequences suggest that the heme environment of MnP is similar to that of other plant and fungal peroxidases (Glenn *et al.*, 1986; Wariishi *et al.*, 1988, 1992; Pribnow *et al.*, 1989; Harris *et al.*, 1991; Banci *et al.*, 1992; Dunford & Stillman, 1976; Mino *et al.*, 1988). Kinetic and spectral characterization of the oxidized intermediates, MnP compounds I, II, and III, indicate that the catalytic cycle of MnP is similar to that of horseradish peroxidase and LiP (Gold *et al.*, 1989; Glenn *et al.*, 1986; Wariishi *et al.*, 1988, 1992;

120

Renganathan & Gold, 1986). The crystal structures of both LiP and MnP have been reported (Edwards *et al.*, 1993; Poulos *et al.*, 1993; Piontek *et al.*, 1993; Sundaramoorthy *et al.*, 1994b). These structures confirm that the heme environments of MnP and LiP are similar to those of cytochrome *c* peroxidase and plant and fungal peroxidases (Poulos *et al.*, 1993; Sundaramoorthy *et al.*, 1994b). However, the crystal structure of MnP revealed a cation binding site. The ligands to this proposed Mn(II) binding site are Glu35, Glu39, Asp179, a heme propionate, and two H_2O molecules (Sundaramoorthy *et al.*, 1994b). MnP is unique in its ability to oxidize Mn(II) to Mn(III) (Glenn & Gold, 1985; Glenn *et al.*, 1986; Wariishi *et al.*, 1992) as shown in Scheme 5.1.

Schem 5.1
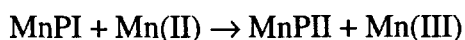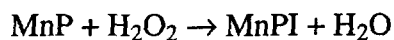
$$MnP + H_2O_2 \rightarrow MnPI + H_2O$$

$$MnPI + Mn(II) \rightarrow MnPII + Mn(III)$$

$$MnPII + Mn(II) \rightarrow MnP + Mn(III) + H_2O$$

The enzyme-generated Mn(III) is stabilized by organic acid chelators such as oxalate which is also secreted by the fungus (Wariishi *et al.*, 1992; Kishi *et al.*, 1994; Kuan *et al.*, 1993). The Mn(III)-organic acid complex oxidizes phenolic substrates, including lignin substructure model compounds (Tuor *et al.*, 1992) and aromatic pollutants (Valli & Gold, 1991; Valli *et al.*, 1992b; Joshi & Gold, 1993), as well as possible mediator molecules (Bao *et al.*, 1994; Wariishi *et al.*, 1989b).

We recently developed a homologous expression system for MnP isozyme 1 (MnP1) (Mayfield *et al.*, 1994b). In this system, the *P. chrysosporium* glyceraldehyde-3-phosphate-dehydrogenase (*gpd*) promoter is used to drive expression of the *mnp*1 gene during the primary metabolic growth phase when endogenous MnP is not expressed. This expression system produces recombinant MnP1 (rMnP1) in amounts comparable to the endogenous MnPs produced by the wild-type strain (Mayfield *et al.*, 1994b). Previously, we used this expression system and the polymerase chain reaction (PCR) to create a site-directed mutation in which Asp179, one of the potential Mn(II) binding ligands in MnP, was converted to an Asn (Kusters-van Someren *et al.*, 1995). Kinetic and spectroscopic analyses demonstrated that this mutation significantly affected the oxidation of Mn(II), probably by decreasing the affinity of the enzyme for Mn(II), confirming that Asp179 is a Mn(II) ligand. To further characterize the Mn(II) binding site, we have mutated the

putative Mn(II) ligands Glu35 and Glu39 and characterized these single mutants and an E35Q-D179N double mutant spectroscopically and kinetically.

5.2 MATERIALS AND METHODS

5.2.1 Organisms

P. chrysosporium wild-type strain OGC101, auxotrophic strain OGC107-1 (Ade 1), and prototrophic transformants were maintained as described (Mayfield *et al.*, 1994b; Alic *et al.*, 1990). *Escherichia coli* XL1-Blue and DH5αF′ were used for subcloning plasmids.

5.2.2 Oligodeoxyribonucleotides

Four oligonucleotides were each used for site-directed mutagenesis of Glu35 and Glu39 of *mnp1* (Pribnow *et al.*, 1989; Godfrey *et al.*, 1990). Oligonucleotide $N10_{norm}$ is a 17-mer corresponding to *mnp1* positions 14–30. Oligonucleotide $B9_{rev}$ is complementary to the *mnp1* sequence over nucleotide positions 592–608. Oligonucleotides $Q35_{norm}$ and $Q35_{rev}$ are a 27-mer and a 29-mer, respectively, and are partially overlapping: $Q35_{norm}$ spans nucleotides 219–245, and $Q35_{rev}$ is complementary to nucleotides 207–235. Oligonucleotides $Q39_{norm}$ and $Q39_{rev}$ are 28 mers and are again partially overlapping: $Q39_{norm}$ spans nucleotides 289–316, and $Q39_{rev}$ is complementary to nucleotides 278–305. Oligonucleotides were synthesized at the Center for Gene Research and Biotechnology, Oregon State University, Corvallis, OR. $Q35_{norm}$ and $Q35_{rev}$ contain the preferred codon and anticodon (Ritch & Gold, 1992), respectively, for Gln, CAG replacing GAA, which encodes Glu35. $Q39_{norm}$ and $Q39_{rev}$ also contain the preferred codon and anticodon, respectively, for Gln, CAG replacing GAG, which encodes Glu39.

5.2.3 Site-directed Mutagenesis by PCR

A 544-bp *Not*1-*Bpu*1102I fragment containing the E35Q or E39Q mutation was generated by overlap extension (Kusters-van Someren, *et al.*, 1995; Ho *et al.*, 1989) using the polymerase chain reaction (PCR). Two fragments which partially overlap were generated by using either oligonucleotides $N10_{norm}$ and $Q35_{rev}$ (or $Q39_{rev}$) or oligonucleotides $Q35_{norm}$ (or $Q39_{norm}$) and $B9_{rev}$ under the conditions described (Kusters-van Someren *et al.*, 1995). The reaction products of both reactions were analyzed by electrophoresis on a 1% agarose gel and the desired fragments were excised and purified

using GeneClean (Bio101). The partially overlapping fragments were combined and used as template DNA in a third reaction with oligonucleotides $N10_{norm}$ and $B9_{rev}$ to generate a 593-bp PCR fragment under the same conditions (Kusters-van Someren et al., 1995). The final PCR product was analyzed by agarose gel electrophoresis, excised, purified by GeneClean and digested with NotI and Bpu1102I (New England Biolabs).

5.2.4 Construction of pAGM6, 8, and 9

The NotI-Bpu1102I fragments containing the E35Q and E39Q mutations were first subcloned into pGM1 (Mayfield et al., 1994b), containing unique NotI-Bpu1102I sites, replacing the wild-type mnp1 fragment with the mutant fragment, to generate pGM8 and pGM9, respectively. For the E35Q-D179N double mutation, the NotI-Bpu1102I fragment containing the E35Q mutation was subcloned into pGM4, which contains the D179N mutation (Kusters-van Someren, et al., 1995), to generate pGM6. The entire NotI-Bpu1102I fragments were analyzed by double-stranded DNA sequencing as described (Kusters-van Someren et al., 1995). Subsequently, the 4.0-kb XbaI-EcoRI fragments of pGM6, 8, and 9, containing the gpd promoter and the mutated mnp1 genes, were subcloned into pOGI18 (Godfrey et al., 1994), generating pAGM6, 8, and 9, respectively. The presence of the mutations in pAGM6, 8, and 9 was confirmed by double-stranded DNA sequencing of the appropriate sequences, using oligonucleotide $N10_{norm}$ as a primer.

5.2.5 Transformation of *Phanerochaete chrysosporium*

P. chrysosporium strain Ade1 (Gold et al., 1982) was transformed as described previously (Mayfield et al., 1994b; Alic et al., 1990), using 1 μg of pAGM 6, 8, or 9 as transforming DNA. Transformants were transferred to minimal slants (Mayfield et al., 1994b; Alic et al., 1990) to confirm adenine prototrophy and assayed for MnP activity using the o-anisidine plate assay as described (Mayfield et al., 1994b). Transformants with the strongest activity were purified by fruiting as described (Alic et al., 1987) and the progeny were rescreened for MnP activity by the o-anisidine plate assay.

5.2.6 Production and Purification of the MnP Mutant Proteins

Cultures were maintained on slants and grown in liquid cultures from conidial inocula (Mayfield et al., 1994b; Kusters-van Someren, 1995). The MnP mutant proteins were purified from the extracellular medium as described for the wild-type recombinant MnP1 (Mayfield et al., 1994b), except that hydrophobic interaction column chromatography was employed as the initial step. Ammonium sulfate (1.0 M) was

added to the concentrated extracellular medium after which the mixture was applied to a Phenyl Sepharose CL-6B column (2.5 × 15 cm), equilibrated with 20 mM sodium acetate (pH 4.5), containing 1.0 M ammonium sulfate. The column was eluted at 4 °C with a linear ammonium sulfate gradient (1.0 to 0.2 M). The fractions containing MnP activity were concentrated and desalted by membrane ultrafiltration. MnP mutant proteins were purified further by a combination of Cibacron Blue 3GA agarose column chromatography and fast-protein liquid chromatography using a Mono Q column (Pharmacia), as described (Mayfield *et al.*, 1994b; Kusters-van Someren *et al.*, 1995).

5.2.7 SDS-PAGE and Western Blot Analysis

Sodium dodecyl sulfate-polyacrylamide gel electrophoresis (SDS-PAGE) was performed using a 12% Tris-glycine gel system (Laemmli, 1970) and a Mini-Protean II apparatus (Bio-Rad). The gels were stained with Coomassie blue. For western (immunoblot) analysis, proteins were electroblotted (Sambrook *et al.*, 1989) onto nitrocellulose (Micron Separations, Inc.) and MnP proteins were detected as described (Mayfield *et al.*, 1994b).

5.2.8 Enzyme Assays and Spectroscopic Procedures

Mn(II) oxidation by MnP was measured by following the formation of Mn(III)-malonate at 270 nm as previously described (Wariishi et al, 1992). The oxidation of ferrocyanide by MnP was followed at 420 nm using the absorptivity of ferricyanide, 1 mM^{-1} cm^{-1} (Cheddar *et al.*, 1989). UV-absorption spectra of the various oxidation states of MnP mutant proteins were recorded at room temperature using a Shimadzu UV-260 spectrophotometer. The enzyme was maintained in 20 mM potassium malonate, pH 4.5. The ionic strength of the buffers was adjusted to 0.1 M using K_2SO_4. Enzyme concentrations were determined at 406 nm using an absorptivity of 129 mM^{-1} cm^{-1} (Glenn & Gold, 1985). Compound I of the MnP mutants was prepared by mixing 1.0 equiv of H_2O_2 with native enzyme. Compound II was prepared by the successive addition of 1.0 equiv of H_2O_2 and 1.0 equiv of ferrocyanide to the native enzyme.

5.2.9 Kinetic Analysis

To determine apparent K_m and k_{cat} values for Mn(II) and ferrocyanide, 1/initial velocity versus 1/[substrate] were plotted at fixed concentrations of H_2O_2 (0.1 mM). Reaction mixtures contained mutant MnP protein (10 µg/ml), H_2O_2, and $MnSO_4$

(0.5–5.0 mM), or ferrocyanide (1.0–5.0 mM) in 50 mM sodium malonate, pH 4.5. To determine apparent K_m values for H_2O_2, 1/initial velocity versus 1/[H_2O_2] were plotted at 5 mM Mn(II). Transient state kinetic experiments on the formation of compound I and the reduction of compound II were carried out at 25.0 ± 1.0 °C using a Dionex DC37 stopped-flow photometer (dead time 2.7 ms) equipped with a 75-watt xenon lamp and interfaced with a Nicolet Explorer III scope kindly provided by Prof. M. Schimerlik, Oregon State University. One reservoir contained buffer and the enzyme (2 μM for compound I formation and 4 μM for compound II reduction experiments). The other reservoir contained the substrate (H_2O_2, Mn(II), p-cresol, or ferrocyanide) in water in at least 10-fold excess with respect to the enzyme. The formation of MnP compound I in 20 mM potassium succinate, pH 4.5 (ionic strength 0.1 M, adjusted with K_2SO_4), was followed at 397 nm, the isosbestic point between compound I and II. The reduction of MnP compound II in 20 mM potassium malonate, pH 4.5, or 1 mM potassium oxalate, pH 4.6 (ionic strength 0.1 M, adjusted with K_2SO_4), was followed at 406 nm, the Soret absorbance maximum of the native enzyme. Compound II of MnP mutant proteins was freshly prepared for each experiment and the reaction was initiated by adding the reducing substrate in 10-fold excess. All of the kinetic traces displayed single exponential character from which pseudo-first-order rate constants were calculated. Several substrate concentrations were used and plots of pseudo-first-order rate constants versus substrate concentration were obtained.

5.2.10 Resonance Raman Spectroscopy

Resonance Raman (rR) spectra were obtained on a custom spectrograph consisting of a McPherson (Acton, MA) Model 2061/207 monochromator operated at a focal length of 0.67 m and a Princeton Instruments (Trenton, NJ) LN1100 CCD detector with a Model ST-130 controller. Laser excitation was from Coherent (Santa Clara, CA) Innova 302 krypton (413.1 nm) and Innova 90-6 argon (514.5 nm) lasers. The laser lines were filtered through Applied Photophysics (Leatherhead, UK) prism monochromators to remove plasma emissions. Incident laser power at the sample was ~20 mW (413.1 nm) and ~55 mW (514.5 nm). Spectra were collected in a 90°-scattering geometry from solution samples contained in glass capillary tubes at room temperature. Rayleigh scattering was attenuated by use of Kaiser Optical (Ann Arbor, MI) notch or super-notch filters. Spectral resolution was set to ~3.0 cm^{-1}. Indene and CCl_4 served as frequency and polarization standards, respectively. Data were calibrated and analyzed with GRAMS/386 spectroscopic software (Galactic Industries Corp., Salem NH). The concentrations of

MnP protein for rR studies were 100–200 μM in phosphate buffer (20 mM, pH 6.0) at constant ionic strength of 0.1 (adjusted with Na_2SO_4).

5.2.11 Chemicals

Phenyl-Sepharose CL-6B, Cibacron Blue 3GA agarose, potassium ferrocyanide, and H_2O_2 (30 % solution) were obtained from Sigma. The concentration of the H_2O_2 stock solution was determined as described (Cotton & Dunford, 1973). p-Cresol was obtained from Aldrich. p-Cresol was purified by silica gel thin-layer chromatography, solvent (hexane:ethyl acetate, 3:1) before use. All other chemicals were reagent grade. Solutions were prepared using deionized water obtained from a Milli Q purification system (Millipore).

5.3 RESULTS

5.3.1 Expression and Purification of Mutant Proteins

The presence of the E35Q and E39Q single mutations and the E35Q-D179N double mutation was confirmed by double-stranded DNA sequencing of the altered cassettes in both pGM6, 8 and 9 and the complete transformation vectors pAGM6, 8, and 9, respectively. Transformants which exhibited readily detectable MnP activity on plate assays were selected and purified by fruiting as described (Alic *et al.*, 1990). The purified transformants expressed extracellular recombinant MnP protein within three days after inoculation of liquid high-carbon, high-nitrogen agitated cultures, as verified by western (immunoblot) detection (data not shown). Endogenous MnP is not expressed under these conditions. The amounts of mutant protein secreted by the pAGM6, 8, and 9 transformants were comparable to the levels of recombinant wild-type MnP1 (rMnP1) we reported previously (Mayfield *et al.*, 1994b), as estimated by western immunoblot analysis (data not shown). However, the transformants exhibited low Mn(II)-oxidizing activity, as measured by the formation of the Mn(III)-malonate complex (Wariishi *et al.*, 1992). MnP proteins E35Q, E39Q, and E35Q-D179N were purified using Phenyl Sepharose, Blue Agarose, and Mono Q chromatographies (Mayfield *et al.*, 1994b; Kusters-van Someren, *et al.*, 1995). Phenyl Sepharose replaced DEAE Sepharose (Mayfield *et al.*, 1994b; Kusters-van Someren, *et al.*, 1995) as an initial purification step since the yield of MnP protein was higher. The major peak eluted from the Mono Q column in the same fraction as rMnP1, when the latter was chromatographed under

identical conditions (data not shown) (Mayfield *et al.*, 1994b). Furthermore, the molecular weights (46 kDa) of the MnP mutant proteins were identical to those of rMnP1 and wild-type MnP1 (data not shown).

5.3.2 Spectral Properties of MnP Mutant Proteins

Figure 5.1 shows the absorption spectra of the native, compound I, and compound II states of the MnP E35Q-D179N double mutant protein. The native protein exhibited a Soret band at 406 nm and visible bands at 500 and 640 nm. The Soret band of compound I was decreased with respect to native MnP and blue shifted from 406 nm to 397 nm. The visible region of compound I displayed a peak at 650 nm with a broad absorption from 530–600 nm. The addition of 1.0 equiv of ferrocyanide to compound I yielded a spectrum for compound II with maxima at 420, 528, and 555 nm. Similar absorption spectra of the native, compound I, and compound II states were observed for the MnP E35Q and E39Q single mutant proteins (data not shown). All of the spectral maxima of the native and various oxidized states of the MnP mutant proteins were essentially identical to those of the wild-type enzyme (Table 5.1), suggesting that substitution of amides for the acidic Mn(II) binding ligands did not alter the heme environment of the protein significantly.

5.3.3 Resonance Raman Spectroscopy

The high-frequency ($\sim$1300–1700 cm^{-1}) rR spectral regions that are characteristic of heme coordination and spin state are shown in Figures 2A and B for Soret-band (413.1-nm) and Q-band (514.5-nm) excitation, respectively. The rR spectrum of wild-type MnP (potassium phosphate buffer, pH 6.0, top trace) is of significantly higher quality and resolution than that reported previously (Mino *et al.*, 1988). The new data show that the broad peak at 1487 cm^{-1} (ν_3) is partially resolved into two components at 1482 and 1492 cm^{-1} (Figure 5.2A) and that the peak at 1623 cm^{-1} ($C=C_{vinyl}$ and ν_{10}) consists of three components at $\sim$1612, 1622, and 1628 cm^{-1} (Figure 5.2B). Although the relative intensities of the 1482/1492 cm^{-1} pair respond to changes in pH and ionic strength, both components are polarized (data not shown) and characteristic of ν_3 of six-coordinate high-spin (6cHS) and five-coordinate high-spin (5cHS) heme species, respectively. Consistent with the appearance of two ν_3 modes, the depolarized bands at $\sim$1612 and 1628 cm^{-1} (Figure 5.2B) are the corresponding ν_{10} porphyrin skeletal vibrations of 6cHS and
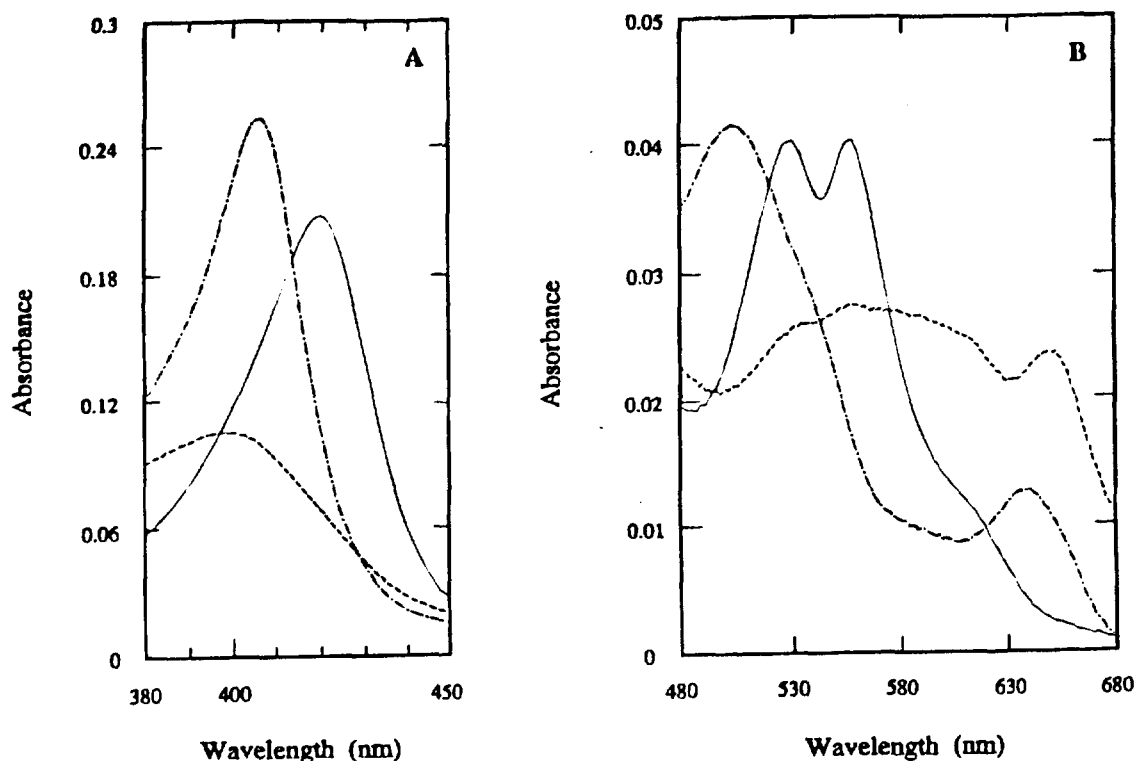
Figure 5.1. Electronic absorption spectra of oxidized states of the MnP E35Q-D179N double mutant. Comparison of UV/vis absorption spectra of native MnP E35Q-D179N (---), compound I (---), and compound II (—). Spectra were recorded in 20 mM potassium malonate, pH 4.5, at 25 °C. The enzyme concentrations were 2 μM (A, Soret spectra) and 4 μM (B, visible spectra). MnP E35Q-D179N compound I (---) was prepared by adding 1 equiv of H_2O_2 to the native enzyme in 20 mM potassium malonate, pH 4.5 (μ = 0.1). MnP E35Q-D179N compound II (—) was prepared by the successive additions of 1.0 equiv of H_2O_2 and 1.0 equiv of ferrocyanide to the native enzyme in the same buffer.

Table 5.1. Absorbance maxima (nm) of native and oxidized intermediates of wild-type MnP1 and MnP1 mutants.

Enzyme	Native	Compound I	Compound II
wt MnP1[a]	406, 502, 632	407, 558, 617 sh[b], 650	420, 528, 555
MnP D179N[c]	406, 502, 635	398, 557, 615 sh, 650	420, 528, 556
MnP E35Q	406, 502, 635	398, 558, 616 sh, 650	420, 528, 555
MnP E39Q	406, 501, 637	400, 557, 615 sh, 649	420, 528, 555
MnP E35Q-D179N	406, 500, 640	397, 555, 615 sh, 650	420, 528, 555

[a] Wariishi *et al.*, 1988

[b] Shoulder

[c] Kusters-van Someren *et al.*, 1995
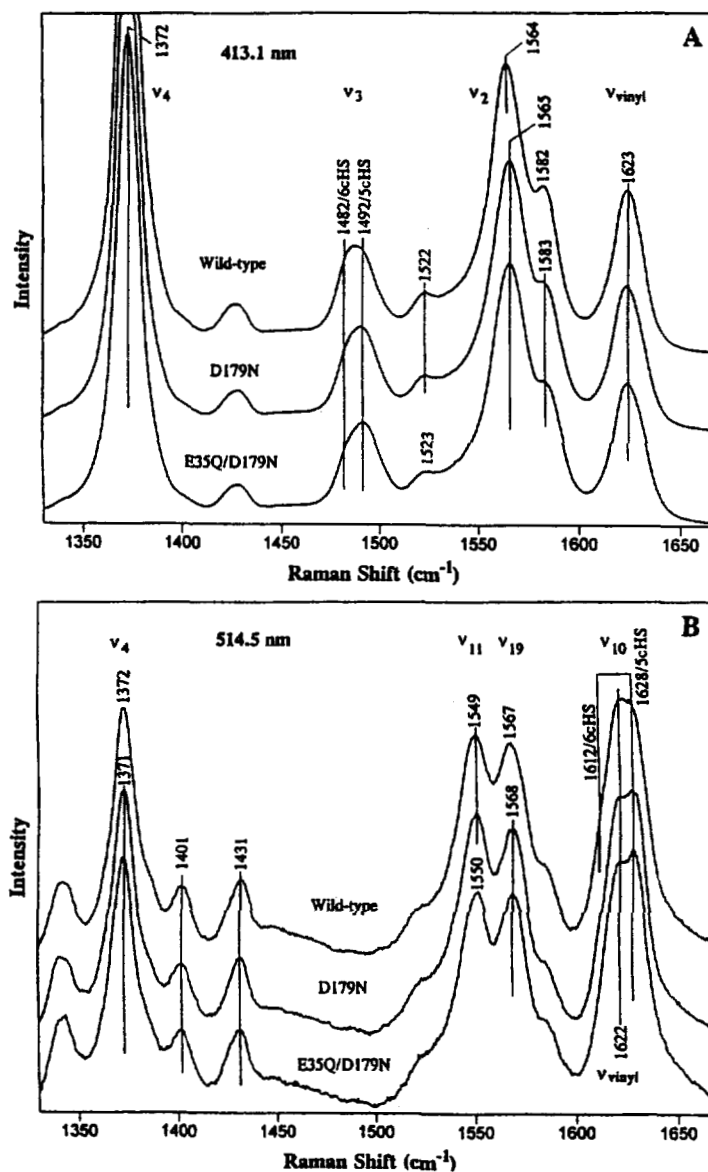
Figure 5.2. Resonance Raman spectra of MnP mutants. (A) Resonance Raman spectra of MnP proteins (~150 μM enzyme in 20 mM phosphate buffer, pH 6.0) obtained with Soret excitation (413.1 nm, 20 mW, 90° scattering geometry, ambient temperature). Samples are the wild-type enzyme (upper), and the mutant enzymes MnP D179N (middle) and E35Q-D179N (lower). Frequencies and assignments for selected heme bands are shown. (B) Resonance Raman spectra of MnP proteins (~150 μM enzyme in 20 mM phosphate buffer, pH 6.0) obtained with Q-band excitation (514.5 nm, 55 mW, 90° scattering geometry, ambient temperature). Samples are the same as in A. Frequencies and assignments for selected heme bands are shown. Polarization data were collected to support the assignments.

5cHS hemes, respectively. The band at 1622 cm^{-1} in the 514.5-nm spectrum is polarized and therefore can be assigned to a C=C$_{vinyl}$ stretching mode. This vinyl mode is almost totally responsible for the strongly polarized band at 1623 cm^{-1} observed with Soret excitation (Figure 5.2A). The present data provide compelling evidence that native wild-type MnP contains a mixture of 6cHS and 5cHS heme species at room temperature.

The rR spectra of the D179N single (Kusters-van Someren, 1995) and the E35Q-D179N double mutations of acidic ligands in the Mn(II)-binding pocket were essentially identical to those of wild-type MnP (Figures 5.2A and B, lower traces). Hence, these mutations did not result in any significant perturbation to the heme moiety. Only minor changes in intensities, but no frequency shifts, were detectable in the heme vibrational spectra as a result of these mutations. For example, in the 413-nm spectra of both mutants (Figure 5.2A), the intensity of the 1492-cm^{-1} component of v_3 was increased relative to that at 1482 cm^{-1}, in contrast to the nearly equal intensities in the spectrum of the wild-type enzyme; in parallel, the proportion of the 1628/1612 cm^{-1} v_{10} components also were increased (Figure 5.2B), suggesting that a slightly greater proportion of the hemes in the mutants were in a 5cHS state.

5.3.4 Steady-state Kinetics

Under steady-state conditions, linear Lineweaver-Burk plots were obtained over a range of Mn(II), ferrocyanide, and H$_2$O$_2$ concentrations in 50 mM malonate, pH 4.5 (data not shown). The apparent K_m and k_{cat} values for Mn(II), ferrocyanide, and H$_2$O$_2$ are listed in Tables 5.2 and 5.3. The apparent K_m values for H$_2$O$_2$ (30–40 µM) and ferrocyanide (3.3–3.6 mM) were similar for the wild-type MnP1, recombinant MnP1 and MnP mutant proteins. In contrast, the apparent K_m values for Mn(II) of MnP E35Q and E39Q were ~60 and ~30-fold higher, respectively, than that for the wild-type MnP1 (Table 5.2); whereas the apparent k_{cat} values of MnP E35Q and E39Q for Mn(II) were 390- and 250-fold lower, respectively, than for the wild-type proteins. Furthermore, the apparent K_m value of the MnP E35Q-D179N double mutant for Mn(II) was ~120-fold higher than that for wild-type MnP1. In addition, the apparent k_{cat} value of the MnP E35Q-D179N double mutant for Mn(II) was approximately 1000 times lower than that for the wild-type MnP1 (Table 5.2).

Table 5.2. Kinetic parameters of wild-type MnP1, rMnP1, MnP D179N, MnP E35Q, MnP E39Q, and MnP E35Q-D179N.[a]

	K_m (µM)	k_{cat} (s^{-1})	
	Mn(II)	H$_2$O$_2$	Mn(II)
wt MnP1	73	42	3.0×10^2
rMnP1	69	39	2.9×10^2
MnP D179N	3.7×10^3	34	1.1
MnP E35Q	4.4×10^3	27	0.77
MnP E39Q	2.0×10^3	37	1.2
MnP E35Q-D179N	8.1×10^3	31	0.29

[a] Reactions were carried out in 50 mM Na-malonate, pH 4.5. Apparent K_m and k_{cat} for Mn(II) were determined using 0.1 mM H$_2$O$_2$. Apparent K_m for H$_2$O$_2$ was determined using 5.0 mM Mn(II).

Table 5.3. Kinetic parameters of MnP proteins for ferrocyanide oxidation.[a]

Enzyme	K_m (mM)	k_{cat} (s^{-1})	k_{cat}/K_m (M^{-1} s^{-1})
wt MnP1	3.6	5.3	1.5×10^3
rMnP1	3.5	5.6	1.6×10^3
MnP D179N	3.5	5.4	1.6×10^3
MnP E35Q	3.3	5.4	1.6×10^3
MnP E39Q	3.5	5.4	1.6×10^3
MnP E35Q-D179N	3.5	5.4	1.5×10^3

[a] Reactions were carried out in 50 mM Na-malonate, pH 4.5. Apparent K_m and k_{cat} for ferrocyanide were determined using 0.1 mM H_2O_2.

5.3.5 Effect of Mutations on Compound I Formation

We demonstrated previously that the rate of MnP compound I formation was not affected by the structure or concentration of the organic acid chelator (Kishi *et al.*, 1994). In our current work, the rate of MnP compound I formation was determined at pH 4.6 in 20 mM potassium succinate. Compound I formation was measured at 397 nm, an isosbestic point between compounds I and II, excluding interference from the possible reduction of compound I. The observed rate constants (k_{1obs}) were linearly proportional to the H_2O_2 concentrations at 10–50-fold excess (data not shown). The second-order rate constants (k_{1app}) obtained for compound I formation for the wild-type protein and the mutant proteins D179N, E35Q, E39Q and E35Q-D179N were similar (Table 5.4).

5.3.6 Effect of Mutations on Compound II Reduction

The rate of compound II reduction is the rate-limiting step in the MnP catalytic cycle (Wariishi *et al.*, 1988, 1989a; Kishi *et al.*, 1994; Kuan *et al.*, 1993). The reductions of the wild-type and mutant proteins were followed at 406 nm under pseudo-first-order conditions using an excess of reducing substrate. The plots of observed pseudo-first-order rate constants versus Mn(II) concentrations leveled off at high Mn(II) concentration in 1 mM potassium oxalate (pH 4.6) (Figure 5.3). This reaction can be explained by a simple binding interaction between reactants, according to equations 1–3:
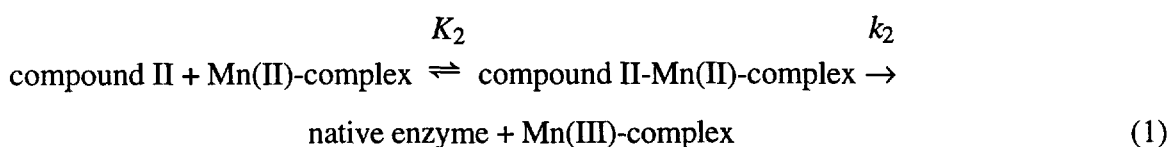
$$\text{compound II} + \text{Mn(II)-complex} \underset{}{\overset{K_2}{\rightleftharpoons}} \text{compound II-Mn(II)-complex} \overset{k_2}{\rightarrow}$$

$$\text{native enzyme} + \text{Mn(III)-complex} \qquad (1)$$

$$k_{2obs} = k_2 \, / \, (1 + K_2 \, / \, [\text{Mn(II)-complex}]) \qquad (2)$$

$$K_2 = [\text{compound II}][\text{Mn(II)-complex}] \, / \, [\text{compound II-Mn(II)-complex}] \qquad (3)$$

where k_2 is a first-order rate constant (s^{-1}) and K_2 is a dissociation constant (M). The calculated values for the first-order rate constant and the dissociation constant are listed in Table 5.5. The equilibrium dissociation constants for the MnP single and double mutants were approximately 100- and 200-fold higher, respectively, than that for the wild-type protein. The first-order rate constants for the single mutants and the double mutant were approximately 200- and 4000-fold lower, respectively, than that for the wild-type protein.

The reduction of compound II to native enzyme also was measured with *p*-cresol and ferrocyanide as the substrates. The plots of pseudo-first-order rate constants versus

Table 5.4. Rate of formation of MnP compound I.

MnP proteins	$k_{1app}{}^a$ (M^{-1} s^{-1})
wt MnP1	$(1.3 \pm 0.1) \times 10^6$
MnP D179N	$(1.1 \pm 0.2) \times 10^6$
MnP E35Q	$(1.1 \pm 0.2) \times 10^6$
MnP E39Q	$(1.2 \pm 0.1) \times 10^6$
MnP E35Q-D179N	$(1.1 \pm 0.2) \times 10^6$

[a] MnP compound I formation was followed at 397 nm, the isosbestic point between compounds I and II. Reactions were carried out in 20 mM K-succinate, pH 4.6 (ionic strength 0.1 M). These rate constants were linearly proportional to [H_2O_2] with a zero intercept.
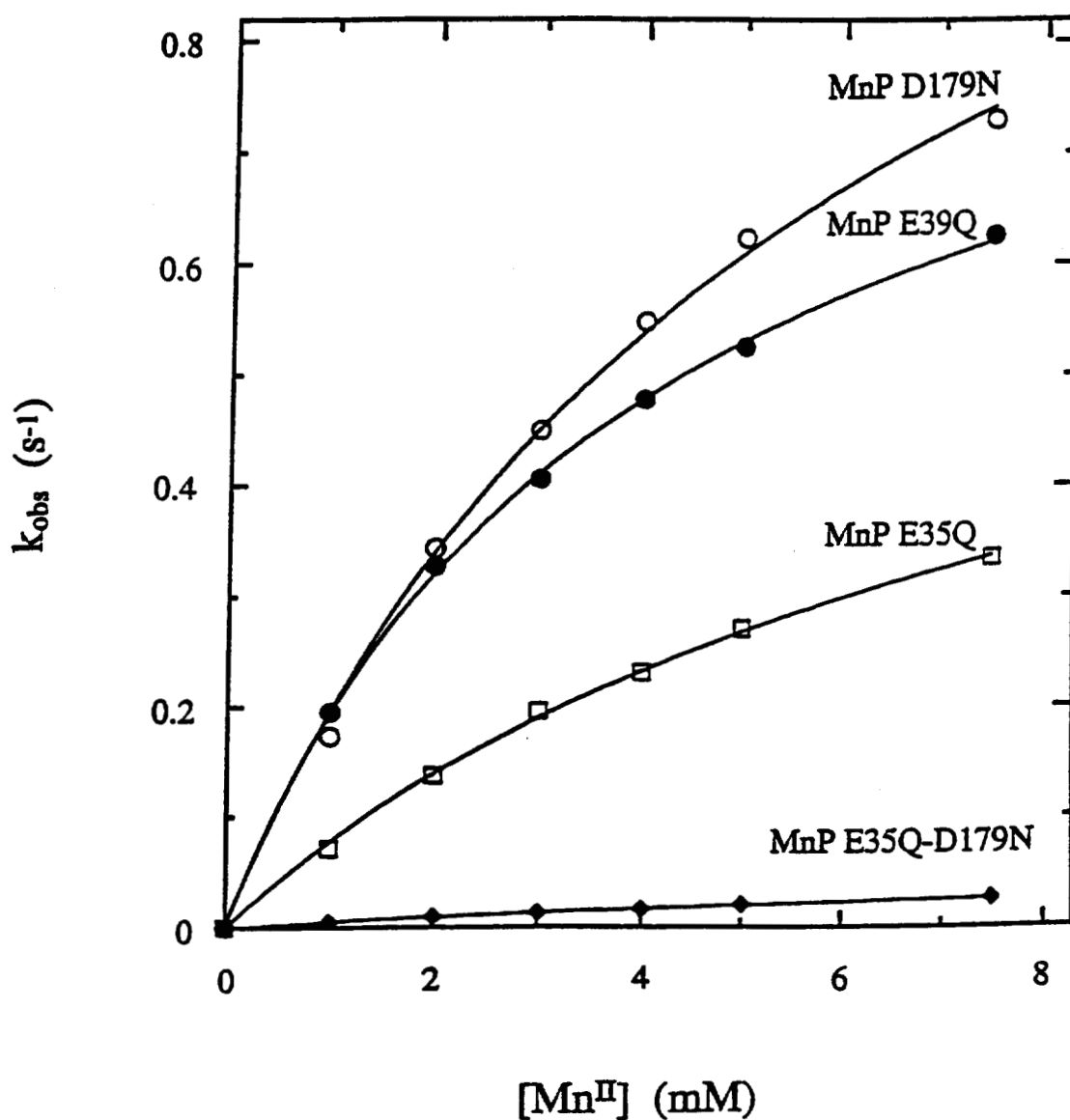
Figure 5.3. Kinetics of reduction of compound II of MnP mutant proteins by Mn(II). Reduction of compound II of MnP D179N (O), E39Q (●), E35Q (□), and E35Q-D179N (♦) by Mn(II) in 1 mM potassium oxalate, pH 4.6. Each trace exhibited single-exponential character. Concentration of enzyme was 2 μM, ionic strength 0.1 M.

Table 5.5. Kinetic parameters for reduction of MnP compound II by Mn(II).[a]

Enzyme	First-order rate constants (s^{-1})	Equilibrium dissociation constants (M)
wt MnP1[b]	$(2.3 \pm 0.2) \times 10^2$	$(5.6 \pm 1.0) \times 10^{-5}$
MnP D179N[c]	1.3 ± 0.1	$(5.6 \pm 0.6) \times 10^{-3}$
MnP E35Q	0.69 ± 0.03	$(8.0 \pm 0.6) \times 10^{-3}$
MnP E39Q	0.94 ± 0.02	$(3.9 \pm 0.2) \times 10^{-3}$
MnP E35Q-D179N	$(6.0 \pm 0.3) \times 10^{-2}$	$(1.1 \pm 0.1) \times 10^{-2}$

[a] Reactions were carried out in 1 mM K-oxalate, pH 4,6, containing 2 µM MnP compound II. The ionic strength was adjusted to 0.1 M.

[b] Kishi et al., 1994

[c] Kusters-van Someren et al., 1995

p-cresol or ferrocyanide concentrations were linear for wild-type MnP1 and MnP mutant proteins (data not shown). The calculated second-order rate constants are listed in Table 5.6. The second-order rate constants of MnP mutants for *p*-cresol and ferrocyanide were similar to those of wild-type MnP1, demonstrating that these mutations did not affect the oxidation of these substrates.

5.4 DISCUSSION

Although the catalytic cycle of MnP is similar to that of other plant and fungal peroxidases (Gold *et al.*, 1989; Gold & Alic, 1993; Wariishi *et al.*, 1988, 1989a; Dunford & Stillman, 1976; Renganathan & Gold, 1986), this enzyme is unique in its ability to oxidize Mn(II) to Mn(III) (Glenn *et al.*, 1986; Wariishi *et al.*, 1989a, 1992). The latter, complexed with an organic acid such as oxalate, diffuses from the enzyme to oxidize either the terminal phenolic substrate (Glenn *et al.*, 1986; Tuor *et al.*, 1992) or a mediator (Bao *et al.*, 1994; Wariishi *et al.*, 1989b). The recent crystal structure (Sundaramoorthy *et al.*, 1994b), as well as homology modeling of MnP (Johnson *et al.*, 1993) indicate that there is a cation binding site on the surface of the protein, consisting of the carboxylates of three acidic amino acid ligands, Asp179, Glu35, and Glu39, and one of the heme propionates. In the crystal structure (Sundaramoorthy *et al.*, 1994b) the final two ligands for the hexacoordinate Mn(II) ion are water molecules but these might be replaced by a chelator such as oxalate during the catalytic cycle. The characterization of our first site-directed MnP mutant, D179N, suggests that this cation site is the productive Mn(II) binding site. Comparison of the Mn(II) binding ligands in MnP and corresponding amino acid residues in the LiP-H8 crystal structure (Pribnow *et al.*, 1989; Poulos *et al.*, 1993; Piontek *et al.*, 1993; Sundaramoorthy *et al.*, 1994b; Ritch & Gold, 1992) reveals that two of three anionic residues found in MnP are replaced by non charged residues in LiP: Ala36 for Glu35 and Asn182 for Asp179. Only Glu39 in MnP is conserved as Glu40 in LiP. In addition, the heme propionate in LiP is not positioned for favorable Mn(II) binding and the location of the extended C-terminal peptide in LiP would interfere with Mn(II) binding (Sundaramoorthy *et al.*, 1994b). Thus LiP lacks an available, stable Mn(II) binding site. Although it recently has been claimed that one of the LiP isozymes, H2, can oxidize Mn(II) (Khindaria *et al.*, 1995; Sutherland *et al.*, 1995), comparison of the LiP-H2 sequence with those of MnP1 and LiP-H8 reveal that LiP-H2 also lacks a favorable Mn(II) binding site, and thus is unlikely to complete its catalytic cycle in the presence of Mn(II) as the only

Table 5.6. Kinetic parameters for the reduction of MnP compound II by ferrocyanide and p-cresol.[a]

Substrate	MnP proteins	Second-order rate constant $(M^{-1} s^{-1})$
ferrocyanide	wt MnP1	$(1.2 \pm 0.1) \times 10^3$
	MnP D179N	$(1.1 \pm 0.2) \times 10^3$
	MnP E35Q	$(1.1 \pm 0.1) \times 10^3$
	MnP E39Q	n.d.[b]
	MnP E35Q-D179N	$(1.0 \pm 0.3) \times 10^3$
p-cresol	wt MnP1	$(1.9 \pm 0.2) \times 10^2$
	MnP D179N	$(1.6 \pm 0.3) \times 10^2$
	MnP E35Q	$(1.9 \pm 0.1) \times 10^2$
	MnP E39Q	$(1.4 \pm 0.4) \times 10^2$
	MnP E35Q-D179N	$(1.9 \pm 0.2) \times 10^2$

[a] Reactions were conducted in 20 mM K-malonate (pH 4.6, ionic strength 0.1 M), containing 2 μM MnP II.

[b] Not determined.

reducing substrate. Contamination of LiP-H2 with MnP during purification may account for the reported oxidation of Mn(II) (Khindaria *et al.*, 1995; Sutherland *et al.*, 1995).

Mutation of each of the ligands in the Mn(II) binding site of MnP would increase our understanding of the unique specificity of this peroxidase. Our earlier results indicate that the Asp179Asn mutation significantly affects the oxidation of Mn(II), probably by decreasing the affinity of the enzyme for Mn(II). However, these results did not rule out the possible involvement of Asp179 in electron transfer. To better understand how the Mn(II) binding site ligands function, we have altered the other amino acid ligands in the Mn(II) binding site: Glu35Gln, Glu39Gln, and Glu35Gln-Asp179Asn.

We recently demonstrated the homologous expression of recombinant MnP isozyme 1 (rMnP1) of *P. chrysosporium* (Mayfield *et al.*, 1994b), wherein expression of the *mnp1* gene is under the control of the *P. chrysosporium gpd* gene promoter. This construct allows expression of rMnP1 during the primary metabolic phase of growth when endogenous MnP is not expressed. Both the spectral and kinetic properties of the recombinant enzyme are very similar to wild-type MnP1, indicating that this expression system is suitable for conducting structure/function studies of MnP by site-directed mutagenesis. Overlap extension PCR was used to create the E35Q, E39Q, and E35Q-D179N mutations. The mutant gene, in pOGI18, was transformed into the Ade1 strain of *P. chrysosporium* as described (Kusters-van Someren *et al.*, 1995). Each mutant protein was purified to homogeneity by a combination of hydrophobic interaction, Blue agarose, and anion-exchange chromatographies.

As with the MnP D179N mutant (Kusters-van Someren *et al.*, 1995), the MnP E35Q, E39Q, and E35Q-D179N mutant proteins are essentially identical to the wild-type enzyme with respect to chromatographic properties and molecular weight, suggesting that these mutations do not lead to gross conformational alterations of the protein. Furthermore, the E35Q, E39Q, and E35Q-D179N mutant, native ferric proteins exhibit essentially identical spectral features to that of wild-type MnP1 (Figure 5.1, Table 5.1) (Wariishi *et al.*, 1988; Mayfield *et al.*, 1994b). The spectra of the catalytic intermediates, compounds I and II, of the mutant proteins also are essentially identical to those of the wild-type MnP oxidized intermediates (Figure 5.1, Table 5.1), suggesting that the heme environment of MnP is not altered significantly by E35Q, E39Q, and E35Q-D179N mutations in the Mn(II) binding site.

Resonance Raman spectroscopy is particularly well suited for the determination of coordination and spin states of hemes and metalloporphyrins (Spiro, 1988). Of the many

porphyrin skeletal vibrational modes, v_3 and v_{10} are generally easily identified and, hence, serve as very useful indicators. Characteristic v_3 values are ~1480, ~1490, and ~1505 cm^{-1} for 6cHS, 5cHS, and 6cLS hemes, respectively. The corresponding set of v_{10} values are ~1610, ~1625, and ~1640 cm^{-1} (Mino *et al.*, 1988; Sun *et al.*, 1993, 1994).

The rR results for wild-type MnP have been obtained at higher resolution and superior S/N as compared to an earlier report from this laboratory (Mino *et al.*, 1988) and show the coexistence of 6cHS and 5cHS heme species at room temperature. The mixture of species is consistent with the presence of a six-coordinate, water-bound heme in equilibrium with a five-coordinate heme lacking an aqua ligand in the distal heme pocket. In the crystal structure of native wild-type MnP, a water molecule is located between the Fe(III) atom of the heme and the distal His46, with an Fe-OH_2 distance of 2.88 Å (Sundaramoorthy *et al.*, 1994b). Similar coordination-state equilibria have been proposed for LiP and cytochrome *c* peroxidase in acidic to neutral buffers (Andersson *et al.*, 1987; Smulevich *et al.*, 1988). The Fe-OH_2 distances in the crystal structures of LiP and cytochrome *c* peroxidase are between 2.42 and 2.73 Å (Poulos *et al.*, 1993; Finzel *et al.*, 1984).

Furthermore, mutations D179N and E35Q-D179N appear to have little or no effect on the structure and coordination-state equilibrium of the heme. Although these residues are involved in the formation of a Mn(II) ion binding site near the heme, one of whose propionate side chains also is implicated as a ligand to the cation site, our UV/vis and resonance Raman data suggest that perturbations caused by removal of these acidic residue(s) from the cation binding site are not transmitted to the nearby heme in a manner detectable by these spectroscopic methods.

In contrast to the negligible effects of these mutations on the spectroscopic properties of MnP, mutations of the Mn(II) binding ligands change the catalytic properties of MnP dramatically. The turnover numbers (k_{cat}) for Mn(II) oxidation by MnP E35Q and E39Q decrease 300-fold with respect to the wild-type enzyme. The apparent K_m values for MnP E35Q and E39Q are 60 and 30 times higher, respectively, than that for wild-type MnP (Table 5.2). Furthermore, the k_{cat} for Mn(II) oxidation by the E35Q-D179N double mutant decreases 1000-fold and the K_m for this double mutant increases 110-fold with respect to the wild-type enzyme (Table 5.2).

These mutations also have a dramatic effect on the reduction of compound II to the native enzyme by Mn(II) (Figure 5.3), which is the rate-limiting step in the MnP catalytic

cycle (Wariishi *et al.*, 1988, 1989a; Kishi *et al.*, 1994; Kuan *et al.*, 1993). At 1 mM oxalate (pH 4.6), the plots of k_{obs} versus Mn(II) concentration are hyperbolic (Figure 5.3), indicating a binding interaction between Mn(II) and MnP. The equilibrium dissociation constants for compound II reduction for the MnP single mutants increase ~100-fold and for the double mutant, ~200-fold (Table 5.5), indicating that the binding affinity of the mutant proteins for Mn(II) is significantly decreased with respect to the wild-type protein. The first-order rate constants for the MnP E35Q, E39Q and E35Q-D179N proteins are approximately 300-, 200- and 4000-fold lower, respectively, than the value obtained for wild-type MnP (Table 5.5), strongly suggesting that this Mn(II) binding site is the productive, and probably the only, substrate oxidation site. The effect of the mutations on the first-order rate constant suggests that the electron-transfer rate is lowered (equations 1–3). This may be a consequence of a higher redox potential for Mn(II) in the Mn binding site of the mutant proteins as compared with that for the wild-type protein. Alternatively, it may represent a much slower rate of electron transfer from a second, weaker Mn binding site.

Interestingly, the K_m and k_{cat} values indicate that oxidation of ferrocyanide by MnP (Table 5.3) is not affected by these mutations in the Mn(II) binding site of MnP. Furthermore, the similarity of the second-order rate constants for MnP compound II reduction by *p*-cresol and ferrocyanide for the mutant and wild-type proteins (Table 5.6) indicate that these reactions are not affected by mutations in Mn(II) binding site. These results indicate that neither ferrocyanide nor *p*-cresol bind or are oxidized at the Mn(II) binding site.

Furthermore, the mutations do not affect either the apparent K_m for H_2O_2 (Table 5.2) or the pre-steady-state rate of compound I formation by H_2O_2 (Table 5.4). This suggests that the environment of the amino acid residues involved in the formation of compound I, including the distal His, distal Arg and proximal His, has not been altered by any of the mutations in Mn(II) binding site. The recent crystal structure of MnP clearly shows that the peroxide and aromatic access channel is distinct from the Mn(II) binding site on the surface of the protein.

Homology modeling (Johnson *et al.*, 1993) and the MnP crystal structure (Sundaramoorthy *et al.*, 1994b) predict that the Mn(II) binding site in MnP consists of the acidic amino acids Asp179, Glu35, and Glu39, and a heme propionate. However, homology modeling also predicts several alternate Mn(II) binding sites (Johnson *et al.*, 1993). Although it is possible that there are other Mn(II) binding sites, the results presented here strongly suggest the Mn(II) binding site shown in Figure 5.4
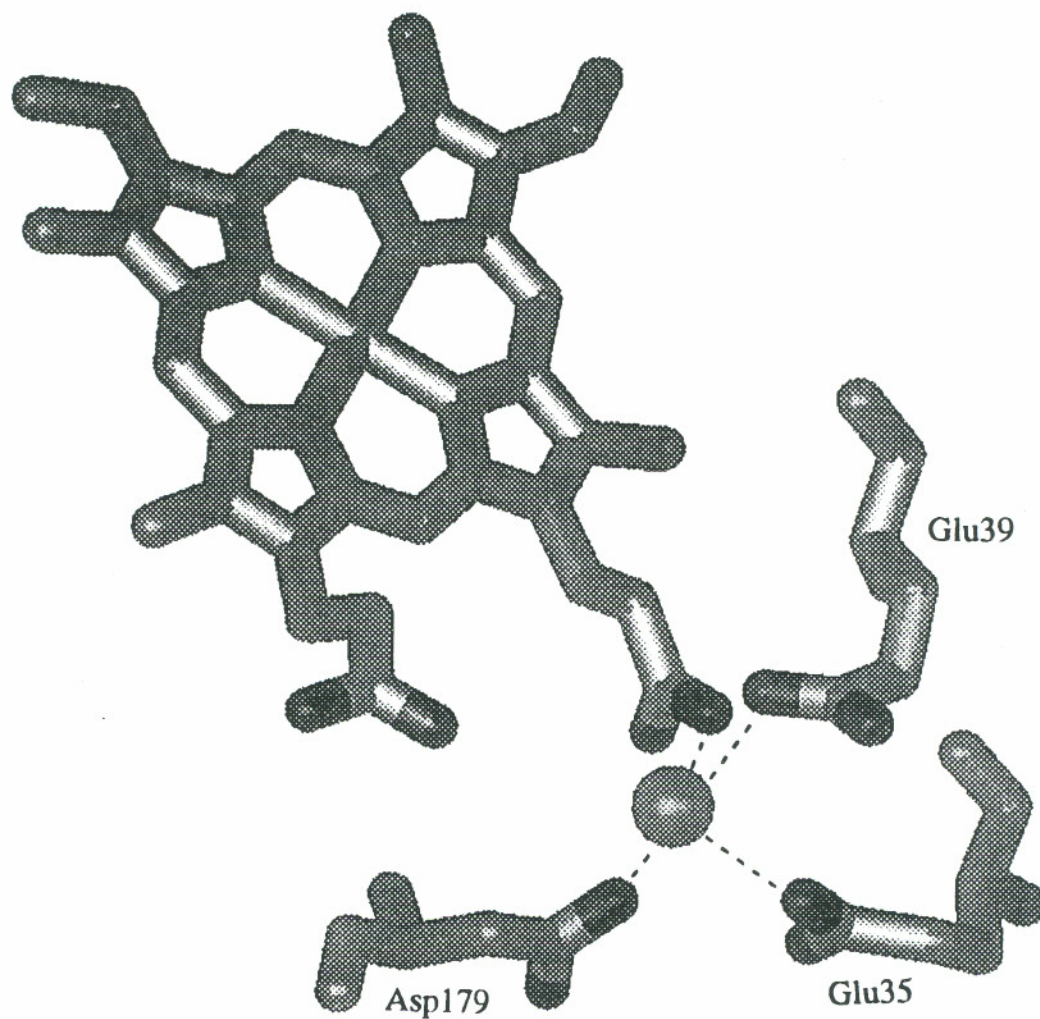
Figure 5.4. The Mn(II) binding site of MnP showing 4 acid ligands—D179, E35, E39, and a heme propionate (Sundaramoorthy *et al.*, 1994b). The dark areas on the models represent oxygen atoms.

(Sundaramoorthy *et al.*, 1994b) is the only productive catalytic site for Mn(II) oxidation, particularly since the double mutation, E35Q-D179N, almost completely destroys MnP oxidation of Mn(II) (Tables 5.2 and 5.5).

In conclusion, the results presented in this study, along with our previous work (Kusters-van Someren *et al.*, 1995), demonstrate that changing any of the acidic amino acid Mn(II) ligands Asp179, Glu35, or Glu39, significantly affects the oxidation of Mn(II), most probably by decreasing the affinity of the enzyme for Mn(II). In contrast, neither the rate of formation of compound I nor the rate of reduction of compound II by *p*-cresol or ferrocyanide is affected by these mutations. These results indicate that the Mn(II) binding site consisting of Asp179, Glu 35 and Glu 39 is the productive site. The coordination of Mn(II) at this site is octahedral, which is typical of Mn(II) coordination complexes (Demmer *et al.*, 1980). Current views envision electron transfer pathways through covalent bonds in proteins (Onuchic & Beratram, 1990). The structure of this site suggests that the electron may be transferred from Mn(II) to the porphyrin via the heme propionate ligand, using a nearly continuous σ-bonded path. Additional mechanistic, structural and mutagenesis studies will be required to elucidate further the electron transfer pathway in this system.

CHAPTER 6

SITE-DIRECTED MUTATIONS AT PHENYLALANINE 190 OF MANGANESE PEROXIDASE: EFFECTS ON STABILITY, FUNCTION, AND COORDINATION

6.1 INTRODUCTION

White-rot basidiomycete fungi are capable of degrading the plant cell wall polymer lignin (Buswell & Odier, 1987; Gold *et al.*, 1989; Kirk & Farrell, 1987) and a variety of aromatic pollutants (Bumpus & Aust, 1987; Hammel, 1989; Joshi & Gold, 1993; Valli & Gold, 1991; Valli *et al.*, 1992b). When cultured under ligninolytic conditions, the lignin degrading fungus *Phanerochaete chrysosporium* secretes two families of extracellular peroxidases, lignin peroxidase (LiP) and manganese peroxidase (MnP), which, along with an H_2O_2-generating system, comprise the major enzymatic constituents of its extracellular lignin-degrading system (Bao *et al.*, 1994; Buswell & Odier, 1987; Gold & Alic, 1993; Hammel *et al.*, 1993; Kirk & Farrell, 1987; Kuwahara *et al.*, 1984; Wariishi *et al.*, 1991b). Both LiP and MnP are able to depolymerize lignin *in vitro* (Bao *et al.*, 1994; Hammel *et al.*, 1993; Wariishi *et al.*, 1991b). MnP activity has been found in all lignin-degrading fungi that have been examined (Hatakka, 1994; Orth *et al.*, 1993; Périé & Gold, 1991).

MnP has been purified and characterized biochemically and kinetically (Glenn & Gold, 1985; Glenn *et al.*, 1986; Gold & Alic, 1993; Gold *et al.*, 1989; Périé *et al.*, 1996; Wariishi *et al.*, 1989a, 1992), and the sequences of cDNA and genomic clones encoding several *P. chrysosporium* MnP isozymes have been determined (Godfrey *et al.*, 1990; Gold & Alic, 1993; Mayfield *et al.*, 1994a; Pease *et al.*, 1989; Pribnow *et al.*, 1989). Spectroscopic studies and DNA sequences suggest that the heme environment of MnP is similar to that of other plant and fungal peroxidases (Banci *et al.*, 1992; Dunford & Stillman, 1976; Glenn *et al.*, 1986; Harris *et al.*, 1991; Mino *et al.*, 1988; Pribnow *et al.*, 1989; Wariishi *et al.*, 1988). Kinetic and spectroscopic characterization of the oxidized intermediates, MnP compounds I and II, indicate that the catalytic cycle of MnP is similar to that of HRP and LiP (Glenn *et al.*, 1986; Gold *et al.*, 1989;

145

Renganathan & Gold, 1986; Wariishi *et al.*, 1988, 1989a, 1992). However, MnP is unique in its ability to oxidize Mn(II) to Mn(III) (Glenn & Gold, 1985; Glenn *et al.*, 1986; Wariishi *et al.*, 1992). The enzyme-generated Mn(III) is stablized by organic acid chelators such as oxalate which is secreted by the fungus (Kishi *et al.*, 1994; Kuan *et al.*, 1993; Wariishi *et al.*, 1992). The Mn(III)–oxalate complex, in turn, oxidizes substrates such as lignin substructure model compounds (Tuor *et al.*, 1992), synthetic lignin (Bao *et al.*, 1994; Wariishi *et al.*, 1991b), and aromatic pollutants (Joshi & Gold, 1993; Valli & Gold, 1991; Valli *et al.*, 1992b).

It has been proposed that a unique Mn binding site observed in the MnP crystal structure (Sundaramoorthy *et al.*, 1994b) is involved in the oxidation of Mn(II). The Mn binding ligands in this proposed binding site are Glu35, Glu39, Asp179, a heme propionate, and two H_2O molecules (Sundaramoorthy *et al.*, 1994b). Using an homologous expression system (Mayfield *et al.*, 1994b) for producing recombinant MnP, we carried out site-directed mutagenesis on the proposed Mn(II) binding site ligands (Kishi *et al.*, 1996; Kusters-van Someren *et al.*, 1995). The results confirmed that Glu35, Glu39, and Asp179 are Mn(II) ligands and that the proposed Mn(II) binding site is the productive site (Kishi *et al.*, 1996; Kusters-van Someren *et al.*, 1995).

Other than this unique Mn binding site, the heme environment of MnP appears to be similar to those of other plant and fungal peroxidases (Edwards *et al.*, 1993; Sundaramoorthy *et al.*, 1994b). All of the catalytic residues, including the distal His and Arg and the proximal His and Asp, are conserved in MnP, LiP, HRP, CCP and CIP (Edwards *et al.*, 1993; Finzel *et al.*, 1984; Gold & Alic, 1993; Kunishima *et al.*, 1994; Petersen *et al.*, 1994; Piontek *et al.*, 1993; Poulos *et al.*, 1993; Sundaramoorthy *et al.*, 1994b). In addition, as in both HRP and LiP (Edwards *et al.*, 1993; Piontek *et al.*, 1993; Poulos *et al.*, 1993), MnP has two Phe residues (Phe 45 and Phe 190) in the heme pocket, whereas both CCP and ascorbate peroxidase contain Trp residues at these positions (Finzel *et al.*, 1984; Patterson & Poulos, 1995). CIP has a Leu (Kunishima *et al.*, 1994; Petersen *et al.*, 1994) replacing the proximal Phe (Phe 190 in MnP1). In addition, comparison of the LiP and MnP crystal structures (Edwards *et al.*, 1993; Piontek *et al.*, 1993; Poulos *et al.*, 1993; Sundaramoorthy *et al.*, 1994b) indicates that the orientation of the plane of the proximal Phe residue of the two enzymes are different. Although the role of the proximal Phe190 in MnP has not been elucidated, it could play a role in protein folding or stability, heme insertion, or stability of the enzyme oxidized intermediates. In this report, we have replaced the proximal Phe190 with Tyr, Leu, Ile, and Ala to examine the role of this amino acid residue in the MnP reaction.

6.2 MATERIAL AND METHODS

6.2.1 Organisms

P. chrysosporium wild-type strain OGC101, auxotrophic strain OGC107-1 (Ade1), and prototrophic transformants were maintained as described previously (Alic *et al.*, 1990). *Escherichia coli* XL1-Blue and DH5αF′ were used for subcloning plasmids.

6.2.2 Oligodeoxyribonucleotides

Each of four oligonucleotides were used for site-directed mutagenesis of Phe190 of the *mnp1* gene (Godfrey *et al.*, 1990; Pribnow *et al.*, 1989). Oligonucleotides $B1_{norm}$ and $D1_{rev}$ were 17-mers, prepared as described previously (Kusters-van Someren *et al.*, 1995). Oligonucleotides $Y190_{norm}$, $L190_{norm}$, and $I190_{norm}$ were 28-mers and $A190_{norm}$, $A190_{rev}$, $Y190_{rev}$, $L190_{rev}$, and $I190_{rev}$ were 27-mers. $Y190_{norm}$, $L190_{norm}$, and $I190_{norm}$ spanned nucleotides 874–901, and $A190_{norm}$ spanned nucleotides 874–900. $A190_{rev}$, $Y190_{rev}$, $L190_{rev}$, and $I190_{rev}$ spanned nucleotides 890–864. Oligonucleotides were synthesized at the Center for Gene Research and Biotechnology, Oregon State University, Corvallis, OR. Oligonucleotides 190_{norm} and 190_{rev} contained the preferred codon and anticodon (Ritch & Gold, 1992), respectively, for corresponding amino acid residues: GCC for A190, TAC for Y190, CTC for L190, and ATC for I190, replacing TTT encoding Phe190.

6.2.3 Site-Directed Mutagenesis by PCR

554-bp *Bpu*1102I–*Dra*III fragments containing the F190A, F190Y, F190L, and F190I mutations were generated by overlap extention (Ho *et al.*, 1989; Kusters-van Someren *et al.*, 1995) using the polymerase chain reaction (PCR). Two partially overlapping fragments were generated using either oligonucleotides $B1_{norm}$ and $A190_{rev}$ (or $Y190_{rev}$, $L190_{rev}$, or $I190_{rev}$) or oligonucleotides $A190_{norm}$ (or $Y190_{norm}$, $L190_{norm}$, or $I190_{norm}$) and $D1_{rev}$ under the conditions described (Kusters-van Someren *et al.*, 1995). These fragments were combined and used as template DNA in a second reaction with oligonucleotides $B1_{norm}$ and $D1_{rev}$ to generate a 608-bp PCR fragment as described (Kusters-van Someren *et al.*, 1995). The final PCR product was analyzed by agarose gel electrophoresis, excised, purified as described (Kusters-van Someren *et al.*, 1995), and digested with *Bpu*1102I and *Dra*III (New England Biolabs).

6.2.4 Construction of pAGM3, 5, 10, and 13

The *Bpu*1102I–*Dra*III fragments containing the F190 mutations were subcloned into pGM1 (Kusters-van Someren *et al.*, 1995; Mayfield *et al.*, 1994b), containing unique *Bpu*1102I and *Dra*III sites, replacing the wild-type *mnp1* fragment with the mutant fragment, to generate pGM3 (F190Y), pGM5 (F190I), pGM10 (F190L), and pGM13 (F190A). The entire *Bpu*1102I–*Dra*III fragments were analyzed by double-stranded DNA sequencing as described (Kusters-van Someren *et al.*, 1995). Subsequently, the 4.0-kb *Xba*I–*Eco*RI fragments of pGM3, 5, 10, and 13, containing the *gpd* promoter and the mutated *mnp1* gene, were subcloned into pOGI18 (Godfrey *et al.*, 1994), generating pAGM3, 5, 10, and 13, respectively. The presence of the mutations in pAGM3, 5, 10, and 13 was confirmed by double-stranded DNA sequencing, using oligonucleotide B1$_{norm}$ as a primer.

6.2.5 Transformation of *Phanerochaete chrysosporium*

P. chrysosporium strain Ade1 (Gold *et al.*, 1982) was transformed as described previously (Alic *et al.*, 1990), using 1 µg of pAGM3, 5, 10, or 13 as transforming DNA. Transformants were transferred to minimal slants (Alic *et al.*, 1990) to confirm adenine prototrophy and, subsequently, were assayed for MnP activity with an *o*-anisidine plate assay as described (Mayfield *et al.*, 1994b). Transformants showing the greatest activity as detected by the plate assay were purified by fruiting as described (Alic *et al.*, 1987).

6.2.6 Production and Purification of the MnP Mutant Proteins

The MnP mutant proteins were produced under primary metabolic conditions when endogenous *mnp* genes were not expressed, as described previously (Kusters-van Someren *et al.*, 1995; Mayfield *et al.*, 1994b), except that cultures were grown at 28 °C on a rotary shaker (150 rpm) for 3 days. The mutant proteins were purified by a combination of phenyl-sepharose CL-6B column chromatography, Cibacron Blue 3GA agarose column chromatography, and FPLC with a Mono Q column (Pharmacia), as described previously (Kishi *et al.*, 1996; Mayfield *et al.*, 1994b).

6.2.7 SDS–PAGE and Western Analysis

Sodium dodecyl sulfate–polyacrylamide gel electrophoresis (SDS–PAGE) was performed with a 12% Tris–glycine gel system (Laemmli, 1970) and a Mini-Protean II apparatus (Bio-Rad). The gels were stained with Coomassie blue. For western

(immunoblot) analysis, proteins were electroblotted onto nitrocellulose (Micron Separations, Inc.), and MnP proteins were detected as described (Pribnow *et al.*, 1989).

6.2.8 Enzyme Assays and Spectroscopic Procedures

Mn(II) oxidation by MnP was measured by following the formation of Mn(III)–malonate as described (Wariishi *et al.*, 1992). The oxidation of ferrocyanide by MnP was followed at 420 nm using the extinction coefficient for ferricyanide of 1.02 mM^{-1} cm^{-1} (Schellenberg & Hellerman, 1958). UV-vis absorption spectra of the various oxidation states of MnP mutant proteins were recorded at 10 °C with a Shimadzu UV-260 spectrophotometer fitted with a circulating water bath. The enzyme was maintained in 20 mM potassium malonate, pH 4.5. The ionic strength of the buffers was adjusted to 0.1 M with K$_2$SO$_4$. Enzyme concentrations were determined at 406 nm with an extinction coefficient of 129 mM^{-1} cm^{-1} (Glenn & Gold, 1985). MnP compounds I and II were prepared as described (Kusters-van Someren *et al.*, 1995; Mayfield *et al.*, 1994b).

Spectrophotometric pH titrations were carried out by addition of small volumes of 2 M NaOH solution to protein solutions (10 µM) prepared in sodium phosphate buffer (0.1 M, 20 °C). The resulting titration data were fitted by the non-linear least squares program Scientist (MicroMath, Orem, UT) to determine the pK_as indicated by the pH-dependent changes in absorbance.

6.2.9 Steady-State Kinetics and Stability Measurements

The apparent K_m and k_{cat} values of the variant enzymes for Mn(II) and ferrocyanide were determined as described (Kusters-van Someren *et al.*, 1995; Mayfield *et al.*, 1994b). Reaction mixtures contained MnP protein (0.5 µg/ml), H$_2$O$_2$ (0.1 mM), and MnSO$_4$ (0.02–0.5 mM), or ferrocyanide (0.1–1.0 mM for F190A and 1.0–5.0 mM for others) in 50 mM sodium malonate, pH 4.5. Apparent K_m values of the mutant enzymes for H$_2$O$_2$ were determined as described (Kusters-van Someren *et al.*, 1995; Mayfield *et al.*, 1994b).

The thermal denaturation of MnP proteins was measured by following the absorbance decrease at the Soret maximum at 406 nm. Reaction mixtures contained 2 µM MnP in 20 mM potassium malonate, pH 4.5. The ionic strength of the solutions was adjusted to 0.1 M with K$_2$SO$_4$.

6.2.10 Magnetic Circular Dichroism (MCD) Spectroscopy

MCD spectra were acquired with a Jasco Model J-720 spectropolarimeter and a 1.5 T electromagnet (Alpha Magnetics). The samples were placed in a 3-mL quartz cuvette (1-cm pathlength) and the cuvette was placed into a water-jacketed cell holder maintained at 298 K. Each spectrum represents an average of six scans (300–700 nm). Protein samples ([wild-type MnP] = 8.7 μM and [F190I] = 7.4 μM) for MCD spectroscopy were prepared in 100 mM sodium phosphate buffer, pH 4.5. The pH of the samples was adjusted by addition of small volumes of 1 M sodium hydroxide solution directly to the cuvette.

6.2.11 Electron Paramagnetic Resonance (EPR) Spectroscopy

EPR spectra of wild-type MnP were obtained at X-band frequencies with a Bruker Model ESP 300E spectrometer equipped with an Oxford Instruments Model 900 liquid helium cryostat, an Oxford Instruments Model ITC4 temperature controller, and a Hewlett-Packard Model 5352B frequency counter. The experimental conditions used were 4 K, microwave power 0.5 mW, microwave frequency 9.45 GHz, modulation frequency 100 kHz, and modulation amplitude 0.5 mT. Enzyme samples for EPR spectroscopy were exchanged into 100 mM sodium phosphate buffer of the appropriate pH through repeated dilution and concentration by centrifugal ultrafiltration with an Amicon microconcentrator (Centricon-10). The final concentration of the protein samples was 1.3 mM.

6.2.12 Chemicals

Phenyl-Sepharose CL-6B, Cibacron Blue 3GA agarose, potassium ferrocyanide, and H_2O_2 (30% solution) were obtained from Sigma. All other chemicals were reagent grade. Solutions were prepared using deionized water obtained from a Milli Q purification system (Millipore).

6.3 RESULTS

6.3.1 Expression and Purification of Mutant Proteins

The F190Y, F190I, F190L, and F190A mutations were confirmed by double-stranded DNA sequencing of the altered restriction fragments in pGM3, 5, 10, and 13 and in the complete transformation vectors, pAGM3, 5, 10, and 13, respectively. Prototrophic transformants with detectable MnP activity in the plate assay were purified by fruiting as described (Alic et al., 1987). When incubated at 28°C, the purified transformants expressed extracellular mutant MnP protein within three days of growth in

liquid, HCHN shake cultures, conditions under which endogenous MnP was not expressed. The amount of variant protein secreted by the F190Y, F190L and F190I transformants, as assayed by monitoring the formation of the Mn(III)–malonate complex (Wariishi et al., 1992), was approximately the same as that of recombinant wild-type MnP1 (rMnP1) (Mayfield et al., 1994b). However, the F190A transformants had 10% of the rMnP1 level of activity. Furthermore, the F190Y, F190L and wild-type transformant exhibited essentially the same amount of MnP activity when grown either at 28 or 37 °C; whereas the F190I and F190A transformants produced only trace amounts of MnP activity when grown at 37 °C, suggesting that the MnP F190I and F190A proteins were unstable at this temperature. The MnP mutant proteins were purified using phenyl-sepharose, Blue Agarose, and Mono Q chromatographies (Kishi et al., 1996; Kusters-van Someren et al., 1995; Mayfield et al., 1994b). In each case, the major variant protein peak eluted from the Mono Q column at essentially the same position as rMnP1 (Mayfield et al., 1994b). Furthermore, the molecular weights (46 kDa), as determined by SDS-PAGE, of the MnP variant proteins were identical to those of rMnP1 (data not shown) (Mayfield et al., 1994b).

6.3.2 Spectral Properties of MnP Mutant Proteins

For each of the variant proteins, the Soret band at 406 nm rapidly decreased and red shifted to yield a band at 397 nm following the addition of 1.0 equiv of H_2O_2 to the native enzyme. In the visible region, compound I displayed a peak at 650 nm with a broad absorption at 530–600 nm (Figure 6.1). Upon the addition of 1.0 equiv of ferrocyanide to the mutant MnP compounds I, compound II spectra, with maxima at 420, 528, and 555 nm, appeared (Figure 6.1). The electronic absorption maxima of compounds I and II for each of the MnP variant proteins were essentially identical to those of the wild-type enzyme (Table 6.1).

6.3.3 Steady-State Kinetics

Under steady-state conditions, linear Lineweaver-Burk plots were obtained over a range of Mn(II), ferrocyanide, and H_2O_2 concentrations in 50 mM malonate, pH 4.5 (data not shown). The apparent K_m values for H_2O_2 (~40 μM) and Mn(II) (~80 μM) for the MnP variant proteins were similar to those for wild-type MnP1 (Table 6.2). The apparent k_{cat} values of the variant proteins for Mn(II) (2.4–2.9 × 10^2 s^{-1}) also were similar to those for wild-type MnP1. In addition, the apparent K_m (~3.5 mM) and k_{cat} (~4.0 s^{-1}) values
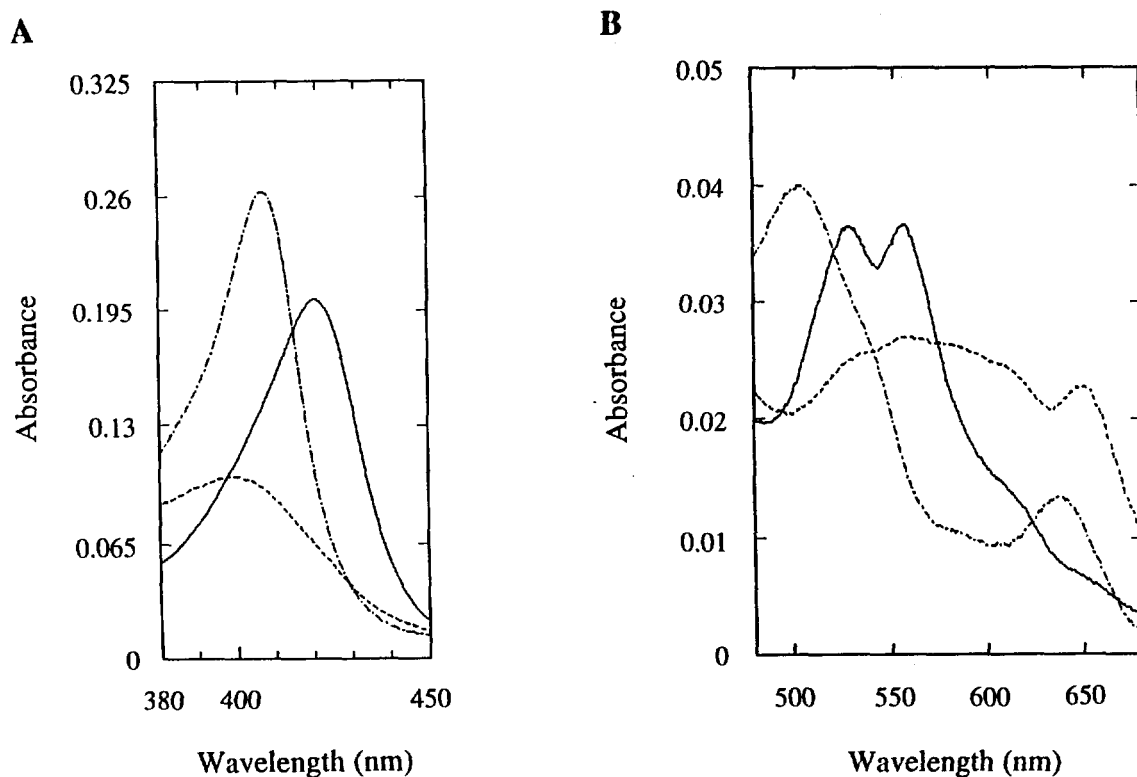
Figure 6.1. Electronic absorption spectra of oxidized states of MnP F190Y: native enzyme
(—•—), compound I (– – –), and compound II (—). Spectra were recorded in 20 mM
potassium malonate, pH 4.5 (μ = 0.1), at 10 °C. The enzyme concentrations were 2 μM
(A, Soret spectra) and 4 μM (B, visible spectra). MnP F190Y compound I was prepared
by adding 1 equiv of H_2O_2 to native MnP F190Y. MnP F190Y compound II was prepared
by the successive additions of 1.0 equiv of H_2O_2 and 1.0 equiv of potassium ferrocyanide
to the native enzyme.

Table 6.1. Absorbance Maxima (nm) of Native and Oxidized Intermediates of Wild-Type MnP1 and MnP F190 Mutants[a]

Enzyme	Native	Compound I	Compound II
wild-type MnP	406, 502, 636	398, 558, 617 (sh)[b], 650	420, 528, 555
MnP F190Y	406, 502, 636	398, 557, 617 (sh)[b], 650	420, 528, 555
MnP F190L	405, 502, 636	397, 558, 617 (sh)[b], 650	420, 528, 555
MnP F190I	405, 501, 635	397, 557, 615 (sh)[b], 468	418, 528, 555
MnP F190A	405, 501, 638	397, 557, 615 (sh)[b], 648	418, 527, 555

[a] Electronic absorption spectra were recorded in 20 mM potassium malonate, pH 4.5 (μ = 0.1), at 10 °C.

[b]Shoulder.

Table 6.2. Steady-State Kinetic Parameters of Wild-Type MnP1, MnP F190Y, MnP F190L, MnP F190I, and MnP F190A[a]

	K_m (μM)			k_{cat} (s^{-1})	
	Mn(II)	H_2O_2	Fe(CN)$_6$	Mn(II)	Fe(CN)$_6$
wild-type MnP	83	39	3.5×10^3	2.9×10^2	4.0
MnP F190Y	80	41	3.8×10^3	2.8×10^2	4.2
MnP F190L	75	41	3.5×10^3	2.9×10^2	3.9
MnP F190I	78	39	3.4×10^3	2.6×10^2	3.4
MnP F190A	74	39	4.2×10^2	2.4×10^2	14.6

[a]Reactions were carried out in 50 mM sodium malonate, pH 4.5, at room temperature. The apparent K_m and k_{cat} for Mn(II) and ferrocyanide were determined in the presence of 0.1 mM H_2O_2. The apparent K_m for H_2O_2 was determined in the presence of 0.5 mM Mn(II).

for ferrocyanide for the F190Y, F190L, and F190I variant proteins were similar to those for the wild-type MnP1 (Table 6.2). In contrast, the MnP F190A apparent K_m value of 0.42 mM for ferrocyanide was ~one-eighth of that for wild-type MnP1, and the MnP F190A apparent k_{cat} value (14.6 s^{-1}) for ferrocyanide was ~4 times higher than for the wild-type MnP1 (Table 6.2).

6.3.4 Thermal Denaturation of MnP F190 Mutant Proteins

The thermal denaturation of the MnP variants was followed over a range of temperatures in 20 mM potassium malonate, pH 4.5. Figure 6.2 shows the natural log plot of the change in absorbance at 406 nm versus time at 49 °C for wild-type MnP and for the F190Y, F190L, and F190I proteins, according to the first-order expression:

$$\ln|A_t - A_\infty| = -kt + \ln|A_0 - A_\infty| \qquad (1)$$

where A_0, A_t, and A_∞ are the Soret absorbance at times 0, t, and the end point, respectively. The rate constants for denaturation (k_{den}) of the MnP proteins were determined from the slopes of the plots, and half-lives ($T_{1/2}$) were calculated for each variant. The $T_{1/2}$ value for the MnP F190I variant at 49 °C (~30 s) was ~one-tenth that observed for the wild-type MnP and for the MnP F190Y and F190L variant proteins (~330 s). The MnP F190A variant was denatured completely within 5 seconds at 49 °C (data not shown).

Arrhenius plots for denaturation ($\ln k_{den}$ versus 1/T) were linear for all forms of MnP studied (Figure 6.3). The activation energies, E_a, derived from the slopes of these plots were very similar (~80 kcal/mol) for the wild-type and MnP F190 variants. However, the temperature dependence in the MnP F190I and F190A variants of the rate of denaturation is shifted significantly with respect to those of the wild-type, F190Y and F190L MnPs.

6.3.5 Stability of MnP Compounds I and II

MnP compound I spontaneously reduced to compound II at pH 4.5 as observed from the increase in absorbance at 417 nm, an isosbestic point in the spectra of compound II and the native protein. The plots of the natural log of absorbance versus time (equation 1) exhibited a linear relationship (Figure 6.4A) from which the rate constants for spontaneous reduction of compounds I to II were calculated.

The spontaneous reduction of compound II also was measured for the MnP variants by following the increase in absorbance of the Soret maximum at 406 nm (Figure 6.4B).
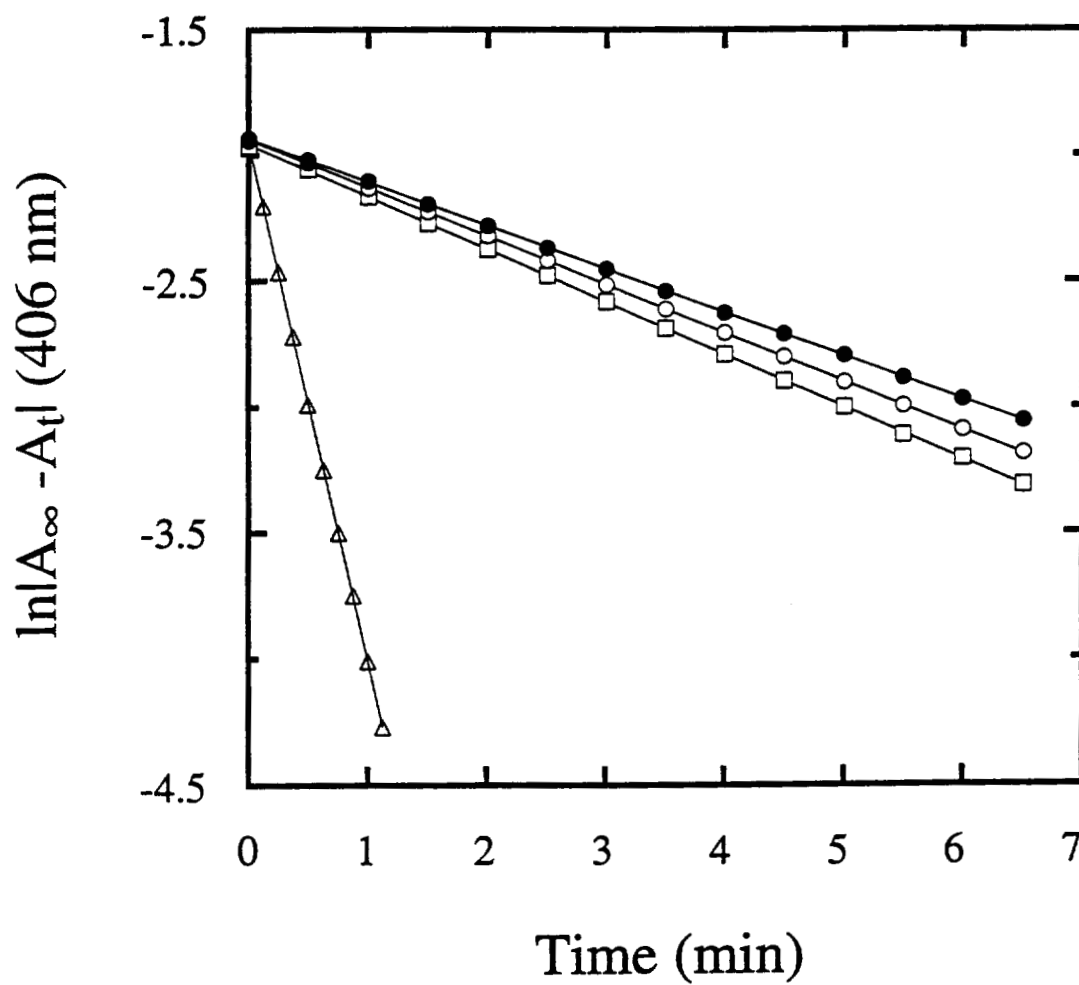
Figure 6.2. First-order plots for the thermal denaturation of wild-type MnP (●), MnP F190Y (O), F190L (□), and F190I (Δ) at 49 °C in 20 mM potassium malonate, pH 4.5 ($\mu = 0.1$). The thermal denaturation of MnP proteins was followed at 406 nm.
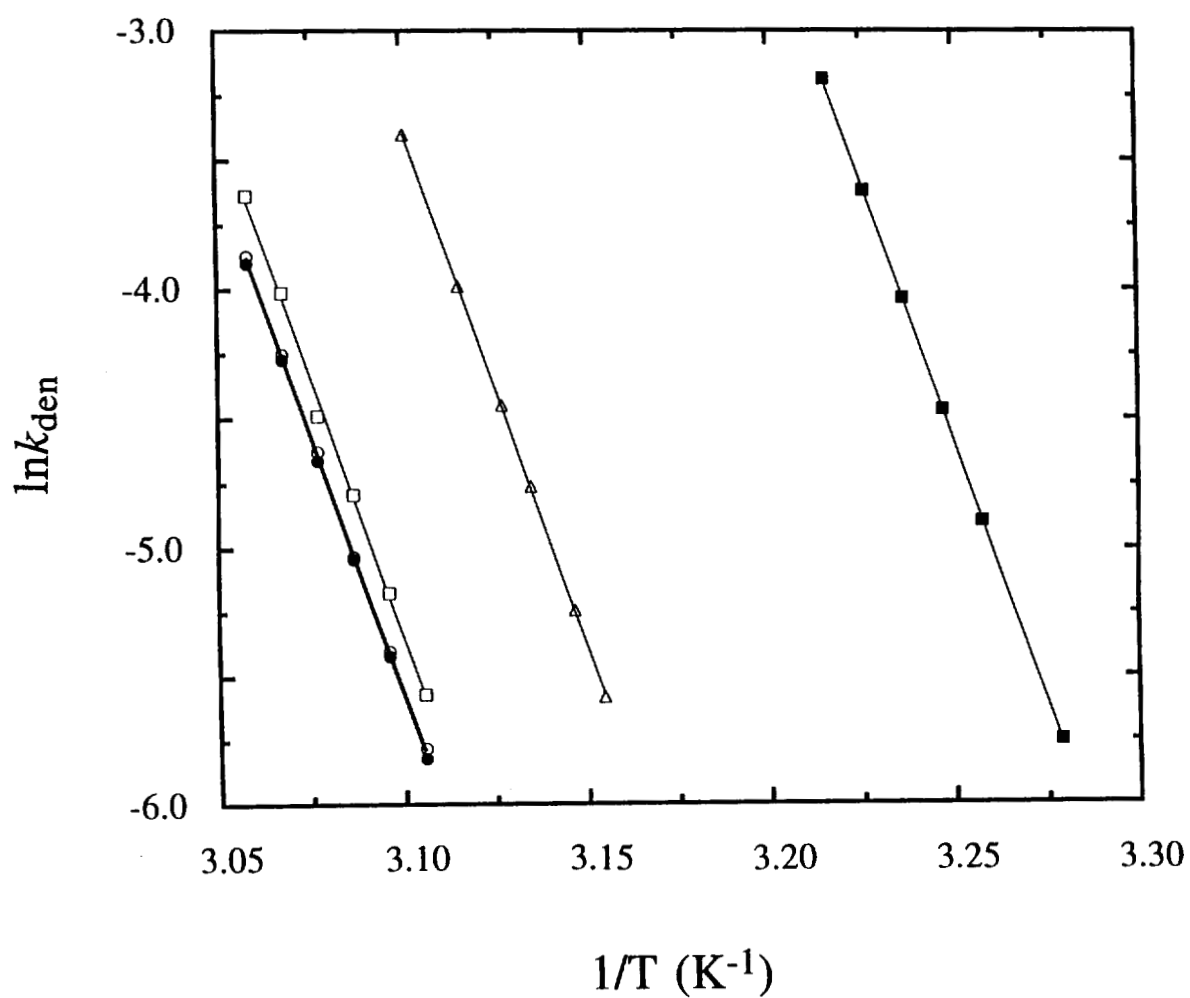
Figure 6.3. Arrhenius plot for the thermal denaturation of wild-type MnP (●), MnP F190Y (O), F190L (☐), F190I (Δ), and F190A (■).
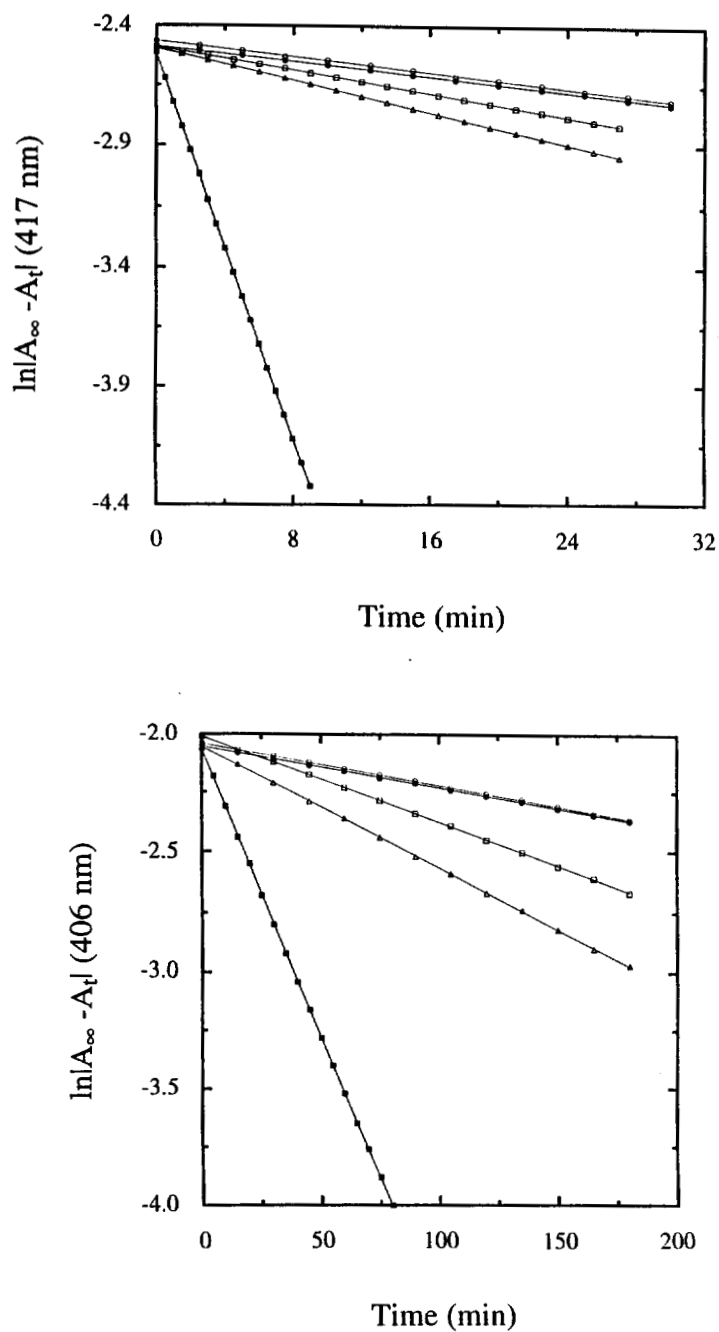
Figure 6.4. First-order plot for the spontaneous decompositions of compound I (A) and compound II (B) of wild-type MnP (●), MnP F190Y (O), F190L (□), F190I (Δ), and F190A (■). The spontaneous decompositions of compounds I and II were followed at 417 and 406 nm, respectively. MnP compounds I and II were prepared at 10 °C as described in the legend to Figure 6.1.

The rate constants for spontaneous reduction of compounds I and II of the F190I and F190L variants were ~2-fold greater than those determined for the wild-type and F190Y variants (Table 6.3). Moreover, the rate constants for spontaneous reduction of the F190A compounds I and II were approximately 30- and 13-fold greater, respectively, than those observed for the wild-type MnP compounds I and II (Table 6.3).

6.3.6 pH-Dependent Shifts in the Electronic Absorption Spectra of MnP F190 Variants

The electronic spectra of the MnP F190I variant exhibited two apparent pH-dependent transitions between pH 5 and 10 (Figure 6.5). At pH 5.3, the spectrum of the MnP F190I variant was typical of a high-spin heme Fe(III) species (λ_{max} = 405, 501, 635 nm). At pH 8.2, the electronic spectrum was characteristic of a hexacoordinate low-spin Fe(III) species with maxima at 412, 534, 560 nm that suggested the presence of a bis-histidinyl coordination environment for the heme iron (Ferrer $et\ al.$, 1994; Turano $et\ al.$, 1995; Vitello $et\ al.$, 1992). Above pH 8.2, further spectroscopic changes were observed, probably owing to the alkaline denaturation of the MnP protein. Similar transitions were observed in the electronic spectra of the wild-type MnP and MnP F190Y, F190L, and F190A variants (data not shown). The pH-dependent changes in absorbance were monitored at 560 nm (Figure 6.6) where the changes in absorbance were most pronounced (Figure 6.5). The pH-linked transitions of all the MnP variants could be fitted to three proton processes. The pK_a values derived from these analyses are listed in Table 6.4. Whereas the pK_a values for wild-type MnP, MnP F190Y, and MnP F190L were similar to each other, the pK_a values obtained for MnPs F190I and F190A, particularly the pK_{a1} and pK_{a2} values, were significantly lower (Table 6.4).

6.3.7 MCD Spectroscopy

To assess the basis for the changes observed in the electronic spectrum of MnP with pH, MCD spectra were obtained at ambient temperature for both the wild-type and variant (F190I) enzymes (Figure 6.7). The MCD spectrum of wild-type MnP exhibited significant pH-dependent changes (Figure 6.7A). The spectrum of the native enzyme (pH 5.9) exhibited a derivative-shaped Soret band (peak, 399 nm; crossover, 408 nm; trough, 418 nm). The visible region (450–700 nm) exhibited additional maxima at ~482 and 650 nm, as well as an additional derivative-shaped band (peak, 529 nm; crossover, 538 nm; trough, 551 nm). The MCD features in the visible region resembled those

Table 6.3. Spontaneous Decomposition of Compounds I and II of the MnP Variants[a]

	Compound I to II[b]		Compound II to native[c]	
	k_1 (s^{-1})	$T_{1/2}$ (min)	k_2 (s^{-1})	$T_{1/2}$ (min)
Wild-type MnP1	1.3×10^{-4}	89	3.0×10^{-5}	3.9×10^2
MnP F190Y	1.3×10^{-4}	89	3.0×10^{-5}	3.9×10^2
MnP F190L	2.4×10^{-4}	48	6.2×10^{-5}	1.9×10^2
MnP F190I	2.8×10^{-4}	41	7.6×10^{-5}	1.5×10^2
MnP F190A	3.4×10^{-3}	3.4	4.1×10^{-4}	0.28×10^2

[a]Reactions were carried out in 20 mM potassium malonate, pH 4.5, at 10 °C (ionic strength adjusted to 0.1 M with K_2SO_4).

[b]The conversion of compound I to II was followed at 417 nm.

[c]The conversion of compound II to native protein was followed at 406 nm.
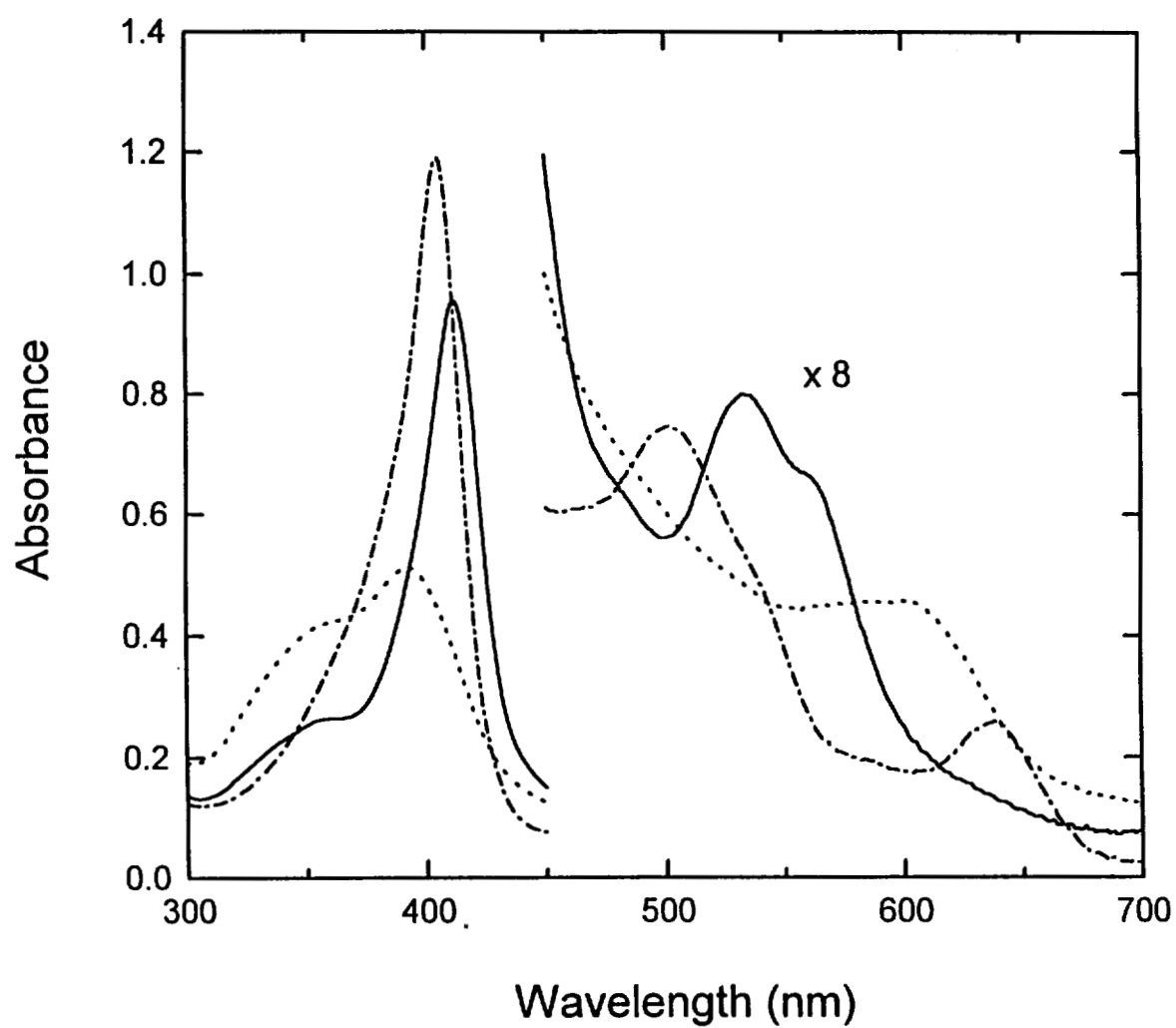
Figure 6.5. Electronic absorption spectra of MnP F190I in 100 mM sodium phosphate buffer (20 °C) at selected pH: pH 5.3 (—•—); pH 8.2 (—); pH 10.2 (– – –).
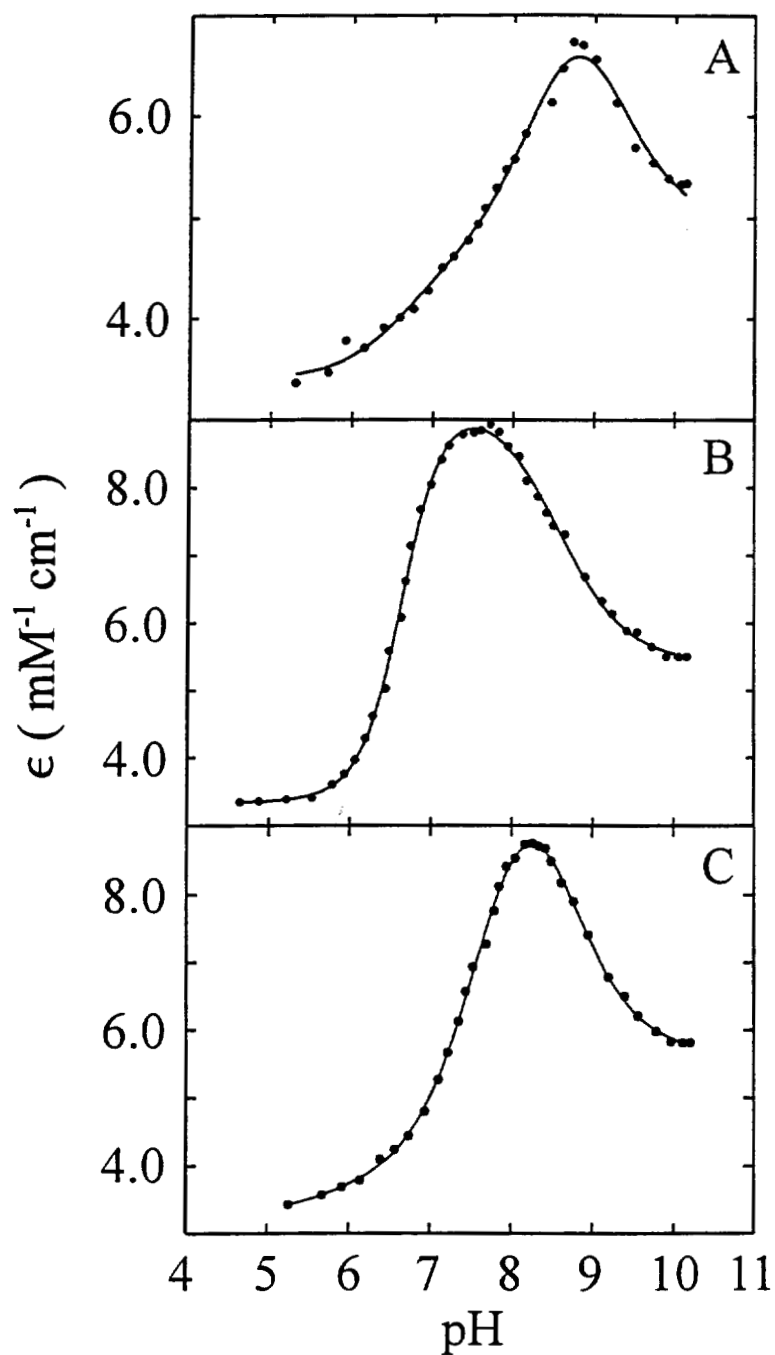
Figure 6.6. Dependence of the absorbance at 560 nm on pH for (A) wild-type MnP, (B) F190A, and (C) F190I in 100 mM sodium phosphate buffer (20 °C). The solid lines represent the nonlinear fits of these data to three single proton processes for wild-type MnP F190I and F190A. Apparent pK_a values for wild-type and variant forms of MnP are listed in Table 6.4.

Table 6.4. Apparent pK_a Values of the pH-Dependent Transitions of Wild-Type MnP, MnP F190Y, F190L, F190I, and F190A in 100 mM Na-Phosphate Buffer (20 °C)

Enzyme	pK_{a1}	pK_{a2}	pK_{a3}
wild-type MnP	6.67 ± 0.18	8.39 ± 0.10	9.15 ± 0.13
MnP F190Y	6.78 ± 0.14	8.62 ± 0.07	8.91 ± 0.14
MnP F190L	6.58 ± 0.26	8.67 ± 0.07	8.89 ± 0.06
MnP F190I	5.69 ± 0.65	7.71 ± 0.04	8.60 ± 0.04
MnP F190A	6.21 ± 0.12	7.08 ± 0.16	8.55 ± 0.05
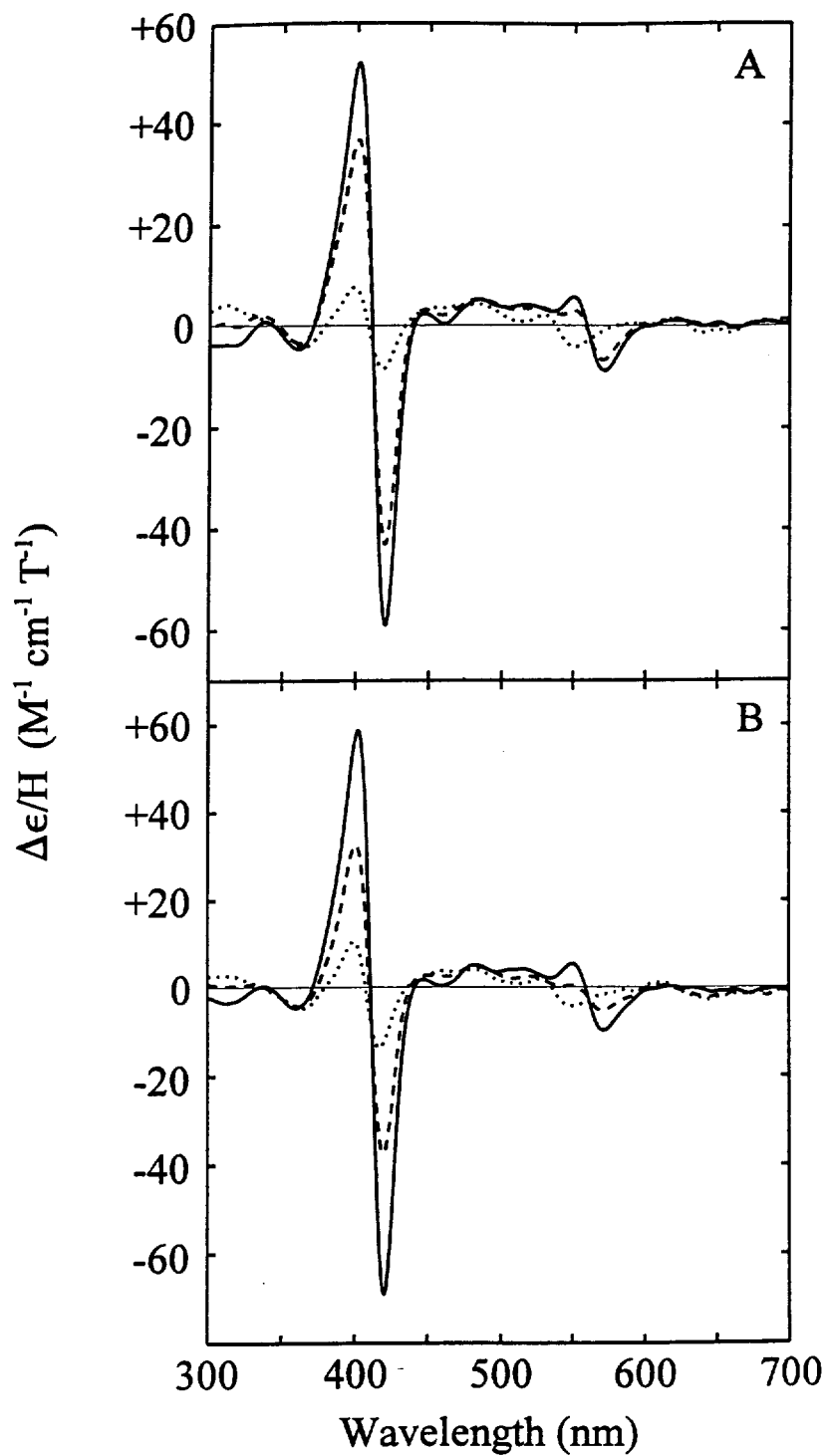
Figure 6.7. Visible MCD spectra (298 K) of ferric manganese peroxidase in 100 mM sodium phosphate buffer: (A) Wild-type enzyme at pH 5.9 (····), pH 6.9 (– – –), and pH 7.8 (—); (B) The F190I variant at pH 5.9 (····), pH 6.5 (– – –), and pH 7.5 (—).

observed for other high-spin heme proteins with a proximal histidine residue [e.g., HRP (Nozawa et al., 1976) and myoglobin (Vickery et al., 1976a)]. At pH 7.8, wild-type MnP exhibited little change in the position of the Soret band (peak, 402 nm; crossover, 411 nm; trough, 421 nm), but a significant increase in intensity of this band that is consistent with an increase in the low-spin component of the heme iron (Vickery et al., 1976a). At this pH, a new derivative-shaped feature appeared (peak, 550 nm; crossover, 559 nm; trough, 571 nm) that resembled similar features observed in the MCD spectra of heme proteins with bisimidazole axial coordination, such as cytochrome b_5 and the imidazole complexes of myoglobin and cytochrome c (Vickery et al., 1976b). The pH-dependent changes observed in the spectrum of the F190I MnP variant (Figure 6.7B) were essentially identical to those of the wild-type enzyme and confirm that the conformational change observed for this variant was unaltered by the F190I substitution at the active site. These pH-dependent changes in the MCD spectra were similar to those reported previously for a variant of CCP (Turano et al., 1995).

6.3.8 EPR Spectroscopy

The EPR spectra (4 K) of wild-type MnP at pH 4.7 and 8.0 are shown in Figure 6.8. At low pH, the native enzyme exhibits a single high-spin axially symmetric species with g values of 5.79 and 1.99 as reported previously (Mino et al., 1988). These properties differentiate MnP and LiP from other well studied peroxidases (e.g., CCP) that have more rhombically distorted electronic environments (Yonetani & Anni, 1987). Unexpectedly, at 4 K, wild-type MnP remained almost completely high-spin at high pH ($g \sim 6.03$ and 1.99) and exhibited only a trace of low-spin component(s), the identity of which is uncertain (Figure 6.8B, expanded region). In contrast, the MCD spectrum acquired at ambient temperature was that of a predominantly low-spin species at pH 7.8. Therefore, wild-type MnP exhibited complex temperature-dependent changes in axial ligation, in which the distal histidine was displaced at low temperatures. Similar temperature dependence of axial ligation has been reported for the D235A variant of CCP and for a variant of horse heart myoglobin, V68H (Ferrer et al., 1994; Lloyd et al., 1995).

6.4 DISCUSSION

Although the catalytic cycle of MnP is similar to that of other plant and fungal peroxidases (Dunford & Stillman, 1976; Gold et al., 1989; Renganathan & Gold, 1986; Wariishi et al., 1988, 1989a), this enzyme is unique in that it oxidizes Mn(II) to Mn(III) (Glenn et al., 1986; Wariishi et al., 1989a, 1992). Mn(III), complexed with an organic
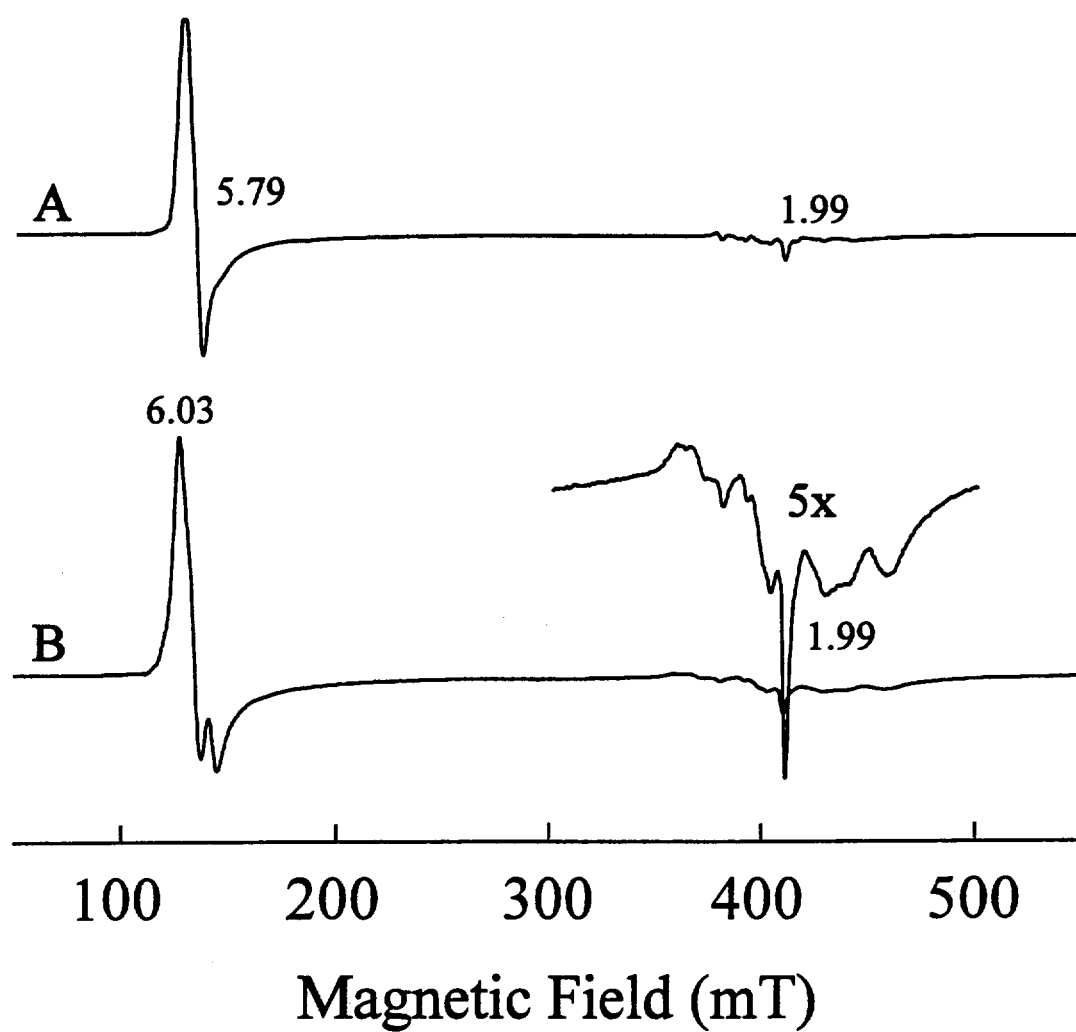
Figure 6.8. X-band EPR spectra (4 K) of wild-type manganese peroxidase (100 mM sodium phosphate buffer) at (A) pH 4.5 and (B) pH 8.0. The expanded region shows the spectrum of the minor, low-spin component.

acid such as oxalate, diffuses from the enzyme to oxidize the terminal organic substrate (Glenn *et al.*, 1986; Tuor *et al.*, 1992). Whereas phenolic compounds can be oxidized directly by MnP compound I, direct oxidation of phenols by MnP compound II is three orders of magnitude slower than the oxidation of Mn(II) by compound II (Kishi *et al.*, 1996; Kusters-van Someren *et al.*, 1995; Wariishi *et al.*, 1988, 1989a). Thus, Mn(II) is required to complete the MnP catalytic cycle (Wariishi *et al.*, 1988, 1989a). The three-dimensional structure of MnP suggests that the ability of MnP to oxidize Mn(II) is due to its unique Mn binding site (Sundaramoorthy *et al.*, 1994b) which includes three acidic amino acid ligands, Asp179, Glu35, and Glu39, and one of the heme propionates. The final two ligands of the hexacoordinate Mn(II) ion are water molecules. Our recent site-directed mutagenesis analysis of the amino acid ligands to Mn demonstrates that this is the productive Mn binding site (Kishi *et al.*, 1996; Kusters-van Someren *et al.*, 1995).

A variety of studies have shown that the heme environment of MnP is similar to that of other plant and fungal peroxidases (Figure 6.9) (Gold & Alic, 1993; Mino *et al.*, 1988; Sundaramoorthy *et al.*, 1994b). Catalytically important amino acid residues found in plant and fungal peroxidases (Edwards *et al.*, 1993; Finzel *et al.*, 1984; Gold & Alic, 1993; Kunishima *et al.*, 1994; Patterson & Poulos, 1995; Petersen *et al.*, 1994; Piontek *et al.*, 1993; Poulos *et al.*, 1993; Sundaramoorthy *et al.*, 1994b), including the distal His46, Arg42, Asn80 and Glu74, and the proximal His173 and Asp242, are all conserved in MnP. In addition to these catalytic amino acid residues, MnP contains two Phe residues in the heme pocket (Figure 6.9). The proximal Phe residue (F190) is conserved in LiP (Edwards *et al.*, 1993; Piontek *et al.*, 1993; Poulos *et al.*, 1993), HRP (Sundaramoorthy *et al.*, 1994b), and peanut peroxidase (Schuller *et al.*, 1996). In contrast, both CCP and ascorbate peroxidase have a Trp at this position and CIP has a Leu (Finzel *et al.*, 1984; Kunishima *et al.*, 1994; Patterson & Poulos, 1995; Petersen *et al.*, 1994). Trp191 in CCP forms an H-bond network through the proximal Asp to the proximal His, which apparently affects the Fe(III)/Fe(II) reduction potential of the heme (Goodin & McRee, 1993; Poulos & Finzel, 1984). In addition, Trp191 in CCP is thought to be the location of the protein-centered radical in compound I (compound ES) (Sivaraja *et al.*, 1989), which is thought to be essential for electron transfer from cytochrome *c* (Mauro *et al.*, 1988). Conversion of Trp191 to a Phe in CCP blocks electron transfer from ferrocytochrome *c* (Mauro *et al.*, 1988). The presence of a less easily oxidizable amino acid residue, such as Phe, at this position, in part explains why compounds I of HRP, LiP, and MnP possess a porphyrin π-cation radical
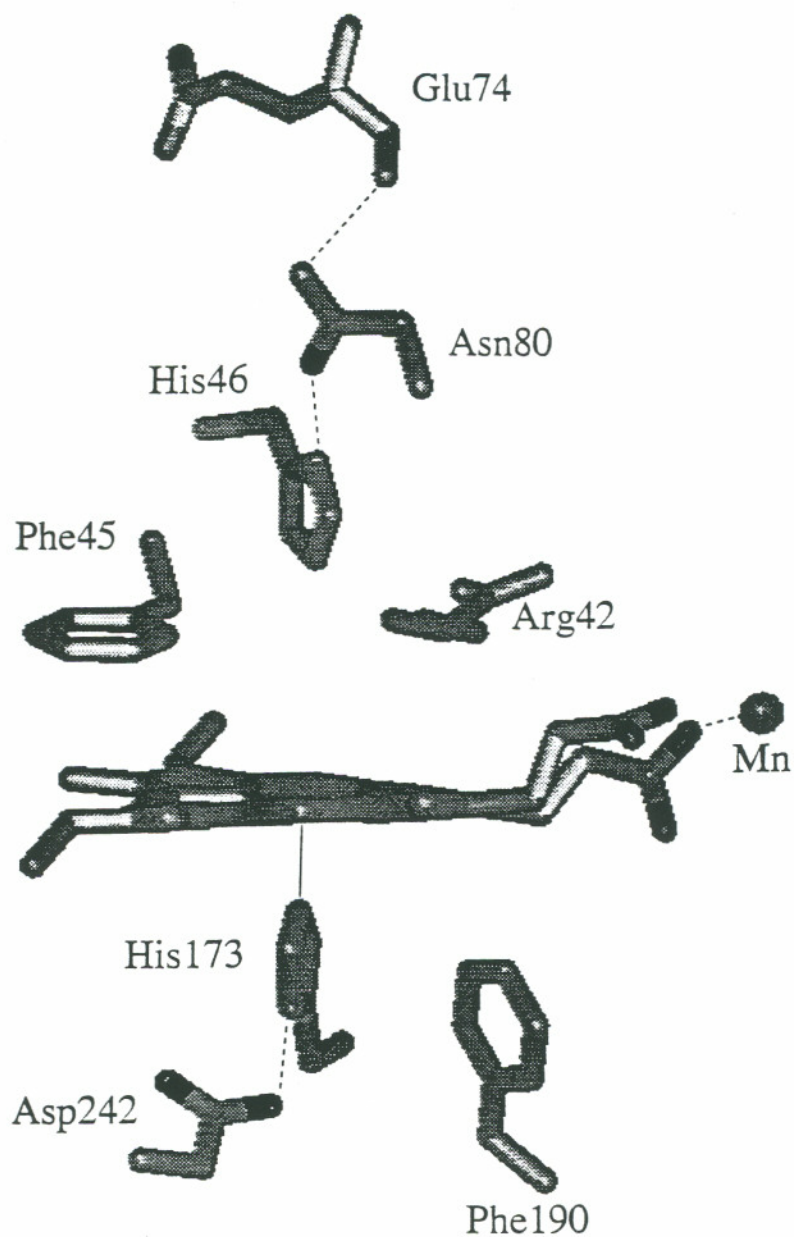
Figure 6.9. Heme environment of MnP (Sundaramoorthy *et al.*, 1994b). Hydrogen bonds are represented by dashed lines.

(Dolphin *et al.*, 1971; Patterson *et al.*, 1995). Although a Trp is located at this position in ascorbate peroxidase (Patterson & Poulos, 1995), a protein-centered Trp radical is not generated in this enzyme. It has been proposed that a cation, possibly a K+, is located close to the proximal Trp residue in ascorbate peroxidase, preventing Trp oxidation to a cation radical (Patterson & Poulos, 1995; Patterson *et al.*, 1995). To study the role of Phe190 in MnP, we replaced this residue with Trp, Tyr, Leu, Ileu, and Ala.

Our attempts to produce the F190W variant protein have not been successful. This variant is not secreted from the cells as demonstrated by western immunoblot analysis (data not shown); similarly, MnP activity is not detectable in the extracellular medium or in the intracellular soluble extract of the F190W transformant. The bulky indole ring of the Trp residue may prevent proper folding of this MnP variant. All of the other variant proteins are secreted into the extracellular medium in active form.

The spectrum of wild-type MnP compound I exhibits a Soret band at 397 nm and a peak at 650 nm with a broad absorption maximum at 530–600 nm (Wariishi *et al.*, 1988). This spectrum is typical of that of an oxyferryl iron with a porphyrin π-cation radical (Dolphin *et al.*, 1971). In contrast, the CCP compound I spectrum is similar to that of HRP compound II (Dunford & Stillman, 1976), a result that presumably reflects the fact that neither derivative possesses a porphyrin π-cation radical. As shown in Figure 6.1, the electronic spectrum of MnP F190Y compound I is essentially identical to that of wild-type MnP, suggesting that this variant also forms a porphyrin π-cation radical. The results summarized in Table 6.1 demonstrate that the absorption maxima for compounds I and II of each of the other variants are essentially identical to those of the wild-type enzyme, suggesting that each of the variants undergoes a normal catalytic cycle. The MnP F190Y variant and the wild-type MnP enzyme exhibit identical steady-state kinetic properties (Table 6.2), and the stability of compounds I of the wild type and F190Y variant are identical (Figure 6.4A and Table 6.3). All of these results strongly suggest that the MnP F190Y variant forms a normal porphyrin π-cation radical instead of a phenoxy radical at Tyr, during the catalytic cycle. Recently, the formation of a Tyr radical has been reported for the HRP F172Y mutant (Miller *et al.*, 1995b). However, in HRP, Phe172 is close to the heme δ-meso edge, whereas Phe190 in MnP may not be in the proper orientation to react with the porphyrin π-cation radical in compound I. In addition, Bonagura et al. (1996) have demonstrated that a stable Trp191 radical cannot be generated in a CCP variant containing a cation binding site near Trp191. Their engineered cation binding site is similar to the proximal Ca(II) binding site in other peroxidases (Bonagura *et al.*, 1996), suggesting that the proximal Ca(II) ion, like the K+ ion in ascorbate peroxidase, prevents the formation

of a protein centered radical in MnP and other peroxidases. This result may explain why a phenoxy radical is not generated at Tyr190 of the F190Y MnP variant.

Since CIP has a Leu in place of Phe190 (Kunishima *et al.*, 1994; Petersen *et al.*, 1994), and CCP and ascorbate peroxidase have a Trp (Finzel *et al.*, 1984; Patterson & Poulos, 1995), peroxidases do not require a proximal Phe residue for catalytic function. Therefore, we mutated MnP Phe190 to Tyr, Leu, Ile, and Ala in an attempt to assess the function of this heme pocket residue. The replacement of Phe190 by Tyr, Leu, Ile, and Ala does not affect significantly the kinetics of the MnP reactions with Mn(II) and H_2O_2 (Table 6.2). The apparent K_m values for Mn(II) and H_2O_2 with all the MnP F190 variants are approximately the same as those for wild-type MnP, suggesting that the mutations at Phe190 do not alter Mn(II) or H_2O_2 binding. The apparent k_{cat} values for Mn(II) also are not affected significantly by the mutations, suggesting that Phe190 does not control the rate of electron transfer from Mn(II), at least at pH 4.5. In contrast, replacement of Phe190 by Ala significantly changes the apparent K_m and k_{cat} for ferrocyanide (Table 6.2). The apparent K_m value decreases ~8 fold and the apparent k_{cat} increases ~4 fold, suggesting that the F190A mutation creates unique access to the heme edge for small molecules such as ferrocyanide. Similarly, replacement of Trp191 with Gly in CCP dramatically increases its binding affinity for imidazole compounds (Fitzgerald *et al.*, 1994).

Both the F190I and F190A variants are significantly less stable than wild-type MnP. The results for the thermal denaturation of the MnP variants (Figure 6.2 and 6.3) suggest that MnP F190I and F190A are one- and two-orders of magnitude less stable, respectively, than wild-type MnP and the MnP F190Y and F190L variants. From the three-dimensional structure of the wild-type enzyme (Sundaramoorthy *et al.*, 1994b), Phe190 is known to be located on a loop between α-helices F and G. It is possible that changing Phe190 to Ile or Ala alters the conformation of the loop to produce movement of these two α-helices with respect to each other. In addition, a Phe, Tyr or Leu residue at position 190 may have a stabilizing hydrophobic interaction with the heme.

Mutations at Phe190 affect the stability of the MnP intermediates, compounds I and II (Figure 6.4A and B, Table 6.3). Although the electronic spectra of compounds I and II of the MnP F190 variants are nearly identical to those of the wild-type MnP (Table 6.1), higher rates of spontaneous reduction of compounds I and II are observed for several of the variants, particularly MnP F190A. These results suggest that the bulky Phe residue acts as a steric barrier that protects the heme from reducing agents.

The electronic absorption spectra of heme-containing proteins are good indicators of high- and low-spin derivatives of Fe(III). The coordination of strong-field ligands such as cyanide generates low-spin derivatives; whereas coordination of weak-field ligands such as fluoride, or penta-coordination, yields high-spin species. Since the energy difference between the high- and low-spin species is small in many heme proteins, mixed-spin Fe(III) heme species often are observed with the coordination of certain ligands such as water, hydroxide, azide, and imidazole (Palmer, 1985; Smith & Williams, 1968). The Fe(III) heme of most peroxidases is coordinated to the protein through the imidazole group of a proximal His residue. The spectroscopic differences among the various derivatives of heme proteins result primarily from differences in coordination on the distal side of the Fe(III). Fe(III) heme proteins typically exhibit four bands in the visible region of the electronic spectrum. Two bands, α and β, appear near 570 and 540 nm, respectively, and two ligand-to-metal charge transfer bands occur near 500 and 630 nm (Palmer, 1985). High-spin derivatives exhibit absorption maxima at the charge-transfer positions and low-spin derivatives predominantly exhibit α and β bands. Upon increasing the pH, changes in the protein ligands to the heme can be observed. Typically, hexacoordinate aquo-, hydroxy-, and bisimidazole forms are observed for various heme proteins (Iizuka & Yonetani, 1970).

At low pH (pH 4.5), both wild-type MnP and the MnP F190 variants exhibit high-spin species with charge transfer bands at 500 and 635 nm (Table 6.1, Figures 6.1 and 6.5). Resonance Raman spectroscopic analysis of the wild-type MnP (Kishi *et al.*, 1996; Mino *et al.*, 1988) has demonstrated that MnP is predominantly pentacoordinate with a minor water-ligated hexacoordinate species. With increasing pH, all of the MnP variants are converted to low-spin species with α and β bands near 560 and 532 nm, respectively (Figure 6.5). The positions of these α and β bands and the characteristic MCD spectra (Figure 6.7) (Dawson & Dooley, 1983; Vickery *et al.*, 1976b) strongly suggest that this transition involves the direct coordination of the distal His to the iron to form a bis-histidinyl complex. With a further increase of pH, all of the MnP variants undergo denaturation (Figure 6.5). Although all of the spectra of the MnP variants exhibit similar transitions upon increasing pH (high spin to low spin to denaturation), coordination of the distal His46 to the heme iron occurs at a significantly lower pH for the MnP F190I and MnP F190A variants relative to the behavior of wild-type MnP or the MnP F190Y and F190L variants (Figure 6.6, Table 6.4). This observation suggests that a hydrogen bond

that is responsible for the first transition is much weaker in the MnP F190I and F190A variants relative to wild-type MnP and the MnP F190Y and F190L variants. Surprisingly, two pK_a values (pK_{a1} and pK_{a2}), rather than one, are obtained in the high-spin to low-spin transition for all the variants (Table 6.4), while only two species are observed in this transition by optical absorption and MCD spectroscopies (Figures 6.5 and 6.7). The first transition (pK_{a1}) may be due to a conformational change that occurs prior to the coordination of the distal His to the Fe(III) heme. Although the pH-dependent transition (pK_{a2}) could represent deprotonation of the distal His46, it has been demonstrated that MnP compound I formation with H_2O_2 is independent of pH from pH 3.1 to 8.3 (Wariishi et al., 1989a), which suggests that His46 is deprotonated in this pH range and that other amino acid residues may be responsible for the pH-dependent transition of MnP. The protonation status of His181 has been proposed to be linked to the transition between the high-spin and low-spin species of CCP variants (Nozawa et al., 1976; Vitello et al., 1992). In CCP, His181 forms a hydrogen bond with the 7-propionate group of the heme (Edwards & Poulos, 1990; Finzel et al., 1984). No similar H-bond to the heme propionate groups of MnP exists. In MnP, the heme 7-propionate is hydrogen bonded to the peptide NH groups of Asp179 and Lys180 and to two water molecules, one of which is coordinated to the Mn(II). The 6-propionate interacts with the Mn(II) ion, the peptide NH group of Arg177, and a water molecule (Sundaramoorthy et al., 1994b). The unique orientation of the 7-propionate in MnP permits formation of an H-bond with the distal Arg42 residue (Sundaramoorthy et al., 1994b). These interractions suggest that the high-to low-spin transition of MnP is not dependent on the interaction of the heme propionate groups with amino acid side chain groups. Although the assignment of the amino acid residues responsible for this high- to low-spin pH transition remains to be clarified, our results suggest that replacement of Phe190 by Ile, or especially Ala, weakens hydrogen bond(s) involved in protein stability and in the pH-linked spin transition. Furthermore, replacing the bulky Phe residue with certain smaller residues such as Ile or Ala may lead to greater flexibility in the heme.

6.4.1 Conclusions

Mutation of the proximal Phe in MnP has little effect on the steady-state kinetic parameters for the substrates H_2O_2 and Mn. However, these mutations result in significant changes in the temperature stability of the variant proteins and in the stability of the oxidized intermediates, compounds I and II. These changes also affect the pH-dependent interconversion of the pentacoordinate, high-spin Fe heme and the hexacoordinate bis-His

ligated low-spin Fe heme species. Furthermore, the F190A variant exhibits an increased ability to oxidize ferrocyanide. Further structural and mechanistic characterizations of these MnP F190 variants are underway.

CHAPTER 7

FINAL COMMENTS AND FUTURE DIRECTIONS

7.1. MANGANESE(II) OXIDATION

MnP shares structural and mechanistic features with other plant and fungal peroxidases; yet MnP is unique in its ability to oxidize Mn(II) to Mn(III). In turn, the Mn(III) stabilized by organic acid chelators such as oxalate oxidizes terminal substrates including lignin and lignin substructures model compounds. X-ray crystallographic and site-directed mutagenesis studies have demonstrated that the ability of MnP to oxidize Mn(II) is due to its unique Mn(II) binding site. The Mn(II) binding site consists of Asp179, Glu35, Glu39, and one of the heme propionates (Figure 1.14). Our site-directed mutagenesis studies clearly showed that this site is the productive site and that MnP possesses only one Mn(II) oxidation site. However, Sutherland et al. (1996) have shown that compound I of all of LiP isozymes from *P. chrysosporium* are able to oxidize Mn(II). The LiP and MnP compound I reduction by Mn(II) should be reinvestigated. Second-order rate constants for the reduction of compound I of the LiP isozymes were 10^3-10^4 $M^{-1}s^{-1}$ at pH 6.0 (Sutherland *et al.*, 1996). In contrast, the reduction of MnP compound I is too fast to monitor at pH 4.5 (Kuan *et al.*, 1993; Sutherland *et al.*, 1996), suggesting that second-order rate constant for the MnP compound I reduction at pH 4.5 is in the range of 10^7 to 10^8 $M^{-1}s^{-1}$. Since the same values for the MnP compound I reduction at pH 6.0 have not been reported, it is unclear that the reduction of LiP compound I by Mn(II) is fast enough to compete with the MnP compound I reduction. The ability of LiP compound I to oxidize Mn(II) may be owing to its particularly high reactivity. There is, however, the possibility that the Mn(II) ion may approach close to the δ-meso edge of the heme. Thus, the Mn(II) ion may directly reduce the porphyrin π-cation radical of compound I without binding to the Mn(II) binding site. Detailed kinetic analysis will clarify the mechanism of compound I reduction by Mn(II) using LiP and MnP (wild-type and Mn(II) binding site mutants).

Kinetic analyses of MnP compound II suggest that the 1:1 Mn(II)-chelator complex rather than the free Mn(II) ion is the substrate for MnP (Chapter 2). However, direct evidence has not been obtained for the binding of the Mn(II)-complex to MnP. In the MnP crystal structure, a free Mn(II) ion is tightly bound to the protein and is not easily released: Chelex-100 or EDTA treatment of MnP could not remove all of Mn(II) bound to the MnP crystal (Sundaramoorthy et al. in preparation). Moreover, two water molecules which are Mn(II) ligands are buried rather than on the surface of protein (Figures 1-14 and 1-15). One of the water molecules acting as a ligand forms an H-bond with a heme propionate. Thus, although these two water molecules may be replaced by a dicarboxylic acid such as oxalate, the binding site would need to rearrange dramatically. Furthermore, a Mn(II)-chelator complex may not fit into this site. In fact, MnP is able to generate the Mn(III)-chelator complex even in the presence of bulk chelators such as phenyl lactate (Wariishi *et al.*, 1992), suggesting that a free Mn(II) would bind to MnP by displacing the chelator with water molecules. Interestingly, a Mn(II) free MnP crystal has been obtained in the presence of the competitive inhibitor, Sm(III) (Sundaramoorthy et al. in preparation). The crystal structure shows that orientation of two of the Mn(II) ligands, Glu35 and Glu39, are different from that in the Mn(II)-bound MnP crystal. The Glu39 side chain swings away from the center of the Mn(II) binding site and the Glu35 side chain has dual conformations. This may provide sufficient space for the binding of the Mn(II)-chelator complex to the site. Further studies including cocrystalization of MnP and Mn(II)-chelator complex and additional kinetic studies are required to determine a real substrate for MnP: a Mn(II)-chelator complex or a free Mn(II).

The MnP crystal structure shows that Arg177 forms an H-bond with one of the Mn(II) ligands, Glu35 (Figures 1-14 and 1-15). This H-bond may help the Glu35 side chain to orient to form a stable Mn(II) binding site. The H-bond may also affect an electrostatic property of the Glu35 side chain controlling the affinity and the redox potential of Mn(II). A site-directed mutagenesis study should help to elucidate the role of the Arg177 in the Mn(II) oxidation by MnP.

7.2. PROXIMAL PHENYLALANINE 190

MnP has two Phe residue in heme binding pocket (Figure 1-12). One of the residues, Phe190, has been replaced by Tyr, Leu, Ile, and Ala residues (Chapter 6). Results demonstrate that the Phe190 residue plays an important role in stabilizing the MnP protein and the oxidized intermediates of MnP. Changing the Phe190 to smaller amino acid

residues, particularly Ile and Ala, destabilizes the heme environment possibly by disrupting an H-bond network near the heme. However, the nature of the H-bond(s) responsible for the stability of MnP is not clear. X-ray crystallography and NMR studies of the F190I and F190A mutants may provide important information to identify amino acid residues controlling the stability of the heme in MnP.

In addition, replacing the Phe190 by Ala residue enhances the rate of ferrocyanide oxidation by MnP (Chapter 6), suggesting that the F190A mutation creates sufficient space for ferrocyanide binding near the heme. Several other substrates such as phenols and small charged molecules can be used to test whether the F190A mutation or other F190 mutations affect the rates of compounds I and II reduction by those substrates. This may provide useful information about factors which govern the binding and oxidation of small molecules near the heme.

7.3. PHENOL OXIDATION

Another unique property of MnP is that the rate of direct phenol oxidation by MnP is more than 1,000 times lower than that of Mn(II) oxidation. Other peroxidases such as HRP and LiP are able to catalyze the oxidation of aromatic compounds. The reason why MnP does not oxidize phenols may be due to the lack of an access channel for aromatics. However, it has been demonstrated that an aromatic peroxide, m-chloro-perbenzoic acid (mCPBA), is able to react with the native MnP (Wariishi et al., 1988, 1989a). In contrast, Harris et al. (1991) showed that a suicide inhibitor, phenylhydrazine, which works for HRP, did not modify the heme of MnP, suggesting that phenylhydrazine cannot approach the δ-meso edge of the heme of MnP. Therefore, the aromatic binding site in MnP appears to depend on the nature of substituents and the oxidation state of enzyme. The site for aromatics oxidation in HRP has been extensively investigated but has not been identified. NMR studies suggest that one or two Phe residues may be involved in the phenol binding in HRP (Chapter 1.3.4.4.). Thus, introduction of Phe residues into the distal or proximal side of MnP may generate the phenol binding site. Site-directed mutagenesis of MnP could be utilized in attempt to create a phenol binding site in MnP. This would clarify the mechanism of aromatic compound oxidation by heme peroxidases.

7.4. ROLE OF HYDROGEN BONDING NETWORK

Most plant and fungal peroxidases possess the catalytically important amino acid

residues such as the distal His, Asn, and Arg, and the proximal His and Asp. The H-bonds between these residues are essential for catalysis and stability of the oxidized intermediates of peroxidases (Chapters 1.3.2. and 1.3.4.). Although these amino acid residues and H-bonds are all conserved in MnP, the catalytic cycle of MnP has several unique properties. The second-order rate constant for MnP compound I formation with H_2O_2 is independent of pH over the range 3.1-8.3 (Wariishi *et al.*, 1989a). The pH dependence of compound I formation with a variety of peroxidases has been studied and indicates that a distal ionizable group with a pK_a value in the range of 3.0-5.5 controls the pH dependence of compound I formation (Dunford & Stillman, 1976; Poulos & Finzel, 1984). Poulos and Kraut (1980b) proposed that the distal ionizable group is the distal His residue. Thus, the pK_a of the distal His in MnP must be significantly lowered. This might occur if the environment of the heme pocket is extremely hydrophobic. It is also possible that a different group rather than the distal His may be responsible for the pH dependence of the peroxidase compound I formation. Site-directed mutagenesis of amino acid residue on the distal side of the heme may provide insight into the mechanism of compound I formation.

In addition, the pH optimum for Mn(II) oxidation by MnP is ~4.5 (Chapter 2). The pH dependence of Mn(II) oxidation involves the pK_a values of chelators which complicates the analysis of the pH dependence of compound I or II reduction (Chapter 2). In addition, Mn(II) binding to MnP is also pH dependent (unpublised data). Thus, for the detailed investigation of the ionizable amino acid groups involved in MnP compound I and II reduction, it may be necessary to utilize substrates such as phenols whose binding would not be affected by pH or chelators. Site-directed mutagenesis will also be useful to clarify the low pH optimum of MnP reaction. Disruption of the H-bonds by changing the distal Asn, or the proximal Asp may significantly alter the pH dependence of the MnP reaction.

Another possibly important amino acid residue in MnP is the distal Glu74 (Figure 1-12). The carbonyl backbone of this residue forms an H-bond with the distal Asn80 and the side chain of the Glu74 binds the proximal Ca(II) ion through a water molecule (Figure 1-13). Thus, this Glu74 may play an important role in orienting the distal Asn and His correctly or in stabilizing the Ca(II) binding site. Interestingly, however, the Glu residue is also conserved in CCP although CCP does not have Ca(II) ions bound to the protein (Chapter 1.3.4.). Studies on site-directed mutants of the Glu74 (and the distal Asn) will elucidate the role of this Glu residue and the H-bond between the Glu and Asn residues.

7.5. ROLE OF CALCIUM(II) IONS

MnP has two Ca(II) ions at the distal and proximal sites (Figures 1-11 and 1-13). It has been demonstrated that the Ca(II) ions are important for both stability and catalysis of HRP and peanut peroxidase (Ogawa *et al.*, 1979; Shiro *et al.*, 1986; Morishima *et al.*, 1986; Haschke & Friedhoff, 1978; Barber *et al.*, 1995). Removal of Ca(II) ions changes the conformation of the heme and the distal and proximal His residues probably by changing the orientation the distal and proximal α helices with respect to the heme. Since one of the Ca(II) ions in the distal site interacts with a Glu74 through a water molecule in MnP, the distal Ca(II) may have a long-range effect on the distal His and Asn residue, which may significantly affect MnP structure and function. Ca(II)-free MnP may be prepared by treating the enzyme with EGTA. Spectroscopic and kinetic studies of the Ca(II)-free MnP should reveal the role of Ca(II) ions in MnP.

In addition to the structural role, the Ca(II) ions may prevent protein-centered radical formation in peroxidases (Chapters 1.3.2.2. and 1.3.4.1.). Ascorbate peroxidase which has a potassium binding site generates a porphyrin π-cation radical rather than a Trp radical (Patterson *et al.*, 1995) and MnP F190Y compound I did not form a Tyr radical (Chapter 6). Furthermore, introducing a cation binding site into CCP prevents the Trp radical formation (Bonagura *et al.*, 1996) (Chapter 1.3.4.1.). Thus, removal of the Ca(II) ions from the MnP F190Y mutant protein may allow the Tyr190 residue to be oxidized to a tyrosyl radical. This will provide another evidence for involvement of Ca(II) ions in determining the location of a free radical in peroxidases.

7.6. RECONSTITUTION OF MANGANESE PEROXIDASE

Reconstitution of heme proteins has been widely used to obtain active recombinant enzymes expressed in prokaryotic systems (Chapter 1.3.3.) and to modify δ-meso edge of the heme (Ortiz de Montellano *et al.*, 1988; Harris *et al.*, 1993; DePillis *et al.*, 1991) and the heme side chains (vinyl, methyl, and propionate groups) (Tamura *et al.*, 1972; DiNello & Dolphin, 1978; Reid *et al.*, 1984, 1986; LaMar *et al.*, 1986). Both removal and reconstitution of CCP, HRP, and ascorbate peroxidase appear to be straightforward (Chapter 1.3.3.): the apoprotein can be obtained simply by extracting these peroxidases with 2-butanone in acid solution. Incubating the apoprotein with the hemin solution easily gives holoenzymes (Yonetani, 1967; Tamura *et al.*, 1972). This suggests that the

apoproteins of these peroxidases possess similar structures to the holoenzymes. In the case of MnP, the heme can also be removed from MnP protein (unpublished data). However, reconstitution of MnP with the heme using the standard methods has not been successful. The heme binding site of MnP may be more hydrophobic than that of other peroxidases, so that the removing the heme from MnP may result in complete denaturation of MnP protein. Thus, various factors must be considered to achieve the successful reconstitution of MnP: different methods to extract the heme, addition of Ca(II) and oxidizing reagents, buffer compositions, temperature, and pH. The reconstitution of MnP will be very useful. First of all the heme propionates can be changed or modified. One of the propionates is a Mn(II) ligand and another forms an H-bond with a water molecule which is also a Mn(II) ligand (Figure 1-14). The modification of the heme propionates would provide useful information for the roles of these propionates on the MnP reaction. In addition, proton NMR studies of MnP reconstituted with specifically deuterated hemes will facilitate the identification of interactions between heme and small molecules and also the characterization of effects on the heme environment by various mutations in the heme pocket.

LITERATURE CITED

Adhi, T. P., Korus, R. A., & Crawford, D. L. (1989) Production of major extracellular enzyme during lignocellulose degradation by two streptomycetes in agitated submerged culture. *Appl. Environ. Microbiol.* **55**, 1165-1168.

Adler, E. (1977) Lignin chemistry—past, present and future. *Wood. Sci. Technol.* **11**, 169-218.

Ahern, T. J., Allan, G. G., & Medcalf, D. G. (1980) New bromoperoxidases of marine origin: partial purification and characterization. *Biochim. Biophys. Acta* **616**, 329-339.

Aitken, M. D., & Irvine, R. L. (1990) Characterization of reactions catalyzed by manganese peroxidase from *Phanerochaete chrysosporium*. *Arch. Biochem. Biophys.* **276**, 405-414.

Akileswaran, L., Alic, M., Clark, E. K., Hornick, J. L., & Gold, M. H. (1992) Isolation and transformation of uracil auxotrophs of the lignin-degrading basidiomycete *Phanerochaete chrysosporium*. *Curr. Genet.* **23**, 351-356.

Alam, S. L., Satterlee, J. D., Mauro, J. M., Poulos, T. L., & Erman, J. E. (1995) Proton NMR studies of cytochrome *c* peroxidase mutant N82A: hyperfine resonance assignments, identification of two interconverting enzyme ofecies, quantitating the rate of interconversion, and determination of equilibrium constants. *Biochemistry* **34**, 15496-15503.

Alic, M., Clark, E. K., Kornegay, J. R., & Gold, M. H. (1990) Transformation of *Phanerochaete chrysosporium* and *Neurospora crassa* with adenine biosynthetic genes from *Schizophyllum commune*. *Curr. Genet.* **17**, 305-311.

Alic, M., Letzring, C., & Gold, M. H. (1987) Mating system and basidiospore formation in the lignin-degrading basidiomycete *Phanerochaete chrysosporium*. *Appl. Environ. Microbiol.* **53**, 1464-1469.

Alic, M., Mayfield, M. B., Akileswaran, L., & Gold, M. H. (1991) Homologous transformation of the lignin-degrading basidiomycete *Phanerochaete chrysosporium*. *Curr. Genet.* **19**, 491-494.

Ander, P. (1994) The cellobiose-oxidizing enzymes CBQ and CBO as related to lignin and cellulose degradation. *FEMS Microbiol. Rev.* **13**, 297-312.

Ander, P., & Eriksson, K.-E. (1976) The importance of phenol oxidase activity in lignin degradation by the white-rot fungus *Sporotrichum pulverulentum*. *Arch. Microbiol.* **109**, 1-8.

Ander, P., & Eriksson, K.-E. (1977) Selective degradation of wood components by white-rot fungi. *Physiol. Plant.* **41**, 239-248.

Ander, P., Eriksson, K.-E., & Yu, H.-s. (1984) Metabolism of lignin-derived aromatic acids by wood-rotting fungi. *J. Gen. Microbiol.* **130**, 63-68.

Ander, P., Mishra, C., Farrell, R. L., & Eriksson, K.-E. (1990) Redox reactions in lignin degradation: interactions between laccase, different peroxidases and cellobiose:quinone oxidoreductase. *J. Biotechnol.* **13**, 525-529.

Ander, P., Sena Martins, G., & Duarte, J. C. (1993) Influence of cellobiose oxidase on peroxidases from *Phanerochaete chrysosporium*. *Biochem. J.* **293**, 431-435.

Ander, P., Stoytschev, I., & Eriksson, K.-E. (1988) Cleavage and metabolism of methoxyl groups from vanillic and ferulic acids by brown-rot and soft-rot fungi. *Cellul. Chem. Technol.* **22**, 255-266.

Andersson, L. A., Renganathan, V., Chiu, A. A., Loehr, T. M., & Gold, M. H. (1985) Spectral characterization of diarylpropane oxygenase, a novel peroxide-dependent, lignin-degrading heme enzyme. *J. Biol. Chem.* **260**, 6080-6087.

Andersson, L. A., Renganathan, V., Loehr, T. M., & Gold, M. H. (1987) Lignin peroxidase: resonance Raman spectral evidence for compound II and for a temperature-dependent coordination-state equilibrium in the ferric enzyme. *Biochemistry* **26**, 2258-2263.

Andrawis, A., Johnson, K. A., & Tien, M. (1988) Studies on compound I formation of the lignin peroxidase from *Phanerochaete chrysosporium*. *J. Biol. Chem.* **263**, 1195-1198.

Aramayo, R., & Timberlake, W. E. (1990) Sequence and molecular structure of the *Aspergillus nidulans* yA (laccase I) gene. *Nucleic. Acids. Res.* **18**, 3415.

Archibald, F., & Roy, B. (1992) Production of manganic chelates by laccase from the lignin-degrading fungus *Trametes* (*Coriolus*) *versicolor*. *Appl. Environ. Microbiol.* **58**, 1496-1499.

Asseffa, A., Smith, S. J., Nagata, K., Gillette, J. Gelboin, H. V., & Gonzalez, F. J. (1989) Novel exogenous heme-dependent expression of mammalian cytochrome P450 using baculovirus. *Arch. Biochem. Biophys.* **274**, 481-490.

Ator, M. A., David, S. K., & Ortiz de Montellano, P. R. (1987) Structure and catalytic mechanism of horseradish peroxidase. Regiospecific meso alkylation of the prosthetic heme group by alkylhydrazines. *J. Biol. Chem.* **262**, 14954-14960.

Ator, M. A., & Ortiz de Montellano, P. R. (1987) Protein control of prosthetic heme reactivity. Reaction of substrates with the heme edge of horseradish peroxidase. *J. Biol. Chem.* **262**, 1542-1551.

Ayers, A. R., Ayers, S. B., & Eriksson, K.-E. (1978) Cellobiose oxidase, purification and partial characterization of a hemoprotein from *Sporotrichum pulverulentum*. *Eur. J. Biochem.* **90**, 171-181.

Bajorath, J., Raghuinathan, S., Hinrichs, W., & Saenger, W. (1989) Long-range structural changes in proteinase K triggered by calcium ion removal. *Nature* **337**, 481-484.

Banci, L., Bertini, I., Bini, T., Tien, M., & Turano, P. (1993) Binding of horseradish, lignin, and manganese peroxidases to their respective substrates. *Biochemistry* **32**, 5825-5831.

Banci, L., Bertini, I., Pease, E. A., Tien, M., & Turano, P. (1992) ^{1}H NMR investigation of manganese peroxidase from *Phanerochaete chrysosporium*. A comparison with other peroxidases. *Biochemistry* **31**, 10009-10017.

Banci, L., Carloni, P., & Savellini, G. G. (1994) Molecular dynamics studies on peroxidases: a structural model for horseradish peroxidase and a substrate adduct. *Biochemistry* **33**, 12356-12366.

Bao, W., Fukushima, Y., Jensen, K. A., Jr., Moen, M. A., & Hammel, K. E. (1994) Oxidative degradation of non-phenolic lignin during lipid peroxidation by fungal manganese peroxidase. *FEBS Lett.* **354**, 297-300.

Bao, W., Usha, S. N., & Renganathan, V. (1993) Purification and characterization of cellobiose dehydrogenase, a novel extracellular hemoflavoenzyme from the white-rot fungus *Phanerochaete chrysosporium*. *Arch. Biochem. Biophys.* **300**, 705-713.

Bar-Lev, S. S., & Kirk, T. K. (1981) Effects of molecular oxygen on lignin degradation by *Phanerochaete chrysosporium*. *Biochem. Biophys. Res. Commun.* **99**, 373-378.

Barber, K. R., Rodríguez-Maranón, M. J., Shaw, G. S., & van Huystee, R. B. (1995) Structural influence of calcium on the heme cavity of cationic peanut peroxidase as determined by ¹H-NMR spectroscopy. *Eur. J. Biochem.* **232**, 825-833.

Barr, D. P., Shah, M. M., Grover, T. A., & Aust, S. D. (1992) Production of hydroxyl radical by lignin peroxidase from *Phanerochaete chrysosporium*. *Arch. Biochem. Biophys.* **298**, 480-485.

Baunsgaard, L., Dalbøge, H., Houen, G., Rasmussen, E. M., & Welinder, K. G. (1993) Amino acid sequence of *Coprinus macrorhizus* peroxidase and cDNA sequence encoding *Coprinus cinereus* peroxidase. A new family of fungal peroxidases. *Eur. J. Biochem.* **213**, 605-611.

Bavendamm, W. (1928) Uber das Vorkommen und den Nachweis von Oxydasen bei holzzerstorenden Pilzen. *Z Pflanzenkr Pflanzenschutz* **38**, 257-276.

Blanchette, R. A. (1991) Delignification by wood-decay fungi. *Ann. Rev. Phytopatol.* **29**, 381-398.

Bollag, J.-M., Shuttleworth, K. L., & Anderson, D. H. (1988) Laccase-mediated detoxification of phenolic compounds. *Appl. Environ. Microbiol.* **54**, 3086-3091.

Bonagura, C. A., Sundaramoorthy, M., Pappa, H. S., Patterson, W. R., & Poulos, T. L. (1996) An engineered cation site in cytochrome *c* peroxidase alters the reactivity of the redox active tryptophan. *Biochemistry* **35**, 6107-6115.

Bourbonnais, R., & Paice, M. G. (1988) Veratryl alcohol oxidases from the lignin-degrading basidiomycete *Pleurotus sajor-caju*. *Biochem. J.* **255**, 445-450.

Bourbonnais, R., & Paice, M. G. (1990) Oxidation of non-phenolic substrates. An expanded role for laccase in lignin biodegradation. *FEBS Lett.* **267**, 99-102.

Bourbonnais, R., & Paise, M. G. (1992) Demethylation and delignification of kraft pulp by *Trametes versicolor* laccase in the presence of 2,2´-azinobis-(3-ethylbenzthiazoline-6-sulphonate). *Appl. Microbiol. Biotechnol.* **36**, 823-827.

Brock, B. J., & Gold, M. H. (1996) 1,4-Benzoquinone reductase from basidiomycete *Phanerochaete chrysosporium*: spectral and kinetic analysis. *Arch. Biochem. Biophys.* **331**, 31-40.

Brock, J. B., Rieble, S., & Gold, M. H. (1995) Purification and characterization of a 1,4-benzoquinone reductase from the basidiomycete *Phanerochaete chrysosporium*. *Appl. Environ. Microbiol.* **61**, 3076-3081.

Brown, J. A., Alic, M., & Gold, M. H. (1991) Manganese peroxidase gene transcription in *Phanerochaete chrysosporium*: activation by manganese. *J. Bacteriol.* **173**, 4101-4106.

Brown, J. A., Glenn, J. K., & Gold, M. H. (1990) Manganese regulates expression of manganese peroxidase by *Phanerochaete chrysosporium*. *J. Bacteriol.* **172**, 3125-3130.

Buffard, D., Breda, C., van Huystee, R. B., Asemota, O., Pierre, M., Dang, H. D. B., & Esnault, R. (1990) Molecular cloning of complementary DNAs encoding two cationic peroxidases from cultivated peanut cells. *Proc. Natl. Acad. Sci. USA* **87**, 8874-8878.

Bumpus, J. A., & Aust, S. D. (1987) Biodegradation of environment pollutants by the white-rot fungus *Phanerochaete chrysosporium*: involvement of the lignin-degrading system. *Bioessays.* **6**, 166-170.

Burdsall, H. H., & Eslyn, W. E. (1974) A new *Phanerochaete* with a *chrysosporium* imperfect state. *Mycotaxon.* **109**, 123-133.

Buswell, J. A., & Eriksson, K.-E. (1988) NAD(P)H dehydrogenase (quinone) from *Sporotrichum pulverulentum*. *Methods Enzymol.* **161**, 271-274.

Buswell, J. A., Hamp, S., & Eriksson, K.-E. (1979) Intracellular quinone reduction in *Sporotrichum pulverulentum* by a NAD(P)H:quinone oxidoreductase. *FEBS Lett.* **108**, 229-232.

Buswell, J. A., & Odier, E. (1987) Lignin degradation. *Crit. Rev. Biotechnol.* **6**, 1-60.

Chance, B., Powers, L., Ching, Y., Poulos, T., Schonbaum, G. R., Yamazaki, I., & Paul, K. G. (1984) X-ray absorption studies of intermediates in peroxidase activity. *Arch. Biochem. Biophys.* **235**, 596-611.

Cheddar, G., Meyer, T. E., Cusanovich, M. A., & Stout, C. D., & Tollin, G. (1989) Redox protein electron-transfer mechanisms: electrostatic interactions as a determinant of reaction site in *c*-type cytochromes. *Biochemistry* **28**, 6318-6322.

Chen, C.-L., & Chang, H.-m. (1985) Chemistry of lignin biodegradation. In *Biosynthesis and Biodegradation of Wood Components* (Higuchi, T., Ed.) pp 535-556, Academic Press, Orland, FL.

Chen, L. L., Chang, H.-m., & Kirk, T. K. (1982) Aromatic acids produced during degradation of lignin in spruce wood by *Phanerochaete chrysosporium*. *Holzforschung* **36**, 3-9.

Choudhury, K., Sundaramoorthy, M., Hickman, A., Yonetani, T., Woehl, E., Dunn, M. F., & Poulos, T. L. (1994) Role of the proximal ligand in peroxidase catalysis. Crystallographic, kinetic, and spectral studies of cytochrome c peroxidase proximal ligand mutants. *J. Biol. Chem.* **269**, 20239-20349.

Choudhury, K., Sundaramoorthy, M., Mauro, J. M., & Poulos, T. L. (1992) Conversion of the proximal histidine ligand to glutamine restores activity to an inactive mutant of cytochrome c peroxidase. *J. Biol. Chem.* **267**, 25656-25659.

Constam, D., Muheim, A., Zimmermann, W., & Fiechter, A. (1991) Purification and characterization of an intracellular NADH:quinone oxidoreductase from *Phanerochaete chrysosporium*. *J. Gen. Microbiol.* **137**, 2209-2214.

Corin, A. F., Hake, R. A., McLendon, G., Hazzard, J. T., & Tollin, G. (1993) Effects of surface amino acid replacements in cytochrome c peroxidase on intracomplex electron transfer from cytochrome c. *Biochemistry* **32**, 2756-2762.

Corin, A. F., McLendon, G., Zhang, Q., Hake, R. A., Falvo, J., Lu, K. S., Ciccarelli, R. B., & Holzschu, D. (1991) Effects of surface amino acid replacements in cytochrome c peroxidase on complex formation with cytochrome c. *Biochemistry* **30**, 11585-11595.

Cormier, M. J., & Prichard, P. M. (1968) An investigation of the mechanifm of the luminescent peroxidation of luminol by stopped flow techniques. *J. Biol. Chem.* **243**, 4706-4714.

Cotton, M. L., & Dunford, H. B. (1973) Studies on horseradish peroxidase. XI. On the nature of compounds I and II as determined from the kinetics of the oxidation of ferrocyanide. *Can. J. Chem.* **51**, 582-587.

Crawford, R. L. (1981) *Lignin biodegradation and transformation.* Wiley-Interscience, New York.

Critchlow, J. E., & Dunford, H. B. (1972a) Studies on horseradish peroxidase. IX. Kinetics of the oxidation of p-cresol by compound II. *J. Biol. Chem.* **247**, 3703-3713.

Critchlow, J. E., & Dunford, H. B. (1972b) Studies on horseradish peroxidase. X. The mechanism of the oxidation of p-cresol, ferrocyanide, and iodide by compound II. *J. Biol. Chem.* **247**, 3714-3725.

Dalbøge, H., Jensen, E. B., & Welinder, K. G. (1992) Patent application no. WO 92/16634.

Dalton, D. A., Diaz del Castillo, L., Kahn, M. L., Joyner, S. L., & Chatfield, J. M. (1996) Heterologous expression and characterization of soybean cytosolic ascorbate peroxidase. *Arch. Biochem. Biophys.* **328**, 1-8.

Daniel, G., Pettersson, B., Volc, J., & Nilsson, T. (1990) Spatial distribution of lignin- and manganese (II) peroxidase(s) during degradation of wood and wood fragments by *Phanerochaete chrysosporium* as revealed by T.E.M. immunogold labelling. In *Biotechnology in Pulp and Paper Manufacture* (Kirk, T. K., & Chang, H.-m., Eds.) pp 99-110, Butterworth-Heinemann, Stoneham, MA.

Daniel, G., Volc, J., Kubatova, E., & Nilsson, T. (1992) Ultrastructural and immunocytochemical studies on the H_2O_2-producing enzyme pyranose oxidase in *Phanerochaete chrysosporium* grown under liquid culture conditions. *Appl. Environ. Microbiol.* **58**, 3667-3676.

Dawson, J. H. (1988) Probing structure-function relations in heme-containing oxygenases and peroxidases. *Science* **240**, 433-439.

Dawson, J. H., & Dooley, D. M. (1983) Magnetic circular dichroism spectroscopy of iron porphyrins and heme proteins. In *Iron Porphyrins* (Lever, A. B. P., & Gray, H. B., Eds.) part 3, pp 1-131, VCH Publishers, New York.

Dawson, J. H., Holm, R. H., Trudell, J. R., Barth, G., Linder, R. E., Bunnenberg, E., Djerassi, C., & Tang, S. C. (1976) Oxidized cytochrome P-450. Magnetic circular dichroism evidence for thiolate ligation in the substrate-bound form. Implications for the catalytic mechanism. *J. Am. Chem. Soc.* **98**, 3707-3708.

Dawson, J. H., & Sono, M. (1987) Cytochrome P450 and chloroperoxidase: thiolate-ligated heme enzymes. Spectroscopic determination of their active site structures and mechanistic implications of thiolate ligation. *Chem. Rev.* **87**, 1255-1276.

de Ropp, J. S., Chen, Z., & La Mar, G. N. (1995) Identification of residues in the aromatic substrate binding site of horseradish peroxidase by ^{1}H NMR studies on isozymes. *Biochemistry* **34**, 13477-13484.

de Ropp, J. S., La Mar, G. N., Wariishi, H., & Gold, M. H. (1991) NMR study of the active site of resting state and cyanide-inhibited lignin peroxidase from *Phanerochaete chrysosporium*. Comparison with horseradish peroxidase. *J. Biol. Chem.* **266**, 15001-15008.

DeLauder, S. F., Mauro, J. M., Poulos, T. L., Williams, J. C., & Schwarz, F. P. (1994) Thermodynamics of hydrogen cyanide and hydrogen fluoride binding to cytochrome *c* peroxidase and its Asn-82→Asp mutant. *Biochem. J.* **302**, 437-442.

Demmer, H., Hinz, I., Keller Rudex, H., Koeber, K., Kottelwesch, H., & Schneider, D. (1980) Complexes and salts of carboxylic acids and their derivatives. In *Coordination Compounds of Manganese* (Schleitzer-Rust, E., Ed.) 8th ed., Vol. 56, pp 1-196, Springer-Verlag, New York.

DePillis, G. D., Sishta, B. P., Mauk, A. G., & Ortiz de Montellano, P. R. (1991) Small substrates and cytochrome *c* are oxidized at different sites of cytochrome *c* peroxidase. *J. Biol. Chem.* **266**, 19334-19341.

DeVault, D. (1980) Quantum mechanical tunnelling in biological systems. *Quart. Rev. Biophys.* **13**, 387-564.

DiNello, R. K., & Dolphin, D. (1978) Interaction of the hemin 2 and 4 substituents with apo horseradish peroxidase. *Biochem. Biophys. Res. Commun.* **80**, 698-703.

DiNello, R. K., & Dolphin, D. H. (1981) Substituted hemins as probes for structure-function relationships in horseradish peroxidase. *J. Biol. Chem.* **256**, 6903-6912.

Dolphin, D., Forman, A., Borg, D. C., Fajer, J., & Felton, R. H. (1971) Compounds I of catalase and horseradish peroxidase: π-cation radicals. *Proc. Natl. Acad. Sci. USA* **68**, 614-618.

Doyle, W. A., & Smith, A. T. (1996) Expression of lignin peroxidase H8 in *Escherichia coli*: folding and activation of the recombinant enzyme with Ca(II) and haem. *Biochem. J.* **315**, 15-19.

Dunford, H. B. (1982) Peroxidases. *Adv. Inorg. Biochem.* **4**, 41-68.

Dunford, H. B. (1991) Horseradish peroxidase: structure and kinetic properties. In *Peroxidases in Chemistry and Biology* (Everse, J., Everse, K. E., & Grisham, M. B., Eds.) Vol. II, pp 25-50, CRC Press, Boca Raton.

Dunford, H. B., & Cotton, M. L. (1975) Kinetics of the oxidation of *p*-aminobenzoic acid catalyzed by horseradish peroxidase compounds I and II. *J. Biol. Chem.* **250**, 2920-2932.

Dunford, H. B., & Stillman, J. S. (1976) On the function and mechanism of action of peroxidase. *Coord. Chem. Rev.* **19**, 187-251.

Dutton, M. V., Evans, C. S., Atkey, P. T., & Wood, D. A. (1993) Oxalate production by basidiomycetes, including the white-rot species *Coriolus versicolor* and *Phanerochaete chrysosporium*. *Appl. Microbiol. Biotechnol.* **39**, 5-10.

Edwards, S. L., Mauro, J. M., Fishel, L. A., Wang, J. M., Miller, M. A., Xuong, N. H., & Kraut, J. (1988) Where is the radical in compound I of cytochrome *c* peroxidase? Clues from crystallography and mutagenesis. *Prog. Clin. Biol. Res.* **274**, 463-475.

Edwards, S. L., Nguyen, H. X., Hamlin, R. C., & Kraut, J. (1987) Crystal structure of cytochrome *c* peroxidase compound I. *Biochemistry* **26**, 1503-1511.

Edwards, S. L., & Poulos, T. L. (1990) Ligand binding and structural perturbations in cytochrome c peroxidase. A crystallographic study. *J. Biol. Chem.* **265**, 2588-2595.

Edwards, S. L., Raag, R., Wariishi, H., Gold, M. H., & Poulos, T. L. (1993) Crystal structure of lignin peroxidase. *Proc. Natl. Acad. Sci. USA* **90**, 750-754.

Effland, M. J. (1977) Modified procedure to determine acid-insoluble lignin in wood and pulp. *Tappi* **60**, 143-144.

Ellfolk, N., & Soininen, R. (1970) *Pseudomonas* cytochrome c peroxidase. I. Purification procedure. *Acta Chem. Scand.* **24**, 2126-2136.

Ellfolk, N., & Soininen, R. (1971) *Pseudomonas* cytochrome c peroxidase. 3. The size and shape of the enzyme molecule. *Acta Chem. Scand.* **25**, 1535-1540.

Enoki, A., & Gold, M. H. (1982) Degradation of the diarylpropane lignin model compound 1-(3′,4′-diethoxyphenyl)-1,3-dihydroxy-2-(4′-methoxyphenyl)-propane and derivatives by the basidiomycete *Phanerochaete chrysosporium*. *Arch. Microbiol.* **132**, 123-130.

Enoki, A., Goldsby, G. P., & Gold, M. H. (1980) Metabolism of the lignin model compounds veratrylglycerol-β-guaiacyl ether and 4-ethoxy-3-methoxyphenyl glycerol-β-guaiacyl ether by *Phanerochaete chrysosporium*. *Arch. Microbiol.* **125**, 227-232.

Enoki, A., Goldsby, G. P., Krisnangura, K., & Gold, M. H. (1981) Degradation of the lignin model compounds 4-ethoxy-3-methoxyphenyl glycerol β-guaiacyl and vanillic acid ethers by *Phanerochaete chrysosporium*. *FEMS Microbiol. Lett.* **10**, 373-377.

Erecínska, M., Oshino, N., Loh, P., & Brocklehurst, E. (1973) *In vitro* studies on yeast cytochrome c peroxidase and its possible function in the electron transfer and energy coupling reactions. *Biochim. Biophys. Acta* **292**, 1-12.

Eriksson, K.-E. L. (1990) Biotechnology in the pulp and paper industry. *Wood Sci. Technol.* **24**, 79-101.

Eriksson, K.-E., Habu, N., & Samejima, M. (1993) Recent advances in fungal cellobiose oxidoreductases. *Enzyme Microb. Technol.* **15**, 1002-1008.

Eriksson, K.-E., Pettersson, B., Volc, J., & Musilek, V. (1986) Formation and partial characterization of glucose-2-oxidase, a H_2O_2 producing enzyme in *Phanerochaete chrysosporium*. *Appl. Microbiol. Biotechnol.* **23**, 257-262.

Erman, J. E., & Vitello, L. B. (1980) The binding of cytochrome c peroxidase and ferricytochrome c. A spectrophotometric determination of the equilibrium association constant as a function of ionic strength. *J. Biol. Chem.* **255**, 6224-6227.

Erman, J. E., Vitello, L. B., Mauro, J. M., & Kraut, J. (1989) Detection of an oxyferryl porphyrin π-cation-radical intermediate in the reaction between hydrogen peroxide and a mutant yeast cytochrome c peroxidase. Evidence for tryptophan-191 involvement in the radical site of compound I. *Biochemistry* **28**, 7992-7995.

Erman, J. E., Vitello, L. B., Miller, M. A., Shaw, A., Brown, K. A., & Kraut, J. (1993) Histidine 52 is a critical residue for rapid formation of cytochrome c peroxidase compound I. *Biochemistry* **32**, 9798-9806.

Eslyn, W. E., Kirk, T. K., & Effland, M. J. (1975) Changes in the chemical composition of wood caused by six soft-rot fungi. *Phytopatology* **65**, 473-476.

Evans, C. S., Gallagher, I. M., Atkey, P. T., & Wood, D. A. (1991) Localization of degradative enzymes in white-rot decay of lignocellulose. *Biodegradation* **2**, 93-106.

Everest, A. M., Wallin, S. A., Stemp, E. D. A., Nocek, J. M., Mauk, A. G., & Hoffman, B. M. (1991) Aromatic hole superexchange through position 82 of cytochrome c is not required for intracomplex electron transfer to zinc cytochrome c peroxidase. *J. Am. Chem. Soc.* **113**, 4337-4338.

Fahreus, G., & Reinhammar, B. (1967) Large scale production and purification of laccase from cultures of the fungus *Polyporus versicolor* and some properties of laccase A. *Acta Chem. Scand.* **21**, 2367-2378.

Faison, B. D., & Kirk, T. K. (1983) Relationship between lignin degradation and production of reduced oxygen species by *Phanerochaete chrysosporium*. *Appl. Environ. Microbiol.* **46**, 1140-1145.

Faison, B. D., & Kirk, T. K. (1985) Factors involved in the regulation of a ligninase activity in *Phanerochaete chrysosporium*. *Appl. Environ. Microbiol.* **49**, 299-304.

Farhangrazi, Z. S., Copeland, B. R., Nakayama, T., Amachi, T., Yamazaki, I., & Powers, L. S. (1994) Oxidation-reduction properties of compounds I and II of *Arthromyces ramosus* peroxidase. *Biochemistry* **33**, 5647-5652.

Farmer, V. C., Henderson, M. E. K., & Russell, J. D. (1960) Aromatic-alcohol-oxidase activity in the growth medium of *Polystictus versicolor*. *Biochem. J.* **74**, 257-262.

Farrell, R. L., Murtagh, K. E., Tien, M., Mozuch, M. D., & Kirk, T. K. (1989) Physical and enzymatic properties of lignin peroxidase isozymes from *Phanerochaete chrysosporium*. *Enzyme Microb. Technol.* **11**, 322-328.

Felton, R. H., Romans, A. Y., Yu, N. T., & Schonbaum, G. R. (1976) Laser Raman spectra of oxidized hydroperoxidases. *Biochim. Biophys. Acta* **434**, 82-89.

Fengel, D., & Wegener, G. (1989) *Wood: Chemistry, Ultrastructure, Reactions*. Walter de Gruyter, Berlin.

Fenn, P., & Kirk, T. K. (1981) Relationship of nitrogen to the onset and suppression of ligninolytic activity and secondary metabolism in *Phanerochaete chrysosporium*. *Arch. Microbiol.* **130**, 59-65.

Ferrer, J. C., Turano, P., Banci, L., Bertini, I., Morris, I. K., Smith, K. M., Smith, M., & Mauk, A. G. (1994) Active site coordination chemistry of the cytochrome *c* peroxidase Asp235Ala variant: spectroscopic and functional characterization. *Biochemistry* **33**, 7819-7829.

Finzel, B. C., Poulos, T. L., & Kraut, J. (1984) Crystal structure of yeast cytochrome *c* peroxidase refined at 1.7-Å resolution. *J. Biol. Chem.* **259**, 13027-13036.

Fishel, L. A., Farnum, M. F., Mauro, J. M., Miller, M. A., Kraut, J., Liu, Y. J., Tan, X. L., & Scholes, C. P. (1991) Compound I radical in site-directed mutants of cytochrome *c* peroxidase as probed by electron paramagnetic resonance and electron-nuclear double resonance. *Biochemistry* **30**, 1986-1996.

Fishel, L. A., Villafranca, J. E., Mauro, J. M., & Kraut, J. (1987) Yeast cytochrome *c* peroxidase: mutagenesis and expression in *Escherichia coli* show tryptophan-51 is not the radical site in compound I. *Biochemistry* **26**, 351-360.

Fitzgerald, M. M., Churchill, M. J., McRee, D. E., & Goodin, D. B. (1994) Small molecule binding to an artificially created cavity at the active site of cytochrome *c* peroxidase. *Biochemistry* **33**, 3807-3818.

Fitzgerald, M. M., Trester, M. L., Jensen, G. M., McRee, D. E., & Goodin, D. B. (1995) The role of aspartate-235 in the binding of cations to an artificial cavity at the radical site of cytochrome *c* peroxidase. *Protein Sci.* **4**, 1844-1850.

Forney, L. J., Reddy, C. A., Tien, M., & Aust, S. D. (1982) The involvement of hydroxyl radical derived from hydrogen peroxide in lignin degradation by the white rot fungus *Phanerochaete chrysosporium*. *J. Biol. Chem.* **257**, 11455-11462.

Freudenberg, K.(1968) The constitution and biosynthesis of lignin. In *Constitution and Biosynthesis of Lignin* (Neish, A. C. & Freudenberg, K., Eds.), pp 47-122, Springer-Verlag, Berlin.

Froehner, S. C., & Eriksson, K.-E. (1974) Purification and properties of *Neurospora crassa* laccase. *J. Bacteriol.* **120**, 458-465.

Fulop, V., Phizackerley, R. P., Soltis, S. M., Clifton, I. J., Wakatsuki, S., Erman, J., Hajdu, J., & Edwards, S. L. (1994) Laue diffraction study on the structure of cytochrome *c* peroxidase compound I. *Structure* **2**, 201-208.

Gazaryan, I. G., Doseeva, V. V., Galkin, A. G., & Tishkov, V. I. (1994) Effect of single-point mutations Phe41→His and Phe143→Glu on folding and catalytic properties of recombinant horseradish peroxidase expressed in *E. coli*. *FEBS Lett.* **354**, 248-250.

Geren, L., Hahm, S., Durham, B., & Millett, F. (1991) Photoinduced electron transfer between cytochrome *c* peroxidase and yeast cytochrome *c* labeled at Cys102 with (4-bromomethyl-4´-methylbipyridine)[bis(bipyridine)]ruthenium(II). *Biochemistry* **30**, 9450-9457.

Germann, U. A., & Lerch, K. (1986) Isolation and partial nucleotide sequence of the laccase gene from *Neurospora crassa*: amino acid sequence homology of the protein to human ceruloplasmin. *Proc. Natl. Acad. Sci. USA* **83**, 8854-8858.

Gilbertson, R. L. (1980) Wood-rotting fungi of North America. *Mycologia.* **72**, 1-49.

Glenn, J. K., Akileswaran, L., & Gold, M. H. (1986) Mn(II) oxidation is the principal function of the extracellular Mn-peroxidase from *Phanerochaete chrysosporium*. *Arch. Biochem. Biophys.* **251**, 688-696.

Glenn, J. K., & Gold, M. H. (1985) Purification and characterization of an extracellular Mn(II)-dependent peroxidase from the lignin-degrading basidiomycete, *Phanerochaete chrysosporium*. *Arch. Biochem. Biophys.* **242**, 329-341.

Glenn, J. K., Morgan, M. A., Mayfield, M. B., Kuwahara, M., & Gold, M. H. (1983) An extracellular H_2O_2-requiring enzyme preparation involved in lignin biodegradation by the white rot basidiomycete *Phanerochaete chrysosporium*. *Biochem. Biophys. Res. Commun.* **114**, 1077-1083.

Glumoff, T., Harvey, P. J., Molinari, S., Goble, M., Frank, G., Palmer, J. M., Smit, J. D., & Leisola, M. S. (1990) Lignin peroxidase from *Phanerochaete chrysosporium*. Molecular and kinetic characterization of isozymes. *Eur. J. Biochem.* **187**, 515-520.

Godfrey, B. J., Akileswaran, L., & Gold, M. H. (1994) A reporter gene construct for studying the regulation of manganese peroxidase gene expression. *Appl. Environ. Microbiol.* **60**, 1353-1358.

Godfrey, B. J., Mayfield, M. B., Brown, J. A., & Gold, M. H. (1990) Characterization of a gene encoding a manganese peroxidase from *Phanerochaete chrysosporium*. *Gene* **93**, 119-124.

Gold, M. H., & Alic, M. (1993) Molecular biology of the lignin-degrading basidiomycete *Phanerochaete chrysosporium*. *Microbiol. Rev.* **57**, 605-622.

Gold, M. H., & Cheng, T. M. (1978) Induction of colonial growth and replica plating of the white-rot basidiomycete *Phanerochaete chrysosporium*. *Arch. Microbiol.* **121**, 37-41.

Gold, M. H., Cheng, T. M., & Mayfield, M. B. (1982a) Isolation and complementation studies of auxotrophic mutants of the lignin-degrading basidiomycete *Phanerochaete chrysosporium*. *Appl. Environ. Microbiol.* **44**, 996-1000.

Gold, M. H., Glenn, J. K., Mayfield, M. B., Morgan, M. A., & Kutsuki, H. (1983) Biochemical and genetic studies on lignin degradation by *Phanerochaete chrysosporium*. In *Recent Advances in Lignin Biodegradation Research* (Higuchi, T., Chang, H.-m & Kirk, T. K., Eds.) pp 219-232, Uni Ltd., Tokyo.

Gold, M. H., Kuwahara, M., Chiu, A. A., & Glenn, J. K. (1984) Purification and characterization of an extracellular H_2O_2-requiring diarylpropane oxygenase from the white rot basidiomycete, *Phanerochaete chrysosporium*. *Arch. Biochem. Biophys.* **234**, 353-362.

Gold, M. H., Mayfield, M. B., Cheng, T. M., Krisnangkura, K., Shimada, M., Enoki, A., & Glenn, J. K. (1982b) A *Phanerochaete chrysosporium* mutant defective in lignin degradation as well as several other secondary metabolic functions. *Arch. Microbiol.* **132**, 115-122.

Gold, M. H., Wariishi, H., & Valli, K. (1989) Extracellular peroxidases involved in lignin degradation by the white-rot basidiomycete *Phanerochaete chrysosporium*. *ACS Symp. Ser.* **389**, 127-140.

Goldsby, G. P., Enoki, A., & Gold, M. H. (1980) Alkyl-phenyl cleavage of the lignin model compounds guaiacylglycerol- and glycerol-β-guaiacyl ether by *Phanerochaete chrysosporium*. *Arch. Microbiol.* **128**, 190-195.

Goodin, D. B., Davidson, M. G., Roe, J. A., Mauk, A. G., & Smith, M. (1991) Amino acid substitutions at tryptophan-51 of cytochrome *c* peroxidase: effects on coordination, species preference for cytochrome *c*, and electron transfer. *Biochemistry* **30**, 4953-4962.

Goodin, D. B., Mauk, A. G., & Smith, M. (1986) Studies of the radical species in compound ES of cytochrome *c* peroxidase altered by site-directed mutagenesis. *Proc. Natl. Acad. Sci. USA* **83**, 1295-1299.

Goodin, D. B., Mauk, A. G., & Smith, M. (1987) The peroxide complex of yeast cytochrome *c* peroxidase contains two distinct radical species, neither of which resides at methionine 172 or tryptophan 51. *J. Biol. Chem.* **262**, 7719-7724.

Goodin, D. B., & McRee, D. E. (1993) The Asp-His-Fe triad of cytochrome c peroxidase controls the reduction potential, electronic structure, and coupling of the tryptophan free radical to the heme. *Biochemistry* **32**, 3313-3324.

Grisebach, H. (1981) In *The Biochemistry of Plants* (Stumpf, P. K., & Conn, E. E., Eds.) Chapt.15, Academic Press, New York.

Guillen, F., Martinez, A. T., & Martinez, M. J. (1992) Substrate specificity and properties of the aryl-alcohol oxidase from the ligninolytic fungus *Pleurotus eryngii*. *Eur. J. Biochem.* **209**, 603-611.

Hahm, S., Durham, B., & Millett, F. (1992) Photoinduced electron transfer between cytochrome c peroxidase and horse cytochrome c labeled at specific lysines with (dicarboxybipyridine)(bisbipyridine)ruthenium(II). *Biochemistry* **31**, 3472-3477.

Hahm, S., Durham, B., & Millett, F. (1993) Reaction of cytochrome c with the radical in cytochrome c peroxidase compound I. *J. Am. Chem. Soc.* **115**, 3372-3373.

Hahm, S., Miller, M. A., Geren, L., Kraut, J., Durham, B., & Millett, F. (1994) Reaction of horse cytochrome c with the radical and the oxyferryl heme in cytochrome c peroxidase compound I. *Biochemistry* **33**, 1473-1480.

Hames, B. D., & Rickwood, D. (Eds.) (1981) *Gel electrophoresis of proteins: A practical approach*. IRL Press, Oxford.

Hammel, K. E. (1989) Organopollutant degradation by lignolytic fungi. *Enzyme Microb. Technol.* **11**, 776-777.

Hammel, K. E., & Moen, M. A. (1991) Depolymrization of a synthetic lignin *in vitro* by lignin peroxidase. *Enzyme Microb. Technol.* **13**, 15-18.

Hammel, K. E., Jensen, K. A., Jr., Mozuch, M. D., Landucci, L. L., Tien, M., & Pease, E. A. (1993) Ligninolysis by a purified lignin peroxidase. *J. Biol. Chem.* **268**, 12274-12281.

Hammel, K. E., Tien, M., Kalyanaraman, B., & Kirk, T. K. (1985) Mechanism of oxidative C_α-C_β cleavage of a lignin model dimer by *Phanerochaete chrysosporium* ligninase. Stoichiometry and involvement of free radicals. *J. Biol. Chem.* **260**, 8348-8353.

Harkin, J. M., & Obst, J. R. (1973) Demethylation of 2,4,6-trimethoxyphenol by phenol oxidase. *Science* **180**, 296-298.

Harmsen, M. C., Schuren, F. H. J., Moukha, S. M., van Zuilen, C. M., Punt, P. J., & Wessels, J. G. H. (1992) Sequence analysis of the glyceraldehyde-3-phosphate dehydrogenase genes from the basidiomycetes *Schizophyllum commune*, *Phanerochaete chrysosporium* and *Agaricus bisporus*. *Curr. Genet.* **22**, 447-454.

Harris, R. Z., Newmyer, S. L., & Ortiz de Montellano, P. R. (1993) Horseradish peroxidase-catalyzed two-electron oxidations. Oxidation of iodide, thioanisoles, and phenols at distinct sites. *J. Biol. Chem.* **268**, 1637-1645.

Harris, R. Z., Wariishi, H., Gold, M. H., & Ortiz de Montellano, P. R. (1991) The catalytic site of manganese peroxidase. Regiospecific addition of sodium azide and alkylhydrazines to the heme group. *J. Biol. Chem.* **266**, 8751-8758.

Hartmann, C., & Ortiz de Montellano, P. R. (1992) Baculovirus expression and characterization of catalytically active horseradish peroxidase. *Arch. Biochem. Biophys.* **297**, 61-72.

Haschke, R. H., & Friedhoff, J. M. (1978) Calcium-related properties of horseradish peroxidase. *Biochem. Biophys. Res. Commun.* **80**, 1039-1042.

Hashimoto, S., Nakajima, R., Yamazaki, I., Tatsuno, Y., & Kitagawa, T. (1986a) Oxygen exchange between the Fe(IV)=O heme and bulk water for the A2 isozyme of horseradish peroxidase. *FEBS Lett.* **208**, 305-307.

Hashimoto, S., Tatsuno, Y., & Kitagawa, T. (1986b) Resonance Raman evidence for oxygen exchange between the Fe(IV)=O heme and bulk water during enzymic catalysis of horseradish peroxidase and its relation with the heme-linked ionization.horseradish peroxidase and its relation with the heme-linked ionization. *Proc. Natl. Acad. Sci. USA* **83**, 2417-2421.

Hashimoto, S., Teraoka, J., Inubushi, T., Yonetani, T., & Kitagawa, T. (1986c) Resonance Raman study on cytochrome *c* peroxidase and its intermediate. Presence of the Fe(IV)=O bond in compound ES and heme-linked ionization. *J. Biol. Chem.* **261**, 11110-11118.

Hatakka, A. (1994) Lignin-modifying enzymes from selected white-rot fungi: production and role in lignin degradation. *FEMS Microbiol. Rev.* **13**, 125-135.

Hayashi, Y., & Yamazaki, I. (1979) The oxidation reduction potential of compound I/compound II and compound II/ferric couples of horsedasish peroxidadse A2 and C. *J. Biol. Chem.* **254**, 9101-9106.

Hazzard, J. T., Poulos, T. L., & Tollin, G. (1987) Kinetics of reduction by free flavin semiquinones of the components of the cytochrome *c*-cytochrome *c* peroxidase complex and intracomplex electron transfer. *Biochemistry* **26**, 2836-2848.

Hazzard, J. Y., & Tollin, G. (1991) Intramolecular electron transfer from the heme to the radical site does not occur in compound II of yeast cytochrome c peroxidase during catalytic turnover. *J. Am. Chem. Soc.* **113**, 8956-8957.

Henikoff, S. (1987) Unidirectional digestion with exonuclease III in DNA sequence analysis. *Methods Enzymol.* **155**, 156-165.

Henriksson, G., Pettersson, G., Johansson, G., Ruiz, A., & Uzcategui, E. (1991) Cellobiose oxidase from *Phanerochaete chrysosporium* can be cleaved by papain into two domains. *Eur. J. Biochem.* **196**, 101-106.

Hewson, W. D., & Dunford, H. B. (1975) Horseradish peroxidase. XVIII. The Arrhenius activation energy for the formation of compound I. *Can. J. Chem.* **53**, 1928-1932.

Hewson, W. D., & Dunford, H. B. (1976) Oxidation of p-cresol by horseradish peroxidase compound I. *J. Biol. Chem.* **251**, 6036-6042.

Higuchi, T. (1985) Biosynthesis of lignin. In *Biosynthesis and Biodegradation of Wood Components* (Higuchi, T., Ed.) pp 141-160, Academic Press, Inc., Orlando, Florida.

Higuchi, T. (1989) Mechanisms of lignin degradation by lignin peroxidase and laccase of white-rot fungi. *ACS Symp. Ser.* **399**, 482-502.

Higuchi, T. (1990) Lignin biochemistry: biosynthesis and biodegradation. *Wood Sci. Technol.* **24**, 23-63.

Hiner, A. N., Hernández-Ruíz, J., García-Cánovas, F., Smith, A. T., Arno, M. B., & Acosta, M. (1995) A comparative study of the inactivation of wild-type, recombinant and two mutant horseradish peroxidase isoenzymes C by hydrogen peroxide and m-chloroperoxybenzoic acid. *Eur. J. Biochem.* **234**, 506-512.

Ho, P. S., Hoffman, B. M., Kang, C. H., & Margoliash, E. (1983) Control of the transfer of oxidizing equivalents between heme iron and free radical site in yeast cytochrome c peroxidase. *J. Biol. Chem.* **258**, 4356-4363.

Ho, S. N., Hunt, H. D., Horton, R. M., Pullen, J. K., & Pease, L. R. (1989) Site-directed mutagenesis by overlap extension using the polymerase chain reaction. *Gene* **77**, 51-59.

Hoffman, B. M. (1991) Electron nuclear double resonance (ENDOR) of metalloenzymes. *Acc. Chem. Res.* **24**, 164-170.

Hoffman, B. M., DeRose, V. J., Doan, P. E., Gurbiel, R. J., Houseman, A. L. P., & Telser, J. (1993) In *Biological Magnetic Resonance* (Berliner, L. J., & Reuben, J., Eds.) Vol. 13, pp 151-218, Plenum Press, New York.

Hoffman, B. M., Roberts, J. E., Kang, C. H., & Margoliash, E. (1981) Electron paramagnetic and electron nuclear double resonance of the hydrogen peroxide compound of cytochrome c peroxidase. *J. Biol. Chem.* **256**, 6556-6564.

Hori, H., & Yonetani, T. (1985) Powder and single-crystal electron paramagnetic resonance studies of yeast cytochrome c peroxidase and its peroxide and its peroxide compound, Compound ES. *J. Biol. Chem.* **260**, 349-355.

Houseman, A. L., Doan, P. E., Goodin, D. B., & Hoffman, B. M. (1993) Comprehensive explanation of the anomalous EPR spectra of wild-type and mutant cytochrome c peroxidase compound ES. *Biochemistry* **32**, 4430-4443.

Huyett, J. E., Doan, P. E., Gurbiel, R., Houseman, A. L. P., Sivaraja, M., Goodin, D. B., & Hoffman, B. M. (1995) Compound ES of cytochrome c peroxidase contains a Trp π-cation radical: characterization by CW and pulsed Q-band ENDOR spectroscopy. *J. Am. Chem. Soc.* **117**, 9033-9041.

Iizuka, T., & Yonetani, T. (1970) Spin changes in hemoproteins. *Adv. Biophys.* **1**, 157-182.

Ishihara, T., & Miyazaki, M. (1972) Oxidation of milled wood lignin by fungal laccase. *Mokuzai Gakkaishi* **18**, 415-419.

Ishikawa, T., Sakai, K., Takeda, T., & Shigeoka, S. (1995) Cloning and expression of cDNA encoding a new type of ascorbate peroxidase from spinach. *FEBS Lett.* **367**, 28-32.

Jeffries, T. W., Choi, S., & Kirk, T. K. (1981) Nutritional regulation of lignin degradation by *Phanerochaete chrysosporium*. *Appl. Environ. Microbiol.* **42**, 290-296.

Jin, L., Schultz, T. P., & Nicholas, D. D. (1990) Structural characterization of brown-rotted lignin. *Horzforschung* **44**, 133-138.

Job, D., Ricard, J., & Dunford, H. B. (1978) Kinetics of formation of the primary compound (compound I) from hydrogen peroxide and turnip peroxidases. *Can. J. Biochem.* **56**, 702-707.

Johnson, F., Loew, G. H., & Du, P. (1993) Prediction of Mn(II) binding site of manganese peroxidase from homology modeling. In *Plant Peroxidases: Biochemistry and Physiology* (Welinder, K. G., Rasmussen, S. K., Penel, C., & Greppin, H., Eds.) pp 31-34, University of Geneva, Geneva, Switzerland.

Johnson, T. M., & Li, J. K.-K. (1991) Heterologous expression and characterization of an active lignin peroxidase from *Phanerochaete chrysosporium* using recombinant baculovirus. *Arch. Biochem. Biophys.* **291**, 371-378.

Joshi, D. K., & Gold, M. H. (1993) Degradation of 2,4,5-trichlorophenol by the lignin-degrading basidiomycete *Phanerochaete chrysosporium. Appl. Environ. Microbiol.* **59**, 1779-1785.

Kang, C. H., Ferguson Miller, S., & Margoliash, E. (1977) Steady state kinetics and binding of eukaryotic cytochromes *c* with yeast cytochrome *c* peroxidase. *J. Biol. Chem.* **252**, 919-926.

Kaput, J., Goltz, S., & Blobel, G. (1982) Nucleotide sequence of the yeast nuclear gene for cytochrome *c* peroxidase precursor. Functional implications of the pre-sequence for protein transport into mitochondria. *J. Biol. Chem.* **257**, 15054-15058.

Karhunen, E., Niku Paavola, M.-L., Viikari, L., Haltia, T., van der Meer, R. A., & Duine, J. A. (1990) A novel combination of prosthetic groups in a fungal laccase; PQQ and two copper atoms. *FEBS Lett.* **267**, 6-8.

Kawai, S., Umezawa, T., & Higuchi, T. (1986) *De novo* synthesis of veratryl alcohol by *Coriolus versicolor. Wood Res.* **73**, 18-21.

Kawai, S., Umezawa, T., & Higuchi, T. (1988a) Degradation mechanisms of phenolic β-1 lignin substructure model compounds by laccase of *Coriolus versicolor. Arch. Biochem. Biophys.* **262**, 99-110.

Kawai, S., Umezawa, T., & Higuchi, T. (1989) Oxidation of methoxylated benzyl alcohols by laccase of *Coriolus versicolor* in the presence of syringaldehyde. *Wood Res.* **76**, 10-16.

Kawai, S., Umezawa, T., Shimada, M., & Higuchi, T. (1988b) Aromatic ring cleavage of 4,6-di(tert-butyl)guaiacol, phenolic lignin model compound, by laccase of *Coriolus versicolor. FEBS Lett.* **236**, 309-311.

Kedderis, G. L., Koop, D. R., & Hollenberg, P. F. (1980) N-Demethylation reactions catalyzed by chloroperoxidase. *J. Biol. Chem.* **255**, 10174-10182.

Kelley, H. C., Davies, D. M., King, M. J., & Jones, P. (1977) Pre-steady-state kinetics of intermediate formation in the deuteroferriheme-hydrogen peroxide system. *Biochemistry* **16**, 3543-3549.

Kelly, R. L., & Reddy, C. A. (1986) Purification and characterization of glucose oxidase from ligninolytic cultures of *Phanerochaete chrysosporoum. J. Bacteriol.* **166**, 269-274.

Kersten, P. J., & Kirk, T. K. (1987) Involvement of a new enzyme, glyoxal oxidase, in extracellular H_2O_2 production by *Phanerochaete chrysosporium*. *J. Bacteriol.* **169**, 2195-2201.

Keyser, P., Kirk, T. K., & Zeikus, J. G. (1978) Ligninolytic enzyme system of *Phanaerochaete chrysosporium*: synthesized in the absence of lignin in response to nitrogen starvation. *J. Bacteriol.* **135**, 790-797.

Khindaria, A., Barr, D. P., & Aust, S. D. (1995) Lignin peroxidases can also oxidize manganese. *Biochemistry* **34**, 7773-7779.

Kirk, T. K. (1971) Effects of microorganisms on lignin. *Ann. Rev. Phytopatol.* **9**, 185-210.

Kirk, T. K. (1975) Effects of a brown-rot fungus, *Lenzites trabea*, on lignin in spruce wood. *Holzforshung* **29**, 99-107.

Kirk, T. K., & Adler, E. (1970) Methoxyl-deficient structural elements in lignin of sweetbum decayed by a brown-rot fungus. *Acta Chem. Scand.* **24**, 3379-3390.

Kirk, T. K., & Chang, H.-m. (1974) Decomposition of lignin by white-rot fungi. I. Isolation of heavily degraded lignins from decayed spruce. *Holzforschung* **28**, 217-222.

Kirk, T. K., & Chang, H.-m. (1975) Decomposition of lignin by white-rot fungi. II. Characterization of heavily degraded lignins from decayed spruce. *Holzforschung* **29**, 56-64.

Kirk, T. K., Conners, W. J., & Ziekus, J. G. (1976) Requirement for a growth substrate during lignin decomposition by two wood-rotting fungi. *Appl. Environ. Microbiol.* **32**, 192-194.

Kirk, T. K., & Cowling, E. B. (1984) The chemistry of solid wood. In *Advances in Chemistry* (Rowell, R. M., Ed.) Vol. 207, pp 435-487, American Chemical Society, Washington, DC.

Kirk, T. K., & Farrell, R. L. (1987) Enzymatic "combustion": the microbial degradation of lignin. *Annu. Rev. Microbiol.* **41**, 465-505.

Kirk, T. K., Harkin, J. M., & Cowling, E. B. (1968) Oxidation of guaiacyl- and veratryl-glycerol-β-gualacyl ether by *Polyporus versicolor* and *Stereum frustulatum*. *Biochim. Biophys. Acta* **165**, 134-144.

Kirk, T. K., & Kelman, A. (1965) Lignin degradation as related to the phenoloxidases of selected wood-decaying basidiomycetes. *Phytopathol* **55**, 739-745.

Kirk, T. K., Nakatsubo, F., & Reid, I. D. (1983) Further study discounts role for singlet oxygen in fungal degradation of lignin model compounds. *Biochem. Biophys. Res. Commun.* **111**, 200-204.

Kirk, T. K., Schultz, E., Connors, W. J., Lorenze, L. F., & Zeikus, J. G. (1978) Influence of culture parameters on lignin metabolism by *Phanerochaete chrysosporium*. *Arch. Microbiol.* **117**, 227-285.

Kirk, T. K., & Shimada, M. (1985) Lignin biodegradation: the microorganisms involved and the physiology and biochemistry of degradation by white-rot fungi. In *Biosynthesis and Biodegradation of Wood Components* (Higuchi, T., Ed.) pp 579-605, Academic Press, Orland, Florida.

Kirk, T. K., & Tien, M. (1983) Biochemistry of lignin degradation by *Phanerochaete chrysosporium*: Investigations with non-phenolic model compounds. In *Recent Advances in Lignin Biodegradation Research* (Higuchi, T., Chang, H.-m., & Kirk, T. K., Eds.) pp 233-245, Uni. Ltd., Tokyo.

Kirk, T. K., Tien, M., Kersten, P. J., Mozuch, M. D., & Kalyanaraman, B. (1986) Ligninase of *Phanerochaete chrysosporium*. Mechanism of its degradation of the non-phenolic arylglycerol β-aryl ether substructure of lignin. *Biochem. J.* **236**, 279-287.

Kishi, K., Kusters-van Someren, M., Mayfield, M. B., Sun, J., Loehr, T. M., & Gold, M. H. (1996) Characterization of manganese(II) binding site mutants of manganese peroxidase. *Biochemistry* **35**, 8986-8994.

Kishi, K., Wariishi, H., Marquez, L., Dunford, H. B., & Gold, M. H. (1994) Mechanism of manganese peroxidase compound II reduction. Effect of organic acid chelators and pH. *Biochemistry* **33**, 8694-8701.

Kjalke, M., Andersen, M. B., Schneider, P., Christensen, B., Schulein, M., & Welinder, K. G. (1992) Comparison of structure and activities of peroxidases from *Coprinus cinereus*, *Coprinus macrorhizus* and *Arthromyces ramosus*. *Biochim. Biophys. Acta* **1120**, 248-256.

Kobayashi, K., Tamura, M., Hayashi, K., Hori, H., & Morimoto, H. (1980) Electron paramagnetic resonance and optical absorption spectrum of the pentacoordinated ferrihemoproteins. *J. Biol. Chem.* **255**, 2239-2242.

Kojima, Y., Tsukuda, Y., Kawai, Y., Tsukamoto, A., Sugiura, J., Sakaimo, M., & Kita, Y. (1990) Cloning, sequence analysis, and expression of ligninolytic phenoloxidase genes of the white-rot basidiomycete *Coriolus hirsutus*. *J. Biol. Chem.* **265**, 15224-15230.

Kremer, S. M., & Wood, P. M. (1992a) Cellobiose oxidase from *Phanerochaete chrysosporium* as a source of Fenton's reagent. *Biochem. Soc. Trans.* **20**, 110S.

Kremer, S. M., & Wood, P. M. (1992b) Evidence that cellobiose oxidase from *Phanerochaete chrysosporium* is primarily an Fe(III) reductase. Kinetic comparison with neutrophil NADPH oxidase and yeast flavocytochrome b_2. *Eur. J. Biochem.* **205**, 133-138.

Kremer, S. M., & Wood, P. M. (1992c) Production of Fenton's reagent by cellobiose oxidase from cellulolytic cultures of *Phanerochaete chrysosporium*. *Eur. J. Biochem.* **208**, 807-814.

Kuan, I.-C., Johnson, K. A., & Tien, M. (1993) Kinetic analysis of manganese peroxidase. The reaction with manganese complexes. *J. Biol. Chem.* **268**, 20064-20070.

Kuan, I.-C., & Tien, M. (1993) Stimulation of Mn peroxidase activity: a possible role for oxalate in lignin biodegradation. *Proc. Natl. Acad. Sci. USA* **90**, 1242-1246.

Kunishima, N., Fukuyama, K., Matsubara, H., Hatanaka, H., Shibano, Y., & Amachi, T. (1994) Crystal structure of the fungal peroxidase from *Arthromyces ramosus* at 1.9 Å resolution. Structural comparisons with the lignin and cytochrome *c* peroxidases. *J. Mol. Biol.* **235**, 331-344.

Kusters-van Someren, M., Kishi, K., Lundell, T., & Gold, M. H. (1995) The manganese binding site of manganese peroxidase: characterization of an Asp179Asn site-directed mutant protein. *Biochemistry* **34**, 10620-10627.

Kutsuki, H., & Gold, M. H. (1982) Generation of hydroxyl radical and its involvement in lignin degradation by *Phanerochaete chrysosporium*. *Biochem. Biophys. Res. Commun.* **109**, 320-327.

Kuwahara, M., Glenn, J. K., Morgan, M. A., & Gold, M. H. (1984) Separation and characterization of two extracellular H_2O_2-dependent oxidases from ligninolytic cultures of *Phanerochaete chrysosporium*. *FEBS Lett.* **169**, 247-250.

Laemmli, U. K. (1970) Cleavage of structural proteins during the assembly of the head of bacteriophage T4. *Nature (London)* **227**, 680-695.

Laker, M. F., Hofmann, A. F., & Meeuse, B. J. (1980) Spectrophotometric determination of urinary oxalate with oxalate oxidase prepared from moss. *Clin. Chem.* **26**, 827-830.

La Mar, G. N., & de Ropp, J. S. (1993) In *Biological Magnetic Resonance* (Berliner, L. J., & Reuben, J., Eds.) Vol. 12, pp 1-78, Plenum Press, New York.

La Mar, G. N., de Ropp, J. S., Latos Grazynski, L., Balch, A. L., Johnson, R. B., Smith, K. M., Parish, D. W., & Chang, R. (1983) Proton NMR characterization of the ferryl group in model heme complexes and hemoproteins: Evidence for the Fe(IV)=O group in ferryl myoglobin and compound II of horseradish peroxidase. *J. Am. Chem. Soc.* **105**, 782-787.

La Mar, G. N., de Ropp, J. S., Smith, K. M., & Langry, K. C. (1981) Proton nuclear magnetic resonance investigation of the electronic structure of compound I of horseradish peroxidase. *J. Biol. Chem.* **256**, 237-243.

La Mar, G. N., Emerson, S. D., Lecomte, J. T. J., Pande, U., Smith, K. M., Craig, G. W., & Kehres, L. A. (1986) Influence of propionate side chains on the equilibrium heme orientation in sperm whale myoglobin. Heme resonance assignments and structure determination by nuclear overhauser effect measurements. *J. Am. Chem. Soc.* **108**, 5568-5573.

La Mar, G. N., Hernández, G., & de Ropp, J. S. (1992) ^{1}H NMR investigation of the influence of interacting sites on the dynamics and thermodynamics of substrate and ligand binding to horseradish peroxidase. *Biochemistry* **31**, 9158-9168.

Leisola, M. S., Kozulic, B., Meussdoerffer, F., & Fiechter, A. (1987) Homology among multiple extracellular peroxidases from *Phanerochaete chrysosporium*. *J. Biol. Chem.* **262**, 419-424.

Leonard, J. J., & Yonetani, T. (1974) Interaction of cytochrome *c* peroxidase with cytochrome *c*. *Biochemistry* **13**, 1465-1468.

Leonowicz, A., Edgehill, R. U., & Bollag, J.-M. (1984) The effect of pH on the transformation of syringic and vanillic acids by the laccases of *Rhizoctonia praticola* and *Trametes versicolor*. *Arch. Microbiol.* **137**, 89-96.

Lerch, K., Deinum, J., & Reinhammer, B. (1978) The state of copper in *Neurospora* laccase. *Biochim. Biophys. Acta* **534**, 7-14.

Limongi, P., Kjalke, M., Vind, J., Tams, J. W., Johansson, T., & Welinder, K. G. (1995) Disulfide bonds and glycosylation in fungal peroxidases. *Eur. J. Biochem.* **227**, 270-276.

Lin, S. Y., & Dence, C. W. (Eds.). (1992) *Methods in Lignin Chemistry*, Springer-Verlag, Berlin, Heidelberg.

Liu, R. Q., Geren, L., Anderson, P., Fairris, J. L., Peffer, N., McKee, A., Durham, B., & Millet, F. (1995a) Design of ruthenium-cytochrome *c* derivatives to measure electron transfer to cytochrome *c* peroxidase. *Biochimie* **77**, 549-561.

Liu, R. Q., Hahm, S., Miller, M., Durham, B., & Millett, F. (1995b) Photooxidation of Trp-191 in cytochrome *c* peroxidase by ruthenium-cytochrome *c* derivatives. *Biochemistry* **34**, 973-983.

Liu, R. Q., Miller, M. A., Han, G. W., Hahm, S., Geren, L., Hibdon, S., Kraut, J., Durham, B.. & Millett, F. (1994) Role of methionine 230 in intramolecular electron transfer between the oxyferryl heme and tryptophan 191 in cytochrome *c* peroxidase compound II. *Biochemistry* **33**, 8678-8685.

Lloyd, E., Hildebrand, D. P., Tu, K. M., & Mauk, A. G. (1995) Conversion of myoglobin into a reversible electron transfer protein that maintains bishistidine axial ligation. *J. Am. Chem. Soc.* **117**, 6434-6438.

Louie, G. V., & Brayer, G. D. (1990) High-resolution refinement of yeast iso-1-cytochrome *c* and comparisons with other eukaryotic cytochromes *c*. *J. Mol. Biol.* **214**, 527-555.

Lundquist, K., & Kirk, T. K. (1978) *De novo* synthesis and decomposition of veratryl alcohol by a lignin-degrading basidiomycete. *Phytochemistry* **17**, 1676.

Maccecchini, M. L., Rudin, Y., & Schatz, G. (1979) Transport of proteins across the mitochondrial outer membrane. A precursor form of the cytoplasmically made intermembrane enzyme cytochrome *c* peroxidase. *J. Biol. Chem.* **254**, 7468-7471.

MacDonald, M. J., Paterson, A. & Broda, P. (1984) Possible relationship between cyclic AMP and idiophasic metabolism in the white rot fungus *Phanerochaete chrysosporium*. *J. Bacteriol.* **160**, 470-472.

Maeda, Y. (1967) Mössbauer effect in peroxidase-hydrogen peroxide compounds. *Biochem. Biophys. Res. Commun.* **26**, 680-685.

Manthey, J. A., & Hager, L. P. (1981) Purification and properties of bromoperoxidase from *Penicillus capitatus*. *J. Biol. Chem.* **256**, 11232-11238.

Marcus, R. A., & Sutin, N. (1985) Electron transfers in chemistry and biology. *Biochim. Biophys. Acta* **811**, 265-322.

Marquez, L., Wariishi, H., Dunford, H. B., & Gold, M. H. (1988) Spectroscopic and kinetic properties of the oxidized intermediates of lignin peroxidase from *Phanerochaete chrysosporium*. *J. Biol. Chem.* **263**, 10549-10552.

Marston, F. A. (1986) The purification of eukaryotic polypeptides synthesized in *Escherichia coli*. *Biochem. J.* **240**, 1-12.

Mauk, M. R., Ferrer, J. C., & Mauk, A. G. (1994) Proton linkage in formation of the cytochrome c-cytochrome c peroxidase complex: electrostatic properties of the high- and low-affinity cytochrome binding sites on the peroxidase. *Biochemistry* **33**, 12609-12614.

Mauro, J. M., Fishel, L. A., Hazzard, J. T., Meyer, T. E., Tollin, G., Cusanovich, M. A., & Kraut, J. (1988) Tryptophan 191-phenylalanine, a proximal-side mutation in yeast cytochrome c peroxidase that strongly affects the kinetics of ferrocytochrome c oxidation. *Biochemistry* **27**, 6243-6256.

Mayfield, M. B., Godfrey, B. J., & Gold, M. H. (1994a) Characterization of the *mnp2* gene encoding manganese peroxidase isozyme 2 from the basidiomycete *Phanerochaete chrysosporium*. *Gene* **142**, 231-235.

Mayfield, M. B., Kishi, K., Alic, M., & Gold, M. H. (1994b) Homologous expression of recombinant manganese peroxidase in *Phanerochaete chrysosporium*. *Appl. Environ. Microbiol.* **60**, 4303-4309.

Mazza, G., Charles, C., Bouchet, M., Richard, J., & Raynaud, J. (1968) Isolation, purification and physico-chemical properties of turnip peroxidases. *Biochim. Biophys. Acta* **167**, 89-98.

McCathy, A. J. (1987) Lignocellulose-degrading actinomycetes. *FEMS Microbiol. Rev.* **46**, 145-163.

McLendon, G., Guarr, T., McGuire, M., Simolo, K., Strauch, S., & Taylor, K. (1985) Long distance electron transfer in polymers and proteins. *Coord. Chem. Rev.* **64**, 113-167.

McRee, D. E., Jensen, G. M., Fitzgerald, M. M., Siegel, H. A., & Goodin, D. B. (1994) Construction of a bisaquo heme enzyme and binding by exogenous ligands. *Proc. Natl. Acad. Sci. USA* **91**, 12847-12851.

Messerschmidt, A., & Huber, R. (1990) The blue oxidases, ascorbate oxidase, laccase and ceruloplasmin. Modelling and structural relationships. *Eur. J. Biochem.* **187**, 341-352.

Messerschmidt, A., Rossi, A., Ladenstein, R., Huber, R., Bolognesi, M., Gatti, G., Marchesini, A., Petruzelli, R., & Finazzi Agro, A. (1989) X-ray crystal structure of the blue oxidase ascorbate oxidase from zucchini. *J. Mol. Biol.* **205**, 513-529.

Meunier, B., Rodriguez-Lopez, J. N., Smith, A. T., Thorneley, R. N., & Rich, P. R. (1995) Laser photolysis behavior of ferrous horseradish peroxidase with carbon monoxide and cyanide: effects of mutations in the distal heme pocket. *Biochemistry* **34**, 14687-14692.

Miller, L. K. (1988) Baculoviruses as gene expression vectors. *Ann. Rev. Microbiol.* **42**, 177-199.

Miller, M. A., Coletta, M., Mauro, J. M., Putnam, L. D., Farnum, M. F., Kraut, J., & Traylor, T. G. (1990a) CO recombination in cytochrome *c* peroxidase: effect of the local heme environment on CO binding explored through site-directed mutagenesis. *Biochemistry* **29**, 1777-1791.

Miller, M. A., Han, G. W., & Kraut, J. (1994a) A cation binding motif stabilizes the compound I radical of cytochrome *c* peroxidase. *Proc. Natl. Acad. Sci. USA* **91**, 11118-11122.

Miller, M. A., Hazzard, J. T., Mauro, J. M., Edwards, S. L., Simons, P. C., Tollin, G., & Kraut, J. (1988) Site-directed mutagenesis of yeast cytochrome *c* peroxidase shows histidine 181 is not required for oxidation of ferrocytochrome *c*. *Biochemistry* **27**, 9081-9088.

Miller, M. A., Liu, R. Q., Hahm, S., Geren, L., Hibdon, S., Kraut, J., Durham, B., & Millett, F. (1994b) Interaction domain for the reaction of cytochrome *c* with the radical and the oxyferryl heme in cytochrome *c* peroxidase compound I. *Biochemistry* **33**, 8686-8693.

Miller, M. A., Mauro, J. M., Smulevich, G., Coletta, M., Kraut, J., & Traylor, T. G. (1990b) CO dissociation in cytochrome *c* peroxidase: site-directed mutagenesis shows that distal Arg 48 influences CO dissociation rates. *Biochemistry* **29**, 9978-9988.

Miller, M. A., Vitello, L., & Erman, J. E. (1995a) Regulation of interprotein electron transfer by Trp 191 of cytochrome *c* peroxidase. *Biochemistry* **34**, 12048-12058.

Miller, V. P., DePillis, G. D., Ferrer, J. C., Mauk, A. G., & Ortiz de Montellano, P. R. (1992) Monooxygenase activity of cytochrome *c* peroxidase. *J. Biol. Chem.* **267**, 8936-8942.

Miller, V. P., Goodin, D. B., Friedman, A. E., Hartmann, C., & Ortiz de Montellano, P. R. (1995b) Horseradish peroxidase Phe172→Tyr mutant. Sequential formation of compound I with a porphyrin radical cation and a protein radical. *J. Biol. Chem.* **270**, 18413-18419.

Mino, Y., Wariishi, H., Blackburn, N. J., Loehr, T. M., & Gold, M. H. (1988) Spectral characterization of manganese peroxidase, an extracellular heme enzyme from the lignin-degrading basidiomycete, *Phanerochaete chrysosporium*. *J. Biol. Chem.* **263**, 7029-7036.

Mliki, A., & Zimmermann, W. (1992) Purification and characterization of an intracellular peroxidase from *Streptomyces cyaneus*. *Appl. Environ. Microbiol.* **58**, 916-919.

Moen, M. A., & Hammel, K. E. (1994) Lipid peroxidation by the manganese peroxidase of *Phanerochaete chrysosporium* is the basis for phenanthrene oxidation by the intact fungus. *Appl. Environ. Microbiol.* **60**, 1956-1961.

Moench, S. J., Chroni, S., Lou, B. S., Erman, J. E., & Satterlee, J. D. (1992) Proton NMR comparison of noncovalent and covalently cross-linked complexes of cytochrome *c* peroxidase with horse, tuna, and yeast ferricytochromes c. *Biochemistry* **31**, 3661-3670.

Moench, S. J., Erman, J. E., & Satterlee, J. D. (1993) Species-specific differences in covalently crosslinked complexes of yeast cytochrome *c* peroxidase with horse and yeast iso-1 ferricytochromes *c*. *Int. J. Biochem.* **25**, 1335-1342.

Morishima, I., Kurono, M., & Shiro, Y. (1986) Presence of endogenous calcium ion in horseradish peroxidase. Elucidation of metal-binding site by substitutions of divalent and lanthanide ions for calcium and use of metal-induced NMR (^{1}H and ^{113}Cd) resonances. *J. Biol. Chem.* **261**, 9391-9399.

Morita, Y., Yamashita, H., Mikami, B., Iwamoto, H., Aibara, S., Terada, M., & Minami, J. (1988) Purification, crystallization, and characterization of peroxidase from *Coprinus cinereus*. *J. Biochem. Tokyo.* **103**, 693-699.

Morohoshi, N., & Haraguchi, T. (1987) Degradation of lignin by the extracellular enzymes of *Coriolus versicolor* VI. Degradation of syringylglycerol-β-syringyl ether by laccase III-c purified from laccase III by isoelectric focusing. *Mokuzai Gakkaishi* **33**, 495-502.

Morohoshi, N., Wariishi, N., Muraiso, C., Nagai, T., & Haraguchi, T. (1987) Degradation of lignin by the extracellular enzymes of *Coriolus versicolor*. IV. Properties of three laccase fractions fractionated from the extracellular enzymes. *Mokuzai Gakkaishi* **33**, 218-225.

Morris, D. R., & Hager, L. P. (1966) Chloroperoxidase. I. Isolation and properties of the crystalline glycoprotein. *J. Biol. Chem.* **241**, 1763-1768.

Morrison, M., & Schonbaum, G. R. (1976) Peroxidase-catalyzed halogenation. *Annu. Rev. Biochem.* **45**, 861-888.

Moss, T. H., Ehrenberg, A., & Bearden, A. J. (1969) Mössbauer spectroscopic evidence for the electronic configuration of iron in horseradish peroxidase and its peroxide derivatives. *Biochemistry* **8**, 4159-4162.

Muheim, A., Fiechter, A., Harvey, P. J., & Schoemaker, H. E. (1992) On the mechanism of oxidation of non-phenolic lignin model compounds by laccase-ABTS couple. *Holzforschung* **46**, 121-126.

Muheim, A., Waldner, R., Leisola, M. S. A., & Fiechter, A. (1990) An extracellular aryl-alcohol oxidase from the white-rot fungus *Bjerkandera adusta*. *Enzyme Microb. Technol.* **12**, 204-209.

Muheim, A., Waldner, R., Sanglard, D., Reiser, J., Schoemaker, H. E., & Leisola, M. S. (1991) Purification and properties of an aryl-alcohol dehydrogenase from the white-rot fungus *Phanerochaete chrysosporium*. *Eur. J. Biochem.* **195**, 369-375.

Musha, Y., & Goring, D. I. A. (1975) Distribution of syringyl and guiacyl moieties in hardwoods as indicated by ultraviolet microscopy. *Wood Sci. Technol.* **9**, 45-58.

Myers, D., & Palmer, G. (1985) Magnetic circular dichroism studies on the heme and tryptophan components of cytochrome c peroxidase. *J. Biol. Chem.* **260**, 3887-3890.

Nagano, S., Tanaka, M., Watanabe, Y., & Morishima, I. (1995) Putative hydrogen bond network in the heme distal site of horseradish peroxidase. *Biochem. Biophys. Res. Commun.* **207**, 417-423.

Nakatsubo, F., Kirk, T. K., Shimada, M., & Higuchi, T. (1981) Metabolism of a phenylcoumaran substructure lignin model compound in ligninolytic cultures of *Phanerochaete chrysosporium*. *Arch. Microbiol.* **128**, 416-420.

Nakatsubo, F., Reid, I. D., & Kirk, T. K. (1982) Incorporation of $^{18}O_2$ and absence of stereospecificity in primary product formation during fungal metabolism of a lignin model compound. *Biochim. Biophys. Acta* **719**, 284-291.

Newmyer, S. L., & Ortiz de Montellano, P. R. (1995) Horseradish peroxidase His-42 → Ala, His-42 → Val, and Phe-41 → Ala mutants. Histidine catalysis and control of substrate access to the heme iron. *J. Biol. Chem.* **270**, 19430-19438.

Nishida, A., & Eriksson, K.-E. (1987) Formation, purification and partial characterization of methanol oxidase, a H_2O_2-producing enzyme in *Phanerochaete chrysosporium*. *Biotechnol. Appl. Biochem.* **9**, 325-338.

Northrup, S. H., Boles, J. O., & Reynolds, J. C. (1988a) Brownian dynamics of cytochrome c and cytochrome c peroxidase association. *Science* **241**, 67-70.

Northrup, S. H., Luton, J. A., Boles, J. O., & Reynolds, J. C. (1988b) Brownian dynamics simulation of protein association. *J. Comput. Aided. Mol. Des.* **1**, 291-311.

Nozawa, T., Kobayashi, N., & Hatano, M. (1976) Magnetic circular dichroism studies on horseradish peroxidase. *Biochim. Biophys. Acta* **427**, 652-662.

Ogawa, S., Shiro, Y., & Morishima, I. (1979) Calcium binding by horseradish peroxidase C and the heme environmental structure. *Biochem. Biophys. Res. Commun.* **90**, 674-678.

Onuchic, J. N., & Beratan, D. N. (1990) A predictive theoretical model for electron tunneling pathways in proteins. *J. Chem. Phys.* **92**, 722-733.

Orth, A. B., Royse, D. J., & Tien, M. (1993) Ubiquity of lignin-degrading peroxidases among various wood-degrading fungi. *Appl. Environ. Microbiol.* **59**, 4017-4023.

Ortiz de Montellano, P. R. (1987) Control of the catalytic activity of prosthetic heme by the structure of hemoproteins. *Acc. Chem. Res.* **20**, 289-294.

Ortiz de Montellano, P. R. (1992) Catalytic sites of hemoprotein peroxidases. *Annu. Rev. Pharmacol. Toxicol.* **32**, 89-107.

Ortiz de Montellano, P. R., Choe, Y. S., DePillis, G., & Catalano, C. E. (1987) Structure-mechanism relationships in hemoproteins. Oxygenations catalyzed by chloroperoxidase and horseradish peroxidase. *J. Biol. Chem.* **262**, 11641-11646.

Ortiz de Montellano, P. R., David, S. K., Ator, M. A., & Tew, D. (1988) Mechanism-based inactivation of horseradish peroxidase by sodium azide. Formation of meso-azidoprotoporphyrin IX. *Biochemistry* **27**, 5470-5476.

Ozaki, S., & Ortiz de Montellano, P. R. (1994) Molecular engineering of horseradish peroxidase. Highly enantioselective sulfoxidation of aryl alkyl sulfides by the Phe-41→Leu mutant. *J. Am. Chem. Soc.* **116**, 4487-4488.

Palmer, G. (1985) The electron paramagnetic resonance of metalloproteins. *Biochem. Soc. Trans.* **13**, 548-560.

Pappa, H. S., Patterson, W. R., & Poulos, T. L. (1996) The homologous tryptophan critical for cytochrome *c* peroxidase function is not essential for ascorbate peroxidase activity. *J. Bioinorg. Chem.* **1**, 61-66.

Pappa, H. S., & Poulos, T. L. (1995) Site-specific cross-linking as a method for studying intramolecular electron transfer. *Biochemistry* **34**, 6573-6580.

Paszczynski, A., Huynh, V. B., & Crawford, R. (1986) Comparison of ligninase-I and peroxidase-M2 from the white-rot fungus *Phanerochaete chrysosporium*. *Arch. Biochem. Biophys.* **244**, 750-765.

Patterson, W. R., & Poulos, T. L. (1994) Characterization and crystallization of recombinant pea cytosolic ascorbate peroxidase. *J. Biol. Chem.* **269**, 17020-17024.

Patterson, W. R., & Poulos, T. L. (1995) Crystal structure of recombinant pea cytosolic ascorbate peroxidase. *Biochemistry* **34**, 4331-4341.

Patterson, W. R., Poulos, T. L., & Goodin, D. B. (1995) Identification of a porphyrin π cation radical in ascorbate peroxidase compound I. *Biochemistry* **34**, 4342-4345.

Pease, E. A., Andrawis, A., & Tien, M. (1989) Manganese-dependent peroxidase from *Phanerochaete chrysosporium*. Primary structure deduced from cDNA sequence. *J. Biol. Chem.* **264**, 13531-13535.

Pease, E. A., Aust, S. D., & Tien, M. (1991) Heterologous expression of active manganese peroxidase from *Phanerochaete chrysosporium* using the baculovirus expression system. *Biochem. Biophys. Res. Commun.* **179**, 897-903.

Peisach, J. (1975) An interim report on electronic control of oxygenation of heme proteins. *Ann. N.Y. Acad. Sci.* **244**, 187-203.

Pelletier, H., & Kraut, J. (1992) Crystal structure of a complex between electron transfer partners, cytochrome *c* peroxidase and cytochrome *c*. *Science* **258**, 1748-1755.

Penner-hahn, J. E., Eble, K. S., McMurry, T. J., Renner, M., Balch, A. L., Groves, J. T., Dawson, J. H., & Hodgson, K. O. (1986) Structural characterization of horseradish peroxidase using EXAF spectroscopy. Evidence for Fe(IV)=O ligation in compounds I and II. *J. Am. Chem. Soc.* **108**, 7819-7825.

Penner-Hahn, J. E., McMurry, T. J., Renner, M., Latos-Grazynsky, L., Eble, K. S., Davis, I. M., Balch, A. L., Groves, J. T., Dawson, J. H., & Hodgson, K. O. (1983) X-ray absorption spectroscopic studies of high valent iron porphyrins. Horseradish peroxidase compounds I and II and synthetic models. *J. Biol. Chem.* **258**, 12761-12764.

Périé, F. H., & Gold, M. H. (1991) Manganese regulation of manganese peroxidase expression and lignin degradation by the white rot fungus *Dichomitus squalens*. *Appl. Environ. Microbiol.* **57**, 2240-2245.

Périé, F. H., Sheng, D., & Gold, M. H. (1996) Purification and characterization of two manganese peroxidase isozymes from the white-rot basidiomycete *Dichomitus squalens*. *Biochim. Biophys. Acta* **1297**, 131-148.

Perry, C. R., Smith, M., Britnell, C. H., Wood, D. A., & Thurston, C. F. (1993) The structure of laccase protein and its synthesis by the commercial mushroom *Agaricus bisporus*. *J. Gen. Microbiol.* **139**, 1209-1218.

Petersen, J. F. W., Kadziola, A., & Larsen, S. (1994) Three-dimential structure of a recombinant peroxidase from *Coprinus cinereus* at 2.6 Å resolution. *FEBS Lett.* **339**, 291-296.

Petersen, J. F., Tams, J. W., Vind, J., Svensson, A., Dalboge, H., Welinder, K. G., & Larsen, S. (1993) Crystallization and X-ray diffraction analysis of recombinant *Coprinus cinereus* peroxidase. *J. Mol. Biol.* **232**, 989-991.

Piontek, K., Glumoff, T., & Winterhalter, K. (1993) Low pH crystal structure of glycosylated lignin peroxidase from *Phanerochaete chrysosporium* at 2.5 Å resolution. *FEBS Lett.* **315**, 119-124.

Poulos, T. L., Edwards, S. L., Wariishi, H., & Gold, M. H. (1993) Crystallographic refinement of lignin peroxidase at 2 Å. *J. Biol. Chem.* **268**, 4429-4440.

Poulos, T. L., & Fenna, R. E. (1994) Peroxidases: structure, function, and engineering. *Met. Biol.* **30**, 25-75.

Poulos, T. L., & Finzel, B. C. (1984) Heme enzyme structure and function. In *Peptide and Protein Reviews* (Hearn, M. T. W., Ed.) pp 115-171, Marcel Dekker, Inc., New York.

Poulos, T. L., Freer, S. T., Alden, R. A., Edwards, S. L., Skogland, U., Takio, K., Eriksson, B., Xuong, N., Yonetani, T., & Kraut, J. (1980) The crystal structure of cytochrome *c* peroxidase. *J. Biol. Chem.* **255**, 575-580.

Poulos, T. L., & Kraut, J. (1980a) A hypothetical model of the cytochrome *c* peroxidase. cytochrome *c* electron transfer complex. *J. Biol. Chem.* **255**, 10322-10330.

Poulos, T. L., & Kraut, J. (1980b) The stereochemistry of peroxidase catalysis. *J. Biol. Chem.* **255**, 8199-8205.

Pribnow, D., Mayfield, M. B., Nipper, V. J., Brown, J. A. & Gold, M. H. (1989). Characterization of a cDNA encoding a manganese peroxidase, from the lignin-degrading basidiomycete *Phanerochaete chrysosporium*. *J. Biol. Chem.* **264**, 5036-5040.

Punt, P. J., Dingemanse, M. A., Jacobs-Meijsing, B. J. M., Pouwels, P. H., & van den Hondel, C. A. M. J. J. (1988) Isolation and characterization of the glyceraldehyde-3-phosphate dehydrogenase gene of *Aspergillus nidulans*. *Gene* **69**, 49-57.

Punt, P. J., Zegers, N. D., Busscher, M., Pouwels, P. H., & van den Hondel, C. A. M. J. J. (1991) Intracellular and extracellular production of proteins in *Aspergillus* under the control of expression signals of the highly expressed *Aspergillus nidulans gpdA* gene. *J. Bacteriol.* **17**, 19-34.

Ramachandra, M., Crawford, D. L., & Hertel, G. (1988) Characterization of an extracellular lignin peroxidase of the lignocellulolytic actinomycete *Streptomyces viridosporus*. *Appl. Environ. Microbiol.* **54**, 3057-3063.

Rayner, A. D. M., & Boddy, L. (1988) *Fungal decomposition of wood. Its bology and ecology*. John Wiley & Sons, Chichester.

Reid, L. S., Lim, A. R., & Mauk, A. G. (1986) Role of heme vinyl groups in cytochrome b_5 electron transfer. *J. Am. Chem. Soc.* **108**, 8197-8201.

Reid, L. S., Mauk, M. R., & Mauk, A. G. (1984) Role of heme propionate groups in cytochrome b_5 electron transfer. *J. Am. Chem. Soc.* **106**, 2182-2185.

Reinhammar, B. (1984) Laccase. In *Copper Proteins and Copper Enzymes* (Lontie, R., Ed.) Vol. 3, pp 1-36, CRC Press, Boca Raton, FL.

Renganathan, V., & Gold, M. H. (1986) Spectral characterizaton of the oxided state of lignin peroxidase, an extracullar heme enzyme from the white-rot basidiomycete *Phanerochaete chrysosporium*. *Biochemistry* **25**, 1626-1631.

Renganathan, V., Miki, K., & Gold, M. H. (1985) Multiple molecular forms of diarylpropane oxygenase, an H_2O_2-requiring, lignin-degrading enzyme from *Phanerochaete chrysosporium*. *Arch. Biochem. Biophys.* **241**, 304-314.

Ritch, T. G., Jr., & Gold, M. H. (1992) Characterization of a highly expressed lignin peroxidase-encoding gene from the basidiomycete *Phanerochaete chrysosporium*. *Gene* **118**, 73-80.

Ritch, T. G., Jr., Nipper, V. J., Akileswaran, L., Smith, A. J., Pribnow, D. G., & Gold, M. H. (1991) Lignin peroxidase from the basidiomycete *Phanerochaete chrysosporium* is synthesized as a preproenzyme. *Gene* **107**, 119-126.

Roberts, J. E., Hoffman, B. M., Rutter, R., & Hager, L. P. (1981) [17]O ENDOR of horseradish peroxidase compound I. *J. Am. Chem. Soc.* **103**, 7654-7656.

Rodriguez-Lopez, J. N., Smith, A. T., & Thorneley, R. N. F. (1996) Role of arginine 38 in horseradish peroxidase. A critical residue for substrate binding and catalysis. *J. Biol. Chem.* **271**, 4023-4030.

Rodríguez-Maranón, M. J., Mercier, D., van Huystee, R. B., & Stillman, M. J. (1994) Analysis of the optical absorption and magnetic circular dichroism spectra of peanut peroxidase: electronic structure of a peroxidase with biochemical properties similar to those of horseradish peroxidase. *Biochem. J.* **301**, 335-341.

Roe, J. A., & Goodin, D. B. (1993) Enhanced oxidation of aniline derivatives by two mutants of cytochrome c peroxidase at tryptophan 51. *J. Biol. Chem.* **268**, 20037-20045.

Sakurada, J., Takahashi, S., & Hosoya, T. (1986) Nuclear magnetic resonance studies on the spatial relationship of aromatic donor molecules to the heme iron of horseradish peroxidase. *J. Biol. Chem.* **261**, 9657-9662.

Saloheimo, M., Niku-Paavola, M.-L., & Knowles, J. K. C. (1991) Isolation and structural analysis of the laccase gene from the lignin-degrading fungus *Phlebia radiata*. *J. Gen. Microbiol.* **137**, 1537-1544.

Sambrook, S. J., Fritch, E. F., & Maniatis, T. (1989) *Molecular cloning: A laboratory manual*, Cold Spring Harbor Laboratory Press, Cold Spring Harbor, New York.

Samejima, M., & Eriksson, K.-E. (1992) A comparison of the catalytic properties of cellobiose:quinone oxidoreductase and cellobiose oxidase from *Phanerochaete chrysosporium*. *Eur. J. Biochem.* **207**, 103-107.

Samejima, M., Phillips, R. S., & Eriksson, K.-E. (1992) Cellobiose oxidase from *Phanerochaete chrysosporium*. Stopped-flow spectrophotometric analysis of pH-dependent reduction. *FEBS Lett.* **306**, 165-168.

Sanders, S. A., Bray, R. C., & Smith, A. T. (1994) pH-dependent properties of a mutant horseradish peroxidase isoenzyme C in which Arg38 has been replaced with lysine. *Eur. J. Biochem.* **224**, 1029-1037.

Sanger, F., Nicklen, S., & Coulson, A. R. (1977) DNA sequencing with chain-terminating inhibitors. *Proc. Natl. Acad. Sci. USA* **74**, 5463-5467.

Sarkanen, K. V., & Ludwig, C. H. (1971) *Lignins. Occurrence, Formation, Structure, and Reactions*, Wiley-Interscience, New York.

Satterlee, J. D., Alam, S. L., Yi, Q., Erman, J. E., Canstaninidis, I., Russell, D. J., & Moench, S. J. (1993) In *Biological Magnetic Resonance* (Berliner, L. J., & Reuben, J., Eds.) Vol. 12, pp 275-298, Plenum Press, New York.

Satterlee, J. D., Alam, S. L., Mauro, J. M., Erman, J. E., & Poulos, T. L. (1994) The effect of the Asn82→Asp mutation in yeast cytochrome c peroxidase studied by proton NMR spectroscopy. *Eur. J. Biochem.* **224**, 81-87.

Satterlee, J. D., Erman, J. E., Mauro, J. M., & Kraut, J. (1990) Comparative proton NMR analysis of wild-type cytochrome c peroxidase from yeast, the recombinant enzyme from *Escherichia coli*, and an Asp-235-Asn-235 mutant. *Biochemistry* **29**, 8797-8804.

Schellenberg, K. A., & Hellerman, L. (1958) Oxidation of reduced diphosphopyridine nucleotide. *J. Biol. Chem.* **231**, 547-556.

Schmidhalter, D. R., & Canevascini, G. (1992) Characterization of the cellulolytic enzyme system from the brown-rot fungus *Coniophora puteana. Appl. Microbiol. Biotechnol.* **37**, 431-436.

Schoemaker, H. E. (1990) On the chemistry of lignin biodegration. *Recl. Trav. Chim. Pays-Bas* **109**, 255-272.

Schoemaker, H. E., Meijer, E. M., Leisola, M., S. A., Haemmerli, S. D., Waldner, R., Sanglard, D., & Schmidt, H. W. H. (1989) Oxidation and reduction in lignin biodegradation. *ACS Symp. Ser.* **399**, 454-471.

Schuller, D. J., Ban, N., van Huystee, R. B., McPherson, A., & Poulos, T. L. (1996) The crystal structure of peanut peroxidase. *Structure* **4**, 311-321.

Schultz, C. E., Rutter, R., Sage, J. T., Debrunner, P. G., & Hager, L. P. (1984) Mössbauer and electron paramagnetic resonance studies of horseradish peroxidase and its catalytic intermediates. *Biochemistry* **23**, 4743-4754.

Shahangian, S., & Hager, L. P. (1981) The reaction of chloroperoxidase with chlorite and chlorine dioxide. *J. Biol. Chem.* **256**, 6034-6040.

Shiro, Y., Kurono, M., & Morishima, I. (1986) Presence of endogenous calcium ion and its functional and structural regulation in horseradish peroxidase. *J. Biol. Chem.* **261**, 9382-9390.

Sitter, A. J., Reczek, C. M., & Terner, J. (1985) Heme-linked ionization of horseradish peroxidase compound II monitored by the resonance Raman Fe(IV) stretching vibration. *J. Biol. Chem.* **260**, 7515-7522.

Sivaraja, M., Goodin, D. B., Smith, M., & Hoffman, B. M. (1989) Identification by ENDOR of Trp191 as the free-radical site in cytochrome *c* peroxidase compound ES. *Science* **245**, 738-740.

Smith, A. T., Du, P., & Loew, G. H. (1995) Homology modeling of horseradish peroxidase. In *Nuclear Magnetic Resonance of Paramagnetic Macromolecules* (La Mar, G. N., Ed.) pp 75-93, Kluwer Academic Publishers, Dordrecht, The Netherlands.

Smith, A. T., Sanders, S. A., Greschik, H., Thorneley, R. N. F., Burke, J. F., & Bray, R. C. (1992a) Probing the mechanism of horseradish peroxidase by site-directed mutagenesis. *Biochem. Soc. Trans.* **20**, 340-345.

Smith, A. T., Sanders, S. A., Thorneley, R. N., Burke, J. F. & Bray, R. R. (1992b) Characterisation of a haem active-site mutant of horseradish peroxidase, Phe41→Val, with altered reactivity towards hydrogen peroxide and reducing substrates. *Eur. J. Biochem.* **207**, 507-519.

Smith, A. T., Santama, N., Dacey, S., Edwards, M., Bray, R. C., Thorneley, R. N., & Burke, J. F. (1990) Expression of a synthetic gene for horseradish peroxidase C in *Escherichia coli* and folding and activation of the recombinant enzyme with Ca(II) and heme. *J. Biol. Chem.* **265**, 13335-13343.

Smith, G. E., Summers, M. D., & Fraser, M. J. (1983) Production of human β interferon in insect cells infected with a baculovirus expression vector. *Mol. Cell. Biol.* **3**, 2156-2165.

Smith, D. W., & Williams, R. J. (1968) Analysis of the visible spectra of some sperm-whale ferrimyoglobin derivatives. *Biochem. J.* **110**, 297-301.

Smulevich, G., Feis, A., Focardi, C., Tams, J., & Welinder, K. G. (1994a) Resonance Raman study of the active site of *Coprinus cinereus* peroxidase. *Biochemistry* **33**, 15425-15432.

Smulevich, G., Mauro, J. M., Fishel, L. A., English, A. M., Kraut, J., & Spiro, T. G. (1988a) Cytochrome *c* peroxidase mutant active site structures probed by resonance Raman and infrared signatures of the CO adducts. *Biochemistry* **27**, 5486-5492.

Smulevich, G., Mauro, J. M., Fishel, L. A., English, A. M., Kraut, J., & Spiro, T. G. (1988b) Heme pocket interactions in cytochrome *c* peroxidase studied by site-directed mutagenesis and resonance Raman spectroscopy. *Biochemistry* **27**, 5477-5485.

Smulevich, G., Miller, M. A., Kraut, J., & Spiro, T. G. (1991) Conformational change and histidine control of heme chemistry in cytochrome *c* peroxidase: resonance Raman evidence from Leu-52 and Gly-181 mutants of cytochrome *c* peroxidase. *Biochemistry* **30**, 9546-9558.

Smulevich, G., Neri, F., Marzocchi, M. P., & Welinder, K. G. (1996) Versatility of heme coordination demonstrated in a fungal peroxidase. Absorption and resonance Raman studies of *Coprinus cinerus* peroxidase and the Asp245→Asn mutant at various pH values. *Biochemistry* **35**, 10576-10585.

Smulevich, G., Neri, F., Willemsen, O., Choudhury, K., Marzocchi, M. P., & Poulos, T. L. (1995) Effect of the His175→Glu mutation on the heme pocket architecture of cytochrome *c* peroxidase. *Biochemistry* **34**, 13485-13490.

Smulevich, G., Paoli, M., Burke, J. F., Sanders, S. A., Thorneley, R. N., & Smith, A. T. (1994b) Characterization of recombinant horseradish peroxidase C and three site-directed mutants, F41V, F41W, and R38K, by resonance Raman spectroscopy. *Biochemistry* **33**, 7398-7407.

Smulevich, G., Wang, Y., Mauro, J. M., Wang, J. M., Fishel, L. A., Kraut, J., & Spiro, T. G. (1990) Single-crystal resonance Raman spectroscopy of site-directed mutants of cytochrome *c* peroxidase. *Biochemistry* **29**, 7174-7180.

Spiro, T. G., Ed. (1988) *Biological Applications of Raman Spectroscopy, Vol. III, Resonance Raman Spectra of Hemes and Metalloproteins*, Wiley, New York.

Stemp, E. D., & Hoffman, B. M. (1993) Cytochrome *c* peroxidase binds two molecules of cytochrome *c*: evidence for a low-affinity, electron-transfer-active site on cytochrome *c* peroxidase. *Biochemistry* **32**, 10848-10865.

Stewart, P., Kersten, P., Vanden-Wymelenberg, A., Gaskell, J., & Cullen, D. (1992) Lignin peroxidase gene family of *Phanerochaete chrysosporium*: complex regulation by carbon and nitrogen limitation and identification of a second dimorphic chromosome. *J. Bacteriol.* **174**, 5036-5042.

Stewart, P., Whitwam, R. E., Kersten, P. J., Cullen, D., & Tien, M. (1996) Efficient expression of a *Phanerochaete chrysosporium* manganese peroxidase gene in *Aspergillus oryzae*. *Appl. Environ. Microbiol.* **62**, 860-864.

Studier, F. W., Rosenberg, A. H., Dunn, J. J., & Dubendorff, J. W. (1990) Use of T7 RNA polymerase to direct expression of cloned genes. *Methods Enzymol.* **185**, 60-76.

Summers, F. E., & Erman, J. E. (1988) Reduction of cytochrome *c* peroxidase compounds I and II by ferrocytochrome *c*. A stopped-flow kinetic investigation. *J. Biol. Chem.* **263**, 14267-14275.

Sun, J., Loehr, T. M., Wilks, A., & Ortiz de Montellano, P. R. (1994) Identification of histidine 25 as the heme ligand in human liver heme oxygenase. *Biochemistry* **33**, 13734-13740.

Sun, J., Wilks, A., Ortiz de Montellano, P. R., & Loehr, T. M. (1993) Resonance Raman and EPR spectroscopic studies on heme-heme oxygenase complexes. *Biochemistry* **32**, 14151-14157.

Sundaramoorthy, M., Choudhury, K., Edwards, S. L., & Poulos, T. L. (1991) Crystal structure and preliminary functional analysis of the cytochrome *c* peroxidase His175Gln proximal ligand mutant. *J. Am. Chem. Soc.* **113**, 7755-7757.

Sundaramoorthy, M., Kishi, K., Gold, M. H., & Poulos, T. L. (1994a) Preliminary crystallographic analysis of manganese peroxidase from *Phanerochaete chrysosporium*. *J. Mol. Biol.* **238**, 845-858.

Sundaramoorthy, M., Kishi, K., Gold, M. H., & Poulos, T. L. (1994b) The crystal structure of manganese peroxidase from *Phanerochaete chrysosporium* at 2.06-Å resolution. *J. Biol. Chem.* **269**, 32759-32767.

Sundaramoorthy, M., Kishi, K., Gold, M. H., & Poulos, T. L. Probing the manganese binding site in manganese peroxidase. in preparation.

Sundaramoorthy, M., Terner, J., & Poulos, T. L. (1995) The crystal structure of chloroperoxidase: a heme peroxidase-cytochrome P450 functional hybrid. *Structure* **3**, 1367-1377.

Sutherland, G. R., Khindaria, A., & Aust, S. D. (1996) The effect of veratryl alcohol on manganese oxidation by lignin peroxidase. *Arch. Biochem. Biophys.* **327**, 20-26.

Sutherland, G. R., Khindaria, A., Chung, N., & Aust, S. D. (1995) The effect of manganese on the oxidation of chemicals by lignin peroxidase. *Biochemistry* **34**, 12624-12629.

Tai, D.-S., Terazawa, M., Chen, C.-L., & Chang, H.-M. (1990) Lignin biodegradation products from birch wood by *Phanerochaete chrysosporium*. *Holzforschung* **44**, 185-190.

Takano, T., & Dickerson, R. E. (1981a) Conformation change of cytochrome *c*. I. Ferrocytochrome *c* structure refined at 1.5 Å resolution. *J. Mol. Biol.* **153**, 79-94.

Takano, T., & Dickerson, R. E. (1981b) Conformation change of cytochrome *c*. II. Ferricytochrome *c* refinement at 1.8 Å and comparison with the ferrocytochrome structure. *J. Mol. Biol.* **153**, 95-115.

Takao, S. (1965) Organic acid production by basidiomycetes. I. Screening of acid-producing strains. *Appl. Microbiol.* **13**, 732-737.

Tams, J. W., Vind, J., & Welinder, K. G. (1993) Site directed mutagenesis of *Coprinus cinerus* peroxidase at the predicted aromatic substrate binding site. In *Plant Peroxidases: Biochemistry and Physiology* (Welinder, K. G., Rasmussen, S. K., Pennel, C., & Greppin, H., Eds.) pp 143-148, University of Geneva, Switzerland.

Tamura, M., Asakura, T., & Yonetani, T. (1972) Heme-modification studies on horseradish peroxidase. *Biochim. Biophys. Acta* **268**, 292-304.

Taube, H. (1948) Catalysis by manganic ion of the reaction of bromine and oxalic acid. Stability of manganic ion complexes. *J. Am. Chem. Soc.* **70**, 3928-3935.

Terner, J., Sitter, A. J., & Reczek, C. M. (1985) Resonance Raman spectroscopic characterizations of horseradish peroxidase. Observation of the Fe(IV)=O stretching vibration of compound II. *Biochim. Biophys. Acta* **828**, 73-80.

Thomas, J. A., Morris, D. R., & Hager, L. P. (1970) Chloroperoxidase. VII. Classical peroxidatic, catalatic, and halogenating forms of the enzyme. *J. Biol. Chem.* **245**, 3129-3134.

Tien, M. (1987) Properties of ligninase from *Phanerochaete chrysosporium* and their possible applications. *Crit. Rev. Microbiol.* **15**, 141-168.

Tien, M., & Kirk, T. K. (1983) Lignin-degrading enzyme from the hymenomycete *Phanerochaete chrysosporium* burds. *Science* **221**, 661-663.

Tien, M., & Kirk, T. K. (1984) Lignin-degrading enzyme from *Phanerochaete chrysosporium*: purification, characterization, and catalytic properties of a unique H_2O_2-requiring oxygenase. *Proc. Natl. Acad. Sci. USA* **81**, 2280-2284.

Trojanowski, J., & Leonowicz, A. (1969) The biodeterioration of lignin by fungi. *Microbios.* **3**, 247-251.

Tuor, U., Wariishi, H., Schoemaker, H. E., & Gold, M. H. (1992) Oxidation of phenolic arylglycerol β-aryl ether lignin model compounds by manganese peroxidase from *Phanerochaete chrysosporium*: oxidative cleavage of an α-carbonyl model compound. *Biochemistry* **31**, 4986-4995.

Turano, P., Ferrer, J. C., Cheesman, M. R., Thomson, A. J., Banci, L., Bertini, I., & Mauk, A. G. (1995) pH, electrolyte, and substrate-linked variation in active site structure of the Trp51Ala variant of cytochrome *c* peroxidase. *Biochemistry* **34**, 13895-13905.

Valli, K., Brock, B. J., Joshi, D. K., & Gold, M. H. (1992a) Degradation of 2,4-dinitrotoluene by the lignin-degrading fungus *Phanerochaete chrysosporium*. *Appl. Environ. Microbiol.* **58**, 221-228.

Valli, K., & Gold, M. H. (1991) Degradation of 2,4-dichlorophenol by the lignin-degrading fungus *Phanerochaete chrysosporium*. *J. Bacteriol.* **173**, 345-352.

Valli, K., Wariishi, H., & Gold, M. H. (1992b) Degradation of 2,7-dichlorodibenzo-*p*-dioxin by the lignin-degrading basidiomycete *Phanerochaete chrysosporium*. *J. Bacteriol.* **174**, 2131-2137.

Van Wyke Coelingh, K. L., Murphy, B. R., Collins, P. L., Lebacq Verheyden, A., & Battey, J. F. (1987) Expression of biologically active and antigenically authentic parainfluenza type 3 virus hemagglutinin-neuraminidase glycoprotein by a recombinant baculovirus. *Virology* **160**, 465-472.

Veitch, N. C. (1995) Aromatic donor molecule binding sites of haem peroxidases. *Biochem. Soc. Trans.* **23**, 232-240.

Veitch, N. C., Tams, J. W., Vind, J., Dalbøge, H., & Welinder, K. G. (1994) NMR studies of recombinant *Coprinus* peroxidase and three site-directed mutants. Implications for peroxidase substrate binding. *Eur. J. Biochem.* **222**, 909-918.

Veitch, N. C., & Williams, R. J. P. (1990) Two-dimensional ^{1}H-NMR studies of horseradish peroxidase C and its interaction with indole-3-propionic acid. *Eur. J. Biochem.* **189**, 351-362.

Veitch, N. C., & Williams, R. J. P. (1991) Two-dimensional proton nuclear magnetic resonance studies of plant peroxidase interactions with aromatic donor molecules. In *Biochemical, Molecular and Physiological Aspects of Plant Peroxidases* (Lobarzewski, J., Greppin, H., Penel, C., & Gaspar, T., Eds.) pp 99-109, University of Geneva, Geneva.

Veitch, N. C., & Williams, R. J. P. (1995) The use of methyl-substituted benzhydroxamic acids as structural probes of peroxidase substrate binding. *Eur. J. Biochem.* **229**, 629-640.

Veitch, N. C., Williams, R. J. P., Bone, N. M., Burke, J. F., & Smith, A. T. (1995) Solution characterisation by NMR spectroscopy of two horseradish peroxidase isoenzyme C mutants with alanine replacing either Phe142 or Phe143. *Eur. J. Biochem.* **233**, 650-658.

Veitch, N. C., Williams, R. J. P., Bray, R. C., Burke, J. F., Sanders, S. A., Thorneley, R. N., & Smith, A. T. (1992a) Structural studies by proton-NMR spectroscopy of plant horseradish peroxidase C, the wild-type recombinant protein from *Escherichia coli* and two protein variants, Phe41-Val and Arg38-Lys. *Eur. J. Biochem.* **207**, 521-531.

Veitch, N. C., Williams, R. J. P., Smith, A. T., Sanders, S. A., Thorneley, R. N., Bray, R. C., & Burke, J. F. (1992b) Investigation of native and mutant plant peroxidases by NMR spectroscopy. *Biochem. Soc. Trans.* **20**, 114S.

Vickery, L., Nozawa, T., & Sauer, K. (1976a) Magnetic circular dichroism studies of myoglobin complexes. Correlations with heme spin state and axial ligation. *J. Am. Chem. Soc.* **98**, 343-350.

Vickery, L., Nozawa, T., & Sauer, K. (1976b) Magnetic circular dichroism studies of low-spin cytochromes. Temperature dependence and effects of axial coordination on the spectra of cytochrome c and cytochrome b_5. *J. Am. Chem. Soc.* **98**, 351-357.

Vicuna, R. (1988) Bacterial degradation of lignin. *Enzyme Microb. Technol.* **10**, 645-655.

Vitello, L. B., Erman, J. E., Mauro, J. M., & Kraut, J. (1990) Characterization of the hydrogen peroxide-enzyme reaction for two cytochrome *c* peroxidase mutants. *Biochim. Biophys. Acta* **1038**, 90-97.

Vitello, L. B., Erman, J. E., Miller, M. A., Mauro, J. M., & Kraut, J. (1992) Effect of Asp-235→Asn substitution on the absorption spectrum and hydrogen peroxide reactivity of cytochrome *c* peroxidase. *Biochemistry* **31**, 11524-11535.

Vitello, L. B., Erman, J. E., Miller, M. A., Wang, J., & Kraut, J. (1993) Effect of arginine-48 replacement on the reaction between cytochrome *c* peroxidase and hydrogen peroxide. *Biochemistry* **32**, 9807-9818.

Waldner, R., Leisola, M. S. A., & Fiechter, A. (1988) Comparison of ligninolytic activites of selected white-rot fungi. *Appl. Microbiol. Biotechnol.* **29**, 400-407.

Wallin, S. A., Stemp, E. D. A., Everest, A. M., Nocek, J. M., Netzel, T. L., & Hoffman, B. M. (1991) Multiphasic intracomplex electron transfer from cytochrome *c* to Zn cytochrome *c* peroxidase: conformational control of reactivity. *J. Am. Chem. Soc.* **113**, 1842-1844.

Wang, J. M., Mauro, M., Edwards, S. L., Oatley, S. J., Fishel, L. A., Ashford, V. A., Xuong, N. H., & Kraut, J. (1990a) X-ray structures of recombinant yeast cytochrome *c* peroxidase and three heme-cleft mutants prepared by site-directed mutagenesis. *Biochemistry* **29**, 7160-7173.

Wang, Y., & Margoliash, E. (1995) Enzymic activities of covalent 1:1 complexes of cytochrome *c* and cytochrome *c* peroxidase. *Biochemistry* **34**, 1948-1958.

Wang, Z. M., Bleakley, B. H., Crawford, D. L., Hertel, G., & Rafii, F. (1990b) Cloning and expression of a lignin peroxidase gene from *Streptomyces viridosporus* in *Streptomyces lividans*. *J. Biotechnol.* **13**, 131-144.

Wariishi, H., Akileswaran, L., & Gold, M. H. (1988) Manganese peroxidase from the basidiomycete *Phanerochaete chrysosporium*: spectral characterization of the oxidized states and the catalytic cycle. *Biochemistry* **27**, 5365-5370.

Wariishi, H., Dunford, H. B., MacDonald, I. D., & Gold, M. H. (1989a) Manganese peroxidase from the lignin-degrading basidiomycete *Phanerochaete chrysosporium*. Transient state kinetics and reaction mechanism. *J. Biol. Chem.* **264**, 3335-3340.

Wariishi, H., Huang, J., Dunford, H. B., & Gold, M. H. (1991a) Reactions of lignin peroxidase compounds I and II with veratryl alcohol. Transient-state kinetic characterization. *J. Biol. Chem.* **266**, 20694-20699.

Wariishi, H., Morohoshi, N. B., & Haraguchi, T. (1987) Degradation of lignin by the extracellular enzymes of *Coriolus versicolor* VII. Effective degradation of syringyl type β-aryl ether lignin model compound by laccase III. *Mokuzai Gakkaishi* **33**, 892-898.

Wariishi, H., Valli, K., & Gold, M. H. (1991b) *In vitro* depolymerization of lignin by manganese peroxidase of *Phanerochaete chrysosporium*. *Biochem. Biophys. Res. Commun.* **176**, 269-275.

Wariishi, H., Valli, K., & Gold, M. H. (1992) Manganese(II) oxidation by manganese peroxidase from the basidiomycete *Phanerochaete chrysosporium*. Kinetic mechanism and role of chelators. *J. Biol. Chem.* **267**, 23688-23695.

Wariishi, H., Valli, K., Renganathan, V., & Gold, M. H. (1989b) Thiol-mediated oxidation of nonphenolic lignin model compounds by manganese peroxidase of *Phanerochaete chrysosporium*. *J. Biol. Chem.* **264**, 14185-14191.

Weinstein, D. A., Krisnangkura, K., Mayfield, M. B., & Gold, M. H. (1980) Metabolism of radiolabeled β-guaiacyl ether-linked lignin dimeric compounds by *Phanerochaete chrysosporium*. *Appl. Environ. Microbiol.* **39**, 535-540.

Welinder, K. G. (1976) Covalent structure of the glycoprotein horseradish peroxidase (EC 1.11.1.7). *FEBS Lett.* **72**, 19-23.

Welinder, K. G. (1985) Plant peroxidases. Their primary, secondary and tertiary structures, and relation to cytochrome *c* peroxidase. *Eur. J. Biochem.* **151**, 497-504.

Welinder, K. G. (1992) Superfamily of plant, fungal and bacterial peroxidases. *Curr. Opin. Struct. Biol.* **2**, 388-393.

Welinder, K. G., Bjornholm, B., & Dunford, H. B. (1995) Functions of electrostatic potentials and conserved distal and proximal His-Asp H-bonding networks in haem peroxidases. *Biochem. Soc. Trans.* **23**, 257-262.

Welinder, K. G., & Nørskov-Lauritsen, L. (1986) Structure of plant peroxidases. Preliminary fitting into the molecular model of yeast cytochrome *c* peroxidase. In *Molecular and Physiological Aspects of Plant Peroxidases* (Greppin, H., Penel, C., & Gaspar, T., Eds.) pp 61-70, University of Geneva, Switzerland.

Wessel, J. G. H. (1987) Growth and development in a model basidiomycete: *Schizophyllum commune*. In *Lignin Enzymic and Microbial Degradation* (Odier, E., Ed.) pp 19-42, INRA Publ., Paris.

Westermark, U., & Eriksson, K.-E. (1974a) Carbohydrate-dependent enzyme quinone reduction during lignin degradation. *Acta Chem. Scand.* **B28**, 204-208.

Westermark, U., & Eriksson, K.-E. (1974b) Cellobiose:quinone oxidoreductase, a new wood-degrading enzyme from white-rot fungi. *Acta Chem. Scand.* **B28**, 209-214.

Whittaker, M. M., Kersten, P. J., Nakamura, N., Sanders Loehr, J., Schweizer, E. S., & Whittaker, J. W. (1996) Glyoxal oxidase from *Phanerochaete chrysosporium* is a new radical-copper oxidase. *J. Biol. Chem.* **271**, 681-687.

Whittaker, M. M. & Whittaker, J. W. (1988). The active site of galactose oxidase. *J. Biol. Chem.* **263**, 6074-6080.

Whitwam, R. E., Gazarian, I. G., & Tien, M. (1995) Expression of fungal Mn peroxidase in *E. coli* and refolding to yield active enzyme. *Biochem. Biophys. Res. Commun.* **216**, 1013-1017.

Wilcox, S. K., Jensen, G. M., Fitzgerald, M. M., McRee, D. E., & Goodin, D. B. (1996) Altering substrate specificity at the heme edge of cytochrome *c* peroxidase. *Biochemistry* **35**, 4858-4866.

Williams, P. G., & Stewart, P. R. (1976) The intramitochondrial location of cytochrome *c* peroxidase in wild-type and petite *Saccharomyces cerevisiae*. *Arch. Microbiol.* **107**, 63-70.

Wood, D. A. (1980) Production, purification and properties of extracellular laccase of *Agaricus bisporus*. *J. Gen. Microbiol.* **117**, 327-338.

Yang, S. F. (1967) Biosynthesis of ethylene. Ethylene formation from methional by horseradish peroxidase. *Arch. Biochem. Biophys.* **122**, 481-487.

Yonetani, T. (1967) Studies on cytochrome *c* peroxidase. X. Crystalline apo-and reconstituted holoenzymes. *J. Biol. Chem.* **242**, 5008-5013.

Yonetani, T. (1976) Cytochrome *c* peroxidase. In *The Enzymes* (Boyer, P. D., Ed.) Vol. 13, pp 345-361, Academic Press, Orland, FL.

Yonetani, T., & Anni, H. (1987) Yeast cytochrome *c* peroxidase. Coordination and spin states of heme prosthetic group. *J. Biol. Chem.* **262**, 9547-9554

Yonetani, T., & Ray, G. S. (1966) Studies on cytochrome *c* peroxidase. III. Kinetics of the peroxidatic oxidation of ferrocytochrome *c* catalyzed by cytochrome *c* peroxidase. *J. Biol. Chem.* **241**, 700-706.

Yonetani, T., & Schleyer, H. (1966) Studies on cytochrome c peroxidase. VII. Electron paramagnetic resonance absorptions of the enzyme and complex ES in dissolved and crystalline forms. *J. Biol. Chem.* **241**, 3240-3243.

Zhou, J. S., & Hoffman, B. M. (1994) Stern-volmer in reverse: 2:1 stoichiometry of the cytochrome c-cytochrome c peroxidase electron-transfer complex. *Science* **265**, 1693-1696.

Zhou, J. S., Nocek, J. M., DeVan, M. L., & Hoffman, B. M. (1995) Inhibitor-enhanced electron transfer: copper cytochrome c as a redox-inert probe of ternary complexes. *Science* **269**, 204-207.

Zimmermann, W. (1990) Degradation of lignin by bacteria. *J. Biotechnol.* **13**, 119-130.

BIOGRAPHICAL SKETCH

Katsuyuki Kishi was born in Okayama, Japan, on February 15, 1965. He received his Bachelor of Science degree from Tokyo University in 1988. He immediately entered the Agricultural Sciences program at Tokyo University and received his Master of Science degree in March, 1990.

In September, 1991, the author began his studies at the Oregon Graduate Institute of Science and Technology where he completed the requirements for the degree of Doctor of Philosophy in Biochemistry.